

Intensification of Biological Nutrient Removal Processes

Stephanie Anne Klaus

Dissertation submitted to the faculty of the Virginia Polytechnic Institute and State University in partial fulfillment of the requirements for the degree of

Doctor of Philosophy
in
Civil Engineering

Amy Pruden-Bagchi, Chair

Charles B. Bott

John T. Novak

Zhen (Jason) He

Zhiwu (Drew) Wang

August 30, 2019

Blacksburg, Virginia

Keywords: Advanced aeration control, anammox, shortcut nitrogen removal, sidestream biological phosphorus removal

Copyright © 2019 Stephanie Anne Klaus

Intensification of Biological Nutrient Removal Processes

Stephanie Anne Klaus

ABSTRACT

Intensification refers to utilizing wastewater treatment processes that decrease chemical and energy demands, increase energy recovery, and reduce the process footprint (or increased capacity in an existing footprint) all while providing the same level of nutrient removal as traditional methods. Shortcut nitrogen removal processes; including nitrite shunt, partial nitrification/anammox, and partial denitrification/anammox, as well as low-carbon biological phosphorus removal, were critically-evaluated in this study with an overall objective of intensification of existing infrastructure.

At the beginning of this study, granular sidestream deammonification was becoming well-established in Europe, but there was virtually no experience with startup or operation of these processes in North America. The experience gained from optimization of the sidestream deammonification moving bed biofilm reactor (MBBR) in this study, including the novel pH-based aeration control strategy, has influenced the startup procedure and operation of subsequent full-scale installations in the United States and around the world.

Long startup time remains a barrier to the implementation of sidestream deammonification processes, but this study was the first to show the benefits of utilizing media with an existing nitrifying biofilm to speed up anammox bacteria colonization. Utilizing media with an established biofilm from a mature integrated fixed film activated sludge (IFAS) process resulted in at least five times greater anammox activity rates in one month than virgin media without a preliminary biofilm. This concept has not been testing yet in a full-scale startup, but has the potential to drastically reduce startup time.

False dissolved oxygen readings were observed in batch scale denitrification tests, and it was determined that nitric oxide was interfering with optical DO sensors, a problem of which the sensor manufacturers were not aware. This led to at least one sensor manufacturer reevaluating their sensor design and several laboratories and full-scale process installations were able to understand their observed false DO readings.

There is an industry-wide trend to utilize influent carbon more efficiently and realize the benefits of mainstream shortcut nitrogen removal. The A/B pilot at the HRSD Chesapeake Elizabeth Treatment provides a unique chance to study these strategies in a continuous flow system with real wastewater. For the first time, it was demonstrated that the presence of influent particulate COD can lead to higher competition for nitrite by heterotrophic denitrifying bacteria, resulting in nitrite oxidizing bacteria (NOB) out-selection. TIN removal was affected by both the type and amount of influent COD, with particulate COD (pCOD) having a stronger influence than soluble COD (sCOD). Based

on these findings, an innovative approach to achieving energy efficient biological nitrogen removal was suggested, in which influent carbon fractions are tailored to control specific ammonia and nitrite oxidation rates and thereby achieve energy efficiency in the nitrogen removal goals downstream.

Intermittent and continuous aeration strategies were explored for more conventional BNR processes. The effect of influent carbon fractionation on TIN removal was again considered, this time in the context of simultaneous nitrification/denitrification during continuous aeration. It was concluded that intermittent aeration was able to achieve equal or higher TIN removal than continuous aeration at shorter SRTs, whether or not the goal is nitrite shunt. It is sometimes assumed that converting to continuous aeration ammonia-based aeration control (ABAC) or ammonia vs. NO_x (AvN) control will result in an additional nitrogen removal simply by reducing the DO setpoint resulting in simultaneous nitrification/denitrification (SND). This work demonstrated that lower DO did not always improve TIN removal and most importantly that aeration control alone cannot guarantee SND. It was concluded that although lower DO is necessary to achieve SND, there also needs to be sufficient carbon available for denitrification.

While the implementation of full-scale sidestream anammox happened rather quickly, the implementation of anammox in the mainstream has not followed, without any known full-scale implementations. This is almost certainly because maintaining reliable mainstream NOB out-selection seems to be an insurmountable obstacle to full-scale implementation. Partial denitrification/anammox was proven to be easier to maintain than partial nitrification/anammox and still provides significant aeration and carbon savings compared to traditional nitrification/denitrification. There is a long-standing interest in combining shortcut nitrogen removal with biological phosphorus removal, without much success. In this study, biological phosphorus removal was achieved in an A/B process with A-stage WAS fermentation and shortcut nitrogen removal in B-stage via partial denitrification.

Intensification of Biological Nutrient Removal Processes

Stephanie Anne Klaus

GENERAL AUDIENCE ABSTRACT

When the activated sludge process was first implemented at the beginning of the 20th century, the goal was mainly oxygen demand reduction. In the past few decades, treatment goals have expanded to include nutrient (nitrogen and phosphorus) removal, in response to regulations protecting receiving bodies of water. The only practical way to remove nitrogen in municipal wastewater is via biological treatment, utilizing bacteria, and sometimes archaea, to convert the influent ammonium to dinitrogen gas. Orthophosphate on the other hand can either be removed via chemical precipitation using metal salts or by conversion to and storage of polyphosphate by polyphosphate accumulating organisms (PAO) and then removed in the waste sludge.

Nitrification/denitrification and chemical phosphorus removal are well-established practices but utilize more resources than processes without nutrient removal in the form of chemical addition (alkalinity for nitrification, external carbon for denitrification, and metal salts for chemical phosphorus removal), increased reactor volume, and increased aeration energy.

Intensification refers to utilizing wastewater treatment processes that decrease chemical and energy demands, increase energy recovery, and reduce the process footprint (or increase capacity in an existing footprint) all while providing the same level of nutrient removal as traditional methods. Shortcut nitrogen removal processes; including nitrite shunt, partial nitritation/anammox, and partial denitrification/anammox, as well as low-carbon biological phosphorus removal, were critically-evaluated in this study with an overall objective of intensification of existing infrastructure.

Partial nitritation/anammox is a relatively new technology that has been implemented in many full-scale sidestream processes with high ammonia concentrations, but that has proven difficult in more dilute mainstream conditions due to the difficulty in suppressing nitrite oxidizing bacteria (NOB). Even more challenging is integrating biological phosphorus removal with shortcut nitrogen removal, because biological phosphorus removal requires the readily biodegradable carbon that is diverted. Partial denitrification/anammox provides a viable alternation to partial nitritation/anammox, which may be better suited for integration with biological phosphorus removal.

ACKNOWLEDGEMENTS

I would like to acknowledge Hampton Roads Sanitation District (HRSD) for funding my research, and thank my advisor Charles Bott for making this opportunity possible. Thanks to my committee chair Amy Pruden for her guidance, and to the rest of my committee, Jason He, Drew Wang, and John Novak for their feedback. Thank you to all of my collaborators, fellow students and interns at HRSD, and the staff at the James River Treatment Plant and Chesapeake Elizabeth Treatment Plant. Thank you to my family for their endless support. And thanks to my partner Dan, for being there every step of the way.

TABLE OF CONTENTS

Abstract.....	ii
General Audience Abstract.....	iv
Acknowledgements.....	v
Table of Contents.....	vi
Table of Figures.....	ix
Table of Tables.....	xiii
Chapter 1: Introduction.....	1
Chapter 2: Literature Review.....	5
Simultaneous Nitrification-Denitrification.....	5
Mainstream Shortcut Nitrogen Removal.....	5
Carbon Removal.....	5
NOB out-selection and anammox retention.....	6
Process control.....	9
Partial Denitrification/Anammox.....	9
RAS fermentation for enhanced reliability and stability of Bio-P.....	9
References.....	10
Chapter 3: Startup of a Full-Scale Partial Nitritation-Anammox MBBR for Sidestream Nitrogen Removal and the Development of a Novel Control System.....	17
Abstract.....	17
Introduction.....	17
Methods and Materials.....	20
Results and Discussion.....	23
Conclusions.....	34
References.....	34
Chapter 4: Methods for Increasing the Rate of Anammox Attachment in a Sidestream Deammonification MBBR.....	37
Abstract.....	37
Introduction.....	37
Materials and Methods.....	39

Results and Discussion.....	44
Conclusions.....	48
References.....	49
Chapter 5: Nitric Oxide Production Interferes with Aqueous Dissolved Oxygen Sensors	51
Abstract.....	51
Introduction.....	51
Materials and Methods.....	52
Results and Discussion.....	54
Conclusions.....	59
References.....	60
Chapter 6: Effect of Influent Carbon Fractionation and Reactor Configuration on Mainstream Nitrogen Removal and NOB Out-Selection	61
Abstract.....	61
Introduction.....	61
Materials and Methods.....	63
Results and Discussion.....	66
Implications for Implementation.....	74
References.....	74
Appendix A: Supporting Information for chapter 6.....	79
Chapter 7: Comparison of Sensor Driven Aeration Control Strategies for Optimization of Nitrogen Removal via Denitrification in Aerated Zones.....	86
Abstract.....	86
Introduction.....	86
Materials and Methods.....	88
Results and Discussion.....	92
Summary and Conclusions.....	106
References.....	107
Appendix B: Supporting Information for chapter 7.....	113
Chapter 8: Integration of Sidestream Biological Phosphorus Removal and Partial Denitrification/Anammox.....	118
Abstract.....	118

Introduction	118
Methods	120
Results and Discussion	124
Conclusions	140
References	140
Appendix C: Supporting Information for Chapter 8	147

TABLE OF FIGURES

Figure 3.1: Ammonium and TIN removal percentages, temperature, nitrite in effluent, and nitrate production ratio. Vertical line indicates end of startup on Day 120.	25
Figure 3.2: Ammonium loading, ammonium removal, and nitrite concentrations in the effluent. Vertical line indicates end of startup on Day 120.	26
Figure 3.3: Biofilm development photos: (A) original seed media prior to placement in reactor; (B) seed media on Day 10; (C) sheared seed media on Day 64; (D) typical seed media on Day 64; (E) new media on Day 64; (F) new media after completion of startup on Day 120; (G) seed media after completion of startup on Day 120.	27
Figure 3.4: Bench-scale new media activity rates. Vertical line indicates end of startup on Day 120.	28
Figure 3.5: Bench-scale seed media activity rates. Vertical line indicates end of startup on Day 120.	29
Figure 3.6: Example of fixed DO control leading to low pH shutoff. In this example, the airflow is programmed to shut off when the pH reaches 6.6 and come back on when pH reaches 6.8.	31
Figure 3.7: Performance of pH-based DO control.	33
Figure 4.1: Performance of the Full-Scale Deammonification MBBR including startup and overall tank conditions during the duration of the attachment experiment. Day 1 to Day 120: Startup Phase, Day 115 to Day 179: Attachment experiment presented in this study	40
Figure 4.2: Time course of influent NH_4^+ (grey circles, right axis), influent sCOD (white triangles), effluent NH_4^+ (black circles), effluent sCOD (white squares), effluent NO_3^- (white circles), and effluent NO_2^- (black triangles) in full-scale deammonification MBBR. Day 1 to Day 120: Startup Phase, Day 115 to Day 179: Attachment experiment presented in this study	41
Figure 4.3: IFAS media and surface modified media AMX activity test results after one month and two months. $\text{AMX NH}_4^+ = \text{AMX activity based on } \text{NH}_4^+ \text{ consumption}$, $\text{AMX NO}_2^- = \text{AMX activity based on } \text{NO}_2^- \text{ consumption}$. Error bars represent the 95% confidence interval.	47
Figure 4.4: IFAS media and surface modified media AMX biomass results after one month and two months.	48
Figure 5.1: Sample A Denitrification Test Nitrogen Measurements and DO Sensor Output. At the beginning of Phase I (time=0) 25 mg/L $\text{NO}_2\text{-N}$ and 400 mg COD/L of sodium acetate was dosed. At the beginning of Phase II once NO_2 was depleted, 15 mg/L NO_3 was dosed. At the beginning of Phase III 200 mg COD/L of sodium acetate was dosed. There was no aeration during this test.	55
Figure 5.2A: Sensor outputs from Sample B denitrification test. NO (red), N_2O (green),	56

Insite DO (cyan), YSI DO (dark blue), YSI membrane (grey), Hach LDO (magenta)	
Figure 5.2B: Sample B Denitrification Test Nitrogen and sCOD measurements. Phase I: No gas sparging; Phase II: Nitrogen gas sparging; Phase III: Air sparging	57
Figure 5.3: Test in Tap Water DO, NO, and N ₂ O Sensor Outputs. NO (red), N ₂ O (green), Insite DO (cyan), YSI DO (dark blue), YSI membrane (grey), Hach LDO (magenta). Phases I and II: Spike of NO gas followed by stripping of NO using N ₂ gas. Phase III: Spike of N ₂ O gas followed by stripping of N ₂ O using N ₂ gas. Phase IV: Sparging air	58
Figure 5.4: pH, DO concentration, and airflow in a sidestream shortcut nitrogen SBR. Republished with permission from Wett and Rauch, 2003.	59
Figure 6.1: Pilot plant configuration. The B-stage was operated with primary clarifier or A-stage effluent. CSTR 1 was anoxic with an internal mixed liquor recycle (IMLR) during MLE configuration.	64
Figure 6.2: % TIN removal vs. tCOD/NH ₄ -N (A), pCOD/NH ₄ -N B), and sCOD/NH ₄ -N (C) in the B-stage influent	68
Figure 6.3: Soluble COD, particulate COD, and nitrite accumulation ratio over time	69
Figure 6.4: Correlation between pCOD and sCOD (mg/L) and nitrite accumulation ratio (NAR%), separated by fully intermittent (FI) (A and B) and MLE configurations (C and D).	70
Figure 6.5: Comparison of NOB divided by AOB rate and NO ₂ denitrification rate divided by NO ₃ denitrification rate from ex-situ maximum activity rate testing, and nitrite accumulation ratio (NAR).	72
Figure 6.6: Prevalence of AOB and NOB (<i>Nitrobacter</i> and <i>Nitrospira</i>), and nitrite accumulation ratio (NAR) over time.	73
Figure 7.1: Phase 1 BNR process configuration. A-stage effluent (ASE) fed the B-stage process. In fully aerated (FA) configuration there was no internal mixed liquor recycle (IMLR). In MLE configuration CSTR 1 was unaerated with IMLR at 300% of influent flow.	93
Figure 7.2: B-stage influent C/N (total COD/NH ₄ ⁺ -N), TIN removal %, and total COD/TIN removal ratio	93
Figure 7.3: SRT, Aerobic Fraction Setpoint (air on time divided by total cycle time), and DO setpoint. Aerobic Fraction and DO setpoints are determined by the AvN controller.	94
Figure 7.4: B-stage influent and effluent nitrogen concentrations	94
Figure 7.5: Phase 2 BNR process configuration. MLE at 300% IMLR with primary clarifier feed.	96
Figure 7.6: TIN removal 5, COD/TIN removal ratio (total COD removed divided by TIN	97

removed) and influent COD/NH ₄ (C/N).	
Figure 7.7: Profile grab samples to quantify SND measured as TIN loss across aerated reactors	99
Figure 7.8: Phase 3 process configurations. A/O with 4 CSTRs (top) and A2O with 5 CSTRs and varying IMLR rates (bottom).	100
Figure 7.9: TIN removal, influent COD/NH ₃ , and total COD/TIN removed ratio during each scenario. Average DO during A2O ABAC was 0.24 mg/L.	102
Figure 7.10: Aerobic TIN removal (SND) vs. Anoxic TIN removal	102
Figure 7.11: Aerobic TIN removal (SND) vs. TIN removal %	103
Figure 7.12: 16S rRNA gene amplicon sequencing results for putative AOB, NOB, PAO and GAO genera.	103
Figure 7.13: Phase 4 process configuration. In A2O configuration there was an anoxic zone with an IMLR of 400% influent flow. In A/O configuration there were four aerated CSTRs and no IMLR.	104
Figure 7.14: SND versus anoxic nitrogen removal	105
Figure 7.15: SND versus ammonia residual in the effluent	105
Figure 8.1: Pilot Configuration	120
Figure 8.2: Fermentate VFA Fractionation as percent of total VFA on a COD basis.	126
Figure 8.3: tCOD, sCOD, and VFA load to the SBPR in mg COD/L divided into the influent flow.	127
Figure 8.4: Influent OP (combined from influent and fermentate), effluent OP, effluent NO ₂ , and VFA load to the sidestream divided into the influent flow.	128
Figure 8.5: Nitrogen profile in time on Day 108 during intermittent aeration in CSTR 4. Grey shaded areas are periods of aeration.	130
Figure 8.6: Maximum anaerobic OP release rate from batch tests (dark green bar), aerobic OP uptake rate from batch tests (light green bar), and influent sCOD/OP ratio (red line). The sCOD/OP ratio was calculated as the five-day moving average of the sCOD added from the fermentate, divided by the sum of the OP in the influent and OP in the fermentate.	131
Figure 8.7: Total TIN in the influent (A-stage effluent (ASE) + fermentate), TIN only from A-stage effluent (ASE), TIN in B-stage effluent (BSE), and TIN in the anammox MBBR effluent.	132

Figure 8.8: TIN removal performance of the MBBR, and glycerol addition (mgCOD/L) to the MBBR.	133
Figure 8.9: qPCR results for Canonical AOB, Comammox, <i>Nitrospira</i> , and <i>Nitrobacter</i> .	134
Figure 8.10: Top 25 genera from 16S amplicon sequencing	135
Figure 8.11: Putative PAO and GAO from 16S amplicon sequencing	135
Figure 8.12: External carbon independent denitrification test on Day 116.	137
Figure 8.13: Rates from external carbon independent denitrification tests over time and VFA load to the SBPR in mg/L as influent flow. Nitrate reduction is positive, nitrite production and OP release are positive.	137
Figure 8.14: Results from the long term denitrification test. The first period is labeled “anaerobic” even though there is nitrate present because this is the OP release and VFA storage period, followed by the aerobic period, then anoxic.	138

TABLE OF TABLES

Table 2.1: NOB out-selection and anammox retention mechanisms for various process configurations	8
Table 3.1: Design parameters	23
Table 3.2: Average influent characteristics	24
Table 3.3: Comparison of aeration control strategies.	33
Table 4.1: Contact Angle and Surface Energy Parameters of the Surface Modified Media and New Media Control. θ_w , θ_D , and θ_F represent the contact angles for water, diiodomethane, and formamide respectively.	44
Table 5.1: List of sensors used in this study	53
Table 6.1: Operational parameters for all phases. The aerobic fraction is the fraction of aerated volume out of the total volume. For the MLE scenarios, the aerobic fraction in parentheses is the aerated fraction in just the aerated tanks, excluding the anoxic zone.	67
Table 7.1: Operating scenarios. All scenarios had a constant influent feed except A2O_ABAC which had a diurnal flow feed pattern.	90
Table 7.2: Summary table for Phases 1 through 3. Phase 4 was not included because the goal was not to maximize TIN removal in that phase.	106
Table 8.1: Sidestream BioP Reactor (SBPR) operation for each phase. sCOD/OP was calculated as sCOD added from the fermentate, divided by the sum of the OP in the influent and OP in the fermentate	125

CHAPTER 1: INTRODUCTION

This study first focused on making improvements to sidestream partial nitrification/anammox processes before focusing on mainstream shortcut nitrogen and biological phosphorus removal. Results for chapters 3 and 4 were collected at a full-scale sidestream process, while results for chapters 5-8 were collected at a mainstream pilot scale system. Note that sidestream in reference to shortcut nitrogen removal refers to treating the dewatered anaerobic digestate, while sidestream in reference to biological phosphorus removal refers to an anaerobic zone that contains only return activated sludge which is not diluted by the influent flow. Also note that partial nitrification/anammox (PNA) is used interchangeably with deammonification.

CHAPTER 2 is a literature review of shortcut nitrogen removal processes and sidestream biological phosphorus removal.

CHAPTER 3 details the startup of the second full-scale process to utilize partial nitrification/anammox in North America, and the first to utilize a moving bed biofilm reactor. It was hypothesized that preventing inorganic carbon limitation was the most important factor in control of sidestream anammox processes. The objective was to demonstrate that pH-based aeration control optimizes performance in a sidestream deammonification MBBR and to provide detailed information on startup strategy.

Klaus, S., Baumler, R., Rutherford, B., Thesing, G., Zhao, H., Bott, C., 2017. Startup of a Partial Nitrification-Anammox MBBR and the Implementation of pH-Based Aeration Control. *Water Environment Research* 89, 500–508.

- Klaus: Data collection, analysis, and writing
- All other co-authors reviewed the manuscript

CHAPTER 4 addresses the challenge of slow start-up times for full-scale sidestream deammonification moving bed biofilm reactors, which is a significant barrier to implementation of this technology. The objective was to test the hypothesis that rates of anammox biofilm growth on HDPE media could be increased through wet chemical surface treatment and through the transfer of media with a mature biofilm from a full-scale mainstream fully nitrifying IFAS process.

Klaus, S., McLee, P., Schuler, A.J., Bott, C., 2016. Methods for Increasing the Rate of Anammox Attachment in a Sidestream Deammonification MBBR. *Water Science and Technology* 74, 110–117.

- Klaus: Data collection, analysis, and writing
- McLee performed the contact angle measurements
- Schuler and Bott reviewed the manuscript

CHAPTER 5 describes the surprising discovery that nitric oxide interferes with dissolved oxygen sensors that are utilized in laboratory and full-scale wastewater treatment facilities. False

dissolved oxygen readings were observed in batch scale denitrification tests, leading to the hypothesis that an intermediate in denitrification was causing interference. The objectives of this study were to demonstrate which denitrification intermediate was interfering with the DO probe readings, to demonstrate that the interference occurs at levels of nitrite that are relevant to wastewater treatment processes, and to test a variety of DO sensors for interference.

Klaus, S., Sadowski, M., Jimenez, J., Wett, B., Chandran, K., Murthy, S., Bott, C.B., 2017. Nitric oxide production interferes with aqueous dissolved oxygen sensors. *Environmental Engineering Science* 34, 687–691.

- Klaus: Data collection, analysis, and writing
- Sadowski and Jimenez: Data collection
- All other co-authors reviewed the manuscript

CHAPTER 6 examines the mechanisms for mainstream NOB out-selection during intermittent aeration in regard to influent carbon fractionation (A-stage effluent versus primary clarifier effluent) and reactor configuration. It was hypothesized that influent particulate COD was leading to NOB out-selection via heterotrophic competition for nitrite. The objectives were to determine the influence of influent COD/NH₄⁺-N ratio on TIN removal, and to determine the effect of operating configurations and influent carbon fractionation on nitrite accumulation and NOB out-selection in an intermittently aerated BNR process.

Effect of Influent Carbon Fractionation and Reactor Configuration on Mainstream Nitrogen Removal and NOB Out-selection. Stephanie A. Klaus, Michael S. Sadowski, Maureen N. Kinyua, Mark W. Miller, Pusker Regmi, Bernhard Wett, Haydee De Clippeleir, Kartik Chandran, Charles B. Bott.

Target Journal: *Environmental Science: Water Research and Technology*

- Klaus: Data collection, analysis, and writing
- Sadowski: Data collection
- Chandran: qPCR analysis and manuscript review
- All other co-authors reviewed the manuscript

CHAPTER 7 compares sensor driven aeration control strategies (both intermittent and continuous) applied to more conventional BNR processes compared to Chapter 6. It was hypothesized that simply reducing the bulk dissolved oxygen concentration would not guarantee increased nitrogen removal in continuously aerated processes. The objective was to test if the same TIN removal and nitrite shunt benefits could be achieved with continuous aeration sensor driven strategies (AvN and ABAC) as with intermittent aeration. This chapter gives insight into how to select an aeration control strategy based on reactor configuration and treatment goals.

Comparison of Sensor Driven Aeration Control Strategies for Optimization of Nitrogen Removal via Denitrification in Aerated Zones. Stephanie A. Klaus and Charles Bott

Target journal: *Water Environment Research*

- Klaus: Data collection, analysis, and writing
- Bott: Reviewed the manuscript

CHAPTER 8 examined the possibility of accumulating nitrite from partial denitrification instead of via partial nitrification. Integrating shortcut nitrogen removal and biological phosphorus removal (bioP) is challenging because of the conflicting influent carbon demands. It was hypothesized that partial denitrification/anammox (PDNA) could be achieved with biological phosphorus removal utilizing an A/B process with a sidestream RAS reactor. The objective was to integrate PDNA and sidestream bioP, utilizing A-stage WAS fermentation as a supplemental carbon source.

Integration of Sidestream Biological Phosphorus Removal and Partial Denitrification/Anammox. Stephanie Klaus, Varun Srinivasan, Dongqi Wang, Chenghua Long, Haydee DeClippeleir, Kartik Chandran, April Gu, Charles B. Bott

Target Journal: *Environmental Science: Water Research and Technology*

- Klaus: Data collection, analysis, and writing
- Srinivasan, Wang, and Long: performed 16S amplicon sequencing, qPCR, and PHA analysis
- DeClippeleir, Chandran, Gu, and Bott reviewed the manuscript

OTHER PUBLICATIONS

In addition to the manuscript chapters presented above, the following are additional publications and patents that were completed during the timeframe of this study.

Klaus, S., Edgerton, A., Bott, C., 2017. How to Operate and Anammox Process. *Water Environment & Technology* 29 (5), 28-33.

Eichler, C.M., Wu, Y., Cox, S.S., Klaus, S., Boardman, G.D., 2018. Evaluation of Sampling Techniques for Gas-Phase Siloxanes in Biogas. *Biomass and Bioenergy* 108, 1–6.

Li, X., Klaus, S., Bott, C., He, Z., 2018. Status, Challenges, and Perspectives of Mainstream Nitrification-Anammox for Wastewater Treatment. *Water Environment Research* 90, 634–649.

Campolong, C., Klaus, S., Rosenthal, A., Sabba, F., Baideme, M., Wells, G., de Clippeleir, H., Chandran, K., Bott, C.B. Nitrogen Polishing in a Partial Denitrification/Anammox MBBR Using Glycerol, Acetate, and Methanol. *In progress. Target: Water Research*

Patents

Bott, C., Klaus, S., 2018. Method for deammonification process control using pH, specific conductivity, or ammonia. US9902635B2. GRANTED.

Murthy, S.N., Clippeleir, H.D., Debarbadillo, C., Bott, C.B., Klaus, S., Wett, B., 2018. Method and apparatus for nutrient removal with carbon addition. US20180009687A1. APPLICATION PENDING.

CHAPTER 2: LITERATURE REVIEW

SIMULTANEOUS NITRIFICATION-DENITRIFICATION

The drivers for implementing ammonia based aeration control (ABAC) are to reduce aeration energy, reduce chemical addition, and prevent peaks in effluent ammonia (Åmand et al, 2013; Rieger et al., 2013). With ABAC, there is the possibility for simultaneous nitrification denitrification (SND) if DO setpoints can get low enough (0.2-0.8 mg/L) (Jimenez et al., 2010). SND is defined as nitrogen loss in aerated reactors. It is typically assumed that converting to ABAC will result in an additional nitrogen removal simply by reducing the DO setpoint resulting in SND. However, the mechanisms for achieving controllable SND are not well understood, and SND is difficult to quantify. Converting to ABAC can lead to more denitrification capacity (therefore more TIN removal) due to less oxygen transfer into anoxic zones but this does not classify as SND. SND is commonly observed in oxidation ditches and in low DO suspended growth systems (Daigger et al., 2014).

In order for SND to occur there needs to be rbCOD available for denitrification in the aerobic zones. This rbCOD could come from internal storage products, or the hydrolysis of pCOD and endogenous decay products. Since aerobic heterotrophs have a clear advantage for soluble substrate, potential conditions that allow for denitrification to occur in aerated zones are:

1. A DO gradient within the floc allows for an anoxic zone for denitrification to occur. This is the most common explanation for SND.
2. A DO gradient within the reactor. Incomplete mixing leads to areas of very low or zero DO. This will not be explored in this study since it is not a reliable way to achieve SND.
3. Organisms that are capable of storing carbon internally in an anaerobic zone, can subsequently denitrify under low DO conditions. This can be carried out by denitrifying phosphorus accumulating organisms (dPAO), denitrifying glycogen accumulating organisms (dGAO), or other heterotrophs (Tsuneda et al., 2006; Rubio-Rincón et al., 2017; Van Loosdrecht et al., 1997). Research has shown that dPAO can reduce nitrate and nitrite during SND (Tsuneda et al., 2006; Zeng et al., 2014; Giraldo et al., 2011).

MAINSTREAM SHORTCUT NITROGEN REMOVAL

CARBON REMOVAL

The following statement is frequently cited in the literature when explaining the benefits of mainstream deammonification: “partial nitritation and anammox results in 60% less aeration, 90% less sludge production and 100% reduction of organic carbon addition compared to conventional nitrification-denitrification” (Cao et al., 2017; Jetten et al., 1997; Mulder, 2003). As Daigger (2014) pointed out, this is completely dependent on carbon removal ahead of the nitrogen removal step. Otherwise, the carbon will get oxidized in B-stage, utilizing aeration energy and creating more biomass. In order to realize the benefits of mainstream deammonification, the carbon needs to be diverted, preferably to an anaerobic digester to recover

energy. It should also be noted that in order to remove 100% of the nitrogen, some organic carbon is required to reduce the small amount of nitrate produced by anammox (Daigger et al., 2014). The concept behind the operation of an A/B process for mainstream deammonification is to balance the carbon that is being captured in A-stage with the remaining carbon that is being fed to B-stage. When the mechanism for nitrogen removal is denitrification by OHO (such as in nitrite shunt), it is desirable to have slowly biodegradable COD (sbCOD) in the B-stage influent (Regmi, 2014). As more nitrogen is removed through the anammox pathway, less carbon is required, and more carbon can be diverted.

The removal of carbon can be accomplished physically (with or without the addition of chemicals to enhance coagulation/flocculation), or biologically. Primary sedimentation tanks should remove from 50 to 70% of the TSS, 25 to 40% of the BOD, and 20 to 35% of the COD (Tchobanoglous et al., 2003). A limitation of primary sedimentation is that soluble and colloidal constituents are not removed. Chemically enhanced primary treatment (CEPT) is the addition of coagulants and/or flocculating agents to the primary settling process to improve physical removal of carbon. Removals of 80 to 90% TSS including some colloidal particles, 50 to 80% BOD, and 45 to 80% COD can be achieved (Tchobanoglous et al., 2003). CEPT can also be used for chemical phosphorus removal. The goal of the high-rate A-stage in an adsorption-bio-oxidation (A/B process) is to provide a controlled carbon loading for B-stage, and by separating the SRTs achieve low cost COD removal at reduced aeration tank volume and aeration energy requirements (Miller et al., 2012).

NOB OUT-SELECTION AND ANAMMOX RETENTION

Deammonification in sidestream processes, treating dewatered anaerobically digested sludge liquor, is well established with over 100 full-scale installations (Lackner et al., 2014). The main challenges of achieving mainstream deammonification are NOB out-selection and anammox retention. NOB repression is easier in sidestream processes due to high free ammonia (FA) concentrations (Anthonisen et al., 1976) and high temperature (Hellinga et al., 1998). Anammox retention becomes more difficult in mainstream because colder temperatures and lower ammonia concentrations result in slower growth rates (Kartal et al., 2010; Vlaeminck et al., 2012; Ma et al., 2016; Lackner et al., 2015). Strategies developed to give AOB an advantage over NOB in mainstream treatment include: maintaining an ammonia residual in the effluent (Regmi et al., 2014; Pérez et al., 2014; Poot et al., 2016; Welker and Lackner, 2016), transient anoxia (Gilbert et al., 2014a; Kornaros et al., 2010), high DO concentration during intermittent aeration (Regmi et al., 2014; Al-Omari et al., 2015), low DO continuous aeration (for biofilm and granule systems) (Sliemers et al., 2005; Pérez et al., 2014; Poot et al., 2016), seeding of AOB from a sidestream process (Al-Omari et al., 2015), aerobic SRT control (Regmi et al., 2014), and exposure of the mainstream biomass to high levels of nitrous acid (Piculell et al., 2016b; Wang et al., 2014). Transient anoxia can be achieved through intermittent aeration either in time (on/off aeration control) or in space (alternating oxic/anoxic zones). The proposed mechanisms of NOB out-selection from transient anoxia are: enzymatic lag (Kornaros et al., 2010), inhibition by

intermediates (Courtens et al., 2015; Park and Chandran 2016), and substrate availability (Gilbert et al., 2014b) (limiting the amount of NO_2^- available aerobically).

Because NOB out-selection is so challenging, it is desirable to combine as many of these strategies as possible. Which strategies can be implemented depends on the type of system that is being operated, and that can be broken down into two categories based on the mechanism for anammox retention. Single SRT systems include: attached growth biofilm systems (Gilbert et al., 2014b; Laurenzi et al., 2016; Gustavsson et al., 2015; Liu et al., 2018) and fully granular systems (Lotti et al., 2014; Gao et al., 2015; Winkler et al., 2012; Morales et al., 2016). Two-SRT systems include: hybrid systems with AOB/NOB/OHO suspended growth and granular anammox (Wett et al., 2015; Han et al., 2016; Cao et al., 2013), and two-phase systems with AOB/NOB/OHO in a separate suspended growth reactor followed by a completely anoxic anammox moving bed biofilm reactor (MBBR) (Regmi et al., 2015; Ma et al., 2011). Aerobic granular sludge and biofilm systems can take advantage of relative diffusion resistance inside and outside of a granule/biofilm to develop and grow different populations simultaneously in a single reactor. However, NOB out-selection can be more challenging because the SRTs of the different populations cannot be separated. Recently, Anoxkaldnes developed “z-carriers”, plastic media capable of out-selecting NOB spatially by limiting the depth of the biofilm (Piculell et al., 2016a). The thickness of the biofilm can be controlled to different depths depending on if it is used in a single stage system, or in the first stage of a two-stage system.

The common mechanism of NOB out-selection to all configurations, is maintaining an ammonia residual to maintain high AOB rates by keeping substrate well above limiting condition. See Table 1 for a summary of NOB out-selection and anammox retention mechanisms. The challenge of suppressing NOB became even more complicated by the discovery in 2015 that certain NOB are capable of oxidizing ammonia directly to nitrate, disrupting the long accepted understanding of nitrification as a two-step process (Kessel et al., 2015). The term Comammox (complete ammonia oxidation) was coined to describe the process (Kessel et al., 2015). The discovery of this pathway may help to explain why NOB out-selection is so difficult (Daims et al., 2016). Research is ongoing to develop molecular tools to identify these bacteria and quantify their presence in wastewater treatment facilities Pinto et al., 2016).

Table 2.1: NOB out-selection and anammox retention mechanisms for various process configurations

Process Configuration	Anammox Retention Mechanism	NOB Out-selection Mechanisms				References
		Ammonia residual?	DO Control	NO ₂ level	SRT separation of microbial populations?	
Biofilm Process	Attached growth on plastic media	Yes (plus FA inhibition if using centrate contact)	Low continuous DO	Low in mainstream, high during centrate contact (HNO ₂ inhibition)	No, unless spatial out-selection using z-carriers	Gilbert et al., 2014; Laureni et al., 2016; Gustavsson et al., 2015; Liu et al., 2018; Piculell et al., 2016
Fully Granular Process	Granules	yes	Continuous DO based on NH ₄ loading	Low	No separation	Lotti et al., 2014; Gao et al., 2015; Winkler et al., 2012; Morales et al., 2016
Hybrid system (Suspended growth with anammox granules)	1. External selector (e.g. hydrocyclone or screens) 2. Bioaugmentation of AMX and AOB	yes	High DO (1.5 mg/L) intermittent DO control	Low as possible going into aerobic zones, higher going into anoxic zones	1. aerobic SRT control 2. external selector 3. Bioaugmentation	Wett et al., 2015; Han et al., 2016; Cao et al., 2013
Two-phase system (Partial nitrification followed by anoxic AMX MBBR)	Biofilm	Yes in Phase 1	Phase 1: High DO (1.5 mg/L) intermittent DO control Phase 2: anoxic	High in phase 1, less than 1 mg/L in phase 2	Phase 1 suspended growth: Aggressive control to keep low aerobic SRT Phase 1 biofilm: spatial out-selection with z-carrier Phase 2: No separation	Regmi et al., 2015; Ma et al., 2011; Piculell et al., 2016

PROCESS CONTROL

Ammonia vs. NO_x (AvN) control for nitrite shunt works by controlling the aerobic fraction to meet an NH_4^+ to NO_x ratio in the effluent. In addition to transient anoxia the controller uses high DO, aerobic SRT control, and high residual ammonia concentration to favor AOB over NOB (Regmi et al., 2014). Although AvN control was developed to achieve nitrite shunt through NOB out-selection, AvN control has the potential to provide more efficient nitrogen removal than ABAC, even if the goal is not nitrite shunt. By setting ammonia and NO_x equal in the effluent, or by specifying a ratio of $\text{NH}_4^+/\text{NO}_x$ somewhat less than one based on the need to comply with an effluent ammonia limit, AvN control oxidizes only the amount of ammonia that can be denitrified utilizing the influent organic carbon that is made available. This maximizes COD utilization efficiency for heterotrophic denitrification using NO_3^- or NO_2^- without the addition of supplemental carbon. This can be achieved with either continuous or intermittent aeration. Another option for the AvN program is the slope-intercept control concept using the following equation: $\text{NH}_4^+ = \text{slope} * \text{NO}_x + \text{intercept}$ where the slope controls the $\text{NH}_4^+/\text{NO}_x$ ratio and the intercept controls the ammonia effluent limit. When implemented for mainstream deammonification, the slope will be higher as more nitrogen is removed through the anammox pathway.

PARTIAL DENITRIFICATION/ANAMMOX

Since successful NOB out-selection relies on leaving an ammonia residual, and because there will always be some residual NO_3^- , some sort of polishing is required to meet a stringent effluent nitrogen limit (Regmi et al., 2015; Le et al., 2019). A completely anoxic MBBR, or combined suspended and granular growth process, can be used to remove additional NO_3^- and NH_4^+ through partial denitrification of NO_3^- to NO_2^- , and the subsequent oxidation of ammonia with the produced nitrite via anammox. Recent research suggests that partial denitrification/anammox may be a viable alternative to sustaining NOB out-selection for partial nitrification (Ma et al., 2016).

RAS FERMENTATION FOR ENHANCED RELIABILITY AND STABILITY OF BIO-P

The fermentation of primary sludge is commonly used to provide volatile fatty acids (VFAs) for biological phosphorus removal (Bio-P) when influent VFA content is insufficient. An alternative approach is to ferment a portion of the return activated sludge (RAS) prior to returning it back to the process, referred to as side-stream Bio-P (Tooker et al., 2016; Andreasen et al., 1997). RAS fermentation was initially investigated as a means to decrease sludge production and nutrient loading to the nutrient removal step, compared to primary sludge fermentation (Andreasen et al., 1997). Also, RAS fermentation is a practical alternative to primary sludge fermentation for facilities that don't have primary treatment. Another example of a sidestream fermentation process is the Cannibal® process, as a means of solids reduction (Novak et al., 2007). While the mechanisms occurring in sidestream Bio-P reactors are largely unknown, the process seems to include a combination of hydrolysis, fermentation, and enrichment of PAO (Vollertsen et al., 2006; Barnard et al., 2010; Houweling et al., 2010). The enrichment of PAO refers to the competition of PAO over GAO, and recent research suggests the possibility of enrichment of

Tetrasphaera over *Accumulibacter* in the sidestream reactor (Nguyen et al., 2011). *Tetrasphaera* are a more recently discovered PAO that have a distinctly different metabolism from the frequently studied *Candidatus Accumulibacter phosphates* (Maszenan et al., 2000; Kristiansen et al., 2013). *Tetrasphaera* seem to occupy a different ecological niche compared to *Accumulibacter*, having the ability to ferment complex organic molecules such as glucose and benefitting from deeper anaerobic conditions (Nguyen et al., 2011; Barnard et al., 2016; Kong et al., 2008). Unlike *Accumulibacter*, all known *Tetrasphaera* have the ability to denitrify nitrite and/or nitrate (Kristiansen et al., 2013). The selection of *Tetrasphaera* over *Accumulibacter* may help to ensure the stability of the Bio-P process. To date there are approximately 85 facilities that have implemented or piloted sidestream Bio-P with many different configurations (Tooker et al., 2016). The most common practice is to send 5-30% of the RAS to a sidestream reactor with an HRT of 16-48 hours (Tooker et al., 2016). Current Bio-P models are not able to predict the benefits of RAS fermentation, suggesting that sidestream Bio-P processes will perform worse than is observed in practice (Dunlap et al., 2016). Future research is needed on mechanisms and population dynamics in sidestream Bio-P reactors as well as on operation and novel applications.

REFERENCES

- Al-Omari, A., Wett, B., Nopens, I., De Clippeleir, H., Han, M., Regmi, P., ... Murthy, S. (2015). Model-based evaluation of mechanisms and benefits of mainstream shortcut nitrogen removal processes. *Water Science and Technology*, 71(6), 840–847.
<https://doi.org/10.2166/wst.2015.022>
- Amand, L., Olsson, G., & Carlsson, B. (2013). Aeration control—a review. *Water Science and Technology*, 67(11), 2374–2398.
- Andreasen, K., Petersen, G., Thomsen, H., & Strube, R. (1997). Reduction of nutrient emission by sludge hydrolysis. *Water Science and Technology; London*, 35(10), 79–85.
- Anthonisen, A. C., Loehr, R. C., Prakasam, T. B. S., & Srinath, E. G. (1976). Inhibition of nitrification by ammonia and nitrous acid. *Journal (Water Pollution Control Federation)*, 835–852.
- Barnard, J., Houweling, D., Analla, H., & Steichen, M. (2010). Fermentation of mixed liquor for phosphorus removal. *Proceedings of the Water Environment Federation*, 2010(18), 59–71.
- Barnard, J. I., Dunlap, P., & Steichen, M. (2017). Rethinking the mechanisms of biological phosphorus removal. *Water Environment Research*, 89(11), 2043–2054.
<https://doi.org/10.2175/106143017X15051465919010>

- Cao, Y. S., Kwok, B. H., Yong, W. H., Chua, S. C., Wah, Y. L., & Yahya, A. G. (2013). The main stream autotrophic nitrogen removal in the largest full scale activated sludge process in Singapore: Process analysis. *Proceedings of WEF/IWA Nutrient Removal and Recovery 2013: Trends in Resource Recovery and Use*, 28–31.
- Cao, Y., van Loosdrecht, M. C. M., & Daigger, G. T. (2017). Mainstream partial nitrification–anammox in municipal wastewater treatment: Status, bottlenecks, and further studies. *Applied Microbiology and Biotechnology*, 101(4), 1365–1383. <https://doi.org/10.1007/s00253-016-8058-7>
- Courtens, E. N. P., De Clippeleir, H., Vlaeminck, S. E., Jordaens, R., Park, H., Chandran, K., & Boon, N. (2015). Nitric oxide preferentially inhibits nitrite oxidizing communities with high affinity for nitrite. *Journal of Biotechnology*, 193, 120–122. <https://doi.org/10.1016/j.jbiotec.2014.11.021>
- Daigger, G. T. (2014). Oxygen and Carbon Requirements for Biological Nitrogen Removal Processes Accomplishing Nitrification, Nitritation, and Anammox. *Water Environment Research*, 86(3), 204–209. <https://doi.org/10.2175/106143013X13807328849459>
- Daigger, G. T., & Littleton, H. X. (2014). Simultaneous Biological Nutrient Removal: A State-of-the-Art Review. *Water Environment Research*, 86(3), 245–257. <https://doi.org/10.2175/106143013X13736496908555>
- Daims, H., Lücker, S., & Wagner, M. (2016). A New Perspective on Microbes Formerly Known as Nitrite-Oxidizing Bacteria. *Trends in Microbiology*, 24(9), 699–712. <https://doi.org/10.1016/j.tim.2016.05.004>
- Dunlap, P., Martin, K. J., Stevens, G., Tooker, N., Barnard, J. L., Gu, A. Z., ... Li, Y. (2016). Rethinking EBPR: What do you do when the model will not fit real-world evidence? *5th IWA/WEF Wastewater Treatment Modeling Seminar*, 39–62.
- Gao, D.-W., Huang, X.-L., Tao, Y., Cong, Y., & Wang, X. (2015). Sewage treatment by an UAFB–EGSB biosystem with energy recovery and autotrophic nitrogen removal under different temperatures. *Bioresource Technology*, 181, 26–31. <https://doi.org/10.1016/j.biortech.2015.01.037>
- Gilbert, E. M., Agrawal, S., Brunner, F., Schwartz, T., Horn, H., & Lackner, S. (2014a). Response of Different Nitrospira Species To Anoxic Periods Depends on Operational DO. *Environmental Science & Technology*, 48(5), 2934–2941. <https://doi.org/10.1021/es404992g>
- Gilbert, E. M., Agrawal, S., Karst, S. M., Horn, H., Nielsen, P. H., & Lackner, S. (2014b). Low Temperature Partial Nitritation/Anammox in a Moving Bed Biofilm Reactor Treating Low Strength Wastewater. *Environmental Science & Technology*, 48(15), 8784–8792. <https://doi.org/10.1021/es501649m>

- Giraldo, E., Jjemba, P., Liu, Y., & Muthukrishnan, S. (2011). Ammonia Oxidizing Archaea, AOA, Population and Kinetic Changes in a Full Scale Simultaneous Nitrogen and Phosphorous Removal MBR. *Proceedings of the Water Environment Federation*, 2011(13), 3156–3168. <https://doi.org/10.2175/193864711802721596>
- Gustavsson, D. J. I., Okhravi, A., Persson, F., Alvarez, N. L., & Jansen, J. L. C. (2015). Experiences of repression of nitrate production in nitrification-anammox on municipal wastewater. *Proceedings of IWA Specialist Conference Nutrient Removal and Recovery: Moving Innovation into Practice*, 18–21.
- Han, M., Vlaeminck, S. E., Al-Omari, A., Wett, B., Bott, C., Murthy, S., & De Clippeleir, H. (2016). Uncoupling the solids retention times of flocs and granules in mainstream deammonification: A screen as effective out-selection tool for nitrite oxidizing bacteria. *Bioresource Technology*, 221, 195–204. <https://doi.org/10.1016/j.biortech.2016.08.115>
- Hellinga, C., Schellen, A., Mulder, J. W., van Loosdrecht, M. v., & Heijnen, J. J. (1998). The SHARON process: An innovative method for nitrogen removal from ammonium-rich waste water. *Water Science and Technology*, 37(9), 135–142.
- Houweling, D., Dold, P., & Barnard, J. (2010). Theoretical limits to biological phosphorus removal: Rethinking the influent COD: N: P ratio. *Proceedings of the Water Environment Federation*, 2010(9), 7044–7059.
- Jetten, M. S. M., Horn, S. J., & van Loosdrecht, M. C. M. (1997). Towards a more sustainable municipal wastewater treatment system. *Water Science and Technology*, 35(9), 171–180. [https://doi.org/10.1016/S0273-1223\(97\)00195-9](https://doi.org/10.1016/S0273-1223(97)00195-9)
- Jimenez, J., Dursun, D., Dold, P., Bratby, J., Keller, J., & Parker, D. (2010). Simultaneous nitrification-denitrification to meet low effluent nitrogen limits: Modeling, performance and reliability. *Proceedings of the Water Environment Federation*, 2010(15), 2404–2421.
- Kartal, B., Kuenen, J. G., & Loosdrecht, M. C. M. van. (2010). Sewage Treatment with Anammox. *Science*, 328(5979), 702–703. <https://doi.org/10.1126/science.1185941>
- Kong, Y., Xia, Y., & Nielsen, P. H. (2008). Activity and identity of fermenting microorganisms in full-scale biological nutrient removing wastewater treatment plants. *Environmental Microbiology*, 10(8), 2008–2019. <https://doi.org/10.1111/j.1462-2920.2008.01617.x>
- Kornaros, M., Dokianakis, S. N., & Lyberatos, G. (2010). Partial Nitrification/Denitrification Can Be Attributed to the Slow Response of Nitrite Oxidizing Bacteria to Periodic Anoxic Disturbances. *Environmental Science & Technology*, 44(19), 7245–7253. <https://doi.org/10.1021/es100564j>
- Kristiansen, R., Nguyen, H. T. T., Saunders, A. M., Nielsen, J. L., Wimmer, R., Le, V. Q., ... Nielsen, P. H. (2013). A metabolic model for members of the genus *Tetrasphaera*

- involved in enhanced biological phosphorus removal. *The ISME Journal*, 7(3), 543–554. <https://doi.org/10.1038/ismej.2012.136>
- Lackner, S., Gilbert, E. M., Vlaeminck, S. E., Joss, A., Horn, H., & van Loosdrecht, M. C. M. (2014). Full-scale partial nitrification/anammox experiences – An application survey. *Water Research*, 55, 292–303. <https://doi.org/10.1016/j.watres.2014.02.032>
- Lackner, S., Welker, S., Gilbert, E. M., & Horn, H. (2015). Influence of seasonal temperature fluctuations on two different partial nitrification-anammox reactors treating mainstream municipal wastewater. *Water Science and Technology*, 72(8), 1358–1363. <https://doi.org/10.2166/wst.2015.301>
- Laureni, M., Falås, P., Robin, O., Wick, A., Weissbrodt, D. G., Nielsen, J. L., ... Joss, A. (2016). Mainstream partial nitrification and anammox: Long-term process stability and effluent quality at low temperatures. *Water Research*, 101, 628–639. <https://doi.org/10.1016/j.watres.2016.05.005>
- Le, T., Peng, B., Su, C., Massoudieh, A., Torrents, A., Al-Omari, A., ... Clippeleir, H. D. (2019). Impact of carbon source and COD/N on the concurrent operation of partial denitrification and anammox. *Water Environment Research*, 91(3), 185–197. <https://doi.org/10.1002/wer.1016>
- Liu, M., Krikorian, E., Knapp, T., Melitas, N., Zhao, H., & Johnson, M. (2018). Mainstream ANITA Mox Pilot Testing at the Joint Water Pollution Control Plant. *Proceedings of the Water Environment Federation*, 2018(5), 169–184.
- Lotti, T., Kleerebezem, R., Hu, Z., Kartal, B., Jetten, M. S. M., & van Loosdrecht, M. C. M. (2014). Simultaneous partial nitrification and anammox at low temperature with granular sludge. *Water Research*, 66, 111–121. <https://doi.org/10.1016/j.watres.2014.07.047>
- Ma, B., Wang, S., Cao, S., Miao, Y., Jia, F., Du, R., & Peng, Y. (2016). Biological nitrogen removal from sewage via anammox: Recent advances. *Bioresour Technol*, 200, 981–990. <https://doi.org/10.1016/j.biortech.2015.10.074>
- Maszenan, A. M., Seviour, R. J., Patel, B. K., Schumann, P., Burghardt, J., Tokiwa, Y., & Stratton, H. M. (2000). Three isolates of novel polyphosphate-accumulating gram-positive cocci, obtained from activated sludge, belong to a new genus, *Tetrasphaera* gen. Nov., and description of two new species, *Tetrasphaera japonica* sp. Nov. And *Tetrasphaera australiensis* sp. Nov. *International Journal of Systematic and Evolutionary Microbiology*, 50(2), 593–603. <https://doi.org/10.1099/00207713-50-2-593>
- Miller, M. W., Bunce, R., Regmi, P., Hingley, D. M., Kinnear, D., Murthy, S., ... Bott, C. B. (2012). A/B process pilot optimized for nitrite shunt: High rate carbon removal followed by BNR with ammonia-Based cyclic aeration control. *Proceedings of the Water Environment Federation*, 2012(10), 5808–5825.

- Morales, N., Val del Río, Á., Vázquez-Padín, J. R., Méndez, R., Campos, J. L., & Mosquera-Corral, A. (2016). The granular biomass properties and the acclimation period affect the partial nitrification/anammox process stability at a low temperature and ammonium concentration. *Process Biochemistry*, *51*(12), 2134–2142.
<https://doi.org/10.1016/j.procbio.2016.08.029>
- Mulder, A. (2003). The quest for sustainable nitrogen removal technologies. *Water Science and Technology*, *48*(1), 67–75. <https://doi.org/10.2166/wst.2003.0018>
- Nguyen, H. T. T., Le, V. Q., Hansen, A. A., Nielsen, J. L., & Nielsen, P. H. (2011). High diversity and abundance of putative polyphosphate-accumulating Tetrasphaera-related bacteria in activated sludge systems. *FEMS Microbiology Ecology*, *76*(2), 256–267.
<https://doi.org/10.1111/j.1574-6941.2011.01049.x>
- Novak, J. T., Chon, D. H., Curtis, B.-A., & Doyle, M. (2007). Biological Solids Reduction Using the Cannibal Process. *Water Environment Research*, *79*(12), 2380–2386.
<https://doi.org/10.2175/106143007X183862>
- Park, M. R., & Chandran, K. (2016). Impact of Hydroxylamine Exposure on Anabolism and Catabolism in Nitrospira Spp. *Proceedings of WEF/IWA Nutrient Removal and Recovery, Denver, CO*.
- Pérez, J., Lotti, T., Kleerebezem, R., Picioreanu, C., & van Loosdrecht, M. C. (2014). Outcompeting nitrite-oxidizing bacteria in single-stage nitrogen removal in sewage treatment plants: A model-based study. *Water Research*, *66*, 208–218.
- Piculell, M., Christensson, M., Jönsson, K., & Welander, T. (2016a). Partial nitrification in MBBRs for mainstream deammonification with thin biofilms and alternating feed supply. *Water Science and Technology*, *73*(6), 1253–1260. <https://doi.org/10.2166/wst.2015.599>
- Piculell, Maria, Suarez, C., Li, C., Christensson, M., Persson, F., Wagner, M., ... Welander, T. (2016b). The inhibitory effects of reject water on nitrifying populations grown at different biofilm thickness. *Water Research*, *104*, 292–302.
<https://doi.org/10.1016/j.watres.2016.08.027>
- Pinto, A. J., Marcus, D. N., Ijaz, U. Z., Santos, Q. M. B. lose, Dick, G. J., & Raskin, L. (2016). Metagenomic Evidence for the Presence of Comammox Nitrospira-Like Bacteria in a Drinking Water System. *MSphere*, *1*(1), e00054-15.
<https://doi.org/10.1128/mSphere.00054-15>
- Poot, V., Hoekstra, M., Geleijnse, M. A., van Loosdrecht, M. C., & Pérez, J. (2016). Effects of the residual ammonium concentration on NOB repression during partial nitrification with granular sludge. *Water Research*, *106*, 518–530.

- Regmi, P. (2014). Feasibility of Mainstream Nitrite Oxidizing Bacteria Out-Selection and Anammox Polishing for Enhanced Nitrogen Removal. *Civil & Environmental Engineering Theses & Dissertations*. <https://doi.org/10.25777/78fk-ef25>
- Regmi, P., Bunce, R., Miller, M. W., Park, H., Chandran, K., Wett, B., ... Bott, C. B. (2015). Ammonia-based intermittent aeration control optimized for efficient nitrogen removal. *Biotechnology and Bioengineering*, 112(10), 2060–2067. <https://doi.org/10.1002/bit.25611>
- Regmi, P., Miller, M. W., Holgate, B., Bunce, R., Park, H., Chandran, K., ... Bott, C. B. (2014). Control of aeration, aerobic SRT and COD input for mainstream nitrification/denitrification. *Water Research*, 57, 162–171.
- Regmi, P. R. (2014). *Feasibility of Mainstream Nitrite Oxidizing Bacteria Out-Selection and Anammox Polishing for Enhanced Nitrogen Removal*.
- Rieger, L., Jones, R. M., Dold, P. L., & Bott, C. B. (2014). Ammonia-based feedforward and feedback aeration control in activated sludge processes. *Water Environment Research*, 86(1), 63–73.
- Rubio-Rincón, F. J., Lopez-Vazquez, C. M., Welles, L., van Loosdrecht, M. C. M., & Brdjanovic, D. (2017). Cooperation between Candidatus Competibacter and Candidatus Accumulibacter clade I, in denitrification and phosphate removal processes. *Water Research*, 120, 156–164. <https://doi.org/10.1016/j.watres.2017.05.001>
- Sliekers, A. O., Haaijer, S. C. M., Stafsnes, M. H., Kuenen, J. G., & Jetten, M. S. M. (2005). Competition and coexistence of aerobic ammonium- and nitrite-oxidizing bacteria at low oxygen concentrations. *Applied Microbiology and Biotechnology*, 68(6), 808–817. <https://doi.org/10.1007/s00253-005-1974-6>
- Tchobanoglus, G., Burton, F., & Stensel, H. D. (2003). Wastewater engineering: Treatment and reuse. *American Water Works Association. Journal; Denver*, 95(5), 201.
- Tooker, N. B., Barnard, J. L., Bott, C., Carson, K., Dombrowski, P., Dunlap, P., ... Phillips, H. (2016). Side-Stream Enhanced Biological Phosphorus Removal as a Sustainable and Stable Approach for Removing Phosphorus from Wastewater. *WEF/IWA Nutrient Removal and Recovery*.
- Tsuneda, S., Ohno, T., Soejima, K., & Hirata, A. (2006). Simultaneous nitrogen and phosphorus removal using denitrifying phosphate-accumulating organisms in a sequencing batch reactor. *Biochemical Engineering Journal*, 27(3), 191–196. <https://doi.org/10.1016/j.bej.2005.07.004>
- van Kessel, M. A. H. J., Speth, D. R., Albertsen, M., Nielsen, P. H., Op den Camp, H. J. M., Kartal, B., ... Lücker, S. (2015a). Complete nitrification by a single microorganism. *Nature*, 528(7583), 555–559. <https://doi.org/10.1038/nature16459>

- van Kessel, M. A. H. J., Speth, D. R., Albertsen, M., Nielsen, P. H., Op den Camp, H. J. M., Kartal, B., ... Lücker, S. (2015b). Complete nitrification by a single microorganism. *Nature*, 528(7583), 555–559. <https://doi.org/10.1038/nature16459>
- van Loosdrecht, M. C. M., Pot, M. A., & Heijnen, J. J. (1997). Importance of bacterial storage polymers in bioprocesses. *Water Science and Technology*, 35(1), 41–47. <https://doi.org/10.2166/wst.1997.0008>
- Vlaeminck, S. E., Clippeleir, H. D., & Verstraete, W. (2012). Microbial resource management of one-stage partial nitritation/anammox. *Microbial Biotechnology*, 5(3), 433–448. <https://doi.org/10.1111/j.1751-7915.2012.00341.x>
- Vollertsen, J., Petersen, G., & Borregaard, V. R. (2006). Hydrolysis and fermentation of activated sludge to enhance biological phosphorus removal. *Water Science and Technology*, 53(12), 55–64. <https://doi.org/10.2166/wst.2006.406>
- Wang, Q., Ye, L., Jiang, G., Hu, S., & Yuan, Z. (2014). Side-stream sludge treatment using free nitrous acid selectively eliminates nitrite oxidizing bacteria and achieves the nitrite pathway. *Water Research*, 55, 245–255. <https://doi.org/10.1016/j.watres.2014.02.029>
- Welker, S., Horn, H., & Lackner, S. (2016). Substrate Contentment: Influence of Residual Ammonium and Dissolved Oxygen Concentrations on Autotrophic Nitrogen Removal. *Proceedings of WEF/IWA Nutrient Removal and Recovery, Denver, USA*.
- Wett, B., Podmirseg, S. M., Gómez-Brandón, M., Hell, M., Nyhuis, G., Bott, C., & Murthy, S. (2015). Expanding DEMON Sidestream Deammonification Technology Towards Mainstream Application. *Water Environment Research*, 87(12), 2084–2089. <https://doi.org/10.2175/106143015X14362865227319>
- Winkler, M.-K. H., Kleerebezem, R., & van Loosdrecht, M. C. M. (2012). Integration of anammox into the aerobic granular sludge process for main stream wastewater treatment at ambient temperatures. *Water Research*, 46(1), 136–144. <https://doi.org/10.1016/j.watres.2011.10.034>
- Zeng, W., Li, B., Wang, X., Bai, X., & Peng, Y. (2014). Integration of denitrifying phosphorus removal via nitrite pathway, simultaneous nitritation–denitritation and anammox treating carbon-limited municipal sewage. *Bioresource Technology*, 172, 356–364. <https://doi.org/10.1016/j.biortech.2014.09.061>

CHAPTER 3: STARTUP OF A FULL-SCALE PARTIAL NITRITATION-ANAMMOX MBBR FOR SIDESTREAM NITROGEN REMOVAL AND THE DEVELOPMENT OF A NOVEL CONTROL SYSTEM

Stephanie Klaus, Rick Baumler, Bob Rutherford, Glenn Thesing, Hong Zhao, Charles Bott

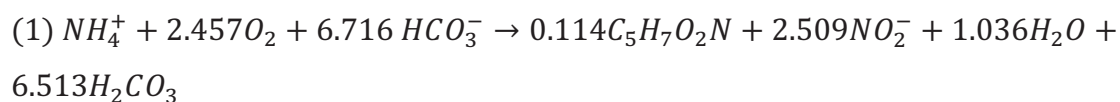
ABSTRACT

The single-stage deammonification moving bed biofilm reactor (MBBR) is a process for treating high strength nitrogen waste streams. In this process, partial nitrification and anaerobic ammonia oxidation (anammox) occur simultaneously within a biofilm attached to plastic carriers. An existing tank at the James River Treatment Plant (76 ML/d) in Newport News, Virginia was modified to install a sidestream deammonification MBBR process. This was the second sidestream deammonification process in North America and the first MBBR type installation. After 4 months the process achieved greater than 85% ammonia removal at the design loading rate of $2.4 \text{ g NH}_4^+/\text{m}^2\cdot\text{d}$ ($256 \text{ kg NH}_4^+/\text{d}$) signaling the end of startup. Based on observations during startup and process optimization phases, a novel pH-based control system was developed that maximizes ammonium removal and results in stable aeration and effluent alkalinity.

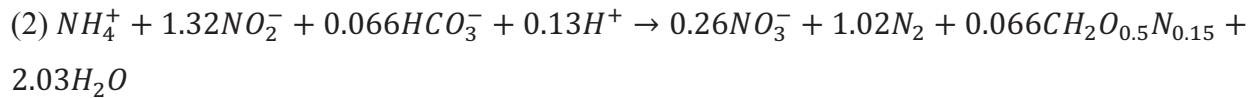
INTRODUCTION

Centrate from dewatered anaerobically digested solids can comprise 15 to 25% of the total incoming nitrogen load for a water resource recovery facility, but only represents about 1% of the total incoming flow. By treating the centrate in a sidestream system, the facility can reduce the nitrogen load on the mainstream process and, by doing so, provide more cost-effective and more efficient overall nitrogen removal (Jetten et al., 2001). The combination of partial nitrification and anaerobic ammonia oxidation (anammox), commonly known as deammonification, is an economical option for sidestream treatment because of decreased aeration energy requirements, no required external carbon or alkalinity, and decreased sludge production over traditional nitrification/denitrification (Ahn, 2006).

In the first step of deammonification, aerobic ammonium oxidizing bacteria (AOB) convert approximately 57% of the incoming ammonia to nitrite according to equation 1 (Grady et al., 2011).



In the second step, anaerobic ammonium oxidizing bacteria (AMX) convert the remaining ammonium and nitrite to nitrogen gas and a small amount of nitrate according to equation 2 (Strous et al., 1998).



The deammonification reaction requires a net consumption of alkalinity (inorganic carbon). There are two components to the inorganic carbon (IC) demand for deammonification: production/consumption of hydrogen ions by AOB/AMX and incorporation of IC into the biomass of AOB and AMX. pH in a sidestream deammonification reactor is mainly governed by alkalinity consumption by AOB, which is a function of aeration intensity or aerobic fraction. Another factor influencing pH is CO₂ stripping due to aeration. Ammonium oxidizing bacteria consume alkalinity, while AMX produce a small amount for a net consumption of approximately 4.0 g CaCO₃/g NH₄⁺ removed (theoretical according to stoichiometry of eqs 1 and 2). Nitrite oxidizing bacteria (NOB) (if present) do not significantly contribute to alkalinity requirements. Centrate/filtrate has a theoretical alkalinity to ammonia ratio of 3.57 CaCO₃/NH₄⁺-N (based on an assumed 1:1 molar ratio of HCO₃⁻:NH₄⁺ coming out of the digester) (Metcalf and Eddy, 2014). The alkalinity/NH₄⁺-N ratio in the centrate dictates the percentage of NH₄⁺ that can be removed without the addition of supplemental alkalinity.

Deammonification can take place in a single reactor or in two separate reactors. In a two-reactor configuration, partial nitrification occurs in an aerobic reactor followed by anammox occurring in an anoxic reactor (Van Dongen et al., 2001). A number of full-scale single reactor configurations are in operation including upflow granular sludge reactors (Abma et al., 2007), moving bed biofilm reactors (MBBRs) (Christensson et al., 2013; Rosenwinkel and Cornelius 2005), and sequencing batch reactor with an AMX selection device (Wett, 2007). In a deammonification MBBR, the conversion of ammonium takes place in the biofilm attached to the plastic media in which AOB exist on the exterior of the biofilm, while AMX exist deeper within the biofilm in an anoxic environment. This process is also characterized by temperatures of 25 to 35 °C, continuous flow, continuous aeration, and a hydraulic retention time (HRT) of approximately 24 hours (Lackner et al., 2014).

The biggest concern during startup of a deammonification MBBR is AMX inhibition by nitrite because AMX cannot initially consume all of the nitrite being produced by AOB. While AMX

appear to be inhibited by the nitrite ion itself, AOB and NOB are susceptible to inhibition by nitrous acid (HNO_2) (Lotti et al., 2012; Strous et al., 1999). Once the AMX capacity is equal to or greater than AOB activity, the limiting factor becomes IC limitation of AOB (Wett and Rauch, 2003). In order to maintain a stable pH and avoid alkalinity limitation an aeration control strategy that takes into account alkalinity is critical. Meeting these operating requirements necessitates utilizing an automatic control system to make continuous process adjustments in order to ensure process reliability. For various deammonification reactor configurations there exists a need for reliable control systems that meet the above objectives, utilize robust sensors, and minimize operator input.

NOB repression is key to deammonification systems because NOB compete with AMX for substrate and space within the biofilm. If all of the nitrate production in the reactor is due to AMX activity, then the nitrate production ratio (eq 4) will be around 11% based on stoichiometry (eq 2). If the nitrate production ratio is any higher than 11%, then it can be assumed that the excess nitrate production is due to NOB activity. Strategies for NOB repression in sidestream systems include high free ammonia (FA) concentration (Anthonisen et al., 1976), low dissolved oxygen concentration (Wiesmann, 1994), high temperature (Hellings et al., 1998), and transient anoxia (Kornaros et al., 2010).

pH-based aeration control is the basis for the DEMON® process, an intermittently aerated deammonification sequencing batch reactor (SBR) in which the length of the aerated and non-aerated phases is controlled by a low and high pH setpoint (Wett, 2007). This process takes advantage of the high accuracy of pH sensors to control within a 0.05 fluctuation in pH based on alkalinity consumption during the aerobic phase and alkalinity production during the anoxic phase. A typical value for the low pH setpoint is 6.8 (Lackner et al., 2014). A deammonification MBBR process can be operated with intermittent aeration (Ling, 2009; Zubrowska-Sudol et al., 2011); however, continuous aeration is preferred due to simplicity of operation, more accurate readings of online signals, and elimination of the need for mechanical mixing during non-aerated phases. Continuous aeration also reduces nitrous oxide (N_2O) emissions (Christensson et al., 2013)

Another control method for a deammonification MBBR described in Christensson et al. (2013) relies on ammonia removal ratio (eq 3) and nitrate production ratio (eq 4) in the reactor to adjust continuous aeration.

$$NH_4^+ \text{ removal} = \frac{EQ \text{ } NH_4^+ - \text{Reactor } NH_4^+}{EQ \text{ } NH_4^+} \times 100 \quad (3)$$

$$NO_3^- \text{ production} = \frac{\text{Reactor } NO_3^-}{EQ \text{ } NH_4^+ - \text{Reactor } NH_4^+} \times 100 \quad (4)$$

The ratios are calculated from online sensor values and the dissolved oxygen (DO) set-point is incrementally increased or decreased to maintain optimum operating conditions. The optimal operating condition is for the ammonia removal to be in the range of 80 to 90% and for nitrate production to be below 12%.

There are a few publications on operation of full-scale deammonification MBBR systems (Christensson et al., 2013; Lackner et al., 2014; Rosenwinkel and Cornelius, 2005) but none give detailed information on optimization of controls. While it is recognized that pH-based aeration control is essential for operating the DEMON® process (Wett, 2007), this is the first full-scale deammonification MBBR to be operated with pH-based aeration control. The objective of this paper is to demonstrate that pH-based aeration control optimizes performance in a sidestream deammonification MBBR and to provide detailed information on startup strategy.

METHODS AND MATERIALS

Deammonification MBBR Installation. The James River Treatment Plant is a 76 ML/d facility located in Newport News, Virginia. Anaerobically digested waste activated sludge and primary sludge was dewatered using centrifuges and the centrate was sent to an equalization basin. An existing below-grade tank was modified for the installation of the sidestream deammonification MBBR (ANITA™ Mox, Kruger Inc., Cary, North Carolina). Centrate was pumped from the equalization basin to the deammonification MBBR for treatment and the effluent was recycled back into the primary clarifiers. Airflow rate to the reactor was controlled and measured by a modulating, motor-actuated control valve. Mechanical mixers kept the media in suspension and the tank completely mixed during periods of non-aeration. Centrate pump speed was controlled by a variable frequency drive and was measured by a flow meter to meet a flow setpoint ranging from 75 to 250 L/min. Two deep-tank electric immersion heaters were used during startup to maintain the tank temperature at 30 °C. A blend of trace metals was added based on micronutrient requirements for bacterial growth (Grady et al., 2011) to prevent micronutrient

deficiencies in both AOB and AMX populations.

Instrumentation and Control. Online sensors from YSI Inc. (Yellow Springs, Ohio) were used to monitor NH_4^+ , NO_3^- , pH, DO, specific conductivity, and temperature in the deammonification MBBR. NH_4^+ and temperature were also monitored in the equalization basin. Ion selective electrode (ISE) probes were used to monitor NH_4^+ and NO_3^- and included an additional sensor for potassium correction of NH_4^+ .

There were three aeration control modes available: Fixed DO control, ammonia-based floating DO control, and pH-based control. Airflow rate to the deammonification MBBR was controlled and measured by a modulating, motor-actuated control valve. The valve receives a command from the Distributed Control System (DCS) and sends a position signal in return. Airflow can be either operated continuously or intermittently. In both continuous airflow mode and intermittent control mode, the airflow can be controlled to meet an airflow setpoint (measured by a flow meter upstream of the valve) or to meet a DO setpoint (measured by a process probe). A low pH setpoint ranging from 6.3 to 6.6 was programmed to safeguard against running out of alkalinity in the deammonification reactor. When the low pH setpoint was reached, the airflow shut off while centrate feed continued to allow the system to recover. In fixed DO control mode cascading proportional integral derivative (PID) control was used to control airflow to the reactor based on a DO setpoint and then valve position was PID controlled based on the airflow setpoint. In ammonia-based floating DO control, the DO setpoint was adjusted to keep ammonia removal and nitrate production ratios within optimum ranges (Christensson et al., 2013). In pH-base aeration control the DO or airflow setpoint was adjusted to meet a pH setpoint.

Bench-Scale Activity Tests. Bench-scale maximum activity tests were performed on a biweekly basis on the seed media, new media, and bulk liquid individually to monitor AMX, AOB, and NOB activity. One liter of seed media and one liter of new media were collected from the deammonification MBBR for each test. Ammonium oxidizing bacteria and NOB activity was measured under aerobic conditions for the seed and new media while AMX activity was measured under anoxic conditions. The bulk liquid test was only performed under aerobic conditions because it was assumed the amount of AMX activity in the bulk was negligible. Temperature was controlled to match the temperature in the full-scale reactor. Dissolved oxygen

was monitored and manually controlled to above 4 mg/L in the aerobic sample to ensure that oxygen was not a limiting factor. For the anoxic test, the reactor was sparged with nitrogen gas to remove as much oxygen as possible and covered with a Styrofoam lid. The nitrogen gas contained 380 ppm (atmospheric concentration) carbon dioxide to prevent a drastic increase in pH. pH was monitored and manually controlled using NaOH and CO₂ to stay within the range of 6.5 to 7.5. Samples were taken at 5- to 30-minute intervals for 5 to 7 samples and analyzed for NH₄⁺, NO₃⁻, and NO₂⁻. Ammonium oxidizing bacteria rates were determined from NO_x production, NOB from NO₃⁻ production, and AMX from both NH₄⁺ and NO₂⁻ consumption. NO₂⁻/NH₄⁺ and NO₃⁻/NH₄⁺ ratios were calculated for the AMX rate experiments to be compared to the stoichiometric values of 1.32 and 0.26, respectively (eq 2).

Biomass Concentration Measurements. The weight of the biomass per square meter of surface area was measured every 2 weeks for both the seed and new media. For this measurement, nine seed pieces and nine new pieces of media were selected at random from the tank. Media samples were dried at 105° C for 2 hours. The dried samples were weighed and the biomass removed by placing the carriers in a 25 mg/L disodium EDTA (ethylenediaminetetraacetic acid) solution and shaking vigorously. The carriers were then rinsed several times using tap water and then dried for more than 2 hours at 105° C. High-pressure tap water was then applied to each media individually to ensure that no dry biofilm remained. The difference in initial and final weight was used to calculate the biomass on the carriers.

Performance Monitoring. Samples for on-site monitoring were collected daily from the deammonification MBBR and equalization basin, immediately filtered through 0.45 micron filter membranes, and analyzed using HACH (Loveland, Colorado) TNT kits and a HACH DR-2800 spectrophotometer. The equalization basin samples were analyzed on-site for NH₄⁺ only as NO₃⁻ and NO₂⁻ were assumed to be close to zero. Samples from the deammonification MBBR were analyzed on-site for NH₄⁺, NO₃⁻, and NO₂⁻. NH₄⁺ and NO₃⁻ values were used to calibrate the ISE probes as necessary. Grab samples from the two locations were also analyzed off-site for the following parameters using standard methods: Total Kjeldahl Nitrogen (TKN), total suspended solids (TSS), volatile suspended solids (VSS), chemical oxygen demand (COD), soluble chemical oxygen demand (sCOD), total phosphorus (TP), orthophosphate (OP), and alkalinity.

RESULTS AND DISCUSSION

Startup Summary. Design parameters (Table 3.1) were based on the average influent (centrate) characteristics shown in Table 3.2. The design flow to the tank, based on centrate production was 284 m³/d. The total volume of the tank was approximately 393 m³ for an HRT of 33 hours at the design flow rate. Because this installation was a retrofit, the HRT was determined by the volume of the existing tank. The expected NH₄⁺ removal was 204 kg N/d based on 80% removal at the design loading rate of 256 kg N/d. To achieve this removal, 133 m³ of media was required in the deammonification reactor, which equated to a fill percentage of 32.2%, 10% of which was pre-colonized (seed) media from an established sidestream deammonification MBBR process in Sjölanda Wastewater Treatment Plant (WWTP), Malmö, Sweden. The percentage of seed media was based on previous startups that have used anywhere in the range of 2 to 15% (Christensson et al., 2013). Seeding with 10% pre-colonized media from the Sjölanda WWTP was chosen to reduce startup time of the deammonification reactor. There are contradicting views on the importance of seeding reactors during startup. According to Christensson et al. (2013) and Lemaire et al. (2011), seeding decreases startup time, while Kandars et al. (2014) and Ling (2009) argue that seeding is not necessary. Regardless of seeding influence on startup time, seeding provides the benefit of immediate nitrite consumption by AMX, which allows for a higher initial ammonia load and reduced risk of nitrite inhibition (Kandars et al., 2014).

Table 3.1: Design parameters.

Parameter	Units	Value
Centrate flow	m ³ /d	284
Centrate NH ₄ ⁺ load	kg N/d	256
Expected NH ₄ ⁺ removal (80%)	kg N/d	204
Tank volume	m ³	393
Total media fill	%	32.2%
Seed media	%	10%
Design NH ₄ ⁺ surface area load	g N/m ² ·d	2.37
Design NH ₄ ⁺ volumetric load	kg N/m ³ ·d	0.64

Table 3.2: Average influent characteristics.

Parameter	Units	Value
NH ₄ ⁺ -N	mg NH ₄ ⁺ -N/L	890 ± 89
Alkalinity	mg CaCO ₃ /L	3400 ± 287
Alk/NH ₄ ⁺ -N	mg CaCO ₃ /mg NH ₄ ⁺ -N	3.83 ± 0.14
COD	mg COD/L	407 ± 74
sCOD	mg COD/L	283 ± 65

Startup of the deammonification MBBR was limited by AMX due to their slow growth rate and sensitivity to nitrite. The objective of the startup was to reach the design ammonia loading rate as quickly as possible without allowing ammonia, pH, or nitrite to reach inhibitory levels.

Therefore, to achieve faster startup, the process must be closely monitored for ammonia, nitrite, nitrate, and pH. Additionally, aeration and ammonia loading, the main control variables, must be monitored. Aeration in the deammonification MBBR can be either continuous or intermittent.

Intermittent aeration is typically utilized during startup, transitioning to continuous aeration for long-term operation. This is because during startup AMX rates are too low to meet loading provided by continuous feed, however once anammox activity rates increase, the system can transition to continuous feed. Typical DO values range from 0.5 to 1.5 mg/L (Christensson et al., 2013). Because ammonia concentrations in the centrate were dependent on digester performance, the only way to control ammonia loading was through the influent flow rate.

During startup, nitrite was controlled below 40 mg NO₂-N/L using intermittent aeration. There is a large amount of variation in reported inhibitory concentrations of nitrite to anammox ranging from 30 to 50 mg NO₂-N/L reported by Fux et al. (2004) to 275 mg NO₂-N/L reported by Kimura et al. (2010). The goal was to maintain alkalinity above 150 mg CaCO₃/L; however, because alkalinity data were collected on a weekly basis, alkalinity would sometimes drop as low as 80 mg CaCO₃/L causing suspected limitations for AOB. One hundred fifty milligrams of CaCO₃/L corresponded to an approximate effluent NH₄⁺-N concentration of 50 to 100 mg/L, which was desirable to prevent substrate limitation to both AOB and AMX. During startup, NH₄⁺ loading to the deammonification reactor was controlled to keep the NH₄⁺ concentration below 350 mg NH₄⁺-N/L to prevent inhibition by FA. At an ammonium concentration of 300 mg NH₄⁺-N/L, pH of 8.0 and temperature of 30 °C, the FA concentration was 25 mg NH₃-N/L. Anthonisen

et al. (1976) demonstrated that AOB were inhibited by FA concentrations in the range of 10 to 150 mg NH₃-N/L while NOB were inhibited at a range of 0.1 to 1 mg NH₃-N/L. Although high pH and ammonia concentrations are undesirable for optimal reactor performance, these conditions provide an effective strategy for temporarily controlling NOB proliferation though NOB adaptation to FA has been reported (Turk and Mavinic 1989; Wong-Chong and Loehr 1978). It is known that AOB are inhibited at a pH around 6.3 however the IC concentration will most likely be the limiting factor so the recommended pH setpoint is in the range of 6.6 to 6.8 (Wett and Rauch, 2003).

Performance During Startup. The deammonification reactor performance for 241 days in terms ammonium and total inorganic nitrogen (TIN) removal, temperature, effluent nitrite concentration and nitrate production ratio are shown in Figure 3.1.

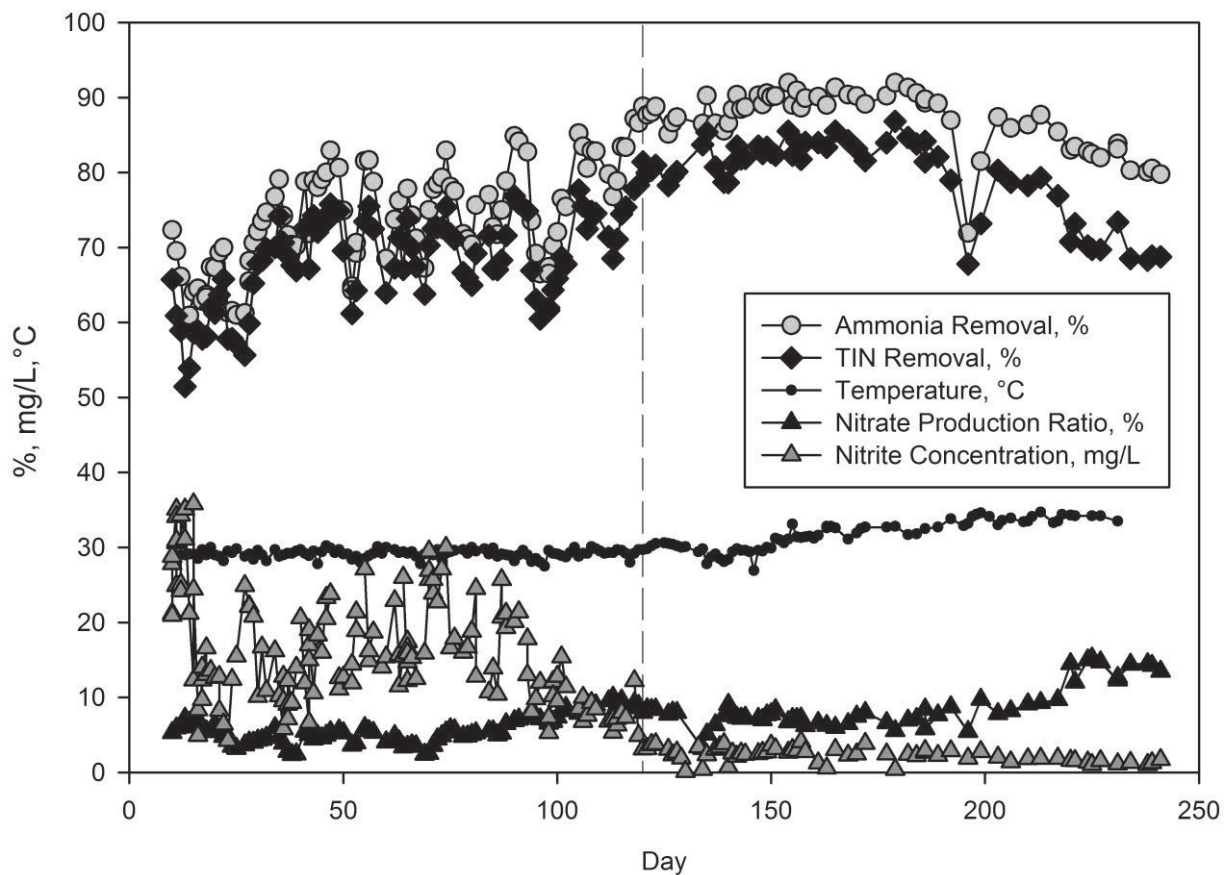


Figure 3.1: Ammonium and TIN removal percentages, temperature, nitrite in effluent, and nitrate production ratio. Vertical line indicates end of startup on Day 120.

Startup was considered complete after 120 days when the reactor was treating all of the available centrate at the design loading rate. For the first week following seeding, the influent centrate was fed intermittently and then transitioned to continuous feed. An immediate reduction in ammonia of above 60% was realized resulting from AMX activity on the seed media. During the 120 days of startup, the ammonia loading rate was limited by AMX activity and was gradually increased as ammonia and nitrite removal increased (Figure 3.2).

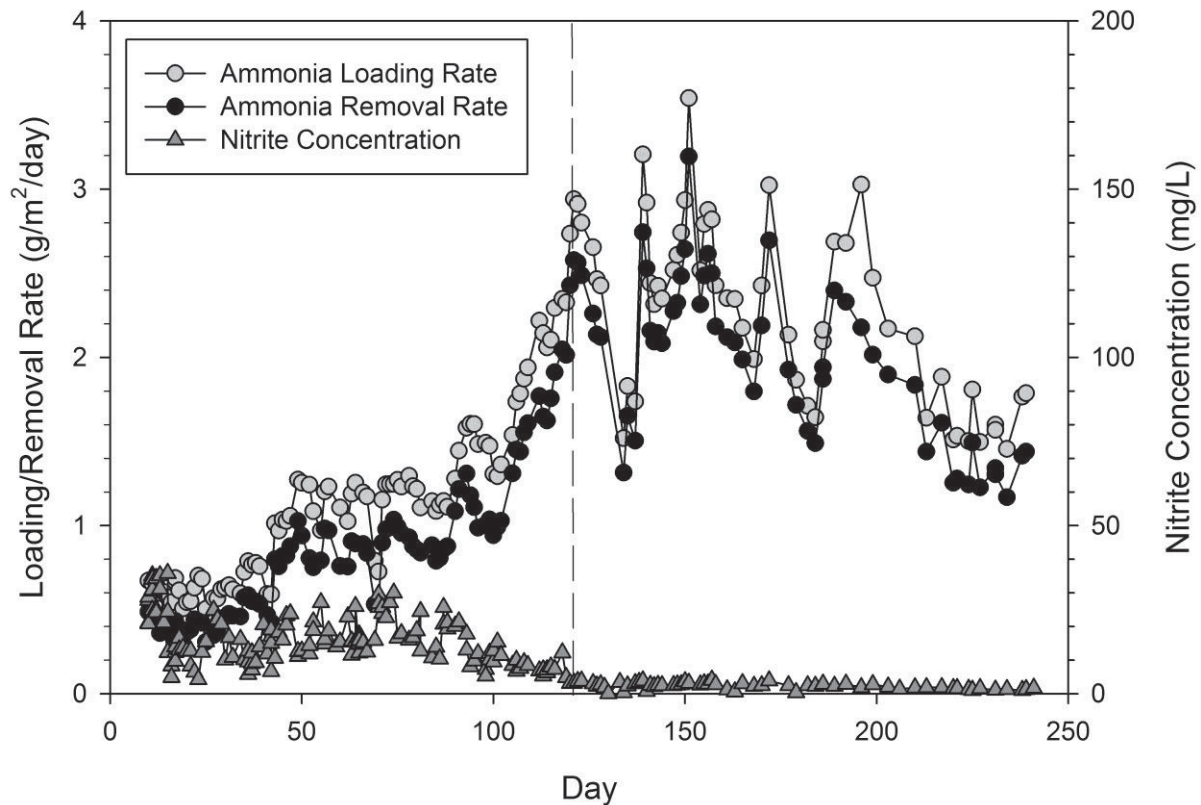


Figure 3.2: Ammonium loading, ammonium removal, and nitrite concentrations in the effluent. Vertical line indicates end of startup on Day 120.

For the first 2 months during startup, the aeration control strategy was intermittent aeration using either an airflow or DO setpoint. This encouraged the growth of AMX by providing a distinct anoxic period and gave more control over the production of nitrite. During intermittent DO control the setpoint ranged from 1.0 to 1.3 mg/L. As AMX activity in the reactor increased, the length of the anoxic period was gradually reduced from 100 to 30 minutes with the intent of transitioning to continuous aeration. During the first 2 months of startup, biomass concentration measurements and visual inspection of the media indicated that a large amount of biomass had been sheared off of the seed media (Figure 3.3B compared to Figure 3.3A) and activity measurements indicated that there was no AMX activity on the new carriers (Figure 3.4). This may have been due in part to high shear forces from the mechanical mixers used during anoxic

periods. For about 25% of the seed media (based on visual inspection), the AMX biomass was sheared almost completely off the media (Figure 3.3C). Soon after the aeration control strategy was switched from intermittent to continuous, biomass on the media increased and AMX was detected on the new carriers (Figure 3.3F). During startup, NO_2^- -N levels were as high as 35 mg/L and then stayed below 3 mg/L after startup was complete (Figure 3.1). NH_4^+ removal ranged from 60 to 85% and TIN removal ranged from 50 to 80% (Figure 3.1).

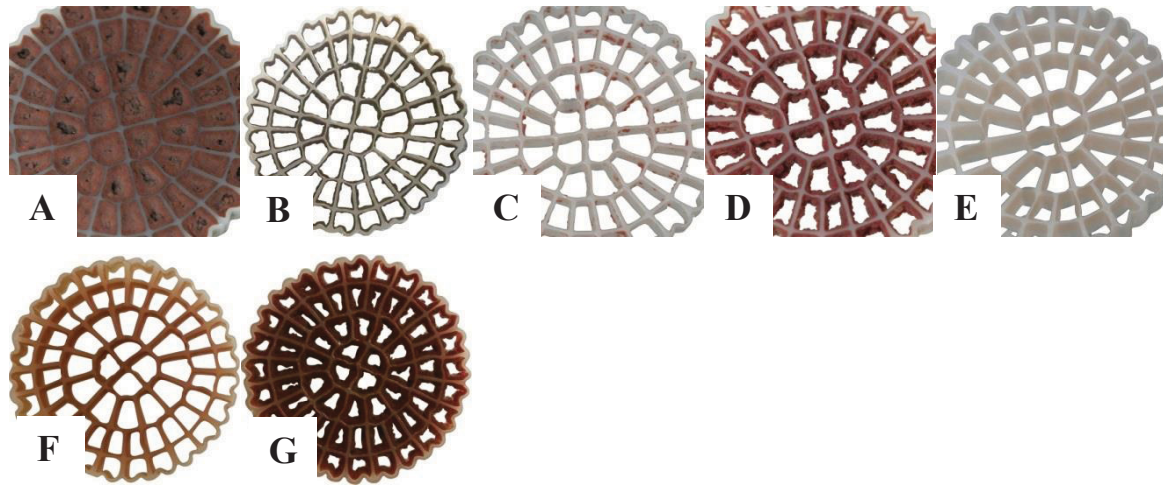


Figure 3.3: Biofilm development photos: (A) original seed media prior to placement in reactor; (B) seed media on Day 10; (C) sheared seed media on Day 64; (D) typical seed media on Day 64; (E) new media on Day 64; (F) new media after completion of startup on Day 120; (G) seed media after completion of startup on Day 120.

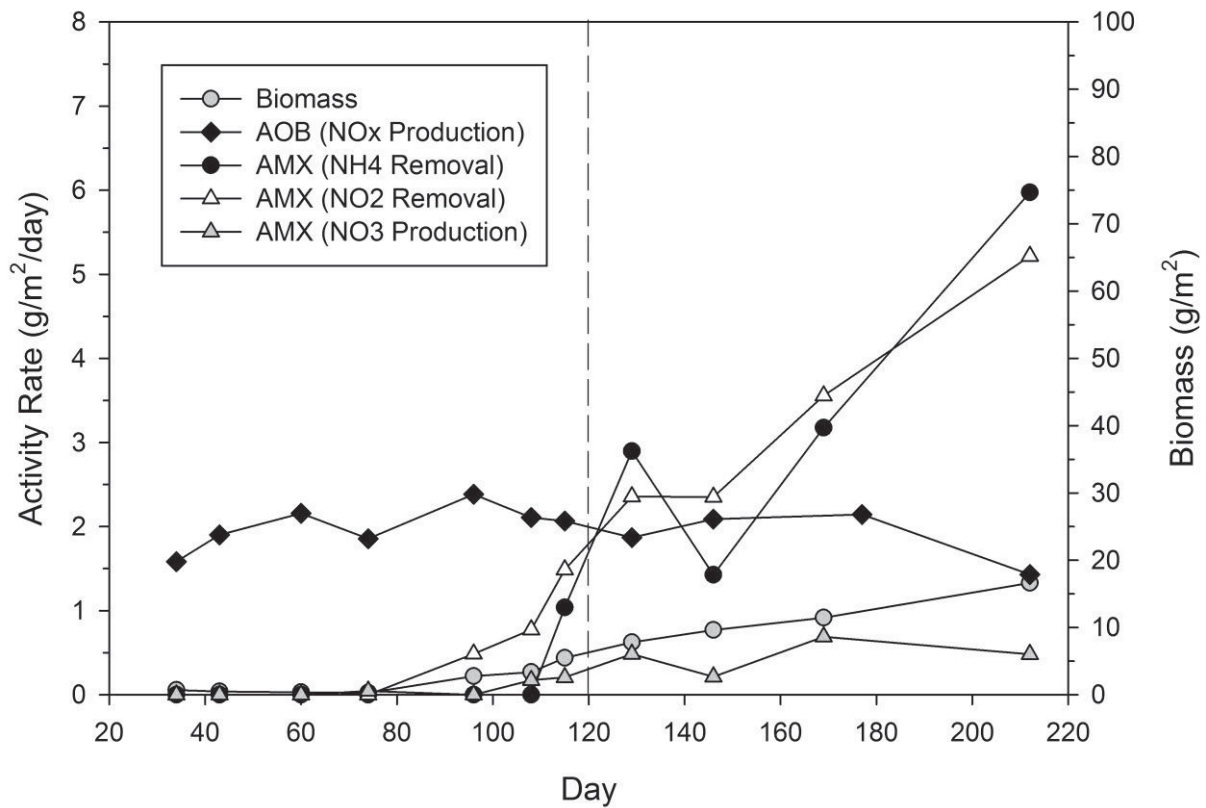


Figure 3.4: Bench-scale new media activity rates. Vertical line indicates end of startup on Day 120.

Activity Tests. Bench-scale activity tests were used to monitor the progress of AMX development on the new and seed media throughout startup as well as determine the presence of NOB in the deammonification MBBR. Results of the activity tests are shown in Figure 3.4 and Figure 3.5. Initially, the AMX rates and biomass density on the seed media were low due to shearing of the biofilm upon placement in the reactor as discussed previously (Figure 3.5). Ammonium oxidizing bacteria activity was first detected on the new media 93 days after seeding (Figure 3.4) as indicated by anoxic nitrite consumption.

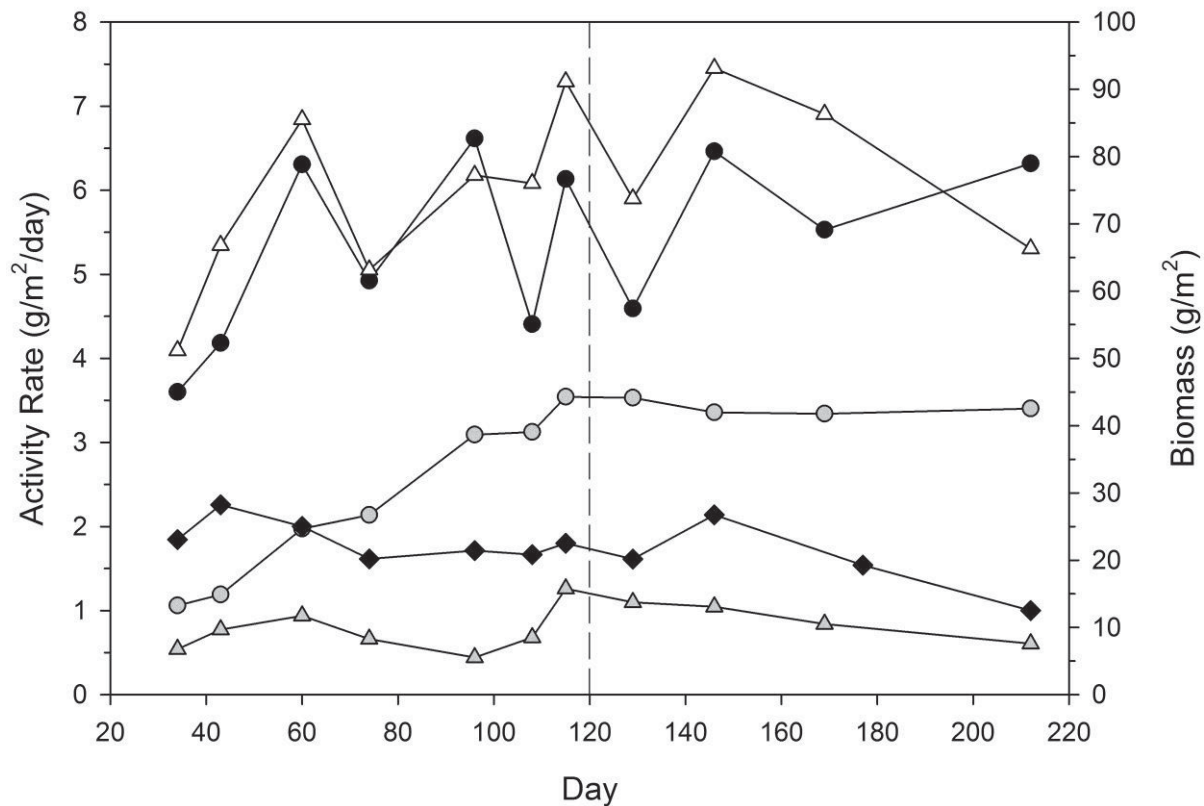


Figure 3.5: Bench-scale seed media activity rates. Vertical line indicates end of startup on Day 120.

On Day 114, anoxic ammonia consumption was detected in addition to nitrite consumption in a ratio indicative of AMX stoichiometry (equation 2). Throughout startup, no NOB activity was detected on the new or seed media. Ammonium oxidizing bacteria activity remained fairly constant on both the new and seed media. According to AMX stoichiometry (equation 2), for every one mole of NH_4^+ consumed, 1.32 mole of NO_2^- is consumed and 0.26 mol of NO_3^- is produced. The new media AMX ratios for $\text{NO}_2^-/\text{NH}_4^+$ and $\text{NO}_3^-/\text{NH}_4^+$ were 1.17 ± 0.37 and 0.16 ± 0.03 , respectively. The seed media AMX ratios for $\text{NO}_2^-/\text{NH}_4^+$ and $\text{NO}_3^-/\text{NH}_4^+$ were 1.14 ± 0.13 and 0.15 ± 0.05 , respectively. The ratios in the activity tests were lower than the stoichiometric ratios most likely due to heterotrophic denitrification, as was evident in the full-scale deammonification MBBR by NO_3^- production ratios less than 11% (Figure 3.1).

It should be noted that as the biofilm became thicker on both the seed and new media, it became increasingly difficult to inhibit AMX activity during the aerobic activity tests. Even at DO concentrations above 6 mg/L, the biofilm thickness limited diffusion of oxygen into the inner layers of the biofilm, thus never completely inhibiting AMX activity. This was evident in the tests as NH_4^+ was being removed that did not end up as NO_x and could not be explained by assimilation. To compensate, the AOB rates were adjusted assuming no NOB activity, which is acceptable because there was no evidence of NOB activity in the full-scale reactor and the small

amount of nitrate produced in the bench scale tests could be explained by AMX. It was also assumed that all excess ammonia removal was due to AMX and so NO_x production by AOB was less than it appeared because NO_2^- was being consumed by AMX.

Performance After Startup. Four months (Day 120) after seeding the reactor, all of the available centrate was being treated at greater than 85% NH_4^+ removal at the design loading rate of $2.4 \text{ g N/m}^2 \cdot \text{d}$, signaling the end of startup (Figure 3.1 and Figure 3.2). After startup was complete, the ammonia loading to the reactor was determined by the centrate production and NH_4^+ concentration. The maximum removal rate was $3.5 \text{ g N/m}^2 \cdot \text{d}$ (Figure 3.2) and the maximum NH_4^+ removal was 92% (87% TIN removal). Similar deammonification processes have achieved 80 to 90% ammonia removal within 2 to 4 months at the design loading rate at three locations in Europe (Christensson et al., 2013). When comparing startup times from different water resource recovery facilities, it should be noted that startup time depends on the centrate production and ammonia concentration (i.e., loading rate) and this will vary from facility to facility. Once startup was complete, the goal became maximizing ammonia removal.

Following startup, it was observed that a constant dissolved oxygen setpoint did not protect against running out of alkalinity in the reactor, which resulted in sporadic and dramatic decreases in pH. A low pH setpoint (air shutoff) was set up to safeguard against running out of alkalinity. However, this scenario resulted in the air frequently switching on and off because the system did not naturally maintain a constant pH at a constant DO setpoint as shown in Figure 3.6. A similar observation was made at a pilot-scale demonstration in which the low pH air shutoff condition was repeatedly triggered as a result of aerating at a constant airflow (Hollowed et al. 2013). As a result of these observations, an aeration control method was added in which airflow was controlled by a constant pH setpoint.

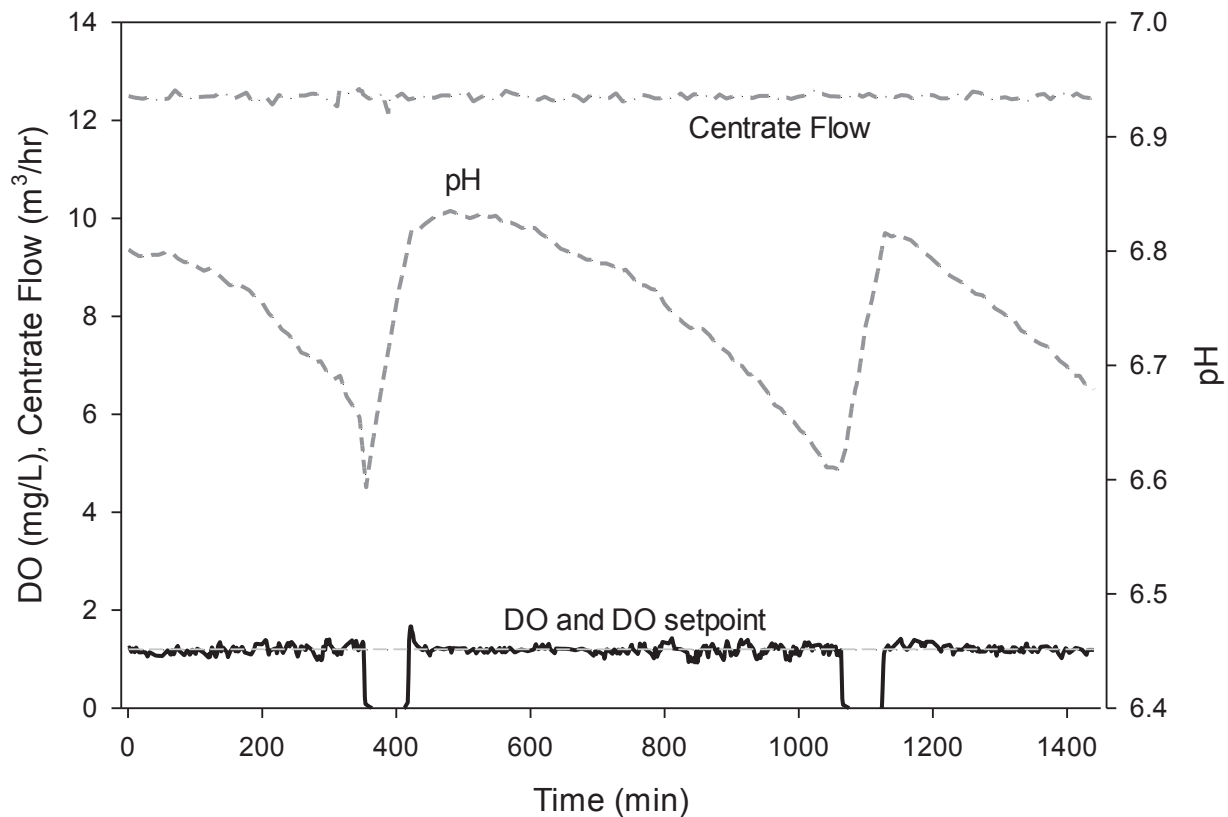


Figure 3.6: Example of fixed DO control leading to low pH shutoff. In this example, the airflow is programmed to shut off when the pH reaches 6.6 and come back on when pH reaches 6.8.

Wett and Rauch (2003) developed a model from full-scale sidestream nitrification data and found that nitrification rates started to slow below 400 mg CaCO_3/L and rates reached close to zero at 150 mg/L CaCO_3 . Guisasola et al. (2007) determined that AOB activities were limited at IC concentrations lower than 150 mg/L CaCO_3 , while NOB were not limited even at a concentration of 5 mg/L CaCO_3 . Chen et al. (2012) found that IC limitation of AOB and AMX occurred at 200 mg/L as CaCO_3 in a bench-scale deammonification reactor and that AOB activity was more affected than NOB activity. Kimura et al. (2011) concluded that AMX was affected by IC limitation at 5 mg CaCO_3/L and, therefore, more sensitive to IC limitation than NOB but not as much as AOB. A review of full-scale sidestream deammonification processes by Lackner et al. (2014) stated that alkalinity was not an important consideration; however, results from this study indicate that alkalinity is the most important consideration for long-term operation of a sidestream deammonification MBBR, which agrees with the work of Wett and Rauch (2003) and Wett (2007).

Comparison of Aeration Control Strategies. In the deammonification MBBR, the ammonium concentration in the effluent corresponded to a given pH and specific conductivity so the three signals can be used interchangeably. It was desirable to maintain a constant pH (i.e., ammonium

and specific conductivity) in the effluent to maintain near-complete use of influent alkalinity and the lowest possible ammonium concentration in the effluent. It is known that in order to maximize NH_4^+ removal in a sidestream deammonification process, it is necessary to maximize the utilization of available alkalinity (Wett, 2007). It was difficult to achieve this using DO control alone due to changes in influent ammonium concentration, alkalinity, and oxygen demand in the reactor. Although any of the three signals (pH, specific conductivity, and ammonia concentration) could have been used for aeration control, the pH signal was chosen because it was the most robust sensor (followed by specific conductivity and then ammonia), and it was the best indicator of residual alkalinity. Specific conductivity is an acceptable substitute for control as it is indicative of the alkalinity and ammonia concentration. The ammonia ISE probe is not as reliable and does not account for changes in alkalinity.

The airflow control valve could be controlled by an airflow or DO setpoint. In both of these methods, if the pH feedback was less than the pH setpoint (indicating that too much alkalinity was being consumed) the airflow decreased, and if the pH feedback was greater than the pH setpoint, the airflow or DO setpoint increased. The airflow control was accomplished with an appropriately tuned PID controller or logic-based algorithm. If NOB growth occurred, resulting in an increase in the effluent nitrate concentration, the pH setpoint was increased (decreasing the airflow rate) at the expense of ammonia removal until the nitrate production ratio was less than the value that would be expected to be produced by AMX alone (11%). Nitrate production typically increased over the course of days as opposed to hours. Although the pH setpoint adjustment could be automated based on nitrate production ratio, this calculation did not need to be made at the same frequency as DO setpoint.

By controlling aeration based on pH, the alkalinity consumed in the reactor was equal to the alkalinity in the influent, maintaining enough residual alkalinity to avoid IC limitation. pH-based aeration control maximized NH_4^+ removal and resulted in more consistent effluent characteristics (Figure 3.7) with less operator input than fixed DO control. Fixed DO control required that DO setpoint be manually adjusted to maximize ammonia removal and avoid alkalinity limitation. pH-control also maintained an NH_4^+ residual which prevents AOB or AMX activity limitations, and the subsequent induction of NOB growth. The main advantage of using pH-based DO control is that the controller will maintain a high NH_4^+ removal rate while protecting against running out of alkalinity even with changes in loading. Figure 3.7 demonstrates that over the course of 2 months, the controller was able to respond to disturbances caused by changes in centrate flow while maintaining an ammonia removal rate in the range of 83 to 92%.

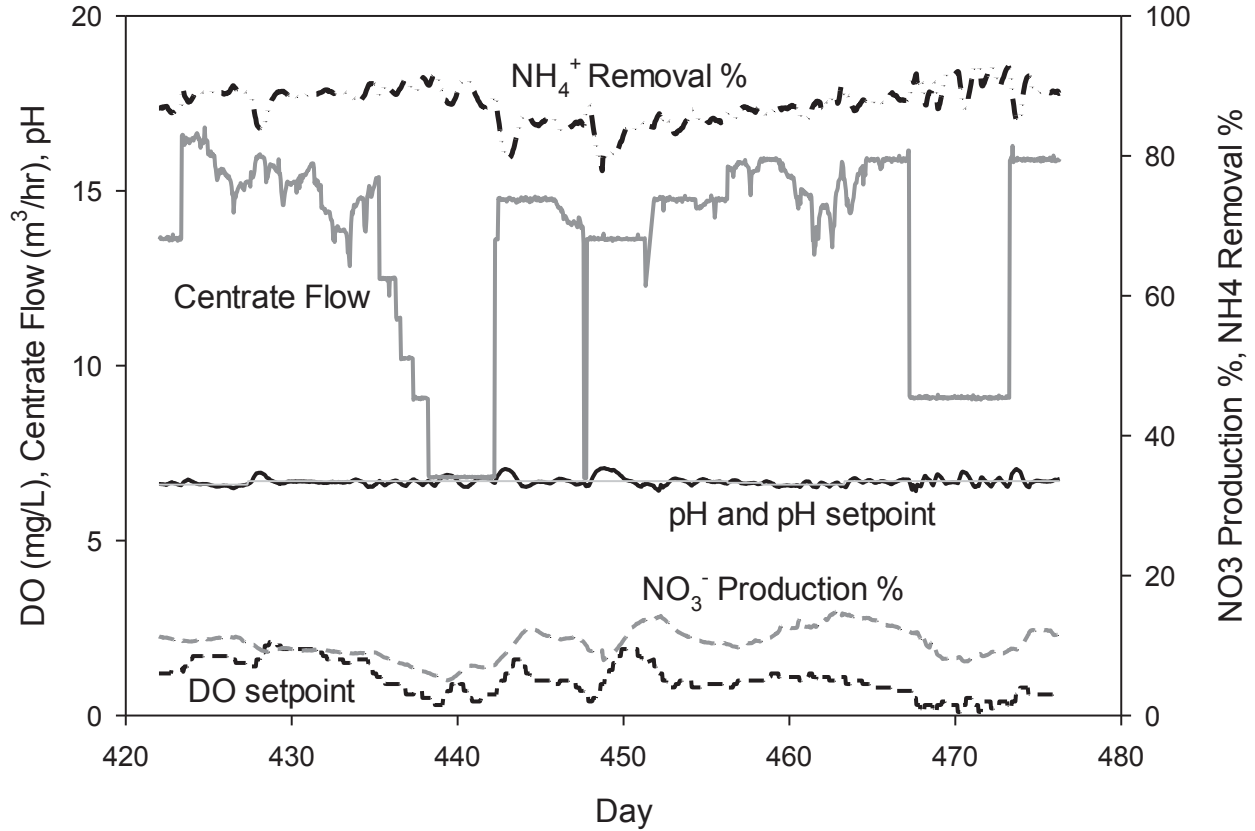


Figure 3.7: Performance of pH-based DO control.

As previously mentioned, DO control is required in order to prevent over-aeration, which inhibits AMX and encourages NOB growth. Floating ammonia-based aeration control maximizes ammonia removal but does not take into account residual alkalinity. pH-based aeration control maximizes ammonia removal and prevents alkalinity limitation using a robust and accurate sensor and is, therefore, the preferred aeration method for sidestream deammonification MBBRs. These observations are summarized in Table 3.3.

Table 3.3: Comparison of aeration control strategies.

	Prevents over-aeration?	Maximizes ammonia removal?	Prevents running out of alkalinity?
Air flow control	no	no	no
Fixed DO control	yes	no	no
Ammonia-based floating DO control	yes	yes	no
pH-based aeration control (airflow or DO)	yes	yes	yes

CONCLUSIONS

The objective of this study was to demonstrate that pH-based aeration control optimizes performance in a sidestream deammonification MBBR and to provide detailed information on startup strategy. The system reached full design capacity after four months and was consistently achieving 80 to 90% NH_4^+ removal at the design loading rate $2.4 \text{ g NH}_4^+\text{-N/m}^2\cdot\text{d}$. Anammox bacteria were not detected on the new media in bench-scale testing until 120 days after seeding and no NOB activity was detected during startup. Upset periods have occurred since startup and all were characterized by a short-term increase in nitrate production and NOB activity, and resulted in a period of decreased NH_4^+ removal, until corrective action could be taken. Startup time could potentially have been shorter if continuous aeration had been used earlier by reducing shear in the reactor that resulted from mechanical mixing. pH-based aeration control proved to be an effective, simple, and stable method that was preferred over DO-based aeration control. pH-based control is crucial in a sidestream deammonification MBBR to maximize ammonia removal while protecting against alkalinity (IC) limitations.

REFERENCES

- Abma, W. R.; Schultz, C. E.; Mulder, J. W.; Van der Star, W. R. L.; Strous, M.; Tokutomi, T.; Van Loosdrecht, M. C. M. (2007) Full-Scale Granular Sludge Anammox Process. *Water Sci. Technol.*, **55** (8-9), 27–33.
- Ahn, Y. Sustainable Nitrogen Elimination Biotechnologies: A Review. (2006) *Process Biochem.*, **41** (8), 1709–1721.
- Anthonisen, A. C.; Loehr, R. C.; Prakasam, T. B. S.; Srinath, E. G. (1976) Inhibition of Nitrification by Ammonia and Nitrous Acid. *J. Water Pollut. Control Fed.*, **48** (5), 835–852.
- Chen, Y.; Li, S.; Fang, F.; Guo, J.; Zhang, Q.; Gao, X. (2012) Effect of Inorganic Carbon on the Completely Autotrophic Nitrogen Removal Over Nitrite (CANON) Process in a Sequencing Batch Biofilm Reactor. *Environ. Tech.*, **33** (23), 2611–2617.
- Christensson, M.; Ekström, S.; Andersson Chan, A.; Le Vaillant, E.; Lemaire, R. (2013) Experience from Start-Ups of the First ANITA Mox Plants. *Water Sci. Technol.*, **67** (12), 2677–2684.
- Fux, C.; Marchesi, V.; Brunner, I.; Siegrist, H. (2004) Anaerobic Ammonium Oxidation of Ammonium-Rich Waste Streams in Fixed-Bed Reactors. *Water Sci. Technol.*, **49** (11-12), 77–82.
- Grady, C.; Daigger, G.; Love, N.; Filipe, C. (2011). *Biological Wastewater Treatment*; IWA Publishing: Boca Raton, Florida.
- Guisasola, A.; Petzet, S.; Baeza, J. A.; Carrera, J.; Lafuente, J. (2007) Inorganic Carbon Limitations on Nitrification: Experimental Assessment and Modelling. *Water Res.*, **41** (2), 277–286.

- Hellinga, C.; Schellen, A.; Mulder, J. W.; van Loosdrecht, M. C. M.; Heijnen, J. J. (1998) The SHARON Process: an Innovative Method for Nitrogen Removal from Ammonium-Rich Waste Water. *Water Sci. Technol.*, **37** (9), 135–142.
- Hollowed, M.; Stec-Uddin, E.; Zhao, H.; McQuarrie, J. (2013) Evaluation of the Anita-Mox Moving Bed Biofilm Reactor Process for Sidestream Deammonification at the Robert W. Hite Treatment Facility, Denver Colorado. *Proc. Water Environ. Fed.*, (4), 389–399.
- Jetten, M. S. M.; Wagner, M.; Fuerst, J.; van Loosdrecht, M.; Kuenen, G.; Strous, M. (2001) Microbiology and Application of the Anaerobic Ammonium Oxidation ('Anammox') Process. *Curr. Opin. Biotechnol.*, **12** (3), 283–288.
- Kanders, L.; Areskoug, T.; Schneider, Y.; Ling, D.; Punzi, M.; Beier, M. (2014) Impact of Seeding on the Start-Up of One-Stage Deammonification MBBRs. *Environ. Technol.*, **35** (21-24), 2767–2773.
- Kimura, Y.; Isaka, K.; Kazama, F.; Sumino, T. (2010) Effects of Nitrite Inhibition on Anaerobic Ammonium Oxidation. *Appl. Microbiol. Biotechnol.*, **86** (1), 359–365.
- Kornaros, M.; Dokianakis, S. N.; Lyberatos, G. (2010) Partial Nitrification/Denitrification Can Be Attributed to the Slow Response of Nitrite Oxidizing Bacteria to Periodic Anoxic Disturbances. *Environ. Sci. Technol.*, **44** (19), 7245–7253.
- Lackner, S.; Gilbert, E.; Vlaeminck, S.; Joss, A.; Horn, H.; van Loosdrecht, M. (2014) Full-Scale Partial Nitritation/Anammox Experiences—An Application Survey. *Water Res.*, **55**, 292–303.
- Lemaire, R.; Liviano, I.; Ekström, S.; Roselius, C.; Chauzy, J.; Thornberg, D.; Thirsing, S.; Deleris, S. (2011) 1-Stage Deammonification MBBR Process for Reject Water Sidestream Treatment: Investigation of Start-Up Strategy and Carriers Design. *Conference Proceedings WEF Nutrient Recovery and Management*, Miami.
- Ling, D. (2009) Experience from Commissioning of Full-Scale Deammon® Plant at Himmerfjärden (Sweden). *Proceedings of 2nd IWA Specialized Conference on Nutrient Management in Wastewater Treatment Processes*, Krakow, Poland; pp 403–410.
- Lotti, T.; van der Star, W. R. L.; Kleerebezem, R.; Lubello, C.; van Loosdrecht, M. C. M. (2012) The Effect of Nitrite Inhibition on the Anammox Process. *Water Res.*, **46** (8), 2559–2569.
- Metcalf and Eddy, Inc. (2014) *Wastewater Engineering Treatment and Reuse*, 5th ed.; McGraw Hill: New York.
- Rosenwinkel, K. H.; Cornelius, A. (2005) Deammonification in the Moving-Bed Process for the Treatment of Wastewater with High Ammonia Content. *Chem. Eng. Technol.*, **28** (1), 49–52.
- Strous, M.; Heijnen, J. J.; Kuenen, J. G.; Jetten, M. S. M. (1998) The Sequencing Batch Reactor as a Powerful Tool for the Study of Slowly Growing Anaerobic Ammonium-Oxidizing Microorganisms. *Appl. Microbiol. Biotechnol.*, **50** (5), 589–596.
- Strous, M.; Kuenen, J.G.; Mike, S.M.J. (1999) Key Physiology of Anaerobic Ammonium Oxidation. *Appl. Environ. Microbiol.*, **65** (7), 3248–3250.

- Turk, O.; Mavinic, D. S. (1989) Maintaining Nitrite Buildup in a System Acclimated to Free Ammonia. *Water Res.*, **23** (11), 1383–1388.
- Van Dongen, L.; Jetten, M.; Van Loosdrecht, M. (2001) *The Combined SHARON/Anammox Process*; STOWA Report; IWA Publishing: London.
- Wett, B. (2007) Development and Implementation of a Robust Deammonification Process. *Water Sci. Technol.*, **56** (7), 81–88.
- Wett, B.; Rauch, W. (2003) The Role of Inorganic Carbon Limitation in Biological Nitrogen Removal of Extremely Ammonia Concentrated Wastewater. *Water Res.*, **37**, 1100–1110.
- Wiesmann, U. (1994) Biological Nitrogen Removal from Wastewater. *Adv. Biochem. Eng.*, **51**, 113–154.
- Wong-Chong, G. M.; Loehr, R. C. (1978) Kinetics of Microbial Nitrification: Nitrite-Nitrogen Oxidation. *Water Res.*, **12** (8), 605–609.
- Zubrowska-Sudol, M.; Yang, J.; Trela, J.; Plaza, E. (2011) Evaluation of Deammonification Process Performance at Different Aeration Strategies. *Water Sci. Technol.*, **63** (6), 1168–1176.

CHAPTER 4: METHODS FOR INCREASING THE RATE OF ANAMMOX ATTACHMENT IN A SIDESTREAM DEAMMONIFICATION MBBR

Stephanie Klaus, Patrick McLee, Andrew J. Schuler, Charles Bott

ABSTRACT

Deammonification (partial nitritation-anammox) is a proven process for the treatment of high-nitrogen waste streams, but long startup time is a known drawback of this technology. In a deammonification moving bed biofilm reactor (MBBR), startup time could potentially be decreased by increasing the attachment rate of anammox bacteria (AMX) on virgin plastic media. Previous studies have shown that bacterial adhesion rates can be increased by surface modification or by the development of a preliminary biofilm. This is the first study on increasing AMX attachment rates in a deammonification MBBR using these methods. Experimental media consisted of three different wet-chemical surface treatments, and also media transferred from a full-scale mainstream fully nitrifying integrated fixed-film activated sludge (IFAS) reactor. Following startup of a full-scale deammonification reactor, the experimental media was placed in the full-scale reactor and removed for activity rate measurements and biomass testing after one and two months. The media transferred from the IFAS process exhibited a rapid increase in AMX activity rates (1.1 g/m²/day NH₄⁺ removal and 1.4 g/m²/day NO₂⁻ removal) as compared to the control (0.2 g/m²/day NH₄⁺ removal and 0.1 g/m²/day NO₂⁻ removal) after one month. Two out of three of the surface modifications resulted in significantly higher AMX activity than the control at one and two months. No NOB activity was detected in either the surface modified media or IFAS media batch tests. The results indicate that startup time of a deammonification MBBR could potentially be decreased through surface modification of the plastic media or through the transfer of media from a mature IFAS process.

INTRODUCTION

The combination of partial nitritation and anaerobic ammonia oxidation (anammox), commonly known as deammonification, is an economical option for sidestream treatment because of decreased aeration energy requirements, no required external carbon or alkalinity, and decreased sludge production over traditional nitrification/denitrification. The ANITA™ Mox process consists of a single-stage deammonification moving bed biofilm reactor (MBBR) for treating high nitrogen waste streams. In this process ammonia oxidizing bacteria (AOB) and anammox bacteria (AMX) exist simultaneously within a biofilm attached to plastic carriers. A key component of the process is controlling dissolved oxygen to limit the growth of nitrite oxidizing bacteria (NOB) which compete with AMX for substrate and to limit oxygen penetration into the biofilm thereby maintaining an anoxic environment for AMX to grow.

Deammonification systems must be closely monitored and controlled during startup to prevent growth of NOB and irreversible nitrite inhibition of AMX. Reducing startup time would be

extremely beneficial as it would require less attention from operators and reduce the risk of irreversibly inhibiting the process. Seeding a reactor with 2-10% pre-colonized media has been shown to reduce startup times from 1 year down to 2-4 months (Lemaire et al. 2011; Christensson et al. 2013). Contrary to reports that seeding decreases startup time, some argue that seeding is not necessary (Ling 2009; Kanders et al. 2014). The debate is whether the origin of the AMX biomass on the virgin media is from the seed media or the wastewater itself. Regardless of the origin of AMX biomass, several months of operation are required for AMX to establish on virgin media, and this could be a barrier to widespread adoption of deammonification technology.

Media in MBBR and integrated fixed-film activated sludge (IFAS) processes is typically made from high density polyethylene (HDPE) due to low cost. However, HDPE has a low surface energy and is hydrophobic making it unfavorable for bacterial growth (Bergbreiter 1994, Goddard and Hotchkiss 2007). Although interactions between surfaces and bacteria are complex and not completely understood, it is well known that bacterial adhesion is affected by surface energy, hydrophobicity, and roughness (An and Friedman 1998, Goddard and Hotchkiss 2007). Bacterial adhesion to a surface occurs in two phases: The initial attachment of a bacterial cell to the substratum, which is governed by physicochemical interactions, followed by biological cell growth and extra cellular polymer production (An and Friedman 1998, Hermansson 1999). The study of bacterial adhesion is broad and typically the goal is to prevent biofilms on surfaces such as ship hulls, food processing equipment, and biomedical devices. However the promotion of biofilms is desirable for biodegradation of plastics (Roy et al. 2011) and biological wastewater treatment (Hadjiev et al. 2007).

Plastic surfaces can be modified using chemical, plasma, or thermal processes to have increased hydrophilicity thereby increasing the rate of bacterial attachment and growth (Bergbreiter 1994). Studies on adhesion of nitrifying bacteria have typically demonstrated that surfaces with higher energy and hydrophilicity correlate with higher nitrification rates, increased biomass accumulation, and increased shear resistance (Khan et al. 2013, Khan et al. 2011, Kim et al. 1997, Lackner et al. 2009, Terada et al. 2004), although one report did conclude that the most hydrophobic surface had the most nitrifying biomass formation (Sousa et al. 1997). Although Chen et al. (2012) examined AMX attachment to surface modified carbon fibers in a deammonification reactor, no studies have been published on increasing AMX attachment to surface modified plastic.

Another potential method of increasing rates of AMX attachment is through the development of a preliminary biofilm composed of nitrifiers and/or heterotrophs. The hypothesis is that the existing biofilm creates a preferential environment for AMX by providing protection from oxygen and NO_2^- in the bulk liquid. While it is known that development of a preliminary biofilm may encourage the attachment of AMX, the transfer of media from a mature mainstream fully nitrifying IFAS process to a sidestream deammonification reactor with the intent of decreasing startup time is a novel approach. Zekker et al. (2012) showed that AMX developed faster in an

anoxic reactor containing media pre-colonized with a nitrifying biomass than in an anoxic reactor containing virgin media. The concern with using media pre-colonized with nitrifying biomass in an aerobic deammonification process versus an anoxic anammox process is the potential proliferation of NOB.

The current study represents the first work on increasing the rates of AMX attachment through surface modification of plastic biofilm carriers. The objectives of this study were to test whether rates of AMX biofilm growth and ammonia/nitrite removal on HDPE media could be increased through wet chemical surface treatment and through the transfer of media with a mature biofilm from a full-scale mainstream fully nitrifying IFAS process.

MATERIALS AND METHODS

Full-Scale Deammonification Reactor Startup

An existing 100,000 gallon tank at the 20 MGD James River Wastewater Treatment Plant (JRWWTP) in Newport News, VA was modified to install the ANITA™ Mox process. This was the first full-scale installation of a sidestream deammonification MBBR process in North America. The mainstream process at JRWWTP utilizes IFAS operated in a MLE configuration. Anaerobically digested waste activated and primary sludge is dewatered using centrifuges and the centrate is sent to an equalization (EQ) basin which is then treated in the deammonification MBBR. The average centrate characteristics throughout the study period (Day 115-Day 197) were 950 mg/L NH_4^+ -N, 1,020 mg/L TKN, 3,450 mg/L as CaCO_3 Alkalinity, 3.63 Alkalinity/ NH_4^+ -N ratio, and 500 mg/L COD.

The reactor was seeded with 10% pre-colonized Anox™ K5 carriers (AnoxKaldnes, Sweden) from an established sidestream deammonification MBBR process (Sjölunda WWTP Malmö, Sweden). The total media fill in the reactor is 32% to meet a design NH_4^+ -N removal rate of 2 g/m²/day. By Day 120 the sidestream deammonification MBBR was achieving greater than 85% NH_4^+ removal at the design loading rate signaling the end of startup (Figure 4.1). Variations in removal percentages during startup up are due to frequent changes in loading rate (Figure 4.1). After startup was complete the removal loading rate and removal percentages were more consistent. Nitrate production ratio was calculated as NO_3^- produced over NH_4^+ removed. A nitrate production ratio of less than 12% indicates that NO_3^- produced is solely from AMX while a ratio greater than 12% indicated the presence of NOB. Figure 4.2 shows the time course of influent and effluent NH_4^+ -N, NO_3^- -N, NO_2^- -N, and sCOD. The temperature was maintained at 30°C using supplemental heating as needed. AMX activity on the virgin carriers was first detected in bench scale activity tests after 3 months of operation. After two months it was determined, by calculating the theoretical biomass production based on AMX yield, that production of AMX biomass was not the limiting factor in biofilm development leading to the hypothesis that attachment of the bacteria to the new virgin media must have been limiting.

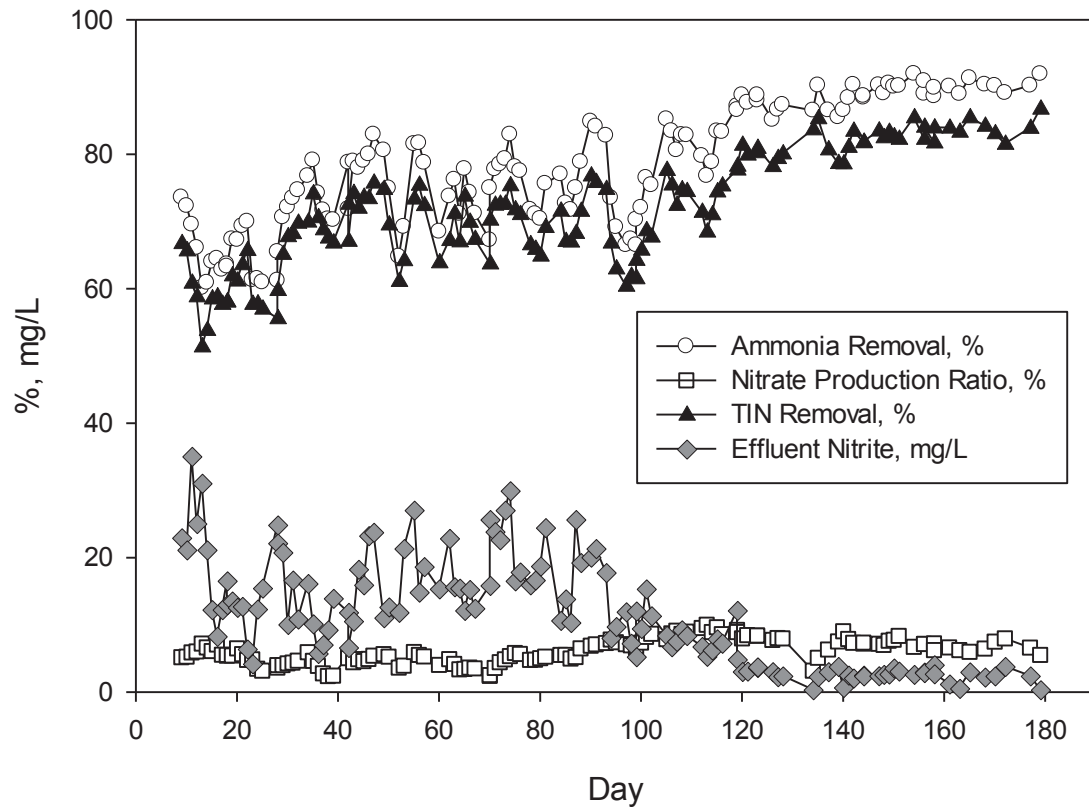


Figure 4.1: Performance of the Full-Scale Deammonification MBBR including startup and overall tank conditions during the duration of the attachment experiment. Day 1 to Day 120: Startup Phase, Day 115 to Day 179: Attachment experiment presented in this study

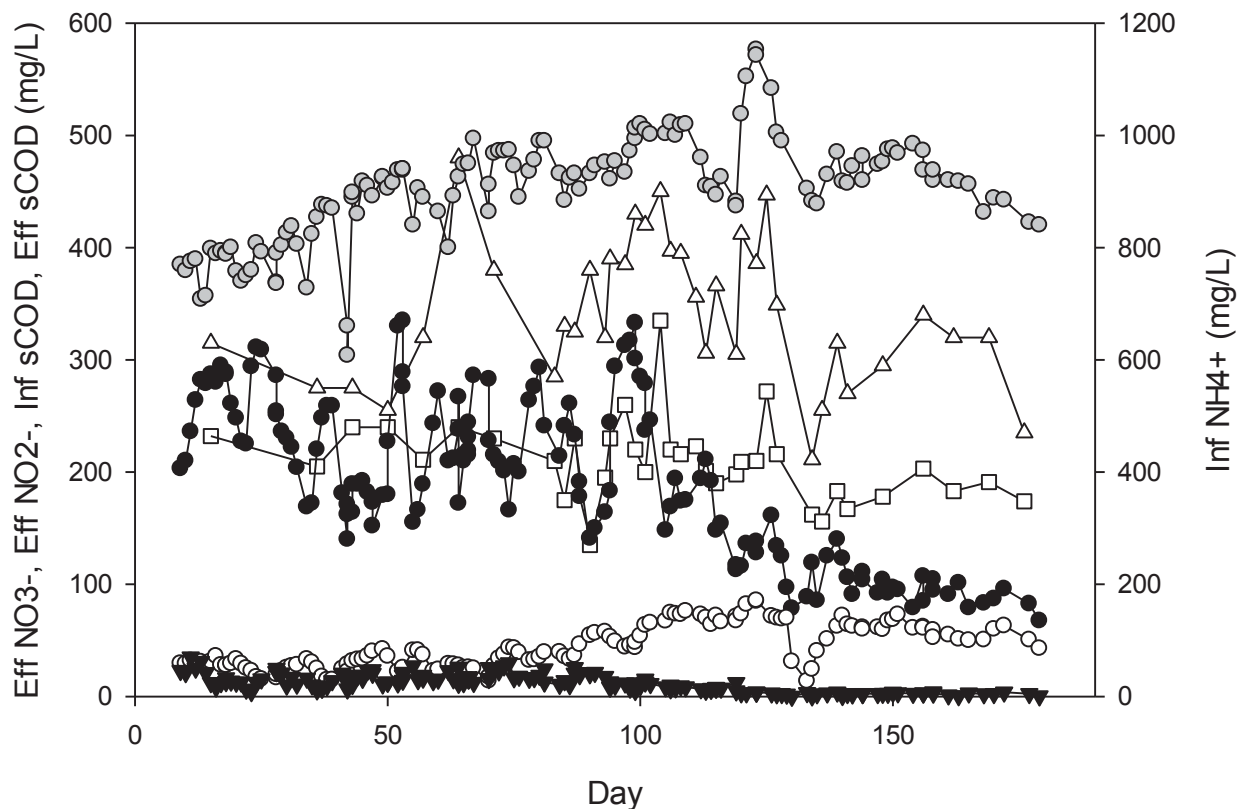


Figure 4.2: Time course of influent NH₄⁺ (grey circles, right axis), influent sCOD (white triangles), effluent NH₄⁺ (black circles), effluent sCOD (white squares), effluent NO₃⁻ (white circles), and effluent NO₂⁻ (black triangles) in full-scale deammonification MBBR. Day 1 to Day 120: Startup Phase, Day 115 to Day 179: Attachment experiment presented in this study

Experimental Media

Wet chemical (as opposed to plasma or thermal) methods of surface modification were explored for this study due to considerations over what would be feasible in a full-scale process. Three-one liter batches of K5 carriers were treated with potassium permanganate, Fenton's Reagent (FeSO₄ plus H₂O₂), and ozone with the intent of oxidizing the surface functional groups thereby increasing the hydrophilicity. Media with biofilm from the existing deammonification MBBR served as a positive control while virgin K5 carriers served as a negative control. All of the media that was chemically oxidized (and the virgin control) was wetted in an aerated container of tap water for 1 week prior to treatment. A small piece of an HPDE sheet was treated along with each batch of media in order to measure contact angle. The experimental media along with the positive and negative control was placed in a perforated aluminum box with individual compartments for each batch of media and placed in the existing sidestream deammonification MBBR on Day 115. Dimensions of the box were approximately 12 inches high x 18 inches wide x 6 inches deep. The box allowed for bulk liquid to flow through the media while allowing the media to be removed from the tank for testing. The box had six individual compartments each

with a volume of three liters. The media fill in each compartment was 30% to reflect conditions in the overall tank. The experimental media was removed once after 30 days and again after 60 days to measure AMX, AOB and NOB activity as well as biomass concentration.

Fenton's Reagent Treatment: The media was placed in deionized water and the pH was adjusted to 3 with H₂SO₄. Next 30% H₂O₂ was added to reach a concentration of 5000 mg/L H₂O₂. Then 6.95 g of FeSO₄ was added to reach a H₂O₂/Fe²⁺ molar ratio of 4. The reaction took place for 24 hours. A sample was periodically tested for peroxide to ensure that a residual was being maintained. The final residual was approximately 15 ppm H₂O₂.

Ozone Treatment: An ozone generator (Ozonology, Inc., Model L-100) was connected to a reactor containing the media in deionized water. Ozone was produced using ambient air at room temperature and was bubbled through the water at the maximum concentration that the generator could provide for 24 hours. A sample was periodically tested to ensure a residual of greater than 0.5 ppm was maintained.

Potassium Permanganate Treatment: Two grams of KMnO₄ was added to 3 liters of deionized water with the media in a glass beaker and continuously stirred for 48 hours at room temperature. A residual was assumed to be maintained as indicated by the purple color of the solution.

IFAS Media: One liter of media (Anox™ K3, AnoxKaldnes, Sweden) with fully nitrifying biofilm was removed from the existing full-scale mainstream IFAS process at JRWWTP on Day 115. The IFAS process has been in operation for approximately 2.5 years.

A batch test was performed to evaluate the effect of short term exposure of the IFAS media to sidestream conditions on NOB activity. Two one liter samples of media were collected from the IFAS process and drained. One sample was placed in bulk from the IFAS process while the other was placed in bulk from the sidestream process. Bench scale activity tests were performed after 4 hours at 20°C to measure AOB and NOB rates. Nearly all NOB activity was assumed to be on the media as demonstrated by Regmi et al. (2011) at JRWWTP.

Contact angle measurements

The pieces of HDPE sheet were analyzed for each surface treatment. The Fenton's reagent and KMnO₄ pieces were cleaned with a 1M H₂SO₄ solution prior to measurement to remove residual metal oxide. The contact angles were determined by goniometry for the three probe liquids ultrapure water, diiodomethane (99%, Sigma-Aldrich, USA), and formamide (>99.5%, Sigma-Aldrich, USA). The sessile drop technique was used (Ramé-Hart Instrument Co., Goniometer Model# 400-22-300 with DROPimage Standard, NJ) as previously described in Khan et al. (2011). At least five 1.5 mL droplets were measured with each liquid.

Surface Energy Calculations

Surface energies were calculated from the contact angle measurements as described in Liu et al. (2008) and Khan et al. (2013) according to the van Oss method (Van Oss et al. 1986). In

summary the total surface energy (γ^{total}) is the sum of the Lifshitz-van der Waals (LW) and Lewis acid-base (AB) components (EQ 1).

$$\gamma^{total} = \gamma^{LW} + \gamma^{AB} \quad EQ 1$$

The acid-base component (γ^{AB}) is related to the electron-acceptor (γ^+) and electron-donor (γ^-) parameters for the given liquid or substrata by EQ 2.

$$\gamma^{AB} = 2\sqrt{\gamma^+ \cdot \gamma^-} \quad EQ 2$$

The Young-Dupré equation (EQ 3) describes the relationship between γ^{LW} , γ^+ , γ^- , and contact angle (θ) for a surface (S) and a drop of liquid (L).

$$\gamma_L(\cos\theta_L + 1) = 2\sqrt{\gamma_S^{LW} \cdot \gamma_L^{LW}} + 2\sqrt{\gamma_S^+ \cdot \gamma_L^-} + 2\sqrt{\gamma_S^- \cdot \gamma_L^+} \quad EQ 3$$

If γ_L^{LW} , γ_L^+ , and γ_L^- are known then γ_S^{LW} , γ_S^+ , and γ_S^- can be calculated from contact angles using three different liquids. Reference values for γ_L^{LW} , γ_L^+ , and γ_L^- were from Good and van Oss (1992) and were confirmed with the supplier.

Bench Scale Maximum Activity Testing

Bench scale maximum activity tests were performed once at 30 days and once at 60 days. AOB and NOB activity was measured under aerobic conditions while AMX activity was measured under anoxic conditions. For all of the samples the biofilm was thin enough that AMX activity was inhibited in the aerobic test. The bulk liquid test was only performed under aerobic conditions since the amount of AMX activity in the bulk was negligible. The bulk liquid AOB activity rates were subtracted from the rates that included media and bulk liquid in order to obtain AOB rates on the media alone. In order to mimic conditions in the full scale reactor the bench scale reactors were filled with 30% media (1 liter) by volume and bulk liquid from the full-scale reactor to reach a total volume of 3 liters. All reactors were fully mixed and dissolved oxygen was monitored and manually controlled to above 4 mg/L in the aerobic test. For the anoxic test the reactor was covered and sparged with a blend of nitrogen gas with 380 ppm of CO₂. pH was monitored and manually controlled to stay within the range of 6.5-7.5. Temperature was controlled using a water bath to match the temperature in the full-scale reactor (30°C). Samples were taken at regular intervals, immediately filtered through 0.45 micron filter membranes, and analyzed for NH₄⁺, NO₃⁻, and NO₂⁻. The maximum activity rates were evaluated by linear regression of the change in nitrogen species over the experimental period. AOB rates were determined from NO_x production, NOB from NO₃⁻ production, and AMX from both NH₄⁺ and NO₂⁻ consumption.

Performance Monitoring of Full-Scale Reactor

Samples for on-site monitoring of the full-scale reactor were immediately filtered through 0.45 micron filter membranes following collection, and analyzed using HACH TNT kits and a HACH DR2800 spectrophotometer. The influent sample was analyzed for NH₄⁺ and the process

(effluent) sample was analyzed for NH_4^+ , NO_3^- , and NO_2^- . sCOD was measured using standard methods.

Biomass Concentration Measurements

The weight of the biomass per square meter of surface area was measured at 30 and 60 days. For this measurement nine pieces of media were removed from each compartment. Measurements were made according to Regmi et al. (2011) with the exception that a 25 mg/L disodium EDTA solution was used to remove biofilm instead of H_2SO_4 .

Statistics

Statistical analysis to test if maximum activity on the experimental media was significantly different from the control was generated using SAS software. The slope of the linear regression from each experimental batch test was tested against the control to determine p values.

RESULTS AND DISCUSSION

Contact Angle and Surface Energy Measurements

The ozone treated HDPE had the lowest water contact angle indicating that it was the most hydrophilic with the new media control being the most hydrophobic (Table 4.1). As expected all three of the surface treatments produced a more hydrophilic surface than the new media control. The surface energy results did not correlate with water contact angle as both the ozone and Fenton's reagent treatment produced a similar surface energy higher than the control, while the potassium permanganate treatment produce a lower surface energy than the control (Table 4.1).

Table 4.1: Contact Angle and Surface Energy Parameters of the Surface Modified Media and New Media Control. θ_w , θ_D , and θ_F represent the contact angles for water, diiodomethane, and formamide respectively.

	Contact Angle (degrees)			Surface Energy Parameters (mJ/m ²)				
	θ_w	θ_D	θ_F	γ^{LW}	γ^+	γ^-	γ^{AB}	γ^{total}
New Media Control	89.5±1.1	51.4±2.0	77.8±3.0	33.5	0.68	7.50	4.52	38.0
Fenton's Reagent	85.4±3.2	42.3±1.0	71.2±1.4	38.5	0.52	7.66	3.99	42.4
KMnO₄	83.4±2.2	53.0±2.5	73.4±3.7	32.6	0.28	10.8	3.47	36.0
Ozone	76.0±3.1	36.2±1.1	55.2±5.3	41.5	0.03	3.84	0.68	42.4

Short-Term Sidestream IFAS Media Experiment

When media from the IFAS tank was placed in bulk liquid from the sidestream deammonification MBBR, NOB activity was reduced by 55% within 4 hours (1.6 g/m²/day to 0.9 g/m²/day). These results suggested that NOB activity would be quickly inhibited, most likely via free ammonia, in sidestream conditions eliminating or reducing the competition with AMX for substrate and space within the biofilm.

Activity and Biomass Results for Experimental Media

There was measureable AMX activity on the new media control after one month (compared to 3 months it took for original new media during startup) implying that shear conditions inside the perforated box did not match the overall tank conditions, or the larger background AMX population in the tank accelerated attachment. After one month the positive control seed media had slightly higher AMX activity (7.6 g/m²/day NH₄⁺ removal and 6.9 g/m²/day NO₂⁻ removal) and higher biomass (47.9 g/m²) than the original seed media in the full scale reactor (5.5 g/m²/day NH₄⁺ removal, 6.9 g/m²/day NO₂⁻ removal, and 42.0 g/m² biomass). This also supports that the experimental media was exposed to lower shear conditions than the overall reactor. After two months the control seed media had slightly less AMX activity (4.5 g/m²/day NH₄⁺ removal and 4.9 g/m²/day NO₂⁻ removal) and about the same biomass (43.6 g/m²) as the original seed media in the full scale reactor (5.5 g/m²/day NH₄⁺ removal, 6.9 g/m²/day NO₂⁻ removal, and 41.7 g/m² biomass) indicating that perhaps the experimental conditions were closer to that of the overall reactor. Regardless of the difference between the experimental conditions and the conditions in the overall tank, the experimental media can still be compared to the new media control.

After one month there was significantly more AMX activity on the IFAS media (1.1 g/m²/day NH₄⁺ removal and 1.4 g/m²/day NO₂⁻ removal) as compared to the control (0.2 g/m²/day NH₄⁺ removal and 0.1 g/m²/day NO₂⁻ removal) (Figure 4.3). Initial biomass on the IFAS media prior to placement in the deammonification reactor was 18.7 g/m². Biomass increased after 1 month and was much higher than on the other experimental media due to the preliminary biofilm (Figure 4.4). At the same time in the full-scale reactor, the maximum AMX rates (from bench scale tests) on the original new media were 1.4 g/m²/day NH₄⁺ removal and 2.4 g/m²/day NO₂⁻ removal (after 5 months of operation). AMX activity and biomass on the IFAS media after two months was again much higher than the control and the surface modified media (Figure 4.3 and 4.4). IFAS AMX activity was 2.0 g/m²/day NH₄⁺ removal and 3.2 g/m²/day NO₂⁻ removal while the new media control was 0.3 g/m²/day NH₄⁺ removal and 1.1 g/m²/day NO₂⁻ removal. After two months AMX activity on the IFAS media was comparable to that on the original new media in the overall reactor (3.2 g/m²/day NH₄⁺ removal and 3.6 g/m²/day NO₂⁻ removal) which had been in the reactor for 6 months. The IFAS media biomass decreased from 1 month to 2 months (Figure 4.4) but was higher than the initial biomass from the IFAS reactor (18.7 g/m²). One explanation for decreased biomass while AMX activity increased could be that more AMX biomass was colonizing the biofilm while inactive biofilm was sloughing off of the media. AOB activity on the IFAS media was slightly higher than the control at both one and two months (approximately 1.5 g/m²/day compared to 1.3 g/m²/day). No NOB activity was detected at either one or two months as indicated by nitrate production ratio less than 12%. These results suggest that media from a mature IFAS process could be used to achieve immediate AMX growth in a sidestream process without risk of NOB proliferation. The ammonia removal rate for the new media control was unusually low for the test at 2 months (Figure 4.3). It is frequently seen in the activity tests that the NO₂⁻ removal results are more consistent than the NH₄⁺ results. Another

common observation is that nitrite removal develops first before NH_4^+ removal as AMX is establishing on the new media.

All three batches of surface-treated media had higher attached biomass than the new media control (Figure 4.4) at both one and two months. Statistical analysis was performed to determine if the AMX activity (based on NO_2^- removal) for the surface modified media was significantly higher ($p \leq 0.05$) than the new media control. Results after one month showed that the AMX activity for both Fenton's reagent treated media and KMnO_4 treated media was significantly higher than the control ($p=0.0037$ and $p<0.0001$ respectively) while the ozone treated media was not significantly higher ($p=0.14$) (Figure 4.3). After two months the AMX activity for Fenton's reagent treated media and KMnO_4 treated media was again significantly higher than the control ($p<0.0001$) while the ozone treated media was not. Although ozone treated media had the lowest water contact angle (Table 4.1) it did not have the highest biomass density or AMX activity. In fact, the ozone treatment seemed to be the least successful of the surface modifications and had lower AMX activity (based on NO_2^- removal) than the control after two months. Surface energy did not appear to correlate with biomass density or AMX activity (Table 4.1, Figure 4.3, Figure 4.4). AOB activity was approximately the same for all of the surface modified media as compared to the control at both one and two months. No NOB activity was detected on any of the experimental media.

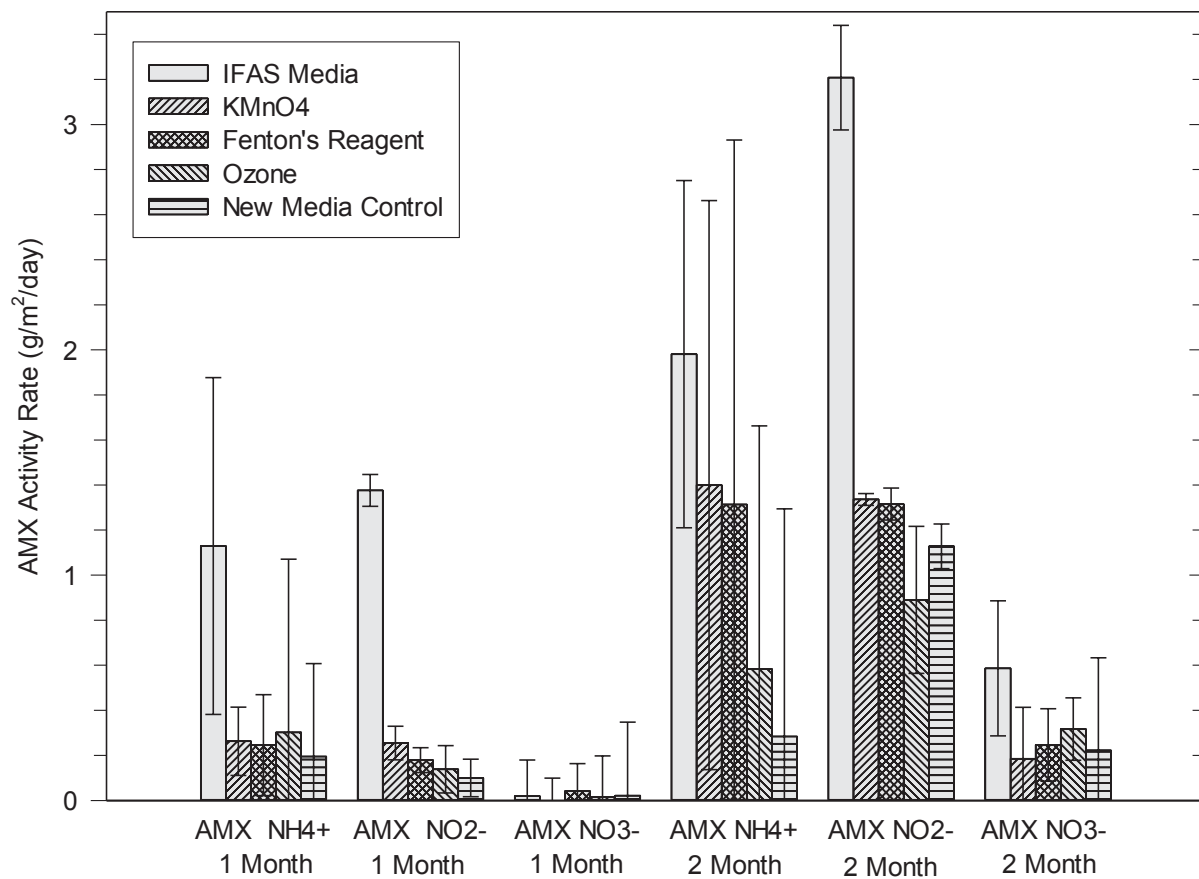


Figure 4.3: IFAS media and surface modified media AMX activity test results after one month and two months. AMX NH₄⁺ = AMX activity based on NH₄⁺ consumption, AMX NO₂⁻ = AMX activity based on NO₂⁻ consumption. Error bars represent the 95% confidence interval.

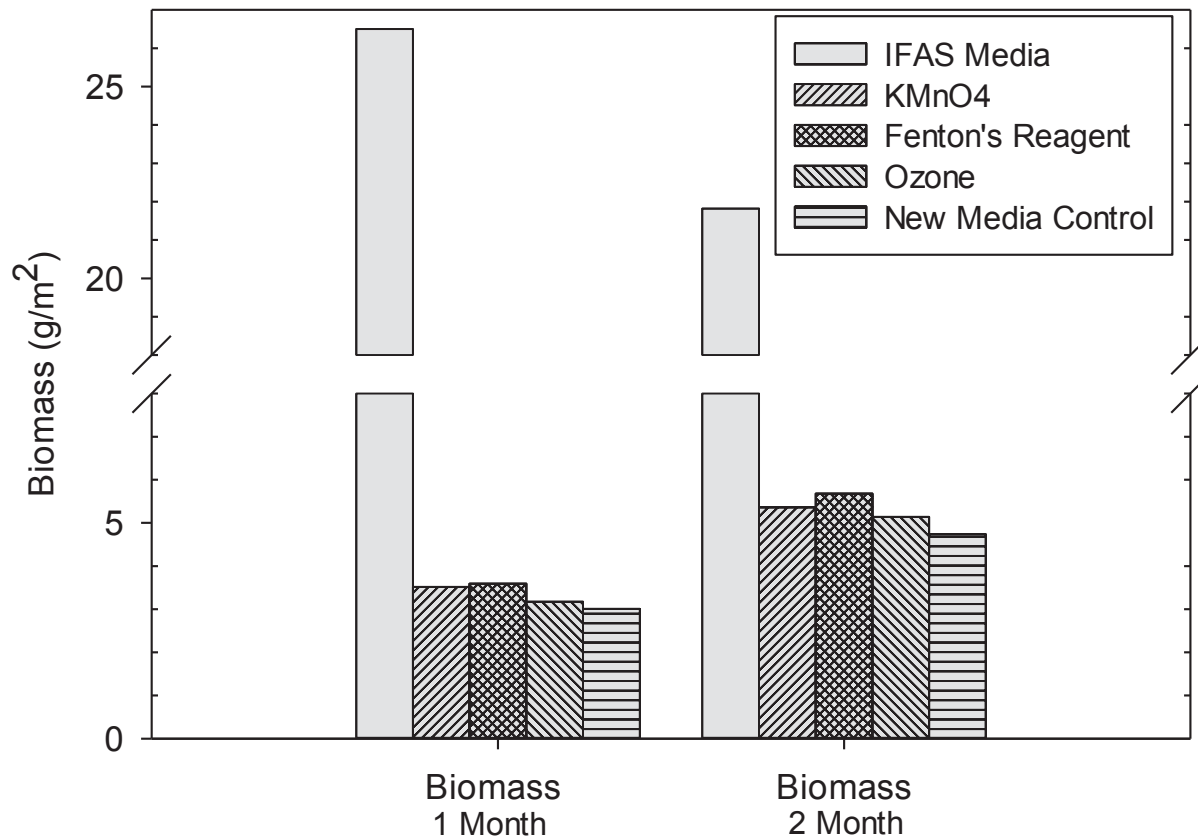


Figure 4.4: IFAS media and surface modified media AMX biomass results after one month and two months.

CONCLUSIONS

The surface modified media had higher biomass density and hydrophilicity than the control new media. AMX activity rates were significantly higher for the Fenton's reagent and potassium permanganate treated media than the new media control after one month and two months while ozone treatment did not result in increased AMX activity. Media from the IFAS tank provided a preliminary biofilm that led to a rapid increase in AMX activity and NOB were inhibited. The large amount of AMX activity in the tank (plus reduced mixing) makes it difficult to make a direct comparison to the original new media during startup. While the results clearly demonstrate that the surface modification and preliminary biofilm led to higher rates of AMX biofilm development compared to the control, further study such as a pilot operation is warranted in order to provide conclusive evidence of reduced startup time.

Acknowledgements

The authors wish to thank the HRSD James River Wastewater Treatment Plant staff for their role in monitoring the full-scale process as well as for construction of the box to house the experimental media. We also thank Virginia Tech's Laboratory for Interdisciplinary Statistical

Analysis (LISA), specifically Jon Atwood for performing the statistical analysis. Patrick McLee was supported by the National Science Foundation, Grant 1337077.

REFERENCES

- An, Y.H. and Friedman, R.J. (1998) Concise review of mechanisms of bacterial adhesion to biomaterial surfaces. *Journal of Biomedical Materials Research* 43(3), 338-348.
- Bergbreiter, D.E. (1994) Polyethylene surface chemistry. *Progress in Polymer Science* 19(3), 529-560.
- Chen, Y.-P., Li, S., Ning, Y.-F., Hu, N.-N., Cao, H.-H., Fang, F. and Guo, J.-S. (2012) Start-up of completely autotrophic nitrogen removal over nitrite enhanced by hydrophilic-modified carbon fiber. *Applied Biochemistry and Biotechnology* 166(4), 866-877.
- Christensson, M., Ekström, S., Andersson Chan, A., Le Vaillant, E. and Lemaire, R. (2013) Experience from start-ups of the first ANITA Mox plants. *Water science and technology : a journal of the International Association on Water Pollution Research* 67(12), 2677-2684.
- Good, R.J., van Oss, C.J., (1992) In: Shrader, M.E., Loeb, G.I. (Eds.), *Modern Approaches to Wettability, Theory and Applications*. Plenum Press, New York.
- Goddard, J.M. and Hotchkiss, J.H. (2007) Polymer surface modification for the attachment of bioactive compounds. *Progress in Polymer Science* 32(7), 698-725.
- Hadjiev, D., Dimitrov, D., Martinov, M. and Sire, O. (2007) Enhancement of the biofilm formation on polymeric supports by surface conditioning. *Enzyme and Microbial Technology* 40(4), 840-848.
- Hermansson, M. (1999) The DLVO theory in microbial adhesion. *Colloids and Surfaces B: Biointerfaces* 14(1), 105-119.
- Kanders, L., Areskoug, T., Schneider, Y., Ling, D., Punzi, M. and Beier, M. (2014) Impact of seeding on the start-up of one-stage deammonification MBBRs. *Environmental Technology* 35(21-24), 2767-2773.
- Khan, M.M.T., Chapman, T., Cochran, K. and Schuler, A.J. (2013) Attachment surface energy effects on nitrification and estrogen removal rates by biofilms for improved wastewater treatment. *Water research* 47(7), 2190-2198.
- Khan, M.M.T., Ista, L.K., Lopez, G.P. and Schuler, A.J. (2011) Experimental and Theoretical Examination of Surface Energy and Adhesion of Nitrifying and Heterotrophic Bacteria Using Self-Assembled Monolayers. *Environmental science & technology* 45(3), 1055-1060.
- Kim, Y.H., Cho, J.H., Lee, Y.W. and Lee, W.K. (1997) Development of a carrier for adhesion of nitrifying bacteria using a thermodynamic approach. *Biotechnology Techniques* 11(11), 773-776.

- Lackner, S., Holmberg, M., Terada, A., Kingshott, P. and Smets, B.F. (2009) Enhancing the formation and shear resistance of nitrifying biofilms on membranes by surface modification. *Water Research* 43(14), 3469-3478.
- Lemaire, R., Liviano, I., Ekström, S., Roselius, C., Chauzy, J., Thornberg, D., Thirsing, S. & Deleris, S. (2011). 1-stage Deammonification MBBR process for reject water sidestream treatment: investigation of start-up strategy and carriers design. In: Conference Proceedings WEF Nutrient Recovery and Management, Miami.
- Ling D. (2009). Experience from commissioning of full-scale DeAmmon® plant at Himmerfjärden (Sweden). In: Proceedings of 2nd IWA Specialized Conference on Nutrient Management in Wastewater Treatment Processes, Krakow, Poland.
- Liu, Y., Gallardo-Moreno, A.M., Pinzon-Arango, P.A., Reynolds, Y., Rodriguez, G. and Camesano, T.A. (2008) Cranberry changes the physicochemical surface properties of *E. coli* and adhesion with uroepithelial cells. *Colloids and Surfaces B: Biointerfaces* 65(1), 35-42.
- Regmi, P., Thomas, W., Schafran, G., Bott, C., Rutherford, B. and Waltrip, D. (2011) Nitrogen removal assessment through nitrification rates and media biofilm accumulation in an IFAS process demonstration study. *Water Research* 45(20), 6699-6708.
- Roy, P.K., Surekha, P. and Rajagopal, C. (2011) Surface oxidation of low- density polyethylene films to improve their susceptibility toward environmental degradation. *Journal of Applied Polymer Science* 122(4), 2765-2773.
- Sousa, M., Azeredo, J., Feijo, J. and Oliveira, R. (1997) Polymeric supports for the adhesion of a consortium of autotrophic nitrifying bacteria. *Biotechnology Techniques* 11(10), 751-754.
- Terada, A., Yamamoto, T., Hibiya, K., Tsuneda, S. and Hirata, A. (2004) Enhancement of biofilm formation onto surface-modified hollow-fiber membranes and its application to a membrane-aerated biofilm reactor. *Water Science and Technology* 49(11-12), 263-268.
- Van Oss, C.J., Good, R.J. and Chaudhury, M.K. (1986) The role of van der Waals forces and hydrogen bonds in “hydrophobic interactions” between biopolymers and low energy surfaces. *Journal of Colloid and Interface Science* 111(2), 378-390.
- Zekker, I., Rikmann, E., Tenno, T., Lemmiksoo, V., Menert, A., Loorits, L., Vabamäe, P., Tomingas, M. and Tenno, T. (2012) Anammox enrichment from reject water on blank biofilm carriers and carriers containing nitrifying biomass: operation of two moving bed biofilm reactors (MBBR). *Biodegradation* 23(4), 547-560.

CHAPTER 5: NITRIC OXIDE PRODUCTION INTERFERES WITH AQUEOUS DISSOLVED OXYGEN SENSORS

Stephanie Klaus, Michael Sadowski, Jose Jimenez, Bernhard Wett, Kartik Chandran, Sudhir Murthy, Charles B. Bott

ABSTRACT

It was observed in previous studies that optical dissolved oxygen (DO) sensors were measuring values up to 1 mg O₂/L in anoxic mixed liquor samples containing nitrite (NO₂⁻). Based on these observations of false DO measurements it was hypothesized that NO₂⁻, N₂O, or NO was interfering with the DO sensors. A variety of DO probes were tested for interference while measuring NO₂⁻, N₂O and NO. It was concluded that NO causes a positive inference with some models of optical DO probes. In bench-scale denitrification tests, 25 mg/L of NO₂⁻ led to the production of enough NO to cause a DO sensor reading of 1 mgO₂/L. These findings are important for any wastewater treatment process that is utilizing online DO measurements in the presence of NO such as shortcut nitrogen removal processes.

INTRODUCTION

Nitrous oxide (N₂O) and nitric oxide (NO) production has been widely studied in wastewater treatment due to the greenhouse gas potential of N₂O and both gasses as indicators of process performance. NO and N₂O are produced either as a byproduct of ammonia oxidation by ammonia oxidizing bacteria (AOB) or as a result of incomplete denitrification by heterotrophic bacteria. There are three main biological pathways for the production of NO and N₂O: The NH₂OH oxidation pathway, AOB denitrification pathway, and heterotrophic denitrification pathway (Ni and Yuan, 2015). Process parameters that increase production of NO and N₂O include high NO₂⁻ concentration, intermittent aeration, low influent COD/N ratio, and low DO concentration (Kampschreur et al., 2009; Wunderlin et al., 2012). Shortcut nitrogen processes such as nitrite shunt and deammonification (partial nitrification/anammox) usually include one or more of these process conditions and are therefore more likely to produce NO and N₂O than conventional nitrogen removal processes (Kampschreur et al., 2008).

N₂O and NO can be measured by Clark-type electrochemical sensors, in which a sensing anode and a reference electrode are placed in an internal electrolyte which is contained in a gas-permeable membrane (Schreiber et al., 2008). Oxygen interference is eliminated in the N₂O sensor through the inclusion of an oxygen-reducing guard cathode (Andersen et al., 2001). There are two main types of dissolved oxygen sensors available for liquid phase measurements: Electrochemical sensors (galvanic or polarographic) and optical sensors with luminescent or fluorescent techniques. Galvanic and polarographic cells operate through the use of an anode and a cathode contained in an electrolyte and isolated from the process medium by an oxygen-permeable membrane (Lee and Tsao, 1979). All optical DO probes operate under the same principle which is the interaction of molecular oxygen with a fluorescing compound. Oxygen quenches the fluorescence which can be measured and related to the concentration of dissolved

oxygen present via the Stern-Volmer equations. The sensor can either measure the fluorescence intensity or the excited state lifetime of the fluorophore (McDonagh et al., 2001).

It was observed in bench scale denitrification rate tests that optical DO probes were registering high readings even though no oxygen was being supplied to the reactor. This was occurring with mixed liquor samples from a full scale nitrite shunt process and from the B-stage of a pilot-scale Adsorption/Bio-Oxidation (A/B) process. The spike in DO probe readings corresponded to the addition of NO_2^- at the beginning of the batch test. This led to the hypothesis that nitrite itself or an intermediate in the denitrification pathway was creating a positive interference with the DO sensor reading. Personal communications by the authors revealed that it is common to observe false DO readings during anoxic denitrification tests but the mechanism has never been studied. The objectives of this study were to determine which intermediate (NO_2^- , N_2O , or NO) was interfering with the DO probe readings, to demonstrate that the interference occurs at levels of NO_2^- that are relevant to wastewater treatment processes, and to test a variety of DO sensors for interference.

MATERIALS AND METHODS

Probe calibration

All DO probes were calibrated in water saturated air prior to measurements. When applicable a two point calibration was performed using a sodium sulfite solution to prepare a zero DO solution. In order to calibrate the nitric oxide and nitrous oxide sensors, a standard stock solution of nitric oxide or nitrous oxide saturated water was prepared. To prepare the nitric oxide stock solution nitric oxide gas (99.9%, Airgas) was bubbled through two washing bottles in series filled with 5 M NaOH. A septum bottle was filled with 10 mL of DI water. The output of the second washing bottle led to the septum vial, piercing the septum with a long needle attached to a diffuser. Nitric oxide was flushed through the setup for 10 min. To make the nitrous oxide stock solution nitrous oxide gas (99.99%, Airgas) was bubbled through a diffuser into a beaker of DI water. The temperature of the saturated solution was measured and was used to calculate the concentration of nitric or nitrous oxide in the saturated solution. The sensor was placed in a covered glass beaker. The beaker was sparged with nitrogen gas (99.999%, Airgas) for five minutes to remove oxygen. A syringe was used to withdraw the stock solution. A three point calibration was performed by spiking two known concentrations of NO or N_2O plus a zero point. The range of the calibration matched the manufacturer's recommended range of each sensor which was 0-42 $\mu\text{g/L-N}$ for NO and 0-14 mg/L-N for N_2O .

Tests in mixed liquor

Sample A was eight liters of return activated sludge (RAS) collected from a full-scale plant performing nitrite shunt. The sample initially contained negligible concentrations of NO_2^- and NO_3^- . At the start of the test, acetate was dosed to an initial concentration of 400 mgCOD/L . Nitrite was dosed at the start of the test to target 25 mgN/L . Once NO_2^- was depleted, NO_3^- was dosed to a target concentration of 15 mgN/L to obtain the specific nitrite and nitrate removal

rates. During the testing, a stand mixer provided adequate mixing to both reactors. The mixing speed was adjusted so that the liquid was adequately mixed while avoiding the creation of a vortex that could entrain air into the liquid. The liquid surface was covered with a floating Styrofoam sheet to further limit the surface transfer of oxygen. Approximately every 20 minutes over the duration of the test, a 15 mL aliquot was removed, filtered and analyzed for NO_3^- -N, NO_2^- -N, NH_4^+ -N. DO was monitored using a Hach LDO 101 probe.

Sample B was four liters of mixed liquor collected from the B-stage of a pilot-scale A/B process operating at 20°C, hydraulic retention time (HRT) of 4 hours and solids retention time (SRT) of approximately 10 days. In this test nitrite and acetate were spiked in the sample while monitoring NO and N_2O as well as DO measurements from the probes listed in Table 5.1. When the DO concentration reached below 0.10 mg/L the reactor was spiked with approximately 25 mg N/L of sodium nitrite and 150 mg COD/L as sodium acetate. The reactor was operated for 2.25 hours and samples were collected at 10 or 15 minute intervals. After 2 hours nitrogen gas was bubbled into the reactor to strip nitric and nitrous oxide and then aerated to compare DO probe readings. All collected samples were filtered through 1.5 μm glass fiber filters and analyzed for NO_3^- -N, NO_2^- -N, NH_4^+ -N, and sCOD. The reactor was continuously mixed through use of a magnetic stir plate. Temperature was controlled by submersion in a water bath to 20°C. The reactor was covered to prevent oxygen transfer. The pH stayed between 6.7 and 7.5.

Table 5.1: List of sensors used in this study

Parameter	Type of Sensor	Model	Manufacturer	Location
Nitric Oxide (NO)	Electrochemical, polarographic	NO-500	Unisense	Aarhus, Denmark
Nitrous Oxide (N_2O)	Electrochemical, polarographic	N_2O -R	Unisense	Aarhus, Denmark
Dissolved Oxygen (DO)	Electrochemical, polarographic	5178	YSI	Yellow Springs, OH, USA
Dissolved Oxygen (DO)	Optical, luminescent	LDO101	Hach	Loveland, CO, USA
Dissolved Oxygen (DO)	Optical, fluorescent	FDO® 70x IQ (SW)	YSI	Yellow Springs, OH, USA
Dissolved Oxygen (DO)	Optical, fluorescent	10	Insite	Slidell, LA, USA

Test in tap water

In this test nitric oxide and nitrous oxide gas were added to tap water to measure the effect of the pure gas on the DO probe measurements. The probes listed in Table 5.1 were placed in a 5L covered reactor with 4L of tap water. The reactor was continuously mixed by a magnetic stir plate. Temperature was controlled by submersion in a water bath to 20°C. First nitric oxide gas (99.9%, Airgas) was bubbled in to the reactor through a diffuser. Then nitrogen gas (99.999%, Airgas) was bubbled through a diffuser to strip the nitric oxide gas. This was repeated again and then nitrous oxide gas (99.99%, Airgas) was bubbled through a diffuser and then stripped using nitrogen gas. The reactor was then aerated to compare DO probe readings in the presence of oxygen.

RESULTS AND DISCUSSION

DO probe interference during denitrification tests

During the denitrification test for Sample A, it appears that the DO readings were affected during the presence of nitrite. Figure 5.1 shows the decreasing nitrite concentration from time zero to approximately 240 minutes and the measured DO response. The probe showed significant DO values over this period despite the reactor not being aerated. Also the DO readings trend with the NO_2^- measurement. During this period the LDO probe was removed several times, washed, and placed in sodium sulfite solution. Each time, the DO would drop rapidly to about 0.1 mg/L. But when the probe was returned to the reactor it exhibited the unexpected high DO response. It is also clear from Figure 5.1 that the presence of NO_3^- does not impact that DO measurement.

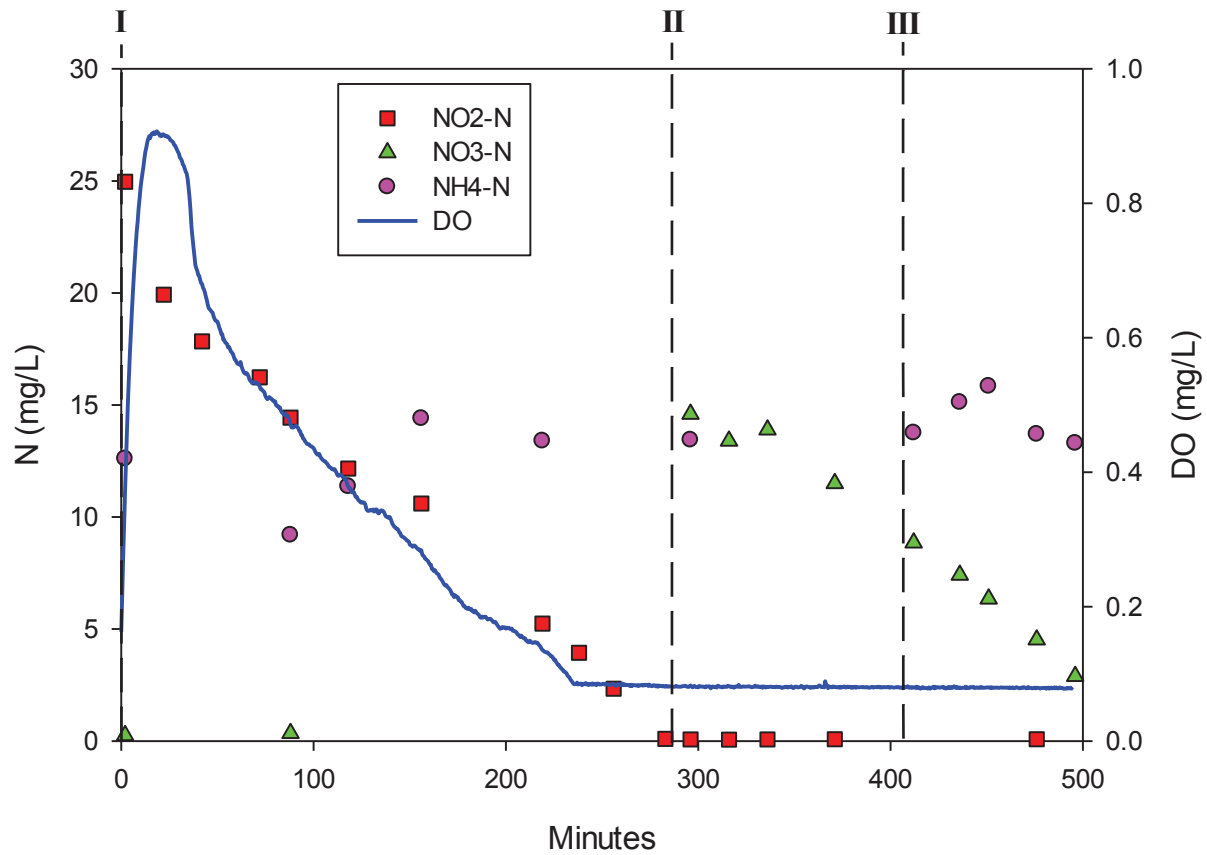


Figure 5.1: Sample A Denitrification Test Nitrogen Measurements and DO Sensor Output. At the beginning of Phase I (time=0) 25 mg/L NO₂-N and 400 mg COD/L of sodium acetate was dosed. At the beginning of Phase II once NO₂ was depleted, 15 mg/L NO₃ was dosed. At the beginning of Phase III 200 mg COD/L of sodium acetate was dosed. There was no aeration during this test.

During the denitrification test for Sample B the NO and N₂O concentrations were measured by online sensors in addition to DO sensor readings. The initial spike of nitrite to the reactor caused an immediate increase in liquid phase NO concentration followed by a slower increase in N₂O concentration (Figure 5.2a). It should be noted that the NO concentration was outside of the range of the calibration (0-42 ug/L-N). However, the important observation is the presence of NO and its effect on the DO sensor. The increase in NO concentration corresponds to an increase in the DO readings of the Hach LDO and YSI FDO probes (Figure 5.2a). When nitrogen gas was sparged in the reactor, the NO was stripped and the DO readings decreased as the NO concentration decreased. NO₃⁻ levels were decreasing in the reactor during the duration of the test however NO₂⁻ and NO were staying constant and N₂O was increasing (Figures 5.2a and 5.2b), so it can be assumed that the denitrification pathway was stopping at N₂O and partial denitrification was occurring (Schulthess et al., 1995). At the end of the test, oxygen was provided to the reactor to demonstrate that all of the probes were functioning properly and DO readings were approximately in agreement. Although both NO and N₂O are listed by the

manufacturer as interfering with the YSI membrane DO probe, the YSI membrane probe did not exhibit the same interference as the Hach LDO and YSI FDO probes. This observation is not necessarily true for all membrane DO probes. Surprisingly the Insite probe did not respond to the high levels of NO even though it uses fluorescent technology similar to the YSI FDO and Hach LDO which did respond to NO. While the cause of this discrepancy is unknown, some potential explanations are differences in: quenching compounds, selectivity of covering membranes, or types of host matrices. Further studies will need to take place to understand, and potentially eliminate, the cause of the interference.

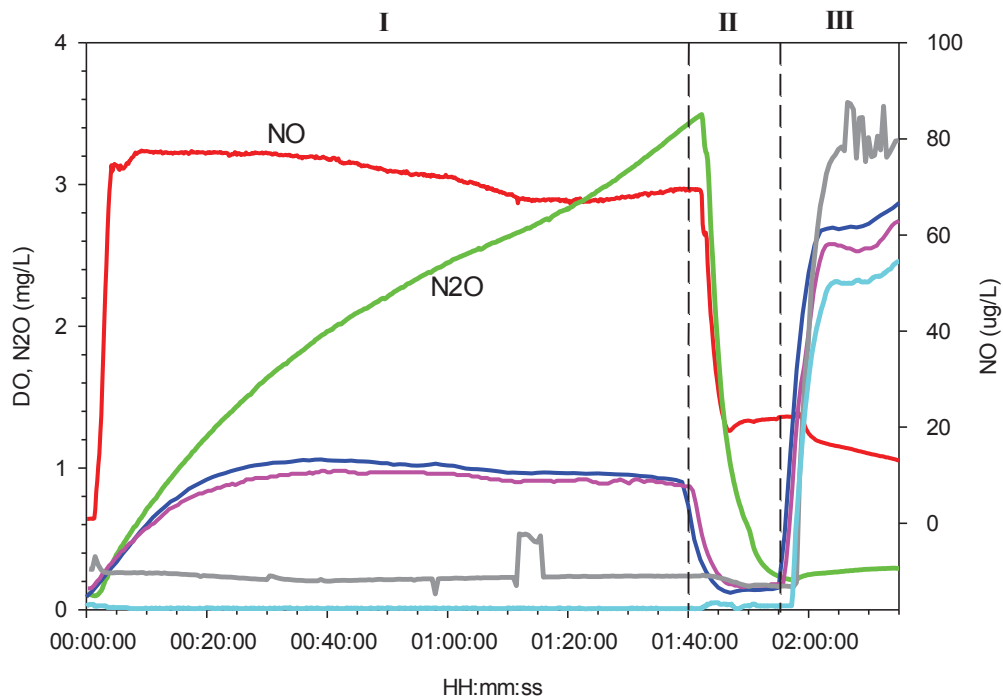


Figure 5.2A: Sensor outputs from Sample B denitrification test. NO (red), N2O (green), Insite DO (cyan), YSI DO (dark blue), YSI membrane (grey), Hach LDO (magenta)

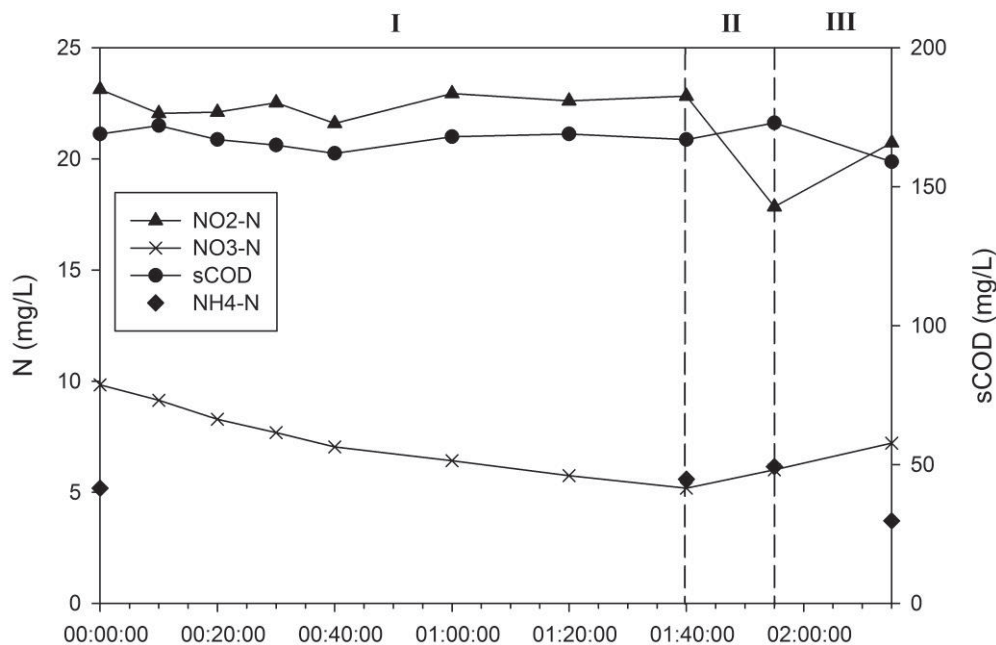


Figure 5.2B: Sample B Denitrification Test Nitrogen and sCOD measurements.
Phase I: No gas sparging; Phase II: Nitrogen gas sparging; Phase III: Air sparging

DO probe interference in tap water with NO and N₂O gas present

The DO readings during the denitrification test appeared to be trending with NO however there was also N₂O present, so an experiment was performed in tap water with just NO or N₂O gas present to demonstrate that NO is the interfering gas and not N₂O. From the results of the test in tap water, it is clear that spikes in the DO readings of the Hach LDO and YSI DO probes occurred with the addition of NO gas and not with the addition of N₂O gas (Figure 5.3). The NO gas also appears to register slightly on the N₂O probe. Again the Insite fluorescent probe and YSI membrane probe were not affected by the presence of NO.

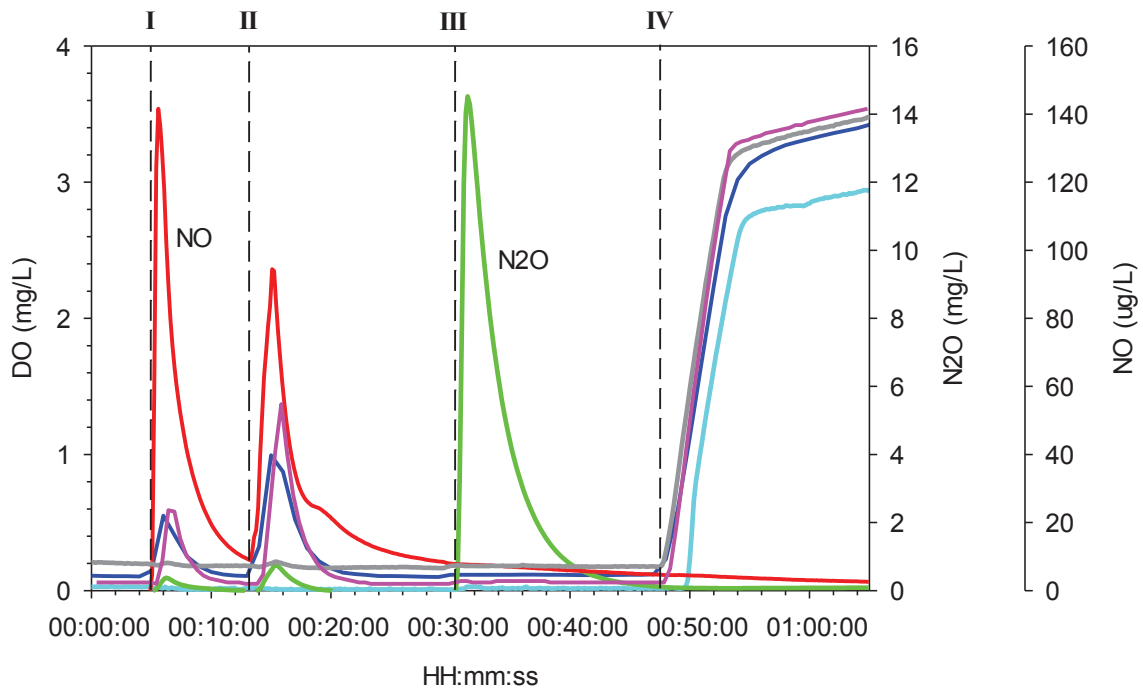


Figure 5.3: Test in Tap Water DO, NO, and N₂O Sensor Outputs. NO (red), N₂O (green), Insite DO (cyan), YSI DO (dark blue), YSI membrane (grey), Hach LDO (magenta). Phases I and II: Spike of NO gas followed by stripping of NO using N₂ gas. Phase III: Spike of N₂O gas followed by stripping of N₂O using N₂ gas. Phase IV: Sparging air

Significance of NO interference on DO measurements in biological nitrogen removal processes

When performing bench-scale denitrification tests, it is important to maintain a completely anoxic sample. If nitric oxide in the sample is causing a falsely high DO reading, the researcher performing the test may come to the incorrect conclusion that either oxygen is getting into the sample, or the DO sensor needs to be replaced. Nitrite concentrations above 25 mg/L (concentration used in this study) are common in sidestream shortcut nitrogen removal processes (Wett and Rauch, 2003; Lackner et al., 2014), and thus DO probe interference may be a concern for full-scale shortcut nitrogen removal processes. In mainstream shortcut nitrogen processes NO₂⁻ levels would not be as high however if operating at low DO (0.2-0.5 mg/L) NO production could potentially have a large effect on DO measurement.

In addition to denitrification bench tests, this phenomenon has also been observed in sidestream shortcut nitrogen removal processes (Wett and Rauch, 2003). The interference with the DO probe was assumed to be associated with high levels of nitrite but the exact mechanism was unknown. These are two examples of DO probe interference in biological nutrient removal processes but there could be other applications in which this interference is occurring such as low DO nitrite shunt processes. Since shortcut nitrogen processes are becoming more popular

and DO probes are crucial to process control, it is critical that any inferences associated with NO_2^- accumulation are understood.

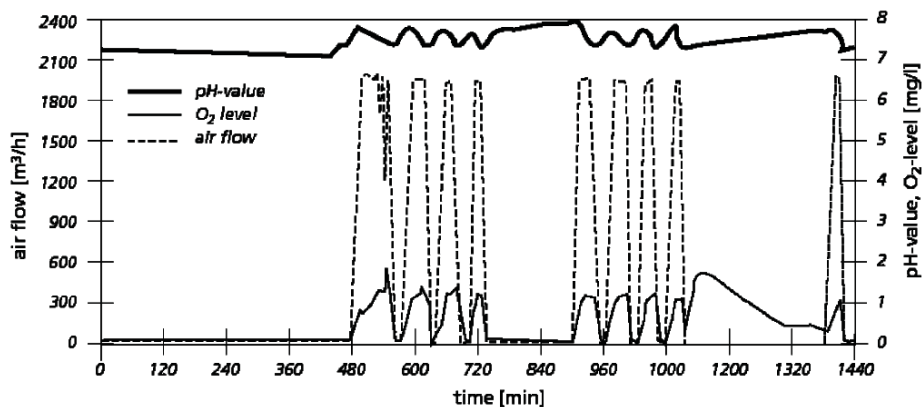


Figure 5.4: pH, DO concentration, and airflow in a sidestream shortcut nitrogen SBR. Republished with permission from Wett and Rauch, 2003.

In an earlier study by Wett and Rauch (2003), it was observed in a full-scale intermittently aerated sidestream SBR performing nitrite shunt that DO probe readings appear to read artificially high immediately after aeration stops (Figure 5.4). This is when NO production would be expected to increase due to transient anoxia and average NO_2^- concentrations of 100 mgN/L (Wett and Rauch, 2003). According to the authors, the increase in DO concentration in the absence of aeration around 1100 minutes was explained as “oxygen sensor was interfered by high NO_x -level during the anoxic settling period” (Wett and Rauch, 2003). A YSI membrane type DO probe was used in this study. In light of data from the present study it seems most likely that the production of NO was the cause of the false DO measurement.

CONCLUSIONS

Based on previous studies, it was determined that NO_2^- accumulation was causing optical DO probes to measure unrealistically high values. This study proves that this interference exists with some optical DO probes but not all. It was also demonstrated that NO_2^- is not directly causing the interference but rather NO is responsible for causing the false DO measurements. The amount of NO produced by a NO_2^- concentration of 25mg/L was enough to cause some DO sensors to read as high as 1 mg/L, even though there was no oxygen present in the sample. This NO_2^- concentration could reasonably be produced in sidestream shortcut nitrogen processes, demonstrating that nitric oxide interference of DO sensor readings is a concern in full-scale processes as well as in bench scale denitrification tests. This phenomenon is not exclusive to the wastewater treatment field and would occur in any aqueous sample when NO is present. Future studies should include quantifying the relationship between NO concentration and DO interference, and determining the mechanism of the interference.

REFERENCES

- Andersen, K., Kjær, T., and Revsbech, N.P. (2001). An oxygen insensitive microsensor for nitrous oxide. *Sensor Actuat. B-Chem.* 81, 42.
- Kampschreur, M.J., van der Star, W.R.L., Wienders, H.A., Mulder, J.W., Jetten, M.S.M., and van Loosdrecht, M.C.M. (2008). Dynamics of nitric oxide and nitrous oxide emission during full-scale reject water treatment. *Water Res.* 42, 812.
- Kampschreur, M.J., Temmink, B.G., Kleerebezem, R., Jetten, M.S.M., and van Loosdrecht, M.C.M. (2009). Nitrous oxide emission during wastewater treatment. *Water Res.* 43, 4093.
- Lackner, S., Gilbert, E., Vlaeminck, S., Joss, A., Horn, H., and van Loosdrecht, M.C.M. (2014). Full-scale partial nitritation/anammox experiences - An application survey. *Water Res.* 55, 292.
- Lee, Y.H., and Tsao, G.T. Dissolved oxygen electrodes. (1979). *Adv. Biochem. Eng.* 13, 35.
- McDonagh, C., Kolle, C., McEvoy, A.K., Dowling, D.L., Cafolla, A.A., Cullen, S.J., and MacCraith, B.D. (2001). Phase fluorometric dissolved oxygen sensor. *Sensor Actuat B-Chem.* 74, 124.
- Ni, B., and Yuan, Z. (2015). Recent advances in mathematical modeling of nitrous oxides emissions from wastewater treatment processes. *Water Res.* 87, 336.
- Schreiber, F., Polerecky, L., and de Beer, D. (2008). Nitric oxide microsensor for high spatial resolution measurements in biofilms and sediments. *Anal. Chem.* 80, 1152.
- Schulthess, R.v., Kühni, M., and Gujer, W. (1995). Release of nitric and nitrous oxides from denitrifying activated sludge. *Water Res.* 29, 215.
- Wett, B., and Rauch, W. (2003). The role of inorganic carbon limitation in biological nitrogen removal of extremely ammonia concentrated wastewater. *Water Res.* 37, 1100.
- Wunderlin, P., Mohn, J., Joss, A., Emmenegger, L., and Siegrist, H. (2012). Mechanisms of N₂O production in biological wastewater treatment under nitrifying and denitrifying conditions. *Water Res.* 46, 1027.

CHAPTER 6: EFFECT OF INFLUENT CARBON FRACTIONATION AND REACTOR CONFIGURATION ON MAINSTREAM NITROGEN REMOVAL AND NOB OUT-SELECTION

Stephanie A. Klaus, Michael S. Sadowski, Maureen N. Kinyua, Mark W. Miller, Pusker Regmi, Bernhard Wett, Haydee De Clippeleir, Kartik Chandran, Charles B. Bott

ABSTRACT

An intermittently aerated, pilot scale biological nitrogen removal process was operated in Modified Lüdbeck Ettinger (MLE) and fully intermittent aeration (all reactors aerated) configurations. The process was fed both A-stage effluent (ASE), and primary clarifier effluent (PCE), which differ in chemical oxygen demand (COD) composition. The objective was to determine the effects of influent carbon fractionation and reactor configuration on nitrite oxidizing bacteria (NOB) out-selection and total inorganic nitrogen (TIN) removal during intermittent aeration. TIN removal was affected by both the type and amount of influent COD, with particulate COD (pCOD) having a stronger influence than soluble COD (sCOD). NOB out-selection was lowest in the MLE configuration, regardless of the feed, and highest in fully intermittent configuration with A-stage feed. During fully intermittent operation with A-stage effluent feed, nitrite accumulation correlated positively with influent particulate COD concentration, and correlated negatively with *ex situ* NOB activity rates. In addition, *ex situ* denitrification batch tests showed that nitrite was consumed faster than nitrate when NOB rates were low. These observations suggested that pCOD improved heterotrophic competition for nitrite, leading to ammonia oxidation rates higher than nitrite oxidation rates. Therefore, the influent COD fractions should be tailored to achieve the desired nitrogen removal goals downstream.

INTRODUCTION

Relative to the practice of conventional full-nitrification (ammonia to nitrate oxidation) followed by denitrification (nitrate reduction to dinitrogen gas, N₂), achieving nitrite shunt (ammonia to nitrite oxidation) is desirable both for decreasing the COD required for denitrification, and for producing an effluent that can be treated by anaerobic ammonia oxidation (anammox). The key to achieving nitrite shunt is the out-selection of nitrite oxidizing bacteria (NOB) while keeping aerobic ammonia oxidizing bacteria (AOB) rates high. NOB out-selection is easier in processes treating internally produced sidestreams, such as post-anaerobic digestion centrate or filtrate, due to the high free ammonia (FA) concentrations in these streams (Anthonisen et al., 1976) as well as their intrinsically high temperature (Hellinga et al., 1998). On the other hand, such factors do not apply to mainstream wastewater such as raw or clarified sewage, owing to the much lower ammonia concentrations and near-ambient temperatures. In mainstream biological nitrogen removal (BNR) processes relying on nitrite-shunt, strategies developed to give AOB an

advantage over NOB in mainstream treatment include: maintaining an ammonia residual in the effluent (Regmi et al., 2014; Pérez et al., 2014; Poot et al., 2016; Welker et al., 2016), transient anoxia (Gilbert et al., 2014; Kornaros et al., 2010), high DO concentration during intermittent aeration (Regmi et al., 2014; Al-Omari et al., 2015), low DO continuous aeration (for biofilm and granule systems) (Pérez et al., 2014; Poot et al., 2016; Sliekers et al., 2005), seeding of AOB from a sidestream process (Al-Omari et al., 2015), stringent aerobic solids retention time (SRT) control (Regmi et al., 2014), and exposure of the mainstream biomass to high levels of nitrous acid (Piculell et al., 2016; Wang et al., 2014). Transient anoxia can be achieved through intermittent aeration either in time (on/off aeration control) or in space (alternating oxic/anoxic zones). The proposed mechanisms of NOB out-selection from transient anoxia include: enzymatic lag (Kornaros et al., 2010), inhibition by intermediates (including nitric oxide and hydroxylamine) (Courtens et al., 2015; Park et al., 2016), and substrate availability (limiting the amount of nitrite available aerobically) (Al-Omari et al., 2015; Malovanyy et al., 2015).

Ammonia vs. NO_x (AvN) control was developed to adapt some of these fundamental concepts into an operational control algorithm, to operationally achieve nitrite shunt (Regmi et al., 2014). AvN control works by controlling the aerobic fraction to meet an NH_4^+ -N to NO_x -N (NO_2^- -N + NO_3^- -N) concentration ratio in the effluent. In addition to transient anoxia the controller uses non-limiting DO, aerobic SRT control, and high residual ammonia concentration to favor AOB activity over NOB. Although AvN control was developed to achieve nitrite shunt through NOB out-selection, AvN control maximizes nitrogen removal efficiency by design, even if the goal is not nitrite shunt. By setting NH_4^+ -N and NO_x -N equal in the effluent, or by specifying a ratio of NH_4^+ -N/ NO_x -N somewhat less than 1:1 based on the need to comply with an effluent ammonia limit, AvN control oxidizes only the amount of ammonia that can be denitrified utilizing the influent organic carbon that is made available. This maximizes COD utilization efficiency for heterotrophic denitrification using nitrate or nitrite, without the addition of supplemental carbon (Batchelor et al., 1983).

As more nitrogen is removed through shortcut nitrogen removal pathways, less carbon is required for chemoorganoheterotrophic denitrification, and more carbon can be diverted, preferably to an anaerobic digester for energy recovery. The removal of carbon can be accomplished physically or biologically. Primary sedimentation tanks should remove from 50 to 70% of the TSS and 20 to 35% of the COD (Tchobanoglous et al., 2003). Another option for carbon removal is a high-rate A-stage biological process. The A-stage process is high-rate activated sludge (HRAS) operated at a low hydraulic retention time (HRT) of about 30 minutes, a low dissolved oxygen (DO) concentration of less or equal to 0.5 mg/L and a low SRT of less than 1 day (Boehnke and Diering, 1997). The goal of the high-rate A-stage is to provide a controlled carbon loading for B-stage, while achieving low cost COD removal at reduced aeration tank volume and aeration energy requirements (Miller et al., 2017). The A-stage process removes both readily biodegradable COD (rbCOD) and slowly biodegradable COD (sbCOD) primarily through sedimentation of primary particles, oxidation of rbCOD, bioflocculation, and

possibly some intracellular storage (Miller et al., 2012; Kinyua et al., 2017; Rahman et al., 2014; Jimenez et al., 2015) while primary clarification removes COD through gravitational settling based on particle size and density. These processes will create effluents with different compositions since A-stage is able to remove rbCOD, while a primary clarifier does not remove soluble and colloidal constituents (Jimenez et al., 2015; de Graaff et al., 2016).

While the effect of aeration (Regmi et al., 2014; Pérez et al., 2014; Poot et al., 2016; Al-Omari et al., 2015; Sliemers et al., 2005), residual ammonia (Regmi et al., 2014; Pérez et al., 2014; Poot et al., 2016; Welker et al., 2016), nitrite concentration (Al-Omari et al., 2015; Malovanyy et al., 2015), and SRT (Regmi et al., 2014; Al-Omari et al., 2015) on NOB out-selection have been extensively studied, the effects of influent carbon fractionation and reactor configuration (i.e. presence of a pre-anoxic zone) have not been examined. It is hypothesized that sbCOD is more desirable in B-stage influent than rbCOD, because it can be utilized for denitrification further downstream in the B-stage reactor. Accordingly, this should lead to increased total inorganic nitrogen (TIN) removal, and potentially increased NOB out-selection through heterotrophic competition for nitrite. The objectives of this study were to: determine the influence of influent COD/NH₄⁺-N ratio on TIN removal, and to determine the effect of operating configurations and influent carbon fractionation on nitrite accumulation and NOB out-selection in an intermittently aerated BNR process

MATERIALS AND METHODS

Pilot Setup

The pilot plant consisted of an HRAS A-stage process, or a primary clarifier, followed by the B-stage process (Figure 6.1). The pilot was fed screened (2.4 mm openings) and degritted municipal wastewater that was first adjusted to 20 degrees C. The A-stage consisted of three bioreactors in series ($V_{total} = 511$ L) followed by an intermediate clarifier. A single modulating valve controlled airflow to the A-stage. A clarifier, separate from the one used in the A-stage process, was operated when the B-stage was fed primary clarify effluent (PCE). Primary clarification was performed in a cone bottom clarifier with a volume of 1170 L at a surface overflow rate (SOR) of 33.2 m³/m²/day and HRT of 1.3 hours. The B-stage consisted of four bioreactors in series ($V_{total} = 606$ L) each with independent aeration control and mechanical mixing. The B-stage system was maintained at a 5-hour HRT. The pilot system was started up without seed, and was operating for three years prior to the beginning of this study.

Operating conditions

B-stage was operated in the following two configurations: 1) a fully intermittent (FI) configuration in which all CSTRs were intermittently aerated for the same interval and duration and 2) a Modified Lüdbeck Ettinger (MLE) configuration in which the first reactor was anoxic, and downstream reactors were intermittently aerated for the same interval and duration (Figure 6.1). The internal mixed liquor recycle (IMLR) rate was constant at 300% of the influent flow

rate. The study compared each aeration strategy with both A-stage effluent (ASE) and primary clarifier effluent (PCE) as influent to the B-stage. The AvN ($\text{NH}_4^+\text{-N}/\text{NO}_x\text{-N}$) ratio setpoint was 1 for the duration of the study. The phases are abbreviated as follows, and were operated in the following order: FI_ASE (87 days), MLE_ASE (45 days), MLE_PCE (39 days), and FI_PCE (20 days).

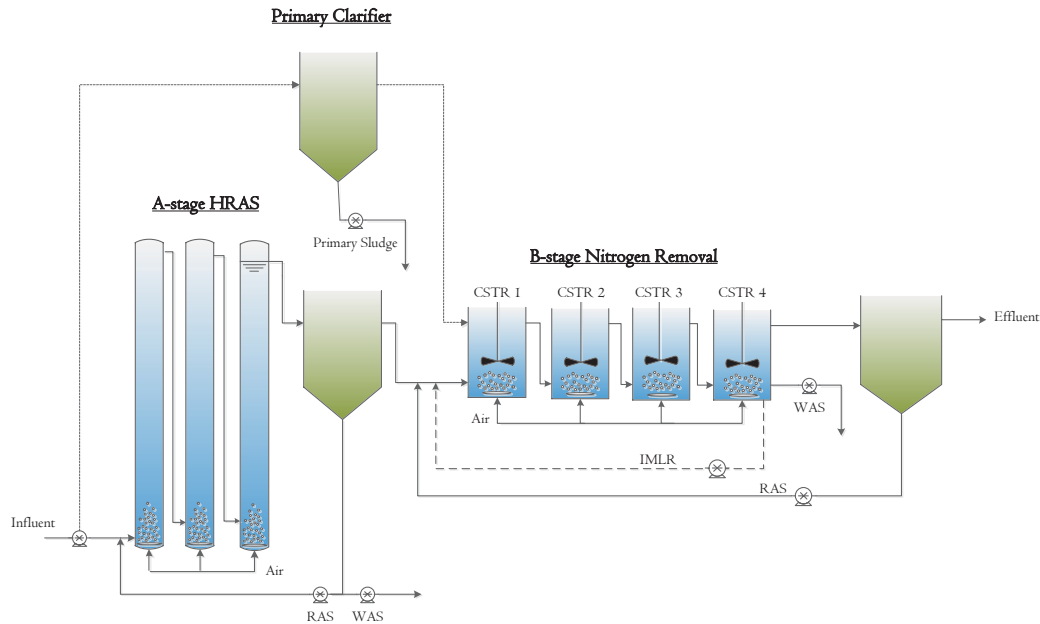


Figure 6.1: Pilot plant configuration. The B-stage was operated with primary clarifier or A-stage effluent. CSTR 1 was anoxic with an internal mixed liquor recycle (IMLR) during MLE configuration.

Automated Process Control

Process automation was achieved using various online sensors and a programmable logic controller (PLC). A-stage aeration control was achieved using a cascade proportional–integral (PI) DO controller, DO sensor (Hach LDO) located in the last bioreactor, mass gas flowmeter, and modulating valve. The A-stage was operated at low DO concentrations (≤ 0.5 mg/L), and an HRT of 30 minutes. The A-stage waste activated sludge (WAS) flow rate was maintained constant and manually changed as needed to obtain the desired COD removal. In the B-stage, the AvN controller, as described in detail by Regmi et al., (2014), consisted of an aeration duration controller that used on-line in situ DO, ammonia, nitrite and nitrate sensors (Hach LDO; WTW VARiON® Plus; s::can spectro::lyser™). In AvN control, the aerobic fraction (air on time divided by total cycle time) was controlled via a proportional–integral–derivative (PID) controller to meet the ($\text{NH}_4^+\text{-N}/\text{NO}_x\text{-N}$) ratio setpoint of 1. During periods of aeration, a DO controller maintained a DO setpoint of 1.6 mg- O_2 /L. Each reactor had a modulating airflow valve and a DO sensor using proportional integral (PI) control to maintain the same DO concentration across all aerated reactors. AvN control was utilized in all phases of the study. pH

was measured in the 3rd CSTR using a ISE Foxboro pH probe (Invensys, London, UK). A stock solution of sodium bicarbonate (80 g NaHCO₃/L) was fed to the third CSTR in order to maintain effluent pH at 6.8.

AOB and NOB Activity Measurements

To measure maximum AOB and NOB activity, once per week a 4 L sample was collected from the 4th CSTR and aerated for 30 minutes to oxidize excess COD. The sample was then spiked with 10,000 mgN/L NH₄Cl and 10,000 mgN/L NaNO₂ stock solutions so that initial concentrations were 20-30 mg NH₄⁺-N/L and 2-4 mg NO₂⁻-N/L respectively. Temperature was controlled at 20°C via submersion in a water bath. The DO concentration was manually maintained between 2.5 and 4 mg/L using diffused compressed air, and DO was measured using a handheld luminescent DO sensor (HACH Loveland, CO). The pH was manually maintained at approximately 7.5 through the addition of sodium bicarbonate. The activity tests were conducted for 1 hour with sample collection every 15 minutes. Samples were analyzed for NH₄⁺-N, NO₂⁻-N, and NO₃⁻-N as described below. The AOB rates were calculated as the slope of the NO_x-N production and NOB rates were calculated as the slope of the NO₃⁻-N production. Calculations explaining how the rates were calculated are located in the Supplementary Information.

Denitrification Rate Measurements

To measure the denitrification rate, batch testing was performed once per week by mixing 2L of RAS from the B-stage secondary clarifier with 2L of either ASE or PCE, which provided the carbon source for denitrification. The mixture was spiked with 20-30 mg-N/L from a dissolved 10,000 mgN/L potassium nitrate solution and 1-3 mg-N/L from a dissolved 10,000 mgN/L sodium nitrite solution. Sampling began when the reactor went anoxic, as measured by a handheld luminescent DO sensor (HACH Loveland, CO). The batch reactor was operated for 1 hour and samples were collected at 15 minute intervals. All collected samples were filtered through 1.5 µm glass fiber filters and analyzed for NO₃⁻-N, NO₂⁻-N, NH₄⁺-N, and sCOD. The batch reactor was continuously mixed through use of a magnetic stir plate. Temperature was controlled by submersion in a water bath. The reactor was covered with a styrofoam lid to minimize oxygen transfer. The pH was manually maintained between 7.0 and 7.5 with the addition of diluted hydrochloric acid or sodium bicarbonate. Just as an imbalance in the AOB and NOB rates creates nitrite accumulation or depletion in the nitrification batch activity test, an imbalance in the denitration rate (NO₃⁻ to NO₂⁻) and denitrition rate (NO₂⁻ to N₂ gas) does the same in the denitrification rate batch test. If denitration and denitrition rates are equal, then the slope of nitrite in the batch test is zero, indicating only full denitrification, no partial denitrification. The nitrate to nitrite (denitration) rate was calculated as the slope of the NO₃⁻-N consumption, and the nitrite to gaseous N (denitrition) rate was calculated as the slope of the NO_x-N consumption. It was assumed in these assays that dinitrogen gas was the main product.

Calculations explaining how the rates were calculated are located in the Supplementary Information and Figure A1.

Microbial Quantification

The abundance of AOB and NOB was quantified using TaqMan quantitative polymerase chain reaction (qPCR). AOB were targeted using the ammonia mono-oxygenase subunit A (*amoA*) gene (Rotthauwe et al., 1997) while NOB were targeted using the *Nitrobacter* 16S rRNA gene (Graham et al., 2007) and *Nitrospira* 16S rRNA gene (Kindaichi et al., 2006). Total bacterial abundance was quantified using eubacterial 16S rRNA gene targeted primers (Ferris et al., 1996). Primer sequences are listed in Table A1. qPCR assays were conducted on a iQ5 real-time PCR thermal cycler (BioRad Laboratories, Hercules, CA). Standard curves for qPCR were generated via serial decimal dilutions of plasmid DNA containing specific target gene inserts. qPCR for standard plasmid DNA and sample DNA were conducted in duplicate and triplicate, respectively. DNA-grade deionized distilled water (Fisher Scientific, MA) was used for non-template controls. Primer specificity and the absence of primer-dimers were confirmed via melt curve analysis of each qPCR profile (Ma et al., 2015; Park et al., 2015).

Analytical Monitoring

Performance was monitored through the collection of 24-hour composite samples using automated samplers. The samplers extracted 250 mL at one-hour intervals allowing average daily influent and effluent characteristics to be measured. Total and volatile suspended solids (TSS and VSS) were analyzed using standard methods 2540D and 2540E respectively (APHA, 2012). MLSS and MLVSS are the TSS and VSS of the mixed liquor suspended solids. Total and soluble COD, orthophosphate (OP), total ammonia nitrogen ($\text{NH}_4^+\text{-N} + \text{NH}_3\text{-N}$), $\text{NO}_2^-\text{-N}$, and $\text{NO}_3^-\text{-N}$ were measured with HACH TNTplus kits and a HACH DR2800 spectrophotometer (HACH Loveland, CO). Nutrient and soluble COD samples were filtered through 0.45 μm and 1.5 μm filters respectively. Particulate COD (pCOD) was calculated as the difference between total COD and sCOD (1.5 μm filtered). The sCOD measurement includes readily biodegradable and colloidal COD fractions. Daily pH and temperature readings of the reactors were recorded using a handheld pH and temperature meter (Beckman Coulter, Brea, CA). Readings for DO were recorded using a handheld luminescent DO sensor (HACH Loveland, CO).

RESULTS AND DISCUSSION

Overall operation

The A-stage SRT ranged from 1 to 7 hours with an average of 3.1 ± 1.1 hours, and was controlled by manually adjusting the wasting rate throughout the ASE feed scenarios, to vary the total COD/ $\text{NH}_4^+\text{-N}$ ratio. The variation in A-stage SRT produced a range of effluent tCOD/ $\text{NH}_4^+\text{-N}$ values from 7 to 15 g/g with an average of 10.7 ± 1.8 . During the PCE scenarios, the total COD varied due to changes in raw influent total COD, but the effluent characteristics

cannot be controlled in the same way as with an A-stage process (Miller et al., 2012; Haider et al., 2003). Throughout the entire study period, the raw influent characteristics (influent for either A-stage or the primary clarifier) were tCOD of 600 ± 109 mg/L, sCOD of 208 ± 28 , and NH_4^+ -N of 32.9 ± 3.6 . For ASE, both the pCOD and sCOD fraction varied, while for PCE only the pCOD fraction varied since sCOD is minimally removed (Figure A2). The average tCOD/ NH_4^+ -N ratio for PCE was higher than ASE (11.3 ± 1.1 and 10.7 ± 1.8 respectively; $p=0.02$), as was the magnitude of tCOD and NH_4^+ -N. Total COD and NH_4^+ -N for PCE was 418 ± 32 mgCOD/L and 37.1 ± 1.8 mgN/L, while it was 311 ± 58 mgCOD/L and 29.1 ± 2.2 mgN/L for ASE. NH_4^+ -N was lower in the ASE due to higher heterotrophic assimilation, which is a benefit of an A-stage over a primary clarifier (Miller et al., 2012). Because of the higher COD in the PCE, the B-stage total SRT had to be lower to keep the MLSS within the target range of 2000 to 4000 mg/L (Table 6.1). The AvN ratio (NH_4^+ -N/ NO_x -N) setpoint throughout the study was 1, and the average AvN ratio from composite samples of the effluent was 0.97 ± 0.3 . The highest nitrite concentrations occurred during the fully intermittent aeration phases (Figure A3). It has been previously suggested that in general, for a given total bioreactor volume, there is an optimum aerated fraction for which total nitrogen removal can be maximized (Batchelor et al., 1983). In this study, for the fully intermittent scenarios, the minimum effluent TIN occurred between an aerobic fraction of 0.4 and 0.5 (Figure A4), which agreed with the results from Batchelor (1983) (minimum effluent TIN at an aerobic fraction of 0.47). Throughout all phases the aerobic SRT remained in the range of 3 to 4 days (Table 6.1). This is within the aerobic SRT range that some NOB out-selection would be expected at 20°C^2 .

Table 6.1: Operational parameters for all phases. The aerobic fraction is the fraction of aerated volume out of the total volume. For the MLE scenarios, the aerobic fraction in parentheses is the aerated fraction in just the aerated tanks, excluding the anoxic zone.

Control Strategy	A-stage Effluent (ASE)		Primary Clarifier Effluent (PCE)	
	MLE	FI	MLE	FI
Total SRT (days)	7.1 ± 1.9	7.9 ± 2.1	5.7 ± 1.2	5.3 ± 0.7
Aerobic SRT (days)	3.0 ± 0.8	3.7 ± 1.1	3.0 ± 1.0	2.9 ± 0.7
Aerobic Fraction (-)	0.43 ± 0.04 (0.56 ± 0.10)	0.47 ± 0.05	0.52 ± 0.09 (0.70 ± 0.12)	0.52 ± 0.07
MLSS (mg/L)	2967 ± 377	2610 ± 595	4232 ± 279	4051 ± 339
MLVSS/MLSS ratio (g/g)	0.84 ± 0.03	0.85 ± 0.02	0.81 ± 0.01	0.81 ± 0.01

Effect of influent C/N ratio on TIN removal

There was not an obvious relationship between TIN removal percentages and operating scenarios, rather there appeared to be an overall trend between influent COD/ $\text{NH}_4^+\text{-N}$ and TIN removal across all scenarios (Figure 6.2A and 6.2B). Figure 6.2A shows an increase in TIN removal, for an increasing tCOD/ $\text{NH}_4^+\text{-N}$ ratio, up to a certain point (around 10 g/g), after which the COD stops providing additional nitrogen removal benefits. The trend is clearer when plotting just the pCOD/ $\text{NH}_4^+\text{-N}$ (Figure 6.2B), and there is no trend with sCOD/ $\text{NH}_4^+\text{-N}$ (Figure 6.2C), suggesting that influent pCOD is the COD fraction contributing most to downstream TIN removal. The FI_ASE scenario was capable of achieving higher TIN removal than the MLE scenarios. This is further evidence of the importance of pCOD since the anoxic periods of intermittent aeration were able to achieve the same amount of denitrification as the anoxic zone at 300% internal recycle. The MLE_ASE scenario did appear to have higher TIN removal than FI_ASE at the lower total COD/ $\text{NH}_4^+\text{-N}$ values (Figure 6.2A), but by looking at Figure 6.2B it appears that is a function of the influent pCOD/N.

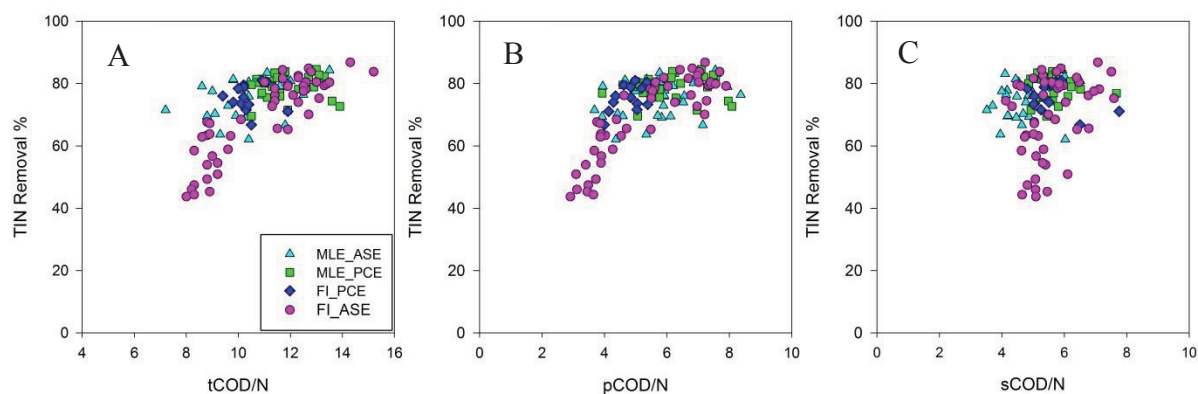


Figure 6.2: % TIN removal vs. tCOD/ $\text{NH}_4\text{-N}$ (A), pCOD/ $\text{NH}_4\text{-N}$ B), and sCOD/ $\text{NH}_4\text{-N}$ (C) in the B-stage influent

This could be due to sCOD being utilized first (for denitrification or oxidized aerobically), while pCOD is used further down the process during anoxic periods for denitrification after it is hydrolyzed (Drewnowski and Makinia, 2011). While this has been previously hypothesized, and the influent tCOD/ $\text{NH}_4^+\text{-N}$ ratio has been shown to correlate positively with TIN removal during intermittent aeration (Regmi et al., 2015), this study directly demonstrates this relationship (Figures 6.2A-C). These trends should hold true for any intermittently aerated process and highlight an opportunity to capture this excess COD upstream and redirect it to an energy recovery process, like anaerobic digestion. These results strongly emphasize that primary effluent COD fractionation, not just the total COD load, should be considered in design and operation of the carbon removal stage. A-stage provides an advantage in that it can be easily controlled to achieve a desired effluent tCOD/ $\text{NH}_4^+\text{-N}$ ratio, while also removing sCOD.

Effect of influent COD fractionation on nitrite accumulation

Nitrite accumulation ratio (NAR) was calculated as $\text{NO}_2^- \text{-N} / \text{NO}_x \text{-N}$ in B-stage effluent and is an indicator of NOB out-selection (Regmi et al., 2014; Pérez et al., 2014; Kornaros et al., 2010). The MLE scenarios had the lowest nitrite accumulation (maximum of 25%), regardless of influent characteristics (Figure 6.3). There was clear nitrite accumulation in the FI_ASE scenario (maximum of 70%), but not as much during the FI_PCE scenario (maximum of 35%). Although it appears that NAR was trending up when the FI_PCE scenario was ended (Figure 6.3), the FI_PCE scenario was too short to draw a clear conclusion between FI_ASE and FI_PCE. Higher nitrite accumulation could also be due to the difference in ASE vs. PCE influent feed characteristics. As discussed previously, the amount of pCOD in the influent to B-stage determined the magnitude of TIN removal (Figure 6.2B), and also seemed to correlate positively with nitrite accumulation during the FI_ASE phase (Figure 6.3).

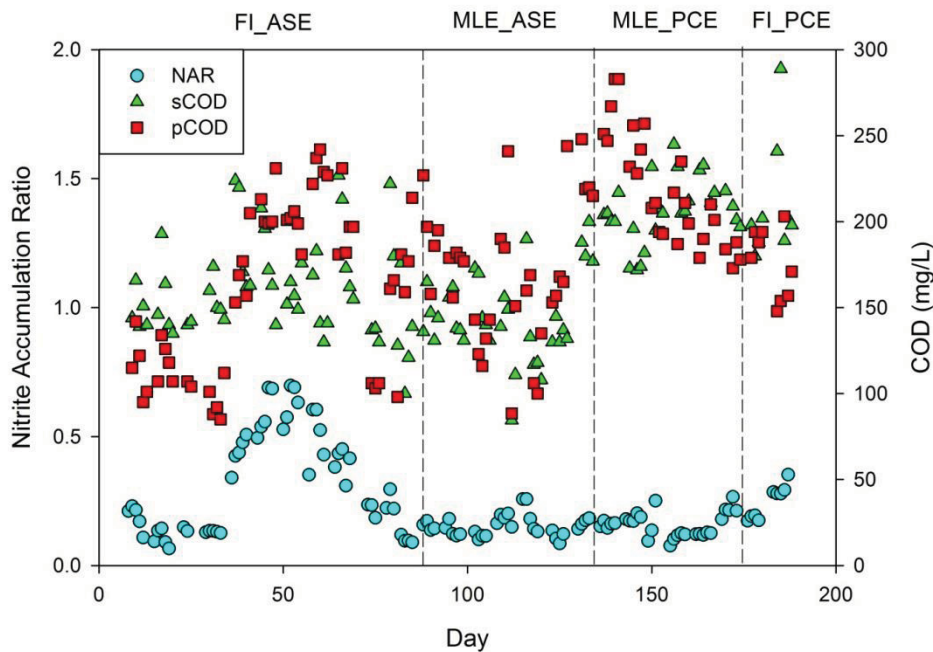


Figure 6.3: Soluble COD, particulate COD, and nitrite accumulation ratio over time

Correlations between sCOD and pCOD and NAR were examined to further elucidate the relationship between influent COD fractions and NAR (Figures 6.4A-D). Fully intermittent scenarios are shown in 4A and 4B and MLE scenarios in 4C and 4D. During the FI_ASE scenario, the influent pCOD fraction correlated positively ($R^2=0.75$, $p=3.6 \times 10^{-15}$) with NAR (Figure 6.4A). There was not a correlation between NAR and pCOD for the FI_PCE phase, possibly because it was not operated long enough. The increased pCOD fraction likely helped to favor heterotrophic competition for nitrite with NOB during transition to non-aerated periods. There was no significant correlation between sCOD and NAR ($p=0.82$) for the FI scenarios

(Figure 6.4B), or between pCOD or sCOD and NAR ($p=0.55$ and $p=0.75$) for the MLE scenarios (Figures 6.4C and 6.4D).

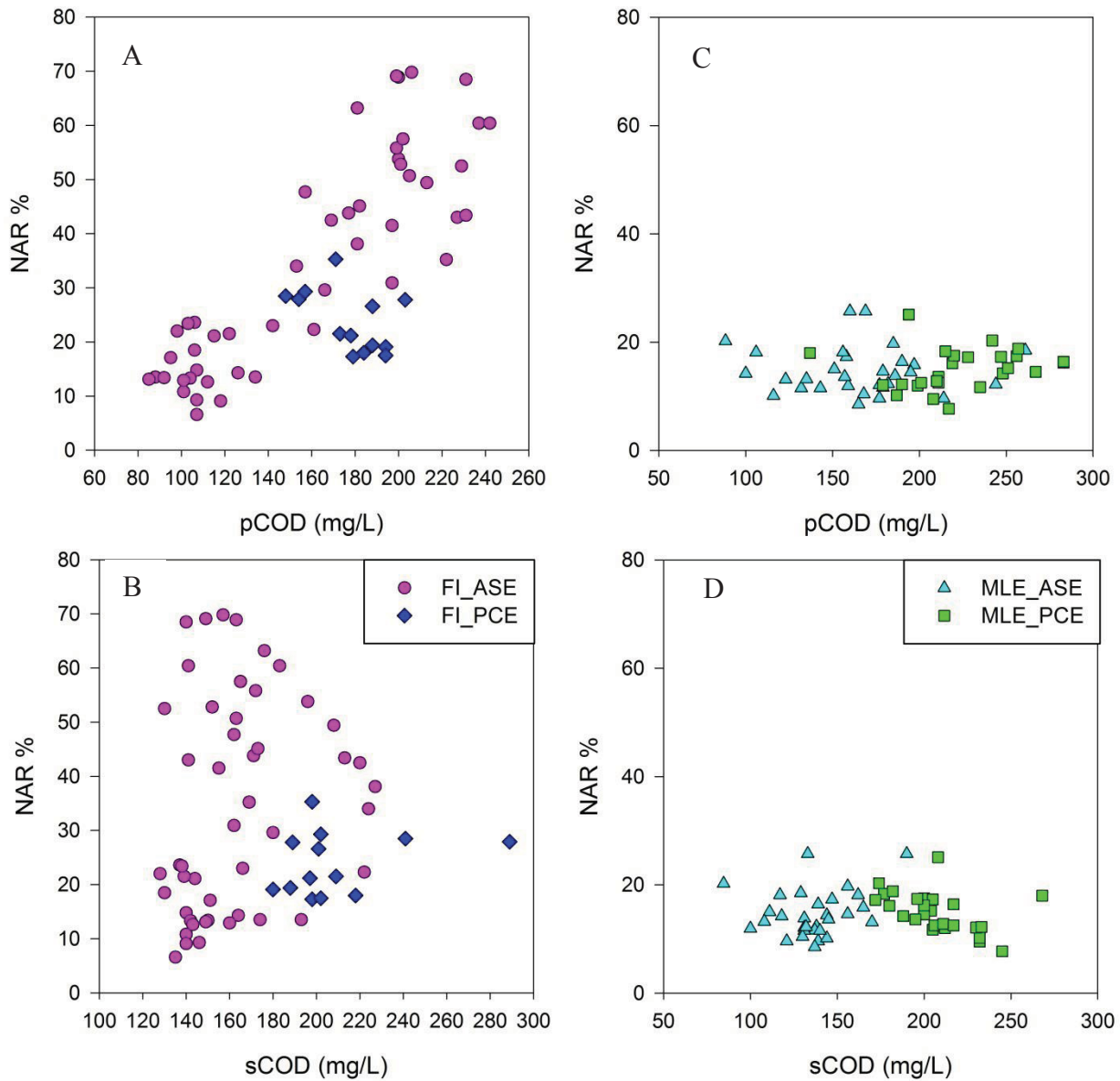


Figure 6.4: Correlation between pCOD and sCOD (mg/L) and nitrite accumulation ratio (NAR%), separated by fully intermittent (FI) (A and B) and MLE configurations (C and D).

It is challenging to explain why the FI aeration scenarios resulted in more NOB out-selection than the MLE scenarios. Three possible reasons include:

1. **Utilization of COD in an upfront anoxic versus intermittently aerated zone.** The COD that could help provide heterotrophic competition in the intermittently aerated zones, may

have been utilized in the anoxic zone for denitrification. Since the hydrolysis rate and hydrolysable COD were not quantified, the fate of the influent COD in the anoxic zone can be inferred from the amount of denitrification taking place. During the MLE scenarios, the IMLR rate was held constant at 300% of the influent flow. Due to lower influent COD during MLE_ASE, the anoxic reactor was typically COD limited (i.e. there was measurable NO_x in the effluent), while during MLE_PCE, the anoxic zone was mostly NO_x limited (i.e. low or non-detect NO_x). Average NO_x grab samples from the effluent of the anoxic zone were 0.21±0.05 mgN/L during MLE_PCE and 0.65±0.89 mgN/L (range 0.11-3.36 mgN/L) during MLE_ASE. While these results could suggest that during the MLE_ASE scenario, there was not enough COD persisting through to provide heterotrophic competition in the intermittently aerated reactors, the same cannot be argued for the MLE_PCE scenario. Also, if it is assumed that it was mostly the sCOD fraction used for denitrification in the anoxic zone, then this should not affect the amount of pCOD making it to the intermittently aerated zones.

2. **Difference in aerobic fraction in the aerated reactors between scenarios.** The aerobic fraction in the last three reactors had to be higher in the MLE configurations in order to maintain the NH₄⁺-N/NO_x-N ratio (Table 6.1). The higher aerobic fraction may not have provided an anoxic period long enough to permit effective heterotrophic competition for nitrite with NOB or to initiate a lag in NOB response (due to a lag in the activity of the nitrite oxidoreductase enzyme in NOB) once the aerobic period returned (Gilbert et al., 2014; Malovanyy et al., 2015). A longer aerobic period could also allow more time to oxidize nitrite to nitrate.
3. **Competitive advantage of NOB over AOB in anoxic zone due to diverse metabolism.** NOB could have an advantage over AOB in the anoxic zone due to their mixotrophic metabolism, allowing them to utilize both organic and inorganic substrates for growth (Steinmüller et al., 1976; Smith and Hoare 1968). This could make it more difficult to out-select NOB when an anoxic zone with sCOD is present, such as in the MLE scenarios.

Relationship between Nitrite Accumulation, NOB rates, and nitrite reduction rates

In addition to nitrite accumulation, another indicator of NOB out-selection was AOB rates higher than NOB rates in bench scale maximum activity tests. NOB/AOB maximum activity rate ratios are shown in Figure 6.5, with lower values indicating more NOB out-selection. NAR correlated negatively with the NOB/AOB rate ratio ($R^2=0.75$, $p=2.4 \times 10^{-8}$) as expected. Also shown on Figure 6.5 are the (NO₂⁻-N denitrification rates)/(NO₃⁻-N denitrification rates) from bench scale maximum activity tests. NO₃⁻-N denitrification refers to the conversion of NO₃⁻-N to NO₂⁻-N (denitration), and NO₂⁻-N denitrification refers to the conversion of NO₂⁻-N to gaseous N (denitritation). When the (NO₂⁻-N denitrification rate)/(NO₃⁻-N denitrification rate) is greater than one, it means that the conversion of nitrite to gaseous N is faster than conversion the nitrate to nitrite. Interestingly, the (NO₂⁻-N denitrification rate)/(NO₃⁻-N denitrification rate) ratio correlated negatively with the NOB/AOB rate ratio (Figure 6.5). In other words, when there was

nitrite accumulation in the batch nitrification tests, there was nitrite depletion during the denitrification tests, and vice versa. Also of note is that the specific NO_2^- -N denitrification rate was greater than the NOB specific rate during the period of high NAR (Figure A5). This observation correlates with the increase in pCOD during that time of operation and thus supports the theory of competition for nitrite by chemoorganoheterotrophic denitrification leading to NOB out-selection. Lemaire et al., (2008) demonstrated through a model based study of a step-feed SBR, that NOB out-selection was established by gradual reduction of the amount of nitrite that is available to provide energy for the growth of NOB. They hypothesized that NOB were out-selected due to the denitrification of nitrite, rather than due to the inhibition of NOB growth kinetics. Dold et al., (2015) modeled nitrite shunt in an SBR and came to a similar conclusion: that nitrite removed by heterotrophic denitrification means less nitrite is available for NOB, reducing the growth of NOB. This would create a cycle over time, where more nitrite is accumulating while NOB population is declining. Ge et al., 2014 had a similar hypothesis for observing NOB out-selection in an alternating aerobic/anoxic step-feed process.

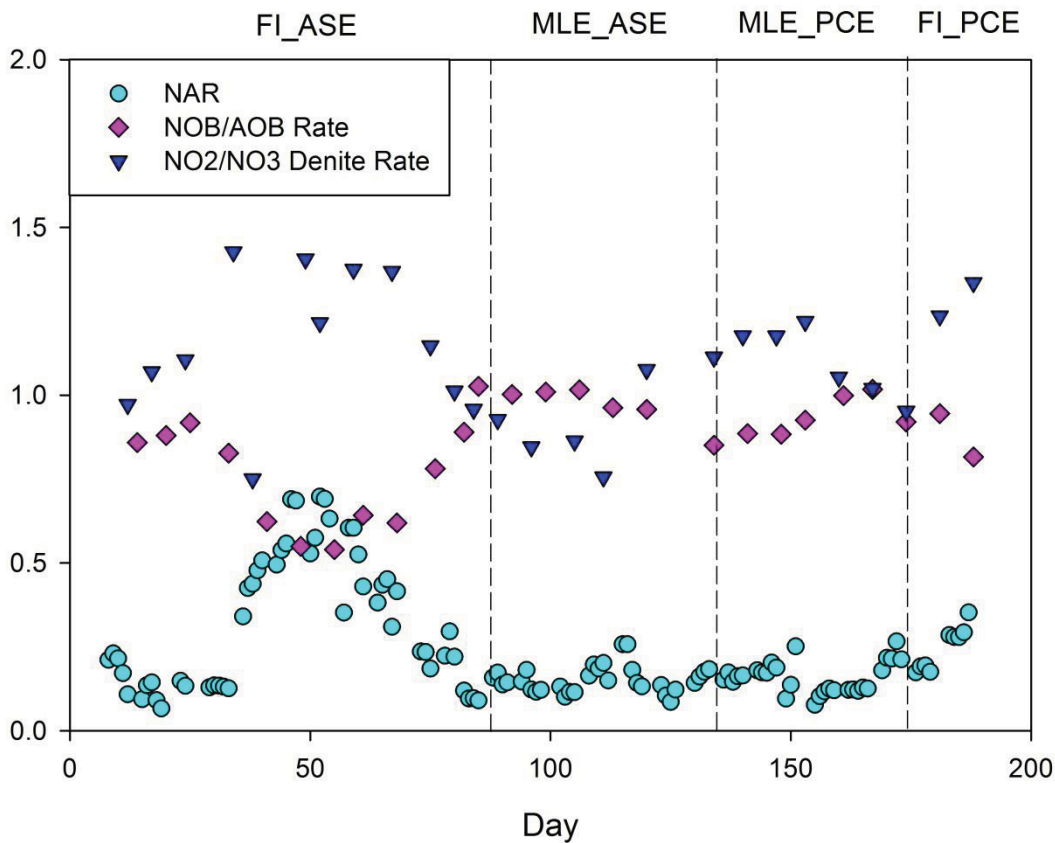


Figure 6.5: Comparison of NOB divided by AOB rate and NO_2 denitrification rate divided by NO_3 denitrification rate from ex-situ maximum activity rate testing, and nitrite accumulation ratio (NAR).

Microbial Ecology

qPCR results showed that the decrease in *Nitrospira* population occurred during periods of nitrite accumulation (Figure 6.6). However, *Nitrospira* population was at least an order of magnitude less than *Nitrobacter*, which stayed high even during periods of nitrite accumulation. Regmi et al. (2014) observed *Nitrospira* concentration was greater than *Nitrobacter* under similar influent characteristics and reactor configuration to this study. During the period of highest nitrite accumulation, the NOB population was greater than the AOB population, even though NOB activity rates were lower than AOB activity rates. These results show that biomass concentrations alone cannot always explain process behavior. In this case, *ex-situ* activity measurements showed that there was an imbalance in process rates causing nitrite accumulation. Multiple reactions need to be taken into account since nitrite is impacted by both nitrification and denitrification processes (biomass concentrations and specific rates). The occurrence of Comammox (Daims et al., 2015) (complete ammonia oxidation to nitrate) by some *Nitrospira* was not included in the targeted microbial analysis and it is unclear how Comammox would influence maximum NOB/AOB activity rate tests.

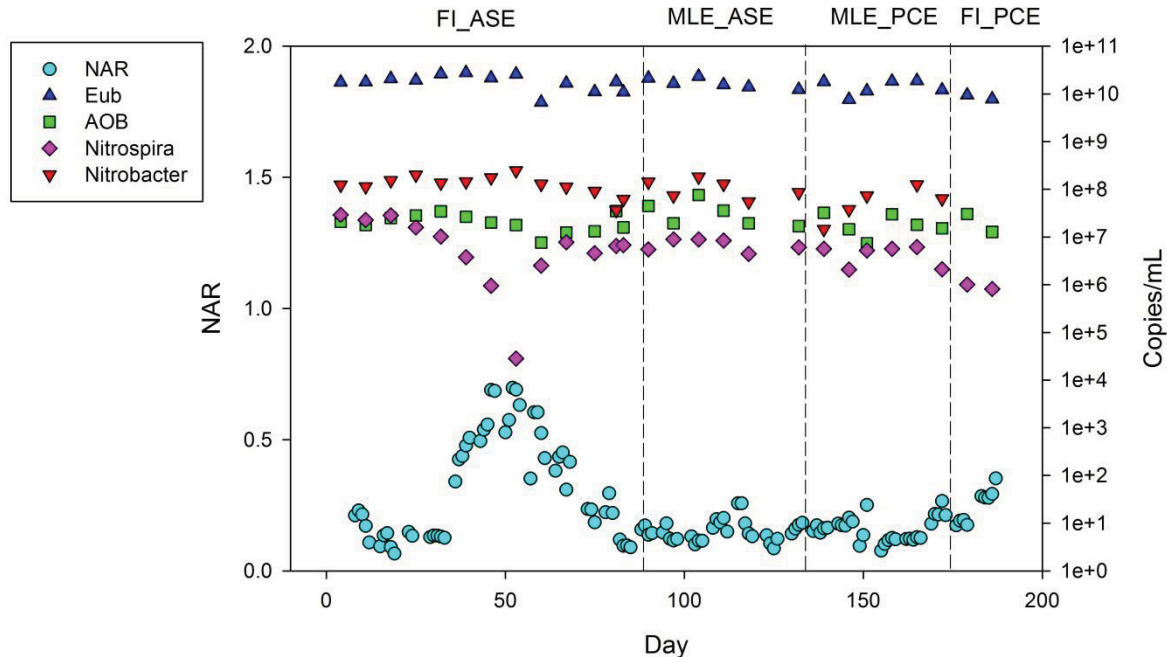


Figure 6.6: Prevalence of AOB and NOB (*Nitrobacter* and *Nitrospira*), and nitrite accumulation ratio (NAR) over time.

IMPLICATIONS FOR IMPLEMENTATION

This work is significant for its primary elucidation of the link between specific COD fractions and implications on both autotrophic nitrogen oxidation and heterotrophic nitrogen reduction, conducted using real wastewater. From these results it appears that fully intermittent aeration without a pre-anoxic zone was a prerequisite to NOB out-selection, and then a higher pCOD increases nitrite accumulation. The effluent nitrite could then be removed, along with effluent ammonia, by an anammox process. The claim that higher COD is beneficial for NOB out-selection may seem contradictory, as it could potentially negate the carbon saving benefit of achieving nitrite shunt. However, the NOB out-selection was correlated specifically with the influx and utilization of particulate COD by nitrite reducing denitrifying bacteria. Therefore, by utilizing an A-stage process, the magnitude of pCOD reaching the B-stage process can be carefully controlled, while still diverting carbon for energy and B-stage capacity savings. By this logic, a step-feed process should enhance the controlled distribution of pCOD even further, especially if it could be fed solely during the anoxic periods of intermittent aeration. By the same logic, chemically enhanced primary treatment would be the least desirable, as it would remove more particulate COD while leaving behind the soluble fraction. These results also point to the difference between achieving nitrite shunt in mainstream versus sidestream processes. Fully autotrophic sidestream processes rely on high free ammonia concentrations and temperature to favor AOB growth over NOB. Mainstream processes don't have the advantage of typical sidestream conditions, so while AOB rates must still be kept high, perhaps the main mechanism for NOB out-selection, in the absence of a large inventory of anammox activity, becomes consumption of nitrite by ordinary heterotrophs for denitrification.

Acknowledgements

The authors thank the Hampton Roads Sanitation District (HRSD) for providing the facilities and equipment for this research. They also thank Zheqin Li for their contribution to the molecular work. This publication was made possible by USEPA grant RD-83556701-1 and WERF grant number INFR6R11. Its contents are solely the responsibility of the grantee and do not necessarily represent the official views of the USEPA and WERF. Further, USEPA and WERF do not endorse the purchase of any commercial products or services mentioned in the publication.

REFERENCES

- Al-Omari, A., Wett, B., Nopens, I., De Clippeleir, H., Han, M., Regmi, P., ... Murthy, S. (2015). Model-based evaluation of mechanisms and benefits of mainstream shortcut nitrogen removal processes. *Water Science and Technology*, 71(6), 840–847.
<https://doi.org/10.2166/wst.2015.022>

- Anthonisen, A. C., Loehr, R. C., Prakasam, T. B. S., & Srinath, E. G. (1976). Inhibition of nitrification by ammonia and nitrous acid. *Journal (Water Pollution Control Federation)*, 835–852.
- Batchelor Bill. (1983). Simulation of Single-Sludge Nitrogen Removal. *Journal of Environmental Engineering*, 109(1), 1–16. [https://doi.org/10.1061/\(ASCE\)0733-9372\(1983\)109:1\(1\)](https://doi.org/10.1061/(ASCE)0733-9372(1983)109:1(1))
- Boehnke, D. B., & Diering, D. B. (1997). Cost-effective wastewater treatment process for removal of... *Water Engineering & Management*, 144(5), 30–34.
- Courtens, E. N. P., De Clippeleir, H., Vlaeminck, S. E., Jordaens, R., Park, H., Chandran, K., & Boon, N. (2015). Nitric oxide preferentially inhibits nitrite oxidizing communities with high affinity for nitrite. *Journal of Biotechnology*, 193, 120–122. <https://doi.org/10.1016/j.jbiotec.2014.11.021>
- Daims, H., Lebedeva, E. V., Pjevac, P., Han, P., Herbold, C., Albertsen, M., ... Wagner, M. (2015). Complete nitrification by Nitrospira bacteria. *Nature*, 528(7583), 504–509. <https://doi.org/10.1038/nature16461>
- de Graaff, M. S., van den Brand, T. P. H., Roest, K., Zandvoort, M. H., Duin, O., & van Loosdrecht, M. C. M. (2016). Full-Scale Highly-Loaded Wastewater Treatment Processes (A-Stage) to Increase Energy Production from Wastewater: Performance and Design Guidelines. *Environmental Engineering Science*, 33(8), 571–577. <https://doi.org/10.1089/ees.2016.0022>
- Dold, P., Du, W., Burger, G., & Jimenez, J. (2015). Is Nitrite-Shunt Happening in the System? Are NOB Repressed? *Proceedings of the Water Environment Federation*, 2015(13), 1360–1374.
- Drewnowski, J., & Makinia, J. (2011). The role of colloidal and particulate organic compounds in denitrification and EBPR occurring in a full-scale activated sludge. *Water Science and Technology*, 63(2), 318–324. <https://doi.org/10.2166/wst.2011.056>
- Ferris, M. J., Muyzer, G., & Ward, D. M. (1996). Denaturing gradient gel electrophoresis profiles of 16S rRNA-defined populations inhabiting a hot spring microbial mat community. *Applied and Environmental Microbiology*, 62(2), 340–346.
- Ge, S., Peng, Y., Qiu, S., Zhu, A., & Ren, N. (2014). Complete nitrogen removal from municipal wastewater via partial nitrification by appropriately alternating anoxic/aerobic conditions in a continuous plug-flow step feed process. *Water Research*, 55, 95–105. <https://doi.org/10.1016/j.watres.2014.01.058>
- Gilbert, E. M., Agrawal, S., Brunner, F., Schwartz, T., Horn, H., & Lackner, S. (2014). Response of Different Nitrospira Species To Anoxic Periods Depends on Operational DO.

- Environmental Science & Technology*, 48(5), 2934–2941.
<https://doi.org/10.1021/es404992g>
- Graham, D. W., Knapp, C. W., Van Vleck, E. S., Bloor, K., Lane, T. B., & Graham, C. E. (2007). Experimental demonstration of chaotic instability in biological nitrification. *The ISME Journal*, 1(5), 385–393. <https://doi.org/10.1038/ismej.2007.45>
- Haider, S., Svardal, K., Vanrolleghem, P. A., & Kroiss, H. (2003). The effect of low sludge age on wastewater fractionation (SS, SI). *Water Science and Technology*, 47(11), 203–209. <https://doi.org/10.2166/wst.2003.0606>
- Hellinga, C., Schellen, A., Mulder, J. W., van Loosdrecht, M. v., & Heijnen, J. J. (1998). The SHARON process: An innovative method for nitrogen removal from ammonium-rich waste water. *Water Science and Technology*, 37(9), 135–142.
- Jimenez, J., Miller, M., Bott, C., Murthy, S., De Clippeleir, H., & Wett, B. (2015). High-rate activated sludge system for carbon management – Evaluation of crucial process mechanisms and design parameters. *Water Research*, 87, 476–482. <https://doi.org/10.1016/j.watres.2015.07.032>
- Kindaichi, T., Kawano, Y., Ito, T., Satoh, H., & Okabe, S. (2006). Population dynamics and in situ kinetics of nitrifying bacteria in autotrophic nitrifying biofilms as determined by real-time quantitative PCR. *Biotechnology and Bioengineering*, 94(6), 1111–1121. <https://doi.org/10.1002/bit.20926>
- Kinyua, M. N., Miller, M. W., Wett, B., Murthy, S., Chandran, K., & Bott, C. B. (2017). Polyhydroxyalkanoates, triacylglycerides and glycogen in a high rate activated sludge A-stage system. *Chemical Engineering Journal*, 316, 350–360. <https://doi.org/10.1016/j.cej.2017.01.122>
- Kornaros, M., Dokianakis, S. N., & Lyberatos, G. (2010). Partial Nitrification/Denitrification Can Be Attributed to the Slow Response of Nitrite Oxidizing Bacteria to Periodic Anoxic Disturbances. *Environmental Science & Technology*, 44(19), 7245–7253. <https://doi.org/10.1021/es100564j>
- Lackner, S., Welker, S., Gilbert, E. M., & Horn, H. (2015). Influence of seasonal temperature fluctuations on two different partial nitrification-anammox reactors treating mainstream municipal wastewater. *Water Science and Technology*, 72(8), 1358–1363. <https://doi.org/10.2166/wst.2015.301>
- Lemaire, R., Marcelino, M., & Yuan, Z. (2008). Achieving the nitrite pathway using aeration phase length control and step-feed in an SBR removing nutrients from abattoir wastewater. *Biotechnology and Bioengineering*, 100(6), 1228–1236. <https://doi.org/10.1002/bit.21844>

- Ma, Y., Sundar, S., Park, H., & Chandran, K. (2015). The effect of inorganic carbon on microbial interactions in a biofilm nitrification–anammox process. *Water Research*, *70*, 246–254. <https://doi.org/10.1016/j.watres.2014.12.006>
- Malovanyy, A., Yang, J., Trela, J., & Plaza, E. (2015). Combination of upflow anaerobic sludge blanket (UASB) reactor and partial nitrification/anammox moving bed biofilm reactor (MBBR) for municipal wastewater treatment. *Bioresour Technol*, *180*, 144–153. <https://doi.org/10.1016/j.biortech.2014.12.101>
- Miller, M. W., Bunce, R., Regmi, P., Hingley, D. M., Kinnear, D., Murthy, S., ... Bott, C. B. (2012). A/B process pilot optimized for nitrite shunt: High rate carbon removal followed by BNR with ammonia-Based cyclic aeration control. *Proceedings of the Water Environment Federation*, *2012*(10), 5808–5825.
- Miller, M. W., Elliott, M., DeArmond, J., Kinyua, M., Wett, B., Murthy, S., & Bott, C. B. (2017). Controlling the COD removal of an A-stage pilot study with instrumentation and automatic process control. *Water Science and Technology*, *75*(11), 2669–2679. <https://doi.org/10.2166/wst.2017.153>
- Park, H., Sundar, S., Ma, Y., & Chandran, K. (2015). Differentiation in the microbial ecology and activity of suspended and attached bacteria in a nitrification-anammox process. *Biotechnology and Bioengineering*, *112*(2), 272–279. <https://doi.org/10.1002/bit.25354>
- Park, M.R.; Chandran, K. Impact of Hydroxylamine Exposure on Anabolism and Catabolism in Nitrospira Spp. In *Proceedings of WEF/IWA Nutrient Removal and Recovery, Denver, USA*; 2016.
- Pérez, J., Lotti, T., Kleerebezem, R., Picioreanu, C., & van Loosdrecht, M. C. (2014). Outcompeting nitrite-oxidizing bacteria in single-stage nitrogen removal in sewage treatment plants: A model-based study. *Water Research*, *66*, 208–218.
- Piculell, M., Suarez, C., Li, C., Christensson, M., Persson, F., Wagner, M., ... Welander, T. (2016). The inhibitory effects of reject water on nitrifying populations grown at different biofilm thickness. *Water Research*, *104*, 292–302. <https://doi.org/10.1016/j.watres.2016.08.027>
- Poot, V., Hoekstra, M., Geleijnse, M. A., van Loosdrecht, M. C., & Pérez, J. (2016). Effects of the residual ammonium concentration on NOB repression during partial nitrification with granular sludge. *Water Research*, *106*, 518–530.
- Rahman, A., Wadhawan, T., Khan, E., Riffat, R., Takács, I., De Clippeleir, H., ... Pathak, B. (2014). Characterizing and quantifying flocculated and adsorbed chemical oxygen demand fractions in high-rate processes. *Proceedings of IWA Specialist Conference, Global Challenges: Sustainable Wastewater Treatment and Resource Recovery, Kathmandu, Nepal*.

- Regmi, P., Bunce, R., Miller, M. W., Park, H., Chandran, K., Wett, B., ... Bott, C. B. (2015). Ammonia-based intermittent aeration control optimized for efficient nitrogen removal. *Biotechnology and Bioengineering*, 112(10), 2060–2067. <https://doi.org/10.1002/bit.25611>
- Regmi, P., Miller, M. W., Holgate, B., Bunce, R., Park, H., Chandran, K., ... Bott, C. B. (2014). Control of aeration, aerobic SRT and COD input for mainstream nitrification/denitrification. *Water Research*, 57, 162–171.
- Rothauwe, J. H., Witzel, K. P., & Liesack, W. (1997). The ammonia monooxygenase structural gene amoA as a functional marker: Molecular fine-scale analysis of natural ammonia-oxidizing populations. *Applied and Environmental Microbiology*, 63(12), 4704–4712.
- Sliekers, A. O., Haaijer, S. C. M., Stafsnes, M. H., Kuenen, J. G., & Jetten, M. S. M. (2005). Competition and coexistence of aerobic ammonium- and nitrite-oxidizing bacteria at low oxygen concentrations. *Applied Microbiology and Biotechnology*, 68(6), 808–817. <https://doi.org/10.1007/s00253-005-1974-6>
- Smith, A. J., & Hoare, D. S. (1968). Acetate Assimilation by *Nitrobacter agilis* in Relation to Its “Obligate Autotrophy.” *Journal of Bacteriology*, 95(3), 844–855.
- Steinmüller, W., & Bock, E. (1976). Growth of *Nitrobacter* in the presence of organic matter. *Archives of Microbiology*, 108(3), 299–304. <https://doi.org/10.1007/BF00454856>
- Tchobanoglous, G., Burton, F.L., Stensel, H.D. Wastewater Engineering: Treatment and Reuse, McGraw-Hill, Boston., 2003.
- Wang, Q., Ye, L., Jiang, G., Hu, S., & Yuan, Z. (2014). Side-stream sludge treatment using free nitrous acid selectively eliminates nitrite oxidizing bacteria and achieves the nitrite pathway. *Water Research*, 55, 245–255. <https://doi.org/10.1016/j.watres.2014.02.029>
- Welker, S.; Horn, H.; Lackner, S. Substrate Contentment: Influence of Residual Ammonium and Dissolved Oxygen Concentrations on Autotrophic Nitrogen Removal. In *Proceedings of WEF/IWA Nutrient Removal and Recovery, Denver, USA; 2016.*

APPENDIX A: SUPPORTING INFORMATION FOR CHAPTER 6

Table A1: Summary of primers utilized for qPCR analysis

Target Gene	qPCR Primer	Nucleotide Sequence (5'-3')	Base Pairs	Reference
Universal 16S rRNA	1055F	ATGGCTGTCGTCAGCT	353	Ferris et al, 1996
	1392R	ACGGGCGGTGTGTAC		
amoA	amoA-1F	GGGGTTTCTACTGGTGGT	491	Rotthauwe et al, 1997
	amoA-2R	CCCCTCKGSAAAGCCTTCTTC		
Nitrospira 16S rRNA	NSPRA-675f	GCGGTGAAATGCGTAGAKATCG	67	Kindaichi et al, 2006
	NSPRA-746r	TCAGCGTCAGRWAYGTTCCAGAG		
	Nspra-723Taq	CGCCGCCTTCGCCACCG		
Nitrobacter 16S rRNA	Nitro-1198f	ACCCCTAGCAAATCTCAAAAAACCG	227	Graham et al, 2007
	Nitro-1423r	CTTCACCCCAGTCGCTGACC		
	Nitro-1374Taq	AACCCGCAAGGGAGGCAGCCGACC		

Explanation of Nitrification and Denitrification Rate Test Calculations

During nitrification, all NO_3^- produced was once NO_2^- . Similarly, during denitrification, all NO_3^- must first be reduced to NO_2^- before N_2 gas. So it is assumed that all NO_3^- reduced to N_2 gas (full denitrification), is at some point NO_2^- . In the AOB/NOB test if nitrite is accumulating then AOB rate is faster than NOB rate. Similarly, in the denitrification batch test, if nitrite is accumulating then the denitrification rate (NO_3^- to NO_2^-) is faster than the denitrification rate (NO_2^- to N_2 gas). See figure A1 for a graphical representation of the potential batch test results.

Nitrification Rate Test Calculations:

AOB (nitrification) and NOB (denitrification) rates are measured simultaneously under aerobic conditions, without substrate limitation. NOB rates are measured as the change in NO_3^- over time and AOB rates are measured as the change in NO_x ($\text{NO}_3^- + \text{NO}_2^-$) over time.

Measured Rates:

$$\begin{aligned} r\text{NO}_2^- &= \text{nitrite rate measured in batch test} \\ r\text{NO}_3^- &= \text{nitrate rate measured in batch test} \\ r\text{NO}_x &= r\text{NO}_2^- + r\text{NO}_3^- \end{aligned}$$

Unknown Rates:

$$\begin{aligned} r\text{NO}_2^-_{\text{NOB}} &= \text{rate of nitrite consumed by NOB} \\ r\text{NO}_2^-_{\text{AOB}} &= \text{rate of nitrite produced by AOB} \\ r\text{NO}_3^-_{\text{NOB}} &= \text{rate of nitrate produced by NOB} \end{aligned}$$

Assume:

$$\begin{aligned} \text{NO}_3^- &\text{ can only be produced by NOB, so } r\text{NO}_3^- = r\text{NOB}_{\text{NO}_3} \\ \text{NO}_2^- &\text{ is produced by AOB and consumed by NOB} \\ r\text{NO}_3^-_{\text{NOB}} &= r\text{NO}_2^-_{\text{NOB}} \end{aligned}$$

Calculations:

$$\text{From equations above: } r\text{NO}_3^- = r\text{NO}_3^-_{\text{NOB}} = -r\text{NO}_2^-_{\text{NOB}}$$

$$\text{Therefore } r\text{NO}_3^- = -r\text{NO}_2^-_{\text{NOB}} \text{ (EQ 1)}$$

$$r\text{NO}_2^- = r\text{NO}_2^-_{\text{AOB}} + r\text{NO}_2^-_{\text{NOB}} \text{ (EQ 2)}$$

$$\text{By substituting EQ 1 into EQ 2: } r\text{NO}_2^-_{\text{AOB}} = r\text{NO}_2^- + r\text{NO}_3^-$$

$$\text{Therefore: } r\text{NO}_2^-_{\text{AOB}} = r\text{NO}_x$$

Denitrification Rate Test Calculations:

The denitration (NO_3^- to NO_2^-) rates and denitritation (NO_2^- to N_2 gas) rates are measured simultaneously under anoxic conditions, without substrate limitation. Denitration rates are measured as the change in NO_3^- over time and denitritation rates are measured as the change in NO_x ($\text{NO}_3^- + \text{NO}_2^-$) over time.

Measured Rates:

$$\begin{aligned}rNO_2^- &= \text{nitrite rate measured in batch test} \\rNO_3^- &= \text{nitrate rate measured in batch test} \\rNO_x &= rNO_2^- + rNO_3^-\end{aligned}$$

Unknown Rates:

$$\begin{aligned}rNO_2^-_{denNO_2-N_2} &= \text{rate of nitrite consumed by denitritation} \\rNO_2^-_{denNO_3-NO_2} &= \text{rate of nitrite produced by denitration} \\rNO_3^-_{denNO_3-NO_2} &= \text{rate of nitrate consumed by denitration}\end{aligned}$$

Assume:

$$\begin{aligned}NO_3^- &\text{ can only be consumed by denitration, so } rNO_3^- = rNO_3^-_{denNO_3-NO_2} \\NO_2^- &\text{ is produced by denitration and consumed by denitritation} \\rNO_3^-_{denNO_3-NO_2} &= rNO_2^-_{denNO_3-NO_2}\end{aligned}$$

Calculations:

$$\text{From equations above: } -rNO_3^- = rNO_3^-_{denNO_3-NO_2} = rNO_2^-_{denNO_3-NO_2}$$

$$\text{Therefore } -rNO_3^- = rNO_2^-_{denNO_3-NO_2} \text{ (EQ 1)}$$

$$rNO_2^- = rNO_2^-_{denNO_3-NO_2} + rNO_2^-_{denNO_2-N_2} \text{ (EQ 2)}$$

$$\text{By substituting EQ 1 into EQ 2: } rNO_2^-_{denNO_2-N_2} = -rNO_3^- + rNO_2^-$$

$$\text{Therefore: } rNO_2^-_{denNO_2-N_2} = -rNO_x$$

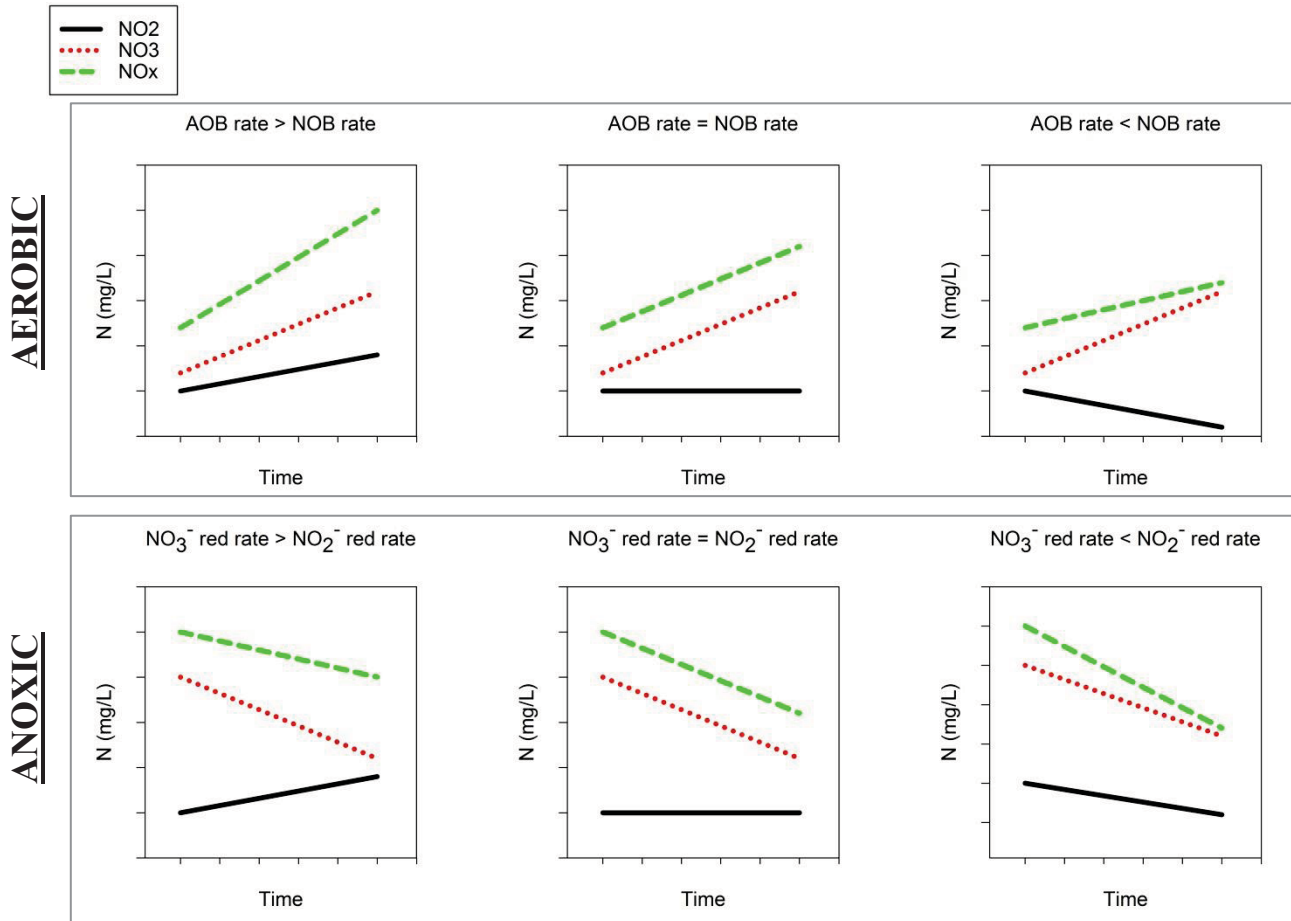


Figure A1: Examples of theoretical batch tests with varying AOB/NOB and NO₃⁻/NO₂⁻ reduction rates

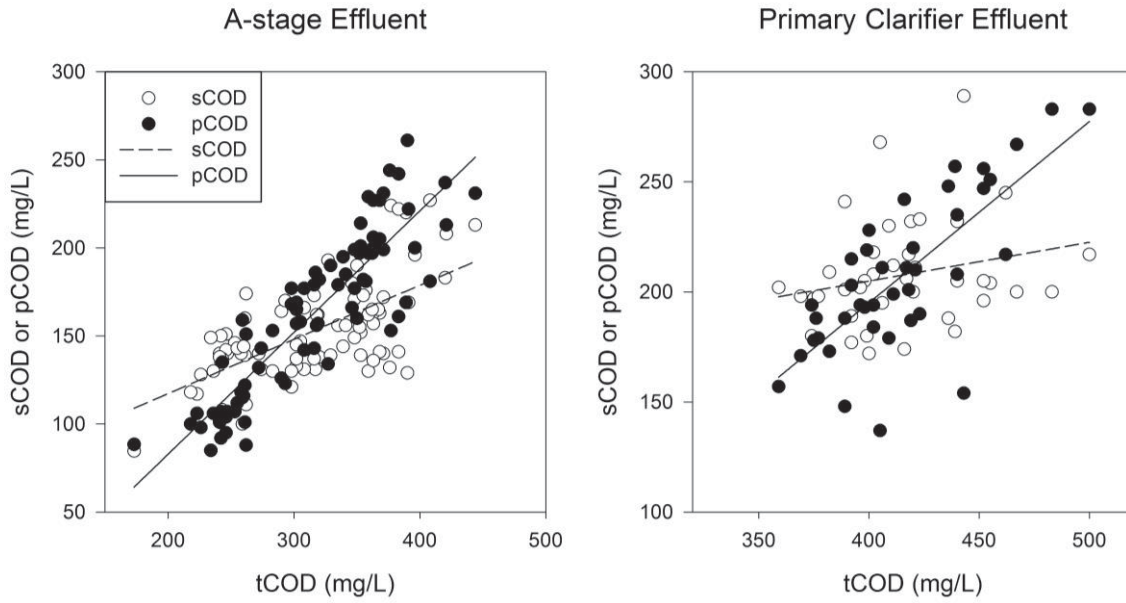


Figure A2: Particulate COD (pCOD) and soluble COD (sCOD, 1.5 μ m filtered) vs. total COD (tCOD) for A-stage effluent and primary clarifier effluent.

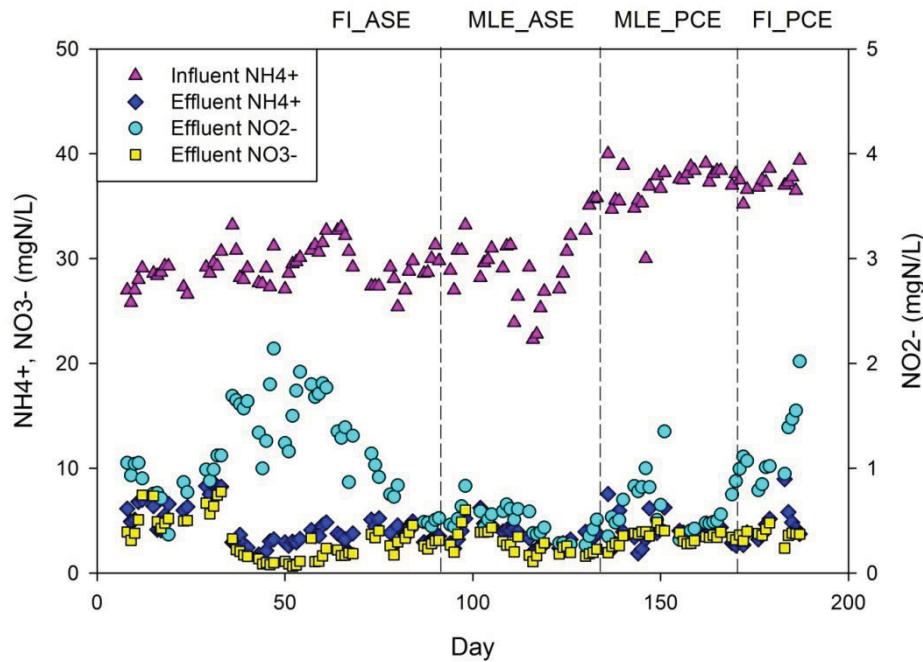


Figure A3: Concentration of influent and effluent ammonia, effluent nitrite, and effluent nitrate over time

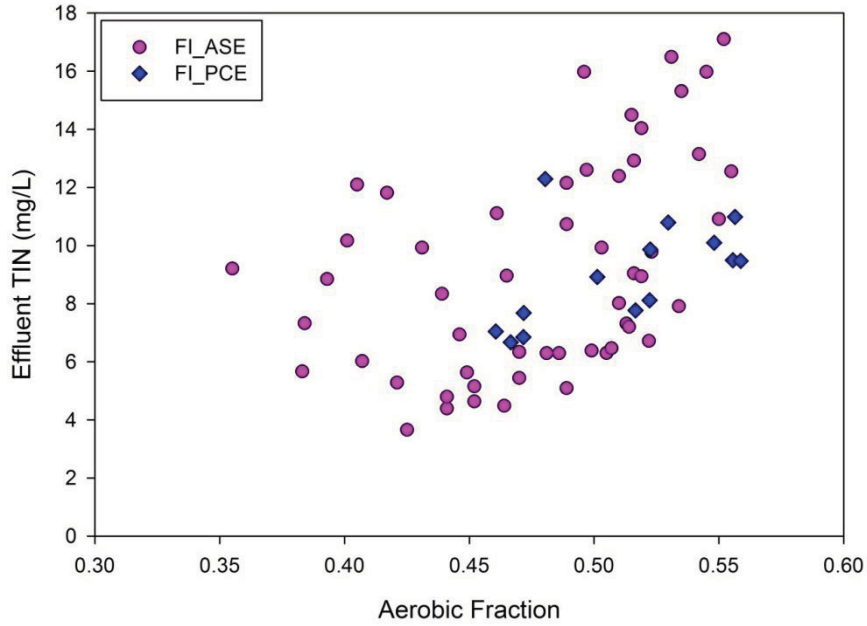


Figure A4: Effluent TIN vs. aerobic fraction for the fully intermittent scenarios (FI_ASE and FI_PCE).

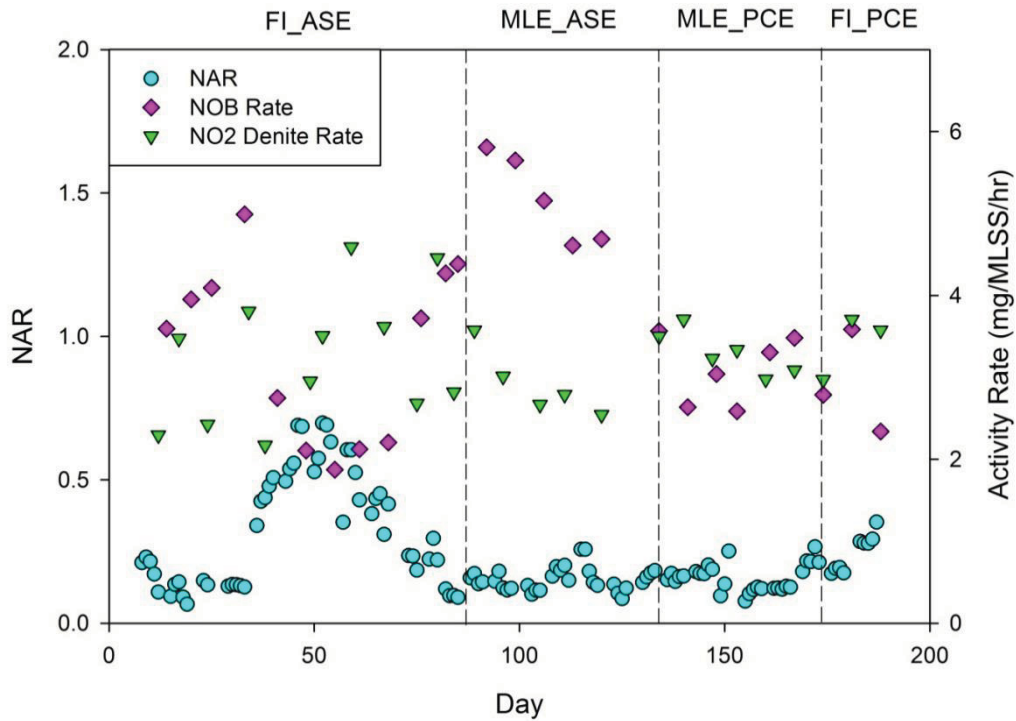


Figure A5: NOB rate and NO_2^- specific denitrification rates from ex-situ maximum activity rate tests in mg/MLSS/hr and nitrite accumulation ratio (NAR).

CHAPTER 7: COMPARISON OF SENSOR DRIVEN AERATION CONTROL STRATEGIES FOR OPTIMIZATION OF NITROGEN REMOVAL VIA DENITRIFICATION IN AERATED ZONES

Stephanie Klaus and Charles B. Bott

ABSTRACT

A pilot scale process was operated with A-stage effluent feed, and primary clarifier effluent feed in MLE, all tanks aerated, A/O, and A2O configurations. Continuous DO control at high DO (2 mg/L), low DO (0.2 mg/L), ammonia based aeration control (ABAC), and ammonia vs. NO_x (AvN) control (both continuous and intermittent operation) were compared on the basis of total inorganic nitrogen (TIN) removal. The highly loaded A/B process configuration (4 hour HRT) with intermittent aeration was capable of achieving a maximum TIN removal of 80%, while the A2O process with PCE feed, an 11 hour HRT, and 0.2-0.3 mg/L continuous aeration achieved a maximum of 88% TIN removal. ABAC and AvN control did not always result in DO setpoints low enough to achieve SND, and even if setpoints were low enough to achieve SND, that did not always result in increased overall TIN removal over continuous DO control of 2 mg/L. While there are other benefits to transitioning to sensor driven aeration control strategies such as ABAC and AvN, increased TIN removal during continuous aeration is not guaranteed.

INTRODUCTION

There is a growing interest in implementing sensor driven aeration control strategies such as ammonia based aeration control (ABAC) and ammonia vs. NO_x (AvN) control. In these control strategies, airflow is controlled to meet either an effluent ammonia setpoint (ABAC) or an ammonia/(nitrate+nitrite) setpoint (AvN). The drivers are to reduce aeration energy and chemical addition (alkalinity and carbon), while preventing peaks in effluent ammonia (Rieger et al., 2014; Vrečko et al., 2006). The advantage of AvN control over ABAC is that it oxidizes only the amount of ammonia that can be denitrified utilizing the influent organic carbon that is made available. This maximizes COD utilization efficiency for denitrification without the addition of supplemental carbon (Regmi et al., 2014; Al-Omari et al., 2015).

Although AvN control was initially developed as an intermittent aeration strategy for a nitrite shunt process (Regmi et al., 2014), it should be noted that both ABAC and AvN can be implemented either with intermittent aeration or continuous aeration. Also, both intermittent aeration ABAC or AvN can facilitate nitrite shunt by leaving an ammonia residual greater than one, providing transient anoxia, and keeping SRT low to facilitate NOB washout (Cao et al., 2017; Regmi et al., 2015). However, if followed by a mainstream anammox process, AvN aeration control is crucial to maintain the balance between NH₄ and NO_x to meet anammox stoichiometry.

Due to limitations on how aeration blowers can be operated, it is considered easier and more practical to utilize continuous aeration than intermittent aeration. Although they achieve the

same effluent goal, it is important to distinguish between continuous and intermittent aeration strategies for nitrogen removal. Intermittent aeration has the advantage of distinct anoxic periods for denitrification, while continuous aeration relies on simultaneous nitrification/denitrification (SND) to achieve nitrogen removal in the aerated zone. Intermittent aeration is not classified as SND, because nitrification and denitrification are taking place at different times. Also, intermittent aeration allows for the aerobic SRT to be adjusted quickly in response to influent ammonia loading, as opposed to only having control over the total SRT in a continuously aerated process.

While increasing denitrification capacity via limiting oxygen transfer into unaerated zones is undisputed, increased denitrification via SND is not guaranteed by implementing ABAC or AvN control. TIN removal can only occur in aerated zones if the DO setpoint can get low enough for SND (0.3-0.7 mg/L) (Jimenez et al., 2010). In ABAC or AvN control, the DO setpoint or aerobic fraction is no longer a user input, and instead the DO setpoint is determined by the SRT (Batchelor, 1983; Schraa et al., 2019). The SRT has to be sufficiently long so that the DO setpoint required to meet the ammonia oxidation requirement, is low enough for SND. This means that the SRT either needs to be increased, and/or that the nitrifying bacteria population needs to be adapted to achieve higher ammonia oxidation rates at lower DO concentrations (Park et al., 2001; Giraldo et al., 2011; Keene et al., 2017).

In order for SND to occur there needs to be an electron donor available for denitrification in the aerobic zones. This can come from internal storage polymers (Van Van Loosdrecht et al., 1997), or the hydrolysis of slowly biodegradable COD (sbCOD) and endogenous decay products to readily biodegradable COD (rbCOD) (Mino et al., 1995; Van Loosdrecht and Henze, 1999). Short-chain fatty acids that have been stored as intracellular polymers (such as PHB and glycogen) under anaerobic conditions, can be used for denitrification by polyphosphate accumulating organisms (PAO), glycogen accumulating organisms (GAO), or other heterotrophic organisms (Tsuneda et al., 2006; Rubio-Rincón et al., 2017; Van Loosdrecht et al., 1997). Studies have shown that denitrification using internally stored polymers can take place in an aerated reactor (SND) (Third et al., 2003; Zeng et al., 2003; Bernat and Wojnowska-Baryła, 2007), or in a dedicated post-anoxic zone (also implied would be anoxic times of intermittent aeration) (Winkler et al., 2011; Vocks et al., 2005; Alleman and Irvine, 1980).

Since aerobic heterotrophs have a clear advantage for soluble substrate in a continuously aerated zone, there needs to be a DO gradient providing an anoxic zone, allowing for denitrification to occur. The DO gradient can be within the floc, or within the reactor due to incomplete mixing (Daigger and Littleton, 2014). Pochana and Keller, 1999 showed that larger floc size resulted in more SND, while Zhu et al., 2007 demonstrated that SND could occur even in very small flocs. There are also novel pathways that allow for denitrification to take place aerobically (Littleton et al., 2003). While there are some guidelines on required influent COD/NH₃ ratio required (greater than 10-11) for SND (Jimenez et al., 2010; Chiu et al., 2007), these studies were performed with acetate as the carbon source, so the effect of real wastewater composition is not known.

While there are many studies on SND in extended aeration processes and oxidation ditches (Liu et al., 2010; Daigger and Littleton, 2000; Bertanza, 1997), membrane bioreactors (MBRs) (Giraldo et al., 2011; Hocaoglu et al., 2011), biofilms (Matsumoto et al., 2007; Randall and Sen, 1996) and granular sludge (Kreuk et al., 2005, Basin et al., 2012), studies of SND in conventional plug-flow type reactors are lacking. This distinction is important because extended aeration processes and MBRs carry high mixed liquor suspended solids (MLSS) and long solids retention times (SRTs) allowing for an endogenous carbon source and the ability to nitrify at very low DO. Oxidation ditches are not typically plug flow, do not have dedicated aerobic zones, and surface aeration is common allowing for oxygen gradients with the reactor. Biofilm and granular sludge processes can more easily provide a distinct anoxic environment (compared to a floc) by limiting the diffusion of oxygen from the bulk liquid. Despite all of the research on SND, it is still not well understood how much SND will occur in well-mixed plug flow systems with defined aerobic and unaerated zones. It is still unknown how to design for SND because it is difficult for current process models to predict. Many studies on SND have been performed in SBRs with synthetic feed (Münch et al., 1996; Oh and Silverstein 1999; Pochana and Keller, 1999) which are difficult to translate to full-scale continuous flow processes.

One driver for implementing nitrite shunt and/or anammox is intensification, meaning removing more nitrogen, in the same (or less) reactor volume, with less chemicals and energy (Stinson et al., 2013). In order to take advantage of these benefits, carbon needs to be removed ahead of the nitrogen removal step, for example by a high rate activated sludge (HRAS) A-stage process (Böhnke and Diering, 1997; Miller et al., 2017). By the above definition of intensification, it is logical to assume that SND during continuous aeration via sensor driven aeration control could be part of an intensified process. While previous research has shown that intermittent aeration (both ABAC and AvN) can be part of an intensified process (Regmi et al., 2015; Al-Omari et al. 2015), one goal of this paper is to determine under what conditions continuous ABAC and AvN aeration control may be part of an intensified process by encouraging SND and/or nitrite shunt.

Since continuous aeration is typically more practical for full-scale plants to implement than intermittent aeration, it is necessary to understand the amount of nitrogen removal that can be achieved via SND during continuous aeration in various configurations with real wastewater. This is the first paper to report on performance of the continuous aeration AvN strategy compared to other advanced aeration control strategies. This pilot offers the unique opportunity to study these aeration controls and SND in a continuous flow process, with many different reactor configurations.

MATERIALS AND METHODS

Pilot Configuration

The pilot plant consisted of an HRAS A-stage process, or a primary clarifier, followed by the B-stage process (Figure B1). The pilot was fed screened (2.4 mm openings) and degrittled municipal wastewater that was first adjusted to 20° C. The A-stage consisted of three bioreactors

in series ($V_{\text{total}} = 511 \text{ L}$) followed by an intermediate clarifier. A single modulating valve controlled airflow to the A-stage. Primary clarification was performed in a cone bottom clarifier with a volume of 1170 L at a surface overflow rate (SOR) of 33.2 $\text{m}^3/\text{m}^2/\text{day}$ and HRT of 1.3 hours.

B-stage was operated in 4 different configurations: Fully aerobic (all CSTRs aerated), Modified Ludzack Ettinger (MLE), A/O process, and A2O process. The fully aerobic and MLE scenarios utilized 4 equally sized completely mixed reactors (CSTR 1 through CSTR 4 in Figure B1) for a total working volume of 606 liters. AO scenarios were operated first with 4 CSTRs in which CSTR 1 was the anaerobic zone, and then 5 CSTRs in which CSTR 0 was the anaerobic zone (Figure B1). For the AO and A2O scenarios with 5 CSTRs, an additional 53 liter anaerobic selector (CSTR 0) was operated upstream of CSTR 1. The anaerobic selector was covered using ping pong balls to minimize oxygen transfer from the atmosphere. During the MLE and A2O scenarios, CSTR 1 was made anoxic and mixed liquor was recycled from CSTR 4 to CSTR 1. Mixing was achieved using variable speed mixers (Caframo 1850, Ontario, Canada), one in each CSTR. Mixing intensity was high enough that solids would not settle when reactors were unaerated, and mixers were kept on at a constant speed even in continuously aerated reactors.

Automated Process Control

Sensors included dissolved oxygen (Insite Model 10, LA, USA), pH (Foxboro/Invensys, UK), ammonium (WTW VARIION, Germany), nitrate and nitrite (Scan Spectrolyser, Austria). Locations of sensors are shown in Figure B2. pH was measured in the 3rd CSTR using a ISE Foxboro pH probe (Invensys, London, UK). A stock solution of sodium bicarbonate (80 g NaHCO_3/L) was fed to the third CSTR in order to maintain effluent pH at 6.8.

Four different aeration control modes were available: continuous aeration DO control, continuous aeration ammonia based aeration control (ABAC), continuous aeration ammonia vs. NO_x control (Cont AvN) and intermittent aeration AvN (Int AvN). The sensors were connected to a programmable logic controller (PLC) and then used for proportion-integral-derivative (PID) or PI control. DO control utilized a PI controller in which DO in each reactor controls air valve position via motor operated valves (MOVs). ABAC utilized a cascading PID loop on top of the DO controller, so that DO setpoint was manipulated to meet an ammonia setpoint in the last CSTR. Continuous AvN aeration was similarly controlled except that the DO setpoint was manipulated to meet a NO_x/NH_4 ratio in the last CSTR instead of ammonia setpoint. Intermittent AvN aeration is similar to continuous AvN control, except that the aerobic fraction (air on time divided by total cycle length) was controlled via PID control as opposed to the DO setpoint. During intermittent AvN control, the DO control PI loop was utilized to meet a constant setpoint of 1.5 mg/L when air was on. A solenoid upstream of the MOVs was opened or closed to meet the aerobic fraction setpoint. For ABAC and AvN control the DO setpoint and/or aerobic fraction was the same in each aerated reactor.

Phases

Operation was divided into four phases, the details of which are shown in Table 7.1. The shaded area indicates that scenario was operated, and the naming code for that phase is shown. The influent flow was constant during each phase except during Phase 3 when there was a diurnal flow variation, shown in Table B1. Scenarios with ASE feed were operated at a 4 hour HRT and scenarios with PCE feed were operated at an 11 hour HRT.

Table 7.1: Operating scenarios. All scenarios had a constant influent feed except A2O_ABAC which had a diurnal flow feed pattern.

Phase	Configuration	CSTRs	Feed	Int AvN	Cont AvN	ABAC	DO set High (2 mg/L)	ABAC Diurnal	DO set low (0.2 mg/L)
1	Fully aerated (FA)	4	ASE	FA_Int_AvN	FA_Cont_AvN				
	MLE	4	ASE	MLE_Int_AvN	MLE_Cont_AvN		MLE_DO_High		
2	MLE	4	PCE	MLE_Int_AvN	MLE_Cont_AvN	MLE_ABAC	MLE_DO_High		
3	A/O	4	PCE						AO_DO_Low
	A2O	5	PCE					A2O_ABAC	A2O_DO_Low
4	A/O	5	PCE						AO_DO_Low
	A2O	5	PCE						A2O_DO_Low

Analysis

Performance was monitored through the collection of 24-hour composite samples using automated samplers. The samplers extracted 250 mL at one-hour intervals allowing average daily influent and effluent characteristics to be measured. Total and volatile suspended solids (TSS and VSS) were analyzed using standard methods 2540D and 2540E respectively (APHA, 2012). Total and soluble COD, OP, total ammonia nitrogen ($\text{NH}_4^+\text{-N} + \text{NH}_3\text{-N}$), $\text{NO}_2^-\text{-N}$, and $\text{NO}_3^-\text{-N}$ were measured with HACH TNTplus kits and a HACH DR2800 spectrophotometer (HACH Loveland, CO). Nutrient and soluble COD samples were filtered through 0.45 μm and 1.5 μm filters respectively. Particulate COD (pCOD) was calculated as the difference between total COD and sCOD (1.5 μm filtered). The sCOD measurement includes readily biodegradable and colloidal COD fractions. Daily pH and temperature readings of the reactors were recorded using a handheld pH and temperature meter (Beckman Coulter, Brea, CA). Readings for DO were recorded using a handheld DO sensor (Insite Model 10, LA, USA). Profile grabs from each CSTR were analyzed for $\text{NH}_4\text{-N}$, $\text{NO}_x\text{-N}$, and $\text{NO}_2\text{-N}$ in order to quantify SND from the first to last CSTR.

SND Calculations

While incomplete mixing in aeration tanks at full-scale facilities may contribute significantly to SND, incomplete mixing was not explored in this study since it is not a reliable way to achieve SND, and cannot be easily replicated at pilot scale. SND was calculated as total inorganic nitrogen (TIN) removed across the aerobic zone. This measurement excludes ammonia generation from ammonification of organic nitrogen (which then gets oxidized to NO_x), and includes ammonia that was removed due to assimilation. Influent organic N that gets ammonified would under predict SND, and NH₄ removed due to assimilation will over predict SND. Example calculations are located in the Supplementary Information. Anoxic nitrogen removal was calculated as NO_x that was denitrified in the anoxic and/or anaerobic zones. A mass balance check was performed by comparing the calculated anoxic nitrogen removal, with the total TIN removal minus the aerobic nitrogen removal. Data points with greater than 20% difference were rejected.

Aerobic TIN removal and anoxic TIN removal were calculated as referenced to the influent flow, for ease of comparison to total TIN removal. Aerobic TIN removal was calculated as TIN in to the aerobic zone (i.e. TIN in the anoxic/anaerobic zone), minus the TIN out (i.e. TIN in the last aerobic reactor). This value was multiplied by the total forward flow (including RAS and IMLR flow), divided by the influent flow. Detailed calculations are shown in the supplementary information.

Mixed Liquor Composite System

During Phase 4 of operation, a system was devised to take composite samples from CSTR1 and CSTR4 while excluding the mixed liquor from the sample. Once every 2 hours, one liter of mixed liquor was pumped into a one liter graduated cylinder. The pump was stopped and the solids were settled for 15 minutes. Then another pump decanted 100mL of the supernatant from the surface of the graduated cylinder. Then the remainder of the mixed liquor was pumped back to the process so the graduated cylinder was emptied for the next cycle. The pumps were controlled by an electronic programmable timer (ChronTrol, San Diego, CA).

DNA Extraction and Amplicon Sequencing

DNA was extracted using the DNeasy Blood & Tissue Mini Kit and the Qiacube robotic workstation (Qiagen). The Ion Torrent Personal Genome Machine (PGM) platform (Thermo Fisher Scientific) was used for amplicon sequencing of the 16S rRNA gene (fusion method with forward primer 1055f (5' ATGGCTGTCGTCAGCT 3') and reverse primer 1392r (5' ACGGGCGGTGTGTAC 3') linked to multiplex barcodes). DNA libraries were quantified with the Bioanalyzer® instrument analysis (Agilent). Libraries were combined, enriched with the Ion PGM™ Hi-Q™ OT2 Kit, and sequenced with the Ion PGM™ Hi-Q™ View Sequencing Kit and Ion 318 Chip v2 (Thermo Fisher Scientific). Sequence reads were trimmed, aligned, and classified using the SILVA (Quast et al., 2013) database through analysis tools available in Mothur (Schloss et al., 2009).

PAO Activity Measurements

Eight liters of mixed liquor were collected in a batch reactor from the last CSTR. The reactor was covered and anaerobic conditions were established. Sodium acetate stock solution (10,000 mgCOD/L) was added to reach 300 mg COD/L in the reactor. Samples were collected every 15 minutes and measured for OP and sCOD. After the anaerobic release phase, sample was then split into two four liter reactor, one for aerobic OP uptake, and one for anoxic OP uptake. The aerobic reactor was aerated using diffused aeration to maintain a DO concentration between 2 and 4 mg/L. Samples were collected every 15 minutes and analyzed for OP. The anoxic reactor was covered and spiked with potassium nitrate stock solution (10,000 mgN/L) to a concentration of 15 mgN/L in the reactor. Samples were collected every 15 minutes and analyzed for OP, sCOD, NO₃, and NO₂. All samples were immediately filtered through 0.45µm cellulose membrane filters and analysis was performed with Test in Tubes (TNT) (HACH Company, Loveland, Colorado).

AOB and NOB Activity Measurements

To measure maximum AOB and NOB activity, a 4 L sample was collected from the 4th CSTR and aerated for 30 minutes to oxidize excess COD. The sample was then spiked with NH₄Cl and NaNO₂ so that initial concentrations were 20-30 mg NH₄⁺-N/L and 2-4 mg NO₂⁻-N/L respectively. Temperature was controlled at 20°C via submersion in a water bath. The DO concentration was manually maintained between 2.5 and 4 mg/L using diffused compressed air. The pH was manually maintained at approximately 7.5 through the addition of sodium bicarbonate. The activity tests were conducted for 1 hour with sample collection every 15 minutes. Samples were analyzed for NH₄⁺-N, NO₂⁻-N, and NO₃⁻-N as described above. The AOB rates were calculated as the slope of the NO_x-N production and NOB rates were calculated as the slope of the NO₃⁻-N production.

Statistical Analysis

Statistical analysis was performed using SigmaPlot (Systat Software, San Jose, CA). the t-test (for a normally distributed data set) and Mann–Whitney rank sum test (for a not normally distributed data set).

RESULTS AND DISCUSSION

Phase 1

In this phase, intermittent AvN and continuous AvN control were compared with A-stage effluent feeding the B-stage nitrogen removal process. The process was operated in both fully aerated (FA) configuration, and with a pre-anoxic zone in MLE configuration (Figure 7.1). TIN removal was highest during MLE_Int_AvN (60.1%±14.1%), followed by FA_Int_AvN (54.4%±13.7%), MLE_Cont_AvN (39.8±11.4), and lastly FA_Cont_AvN (20.5±14.1). TIN removal during MLE DO control was low (25.2%±7.2%) since denitrification can only occur in

the anoxic zone, and the ASE had variable and relatively low sCOD (78.3 ± 9.7 mg COD/L) (Figure 7.2). TIN removal was higher during MLE_Int_AvN ($60.1\% \pm 14.1\%$), which could be due in part to higher influent sCOD (103 ± 17 mg COD/L) leading to more denitrification in the anoxic zone, but the majority of the improvement was more likely from sbCOD being used for denitrification during anoxic periods. In all three of the MLE scenarios, the anoxic zone was always carbon limited as indicated by grab samples in the anoxic zone always containing some NO_x (average value 4.7 ± 3.2). DO control represented the baseline in terms of TIN removal in the aerated reactors. In other words, TIN removal in the other scenarios should not be less than in the high DO period, because at least some denitrification in the aerobic zone was expected.

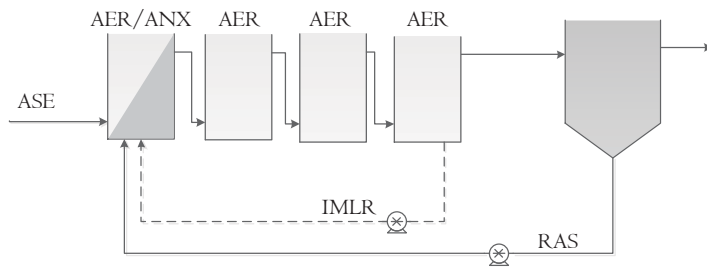


Figure 7.1: Phase 1 BNR process configuration. A-stage effluent (ASE) fed the B-stage process. In fully aerated (FA) configuration there was no internal mixed liquor recycle (IMLR). In MLE configuration CSTR 1 was unaerated with IMLR at 300% of influent flow.

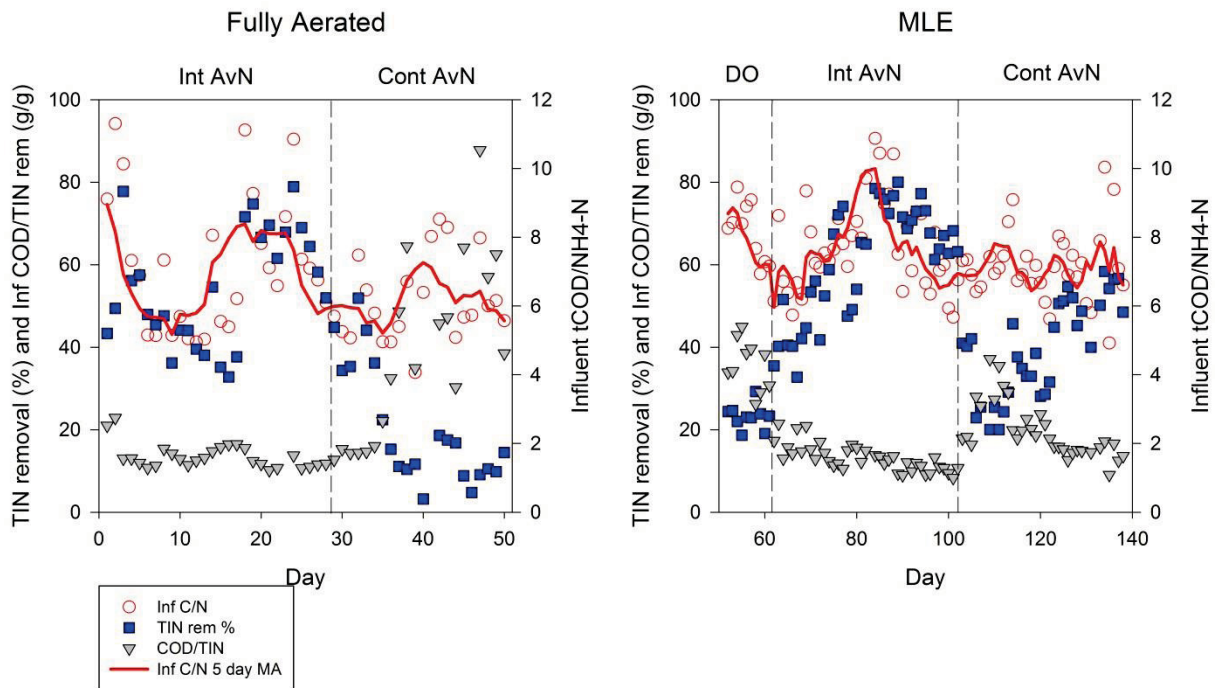


Figure 7.2: B-stage influent C/N (total COD/NH₄⁺-N), TIN removal %, and total COD/TIN removal ratio

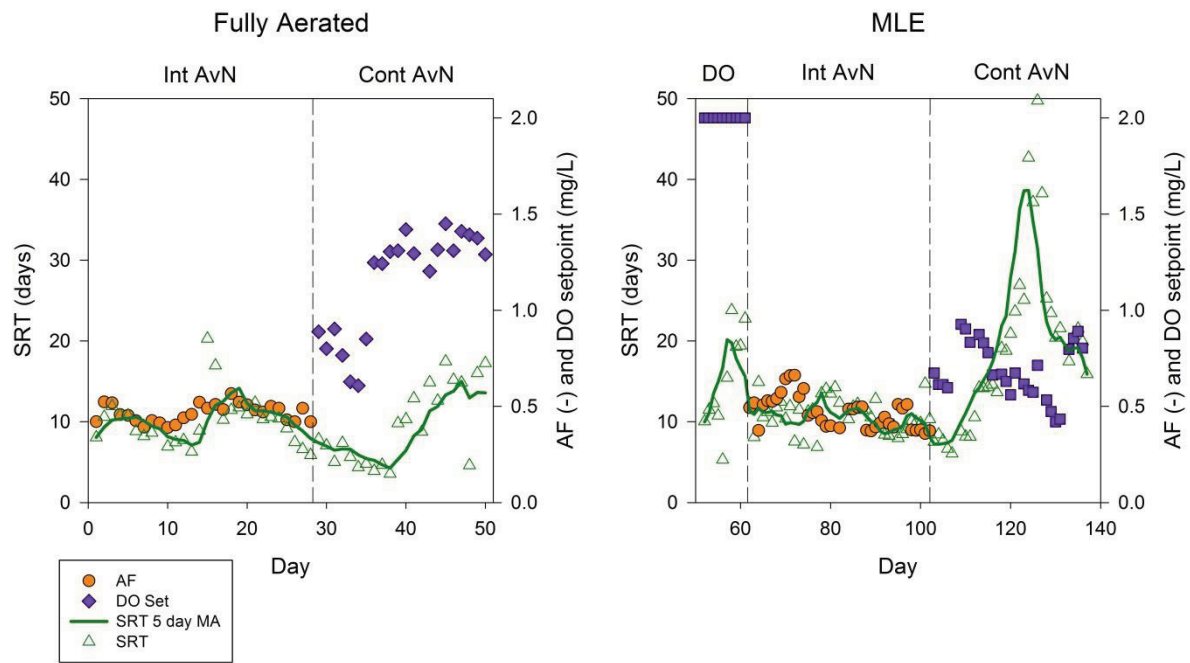


Figure 7.3: SRT, Aerobic Fraction Setpoint (air on time divided by total cycle time), and DO setpoint. Aerobic Fraction and DO setpoints are determined by the AvN controller.

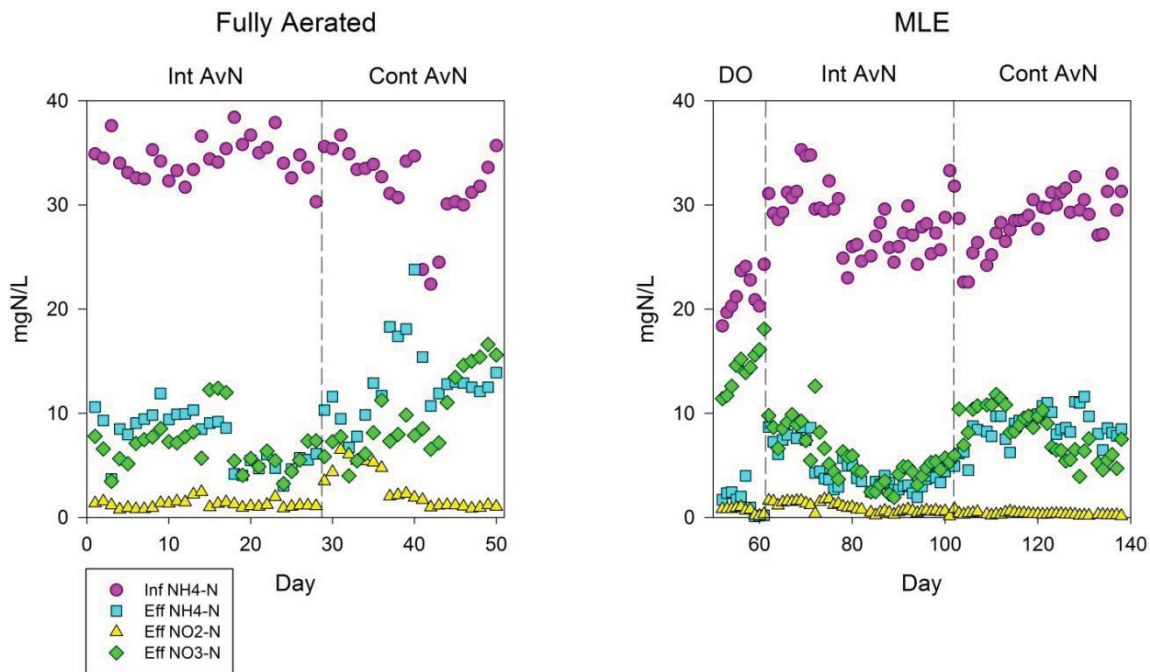


Figure 7.4: B-stage influent and effluent nitrogen concentrations

In both fully aerated and MLE scenarios, a gradual loss of TIN removal was observed when switching from intermittent AvN to continuous AVN (Figure 7.2). In the fully aerated scenarios, this can only mean that SND was not taking place to the same extent that denitrification was taking place during the anoxic periods of intermittent aeration. In the MLE scenarios, the decrease in TIN removal can also be due a decrease in influent sCOD, which would decrease the amount of NO_x reduction occurring in the anoxic zone. However, the influent COD was fairly constant during the transition, so it can be assumed that the change from intermittent to continuous aeration was mostly responsible for the loss of TIN removal (Figure 7.2).

TIN removal was low (20.5%±14.1%) in the fully aerated continuous AvN operation, which was most likely due to the DO setpoint required to meet the AvN ratio being above 1 mg/L, so little SND could occur (Figures 7.2 and 7.3). With a DO setpoint that high, nitrogen loss was most likely occurring through assimilation of ammonia into biomass, and through denitrification in the clarifier. The SRT was increased to try and bring the DO setpoint down, but the setpoint remained high (Figure 7.3). After the transition from MLE_Int_AvN to MLE_Cont_AvN led to a decrease in TIN removal, the SRT was increased even more than during FA_Cont_AvN (Figure 7.3). This time the DO setpoint trended down (as low as 0.42 mg/L, Figure 7.3), and the TIN removal trended up (as high as 58.2%, Figure 7.2). However, although the TIN removal in MLE_Cont_AvN was approaching the values achieved in MLE_Int_AvN at a similar influent C/N (Figure 7.5), the SRT was close to double (approximately 10 days in MLE_Int_AvN vs 20 days in MLE_Cont_AvN).

During the intermittently aerated scenarios, TIN removal trended with influent C/N (Figure 7.2). This trend was also apparent by the COD/TIN removal ratio which was lower and less variable (13.6±3.0 g/g during FA_Int_AvN and 13.7±4.2 g/g during MLE_Int_AvN) than during continuous aeration (49.6±42.7 g/g during FA_Cont_AvN and 19.6±6.5 g/g during MLE_Cont_AvN). COD/TIN removal ratio was calculated as total COD removed divided by TIN removed. In the fully aerated configuration, this was a direct comparison of how efficiently the COD was used for denitrification across the aerobic zone. This was not the case in MLE configuration, because COD was also being utilized for denitrification in the pre-anoxic zone, but the COD/TIN removal ratio can still be used to compare overall efficiency of COD utilization. COD/TIN removal ratios indicated that influent carbon was not used as efficiently in the continuous AvN operation (higher ratio means worse efficiency) because the DO setpoint was frequently too high to achieve the same level of denitrification in the aerated zones as intermittent AvN.

There was a transient spike in nitrite (maximum value of 6.5 mg N/L) during the transition from intermittent aeration to continuous aeration with all tanks aerated that was not able to be sustained (Figure 7.5). Excluding the temporarily high values, the average effluent NO₂⁻ was 1.4±0.5 mg N/L during FA_Cont_AvN operation, which was similar to the value during FA_Int_AvN (1.3±0.4 mg N/L). Effluent NO₂⁻ was 0.9±0.5 mg/L during MLE_Int_AvN, and was lowest during MLE_Cont_AvN (0.3 mg N/L). The fully aerated scenarios had higher

effluent NO_2^- than the MLE scenarios, which was observed previously (Kinyua et al., 2018). There was not a clear difference in maximum AOB and NOB activity rates between operation periods (Figure B3). For the entire phase, average AOB rates were 5.5 ± 1.4 mgN/gVSS/hr, and the average NOB rate was 4.8 ± 1.0 mgN/gVSS/hr. The NOB/AOB rates throughout the test did not indicate NOB out-selection, with an average ratio of 0.9 ± 0.2 g/g, which is above the expected value (Dold et al., 2015).

The intermittent aeration scenarios were able to achieve higher levels of TIN removal at a shorter total process SRT. By controlling the A-stage effluent C/N in the range of 8-10 it would be possible for TIN removal in B-stage remain high (70-80% removal), which is consistent with previous studies at this pilot (Miller et al., 2012; Regmi et al., 2014). TIN removal during continuous AvN operation was poor because the loading was high (NH_4 and or HRT), causing the DO setpoint to be too high for SND. Since the goal of the A/B process is intensification, it would not be practical to operate continuous aeration if it required a >20 day SRT to achieve the effluent nitrogen goals. These results clearly demonstrate that although the two control strategies use similar logic to meet the same effluent goal, they are not equal in terms of performance.

Phase 2

In Phase 1, the MLE results were influenced by influent C/N variations, and by the DO setpoints being too high to achieve reliable SND. In Phase 2, to make the scenarios more applicable to conventional BNR facilities, primary clarifier effluent was used for B-stage influent feed, and the process was operated in an MLE configuration at an 11 hour HRT and 16 day SRT (Figure 7.5). Profile grab samples were taken to be able to quantify the amount of denitrification taking place in the aerated zones (SND). After a change in aeration control strategy, the system reached steady state in 1-2 HRTs, so each strategy was operated for 3-5 days, with one day transition in between. This allowed for influent characteristics to remain relatively constant in order to better compare scenarios. The hypothesis was that by increasing the HRT and SRT, the DO setpoint required to meet the ammonia setpoint in the effluent will be low enough to achieve more reliable SND, so that continuous ABAC and AvN had the opportunity to remove the same or greater TIN than intermittent AvN.

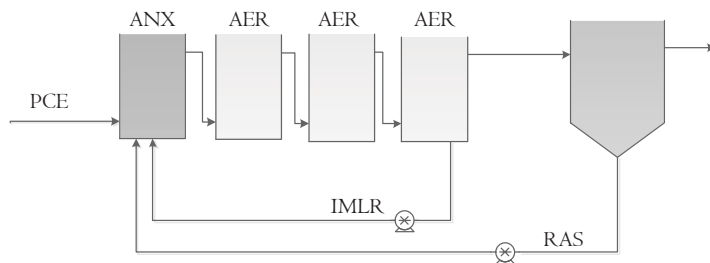


Figure 7.5: Phase 2 BNR process configuration. MLE at 300% IMLR with primary clarifier feed.

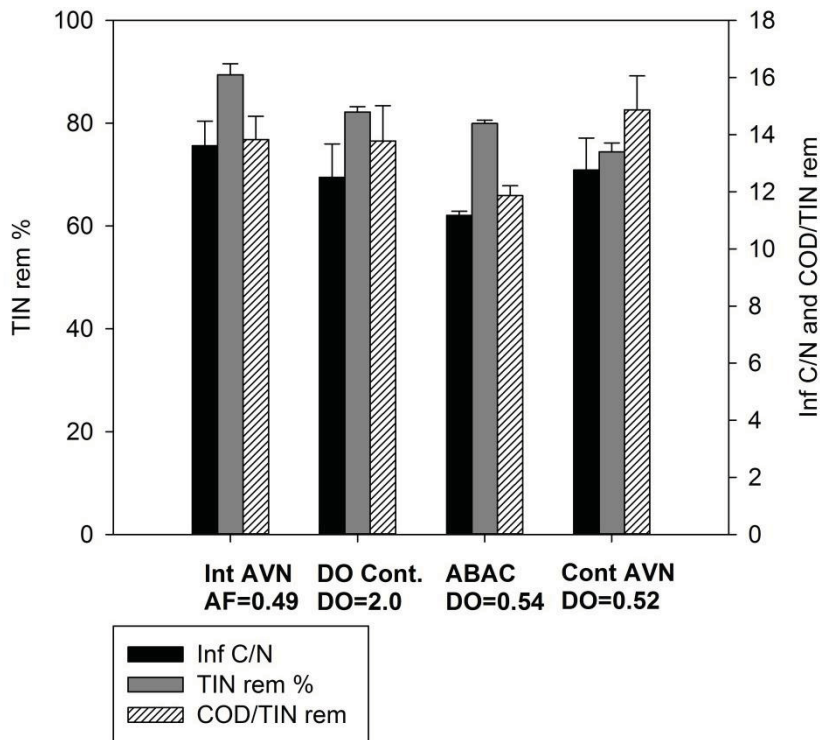


Figure 7.6: TIN removal 5, COD/TIN removal ratio (total COD removed divided by TIN removed) and influent COD/NH4 (C/N).

Average influent characteristics during this phase were total COD of 435 ± 41 mg/L, sCOD of 223 ± 31 , and TKN of 40.8 ± 2.9 . Average MLSS was 3.3 ± 0.5 g/L and average SRT was 16.6 ± 1.6 days. MLE_Int AvN had the highest TIN removal ($89.4 \pm 2.1\%$) followed by MLE_DO_High ($82.2 \pm 1.0\%$), MLE_ABAC ($80.0 \pm 0.7\%$), and MLE_Cont_AvN ($74.4 \pm 1.7\%$) (Figure 7.6). Influent C/N was the highest for MLE_Int_AvN (13.6 ± 0.9) which may have contributed in part to higher TIN removal, but this was reflected in the COD/TIN removal ratios. DO control and continuous AvN had similar influent C/N ratios (12.5 ± 1.2 and 12.8 ± 1.1 gCOD/gN respectively) but continuous AvN control had a significantly lower TIN removal ($p = 1.7 \times 10^{-3}$) than DO control (Figure 7.6). The COD/TIN removal ratio was also the highest for MLE_Cont_AvN, indicating that the COD was used the least efficiently for denitrification. As expected, the DO setpoints in this phase for ABAC and continuous AvN (0.54 ± 0.05 and 0.52 ± 0.07 mg/L respectively) were lower than in Phase 1 for MLE_Cont_AvN (average of 0.69 ± 0.14 and ranged from 0.4 to 0.9 mg/L) due to the longer SRT.

In order to understand why TIN removal was higher during DO control than ABAC and continuous AvN control, TIN removal across the aerobic zone was compared (Figure 7.7). The SND as forward flow was 5.5 mg/L for DO control, 3.8 mg/L for ABAC, 13.0 mg/L for continuous AvN, and 22.8 mg/L for intermittent AvN. This is equivalent to 18%, 14%, 52%, and 76% of total TIN removal respectively. Although TIN loss during intermittent aeration does not

classify as SND by definition, here aerobic TIN loss is being used to compare the efficiency of the different scenarios. The DO setpoints between ABAC and Cont AvN were not significantly different ($p = 0.77$) and so cannot explain the difference in observed SND. In this case, it was not worth leaving behind a higher ammonia residual in continuous AvN vs ABAC, because the DO setpoint did not decrease enough to create more SND.

Out of the continuous aeration strategies, DO control and ABAC had the highest TIN removals but lowest SND, and continuous AvN had the lowest TIN removal but highest SND. This is because of the presence of a pre-anoxic zone in MLE, that was not limited by influent COD from the PCE feed. AvN controller maximizes TIN removal in the aerated zone by balancing nitrification with denitrification. If denitrification occurs in the anoxic zone, the controller will adjust and oxidize more ammonia, however the controller does not account for the capacity of the anoxic zone. If there is the capacity to reduce more NO_x in a pre-anoxic zone, then there is no reason to leave NH_4 in the effluent. That NH_4 should be oxidized and then denitrified in an upfront anoxic zone through internal recycle. By that logic, it is possible that intermittently aerated ABAC (with an effluent setpoint of 1 mg/L or less), would achieve even higher TIN removal than intermittent AvN in this case.

It was clear that intermittent AvN performed the best from a TIN removal stand point, by taking the advantage of influent carbon in the most efficient way (i.e. dedicated anoxic zones led to the most denitrification). It may appear obvious that the ammonia residual left behind in continuous AvN control led to less TIN removal overall, but it is not clear why this strategy achieved the most SND out of the continuous aeration strategies.

In summary, if the anoxic zone is being utilized to its full denitrification potential, and there is no denitrification occurring in the aerobic reactors, there will be no difference in TIN removal between aeration control strategies. This should be true for any process with a pre-anoxic zone, and no second anoxic zone. In fact, a constant DO setpoint of 2mg/L should lead to the highest TIN removal under these conditions, assuming the anoxic zone is not carbon limited, since all of the NH_4^+ is being oxidized. This led to the realization of the importance of quantifying SND through nitrogen profiling. Without the application of a well-calibrated process model, it is difficult to quantify the amount of nitrate and nitrite that is being reduced in the aerated zone because of the multitude of biological processes involving nitrogen in the aerobic zone. Specifically, it is difficult to know if nitrogen loss is due to NO_x reduction or ammonia assimilation, combined with ammonia generation due to organic nitrogen ammonification.

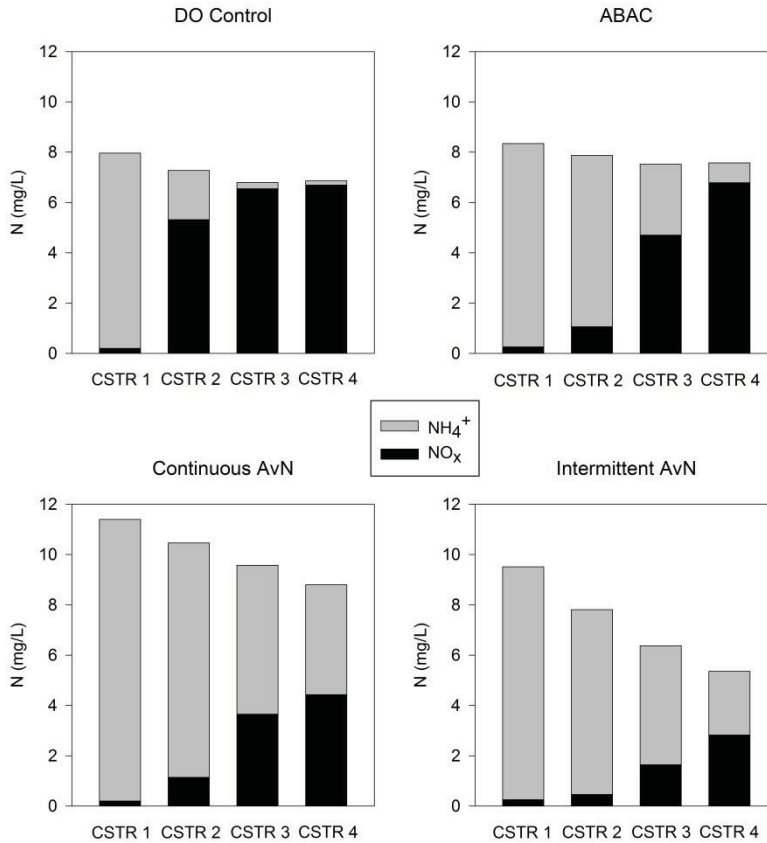


Figure 7.7: Profile grab samples to quantify SND measured as TIN loss across aerated reactors

Phase 3

The SRT was increased to around 20 days (maintaining an 11 hour HRT), so that the system could fully nitrify at very low DO (around 0.2 mg/L), and SND could theoretically be maximized. A/O in this phase was operated with 4 CSTRs, then an anaerobic selector was added to make 5 CSTRs in series for the A2O scenarios (Figure 7.8). During one of the A2O scenarios, the pilot was operated with diurnal loading and ABAC control. The hypothesis was that in full scale ABAC, SND is occurring during low flow conditions, which leads to temporarily very low DO setpoints (possibly even zero DO), so ABAC should produce more SND than constant DO control at a constant loading. A/O constant DO of 0.2 was operated for 38 days, A2O constant DO of 0.2 was operated for 22 days, A2O diurnal flow with ABAC was operated for 56 days, A2O diurnal flow with DO setpoint of 0.3 was operated for 15 days.

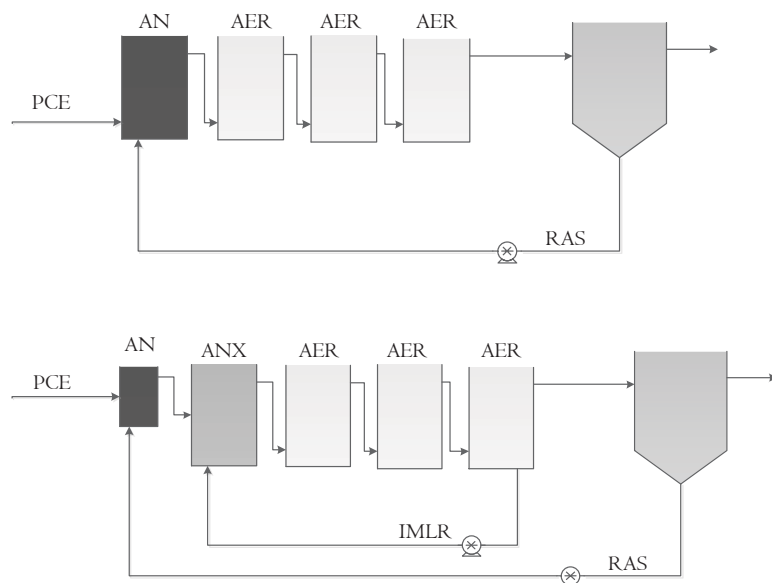


Figure 7.8: Phase 3 process configurations. A/O with 4 CSTRs (top) and A2O with 5 CSTRs and varying IMLR rates (bottom).

At a longer SRT (20.9 ± 2.9 days for all phases) the process was able to fully nitrify at a lower DO concentration (between 0.2 and 0.3 mg/L). Total B-stage influent (primary clarifier effluent) COD was 468 ± 70 , sCOD was 218 ± 41 , and ffCOD was 111 ± 24 . Influent COD/NH₄ ratios were fairly consistent for each phase, and are shown in Figure 7.8. Throughout all phases the effluent ammonia was typically below 1 mg N/L, with an average value of 0.37 ± 0.49 mgN/L (Figure 7.9). The average DO during A2O ABAC was 0.24 ± 0.02 mg/L with values ranging from approximately 0.1 to 0.4 mg/L throughout the day due to the diurnal flow. Examples of controller performance for ABAC with diurnal flow pattern, and constant DO control at a DO of 0.2 mg/L are shown in Figures B4 and B5.

As expected, the overall TIN removal during A/O operation ($61.2 \pm 3.7\%$) was much lower than the lowest TIN removal A2O phase (80.5 ± 3.5). During A2O operation with 0.2 DO setpoint, the overall TIN removal was 80.5 ± 3.5 mgN/L, and 86.0 ± 2.9 mgN/L at a 0.3 DO setpoint. TIN removal was 83.8 ± 3.0 mgN/L during A2O ABAC operation, and the average DO setpoint during ABAC was 0.24 mg/L. The fact that TIN removal among A2O scenarios was lowest at the lowest DO (0.2 mg/L) may be explained by lower influent C/N ratio (Figure 7.8). TIN removal was not improved by operating ABAC with a diurnal influent flow compared to continuous aeration with continuous influent flow (Figure 7.9). This indicates that another factor besides DO concentration was the limiting factor for SND.

Figures 7.10 and 7.11 are from A/O and A2O phases at a constant DO of 0.2 mg/L. During transition from A/O to A2O the IMLR was increased from 1Q to 3Q, and to 4Q. There was a negative correlation ($R^2=0.52$, $p<0.001$) between SND and anoxic nitrogen removal for the A2O scenarios (Figure 7.10). The hypothesis was that there was a fixed amount of denitrification that

can occur across the process, which is determined by the amount of influent COD. Perhaps if there is more COD utilized in the anoxic zone for denitrification, then that COD is not available for denitrification in the aerobic zone. Figure 7.11 shows that there is not a relationship between the amount of SND and TIN removal. This suggests that there is a total amount of TIN removal that can be achieved (most likely to carbon availability), and if denitrification increases in one zone, it will decrease in the other (Figure 7.10).

Biological Phosphorus Removal and Nitrification Rates

There was not an indication of NOB out-selection during this phase. The maximum effluent nitrite value for all phases was 0.36 mgN/L, and the average was 0.07 ± 0.07 mgN/L. AOB/NOB activity rate tests were performed on days 47, 54, 67, and 76. The average AOB rate was 3.50 ± 0.25 mgN/gMLVSS/hr and the average NOB rate was 2.85 ± 0.31 mgN/gMLVSS/hr. The average NOB/AOB rate ratio was 0.81 ± 0.05 g/g. This is close to the theoretical value (0.78 g/g) that would be expected if AOB and NOB populations were equal in a fully nitrifying process (Dold et al., 2015).

PAO and dPAO maximum activity rate tests were performed on day 60. The average anaerobic OP release rate for the two tests was 24.8 ± 2.9 mgP/gMLVSS/hr and the average OP release to acetate uptake rate was 0.64 ± 0.06 gP/gCOD. The aerobic OP uptake rate was 15.8 mgP/gMLVSS/hr. The anoxic OP and NO₃ uptake rates were 3.0 mgP/gMLVSS/hr and 1.1 mgN/gMLVSS/hr. Therefore the maximum anoxic OP uptake rate was approximately 19% of the aerobic maximum OP uptake rate which is consistent with other studies (Kuba et al., 1997). It was difficult to quantify dPAO activity in the pilot process, as release and uptake could be occurring simultaneously in the anoxic zone. It is even more difficult to differentiate between aerobic OP uptake and anoxic OP uptake in aerated zones since both could be happening simultaneously at low DO. As such, it is also difficult to differentiate between denitrification in the aerobic zone by OHO or dPAO.

Dechloromonas spp. and ‘*Candidatus Accumulibacter*’ spp. were the main PAO detected via genus-level analysis of 16S rRNA gene amplicon sequencing (Figure 7.12), with some ‘*Candidatus Competibacter*’ spp. present. Only a small percentage of *Nitrosomonas* were detected, and *Nitrospira* was by far the dominant nitrifier. Although no analysis was performed to detect Comammox, these results could suggest that some of the ammonia oxidation was being performed by *Nitrospira* (van Kessel et al., 2015). Recent research demonstrated Comammox *Nitrospira* selection in a low DO reactor (Roots et al., 2019).

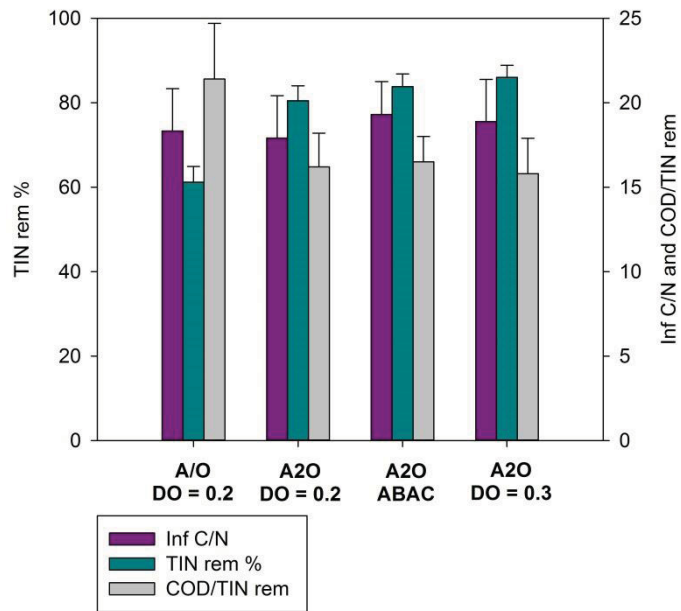


Figure 7.9: TIN removal, influent COD/NH₃, and total COD/TIN removed ratio during each scenario. Average DO during A2O ABAC was 0.24 mg/L.

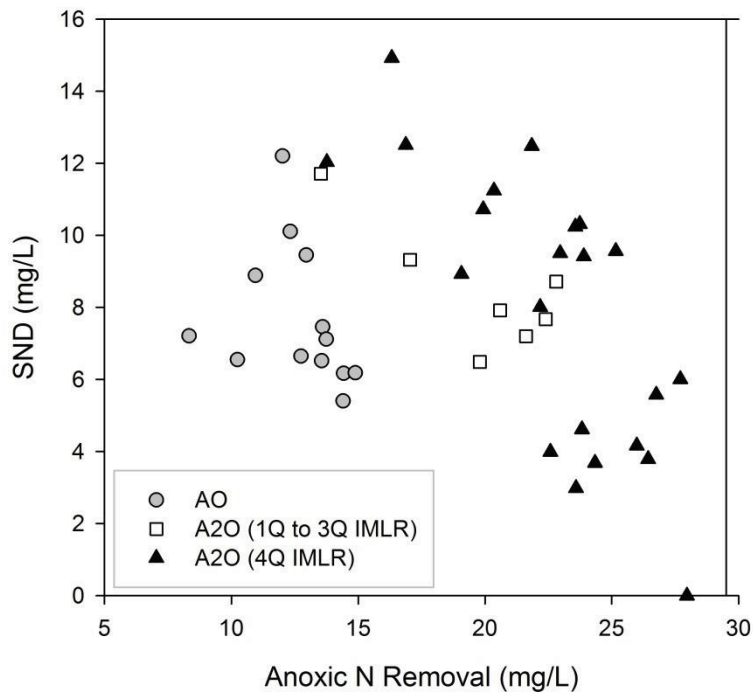


Figure 7.10: Aerobic TIN removal (SND) vs. Anoxic TIN removal

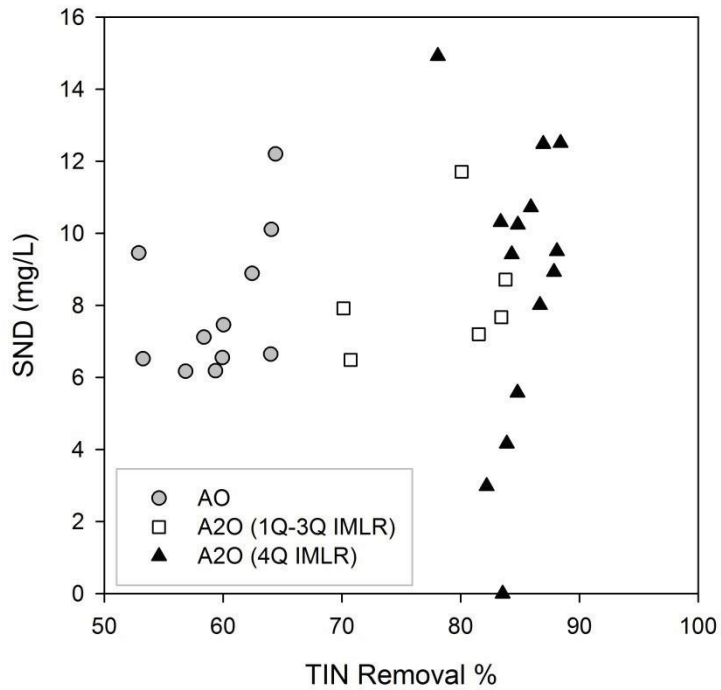


Figure 7.11: Aerobic TIN removal (SND) vs. TIN removal %

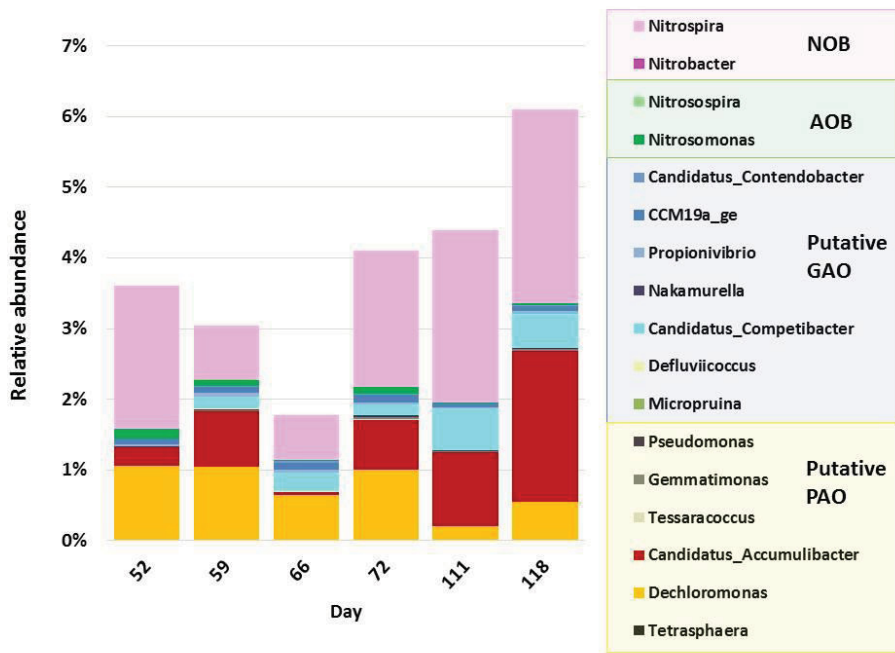


Figure 7.12: 16S rRNA gene amplicon sequencing results for putative AOB, NOB, PAO and GAO genera.

Phase 4

Immediately following Phase 3, the DO concentration was decreased to 0.1 mg/L, and the effluent ammonia was allowed to vary. The SRT and HRT were the same in Phase 4 as in Phase 3 (approximately 20 days and 11 hours respectively). A/O configuration in Phase 4 was different from Phase 3 in that the anaerobic selector had been installed, so there were four aerobic reactors instead of three (Figure 7.13). In order to confirm the relationship between SND and the anoxic nitrogen removal, mixed liquor composite samples were taken from influent and effluent of the aerobic zone as described in the methods.

A similar relationship was observed from the mixed liquor composites between SND and anoxic nitrogen removal (Figure 7.14) as in Phase 3 (Figure 7.10). The initial assumption for Phases 3 and 4 was that with lower DO, SND would increase, which would increase TIN removal. The surprising result was that the amount of SND was related to the ammonia residual (Figure 7.15), presumably because of the relationship between anoxic nitrogen removal and SND (Figure 7.14). Although the higher ammonia residual led to more SND, it did not lead to more total TIN removal. This leads to the conclusion that lower DO is necessary to achieve SND, but then there appears to be a limitation of carbon availability for denitrification once the DO is low enough. If the capacity is available in an upfront anoxic zone, the carbon will be used for denitrification there, if there is less denitrification up front, more TIN removal will occur in the aerobic zone.

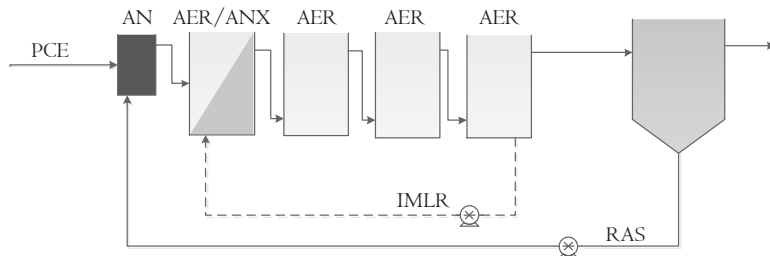


Figure 7.13: Phase 4 process configuration. In A2O configuration there was an anoxic zone with an IMLR of 400% influent flow. In A/O configuration there were four aerated CSTRs and no IMLR.

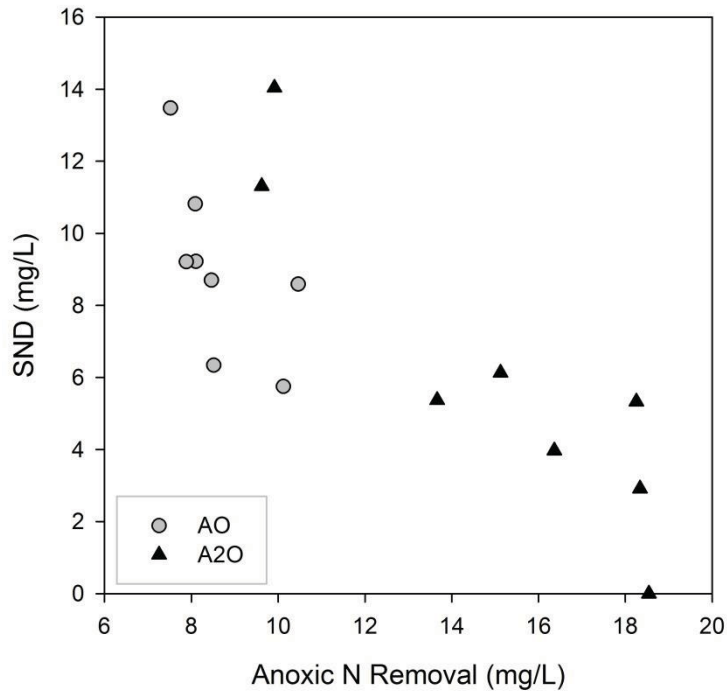


Figure 7.14: SND versus anoxic nitrogen removal

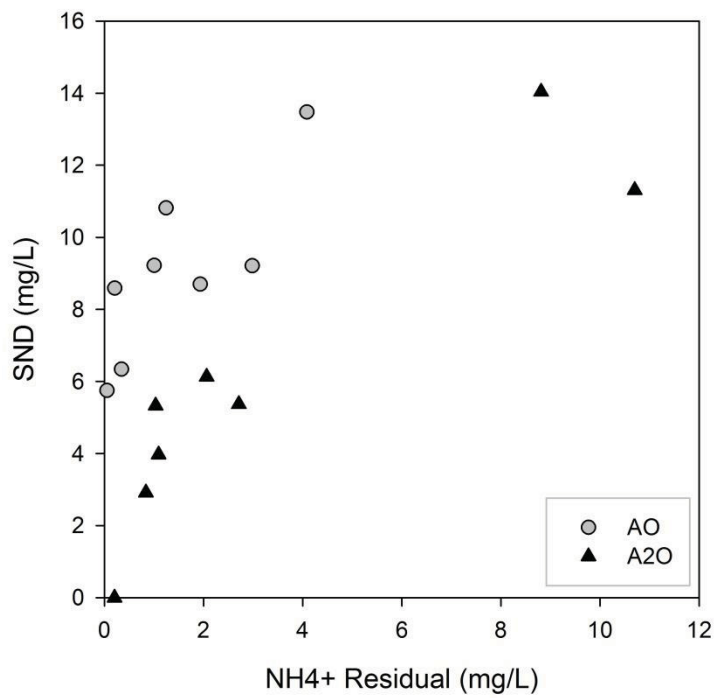


Figure 7.15: SND versus ammonia residual in the effluent

SUMMARY AND CONCLUSIONS

Table 7.2: Summary table for Phases 1 through 3. Phase 4 was not included because the goal was not to maximize TIN removal in that phase.

		Average Inf C/N	Average TIN rem %	Maximum TIN rem %
Phase 1 ASE 4 hr HRT	FA_Int_AvN	7.2±1.9	54.4±13.7	78.9
	FA_Cont_AvN	6.1±1.2	20.5±14.1	51.9
	MLE_DO=2	8.0±1.0	23.1±2.8	29.3
	MLE_Int_AvN	7.8±1.3	60.1±14.1	80.0
	MLE_Cont_AvN	7.2±1.0	39.8±11.4	58.4
Phase 2 MLE 11 hr HRT 16 day SRT	Int AVN	13.6±0.9	89.4±2.1	91.9
	DO = 2	12.5±1.2	82.2±1.0	83.6
	ABAC	11.4±0.3	80.0±0.7	80.5
	Cont AVN	12.8±1.1	74.4±1.7	77.3
Phase 3 AO/A2O 11 hr HRT 21 day SRT	A/O	13.2±1.8	61.2±3.7	70.7
	A2O DO 0.2	12.9±1.8	80.5±3.5	84.8
	A2O ABAC	13.9±1.4	83.8±3.0	88.7
	A2O DO 0.3	13.6±1.8	86.0±2.9	88.4

Intermittent aeration lends itself to intensification because high TIN removal can be achieved at a shorter SRT (Table 7.2). In order for continuous aeration to achieve the same level of TIN removal as intermittent aeration, the SRT needed to be much longer. This demonstrated that in these configurations, attempting to achieve SND via low DO is not part of a strategy for intensification. The highly loaded A/B process configuration (4 hour HRT) with intermittent aeration was capable of achieving a maximum TIN removal of 80%, while the A2O process with PCE feed, an 11 hour HRT, and 0.2-0.3 mg/L continuous aeration achieved a maximum of 88% TIN removal. The highest TIN removal was achieved in phase 2 during intermittent aeration (91.9%). These results suggest that intermittent aeration would result in greater TIN removal in a smaller footprint than continuous aeration.

By optimizing the nitrification process thereby reducing the bulk DO concentration, denitrification capacity can be increased by limiting the transfer of oxygen into anoxic zones, and by recovering excess capacity for anoxic volume (Amand et al., 2013; Rieger et al., 2012a). An increase in TIN removal ranging from 30-50% was reported for five different treatment facilities by optimizing the nitrification and denitrification capacity (Rieger et al., 2012b). Also, decreasing the bulk DO concentration and oxidizing less ammonia, results in aeration and chemical savings. In addition, it is often assumed that implementing ABAC or AvN control will result in increased TIN removed through simultaneous nitrification/denitrification (SND) in the aerobic zone (Jimenez et al., 2013; Wankmuller et al., 2017). However, this study showed that lower DO did not always improve TIN removal and most importantly that aeration control alone cannot guarantee SND. No conclusions can be made about the carbon source for SND, if it was

internally stored or sbCOD, or if it was associated with dPAO. In Phase 1 rbCOD was low coming from A-stage, so sbCOD during intermittent aeration was probably responsible for most TIN removal. In all other phases rbCOD could have been stored, or sbCOD could be hydrolyzed to provide carbon for denitrification in the aerobic zone.

In A2O configuration the TIN removal efficiency was the same, regardless of the amount of SND that occurred. This suggests that process configurations with a pre-anoxic zone (e.g. MLE or A2O) are less likely to benefit from increased TIN removal by implementing low DO aeration control strategies than configurations without (A/O). Keeping in mind that TIN removal was higher for A2O configuration than A/O configuration (Table 7.2). Also, in a process with a pre-anoxic zone, it does not make sense to leave behind an ammonia residual that could be oxidized and then denitrified in a pre-anoxic zone.

If the goal of implementing sensor driven aeration control is increased TIN removal, intermittent aeration is the best option because allows for the most denitrification in the aerobic zone because of the defined anoxic periods. Intermittent aeration (either ABAC or AvN) will adjust the aerobic volume to meet the treatment goals, and in addition, intermittent AvN will maximize TIN removal. Continuous AvN or ABAC is not a substitute for intermittent AvN or ABAC because the TIN removal is dependent on SND, which will require a longer SRT to achieve the same amount of TIN removal. Al-Omari et al., 2015 modeled intermittent ABAC and AvN, and showed that AvN had an increased TIN removal efficiency of 7.3% over ABAC. Intermittent ABAC was not operated in this study, but it could be that intermittent AvN has an increased TIN removal compared to ABAC because the increase in dedicated anoxic time is able to increase denitrification, while in continuous AvN, the decrease in DO setpoint is not enough to increase SND. Even if there would be a slight increase in SND, it would have to be enough to make up for the ammonia residual in the effluent, which was not the case in Phase 2 of this study.

Acknowledgements

The authors would like to acknowledge Catherine Hoar of Dr. Kartik Chandran's lab, Department of Earth and Environmental Engineering, Columbia University for performing the 16S rRNA gene amplicon sequencing analysis.

REFERENCES

- Alleman, J. E., & Irvine, R. L. (1980). Storage-induced denitrification using sequencing batch reactor operation. *Water Research*, 14(10), 1483–1488.
- Al-Omari, A., Wett, B., Nopens, I., De Clippeleir, H., Han, M., Regmi, P., ... Murthy, S. (2015). Model-based evaluation of mechanisms and benefits of mainstream shortcut nitrogen removal processes. *Water Science and Technology*, 71(6), 840–847.
<https://doi.org/10.2166/wst.2015.022>
- Amand, L., Olsson, G., & Carlsson, B. (2013). Aeration control—a review. *Water Science and Technology*, 67(11), 2374–2398.

- Bassin, J. P., Kleerebezem, R., Dezotti, M., & van Loosdrecht, M. C. M. (2012). Simultaneous nitrogen and phosphate removal in aerobic granular sludge reactors operated at different temperatures. *Water Research*, *46*(12), 3805–3816.
<https://doi.org/10.1016/j.watres.2012.04.015>
- Batchelor, B. (1983). Simulation of single-sludge nitrogen removal. *Journal of Environmental Engineering*, *109*(1), 1–16.
- Bernat, K., & Wojnowska-Baryła, I. (2007). Carbon source in aerobic denitrification. *Biochemical Engineering Journal*, *36*(2), 116–122.
- Bertanza, G. (1997). Simultaneous nitrification-denitrification process in extended aeration plants: Pilot and real scale experiences. *Water Science and Technology; London*, *35*(6), 53–61.
- Boehnke, D. B., & Diering, D. B. (1997). Cost-effective wastewater treatment process for removal of... *Water Engineering & Management*, *144*(5), 30–34.
- Cao, Y., van Loosdrecht, M. C. M., & Daigger, G. T. (2017). Mainstream partial nitrification–anammox in municipal wastewater treatment: Status, bottlenecks, and further studies. *Applied Microbiology and Biotechnology*, *101*(4), 1365–1383.
<https://doi.org/10.1007/s00253-016-8058-7>
- Chiu, Y.-C., Lee, L.-L., Chang, C.-N., & Chao, A. C. (2007). Control of carbon and ammonium ratio for simultaneous nitrification and denitrification in a sequencing batch bioreactor. *International Biodeterioration & Biodegradation*, *59*(1), 1–7.
<https://doi.org/10.1016/j.ibiod.2006.08.001>
- Daigger, G. T., & Littleton, H. X. (2000). Characterization of Simultaneous Nutrient Removal in Staged, Closed-Loop Bioreactors. *Water Environment Research*, *72*(3), 330–339.
<https://doi.org/10.2175/106143000X137554>
- Daigger, G. T., & Littleton, H. X. (2014). Simultaneous Biological Nutrient Removal: A State-of-the-Art Review. *Water Environment Research*, *86*(3), 245–257.
<https://doi.org/10.2175/106143013X13736496908555>
- Dold, P., Du, W., Burger, G., & Jimenez, J. (2015). Is Nitrite-Shunt Happening in the System? Are NOB Repressed? *Proceedings of the Water Environment Federation*, *2015*(13), 1360–1374.
- Giraldo, E., Jjemba, P., Liu, Y., & Muthukrishnan, S. (2011). Ammonia Oxidizing Archaea, AOA, Population and Kinetic Changes in a Full Scale Simultaneous Nitrogen and Phosphorous Removal MBR. *Proceedings of the Water Environment Federation*, *2011*(13), 3156–3168. <https://doi.org/10.2175/193864711802721596>

- Hocaoglu, S. M., Insel, G., Ubay Cokgor, E., & Orhon, D. (2011). Effect of sludge age on simultaneous nitrification and denitrification in membrane bioreactor. *Bioresource Technology*, *102*(12), 6665–6672. <https://doi.org/10.1016/j.biortech.2011.03.096>
- Jimenez, J., Bott, C., Regmi, P., & Rieger, L. (2013). Process control strategies for simultaneous nitrogen removal systems. *Proceedings of the Water Environment Federation*, *2013*(4), 492–505.
- Jimenez, J., Dursun, D., Dold, P., Bratby, J., Keller, J., & Parker, D. (2010). Simultaneous nitrification-denitrification to meet low effluent nitrogen limits: Modeling, performance and reliability. *Proceedings of the Water Environment Federation*, *2010*(15), 2404–2421.
- Keene, N. A., Reusser, S. R., Scarborough, M. J., Grooms, A. L., Seib, M., Santo Domingo, J., & Noguera, D. R. (2017). Pilot plant demonstration of stable and efficient high rate biological nutrient removal with low dissolved oxygen conditions. *Water Research*, *121*, 72–85. <https://doi.org/10.1016/j.watres.2017.05.029>
- Kinyua, M., Klaus, S., Sadowski, M., Regmi, P., Wett, B., De Clippeleir, H., Chandran, K., Bott, C.B. (2018). Effect of Influent Carbon Fractionation and Reactor Configuration on Nitrogen Removal and NOB Out Selection during Intermittent Aeration *IWA Nutrient Removal and Recovery Conference 2018, Brisbane, Australia*.
- Kreuk, M. K. de, Heijnen, J. J., & Loosdrecht, M. C. M. van. (2005). Simultaneous COD, nitrogen, and phosphate removal by aerobic granular sludge. *Biotechnology and Bioengineering*, *90*(6), 761–769. <https://doi.org/10.1002/bit.20470>
- Littleton, H. X., Daigger, G. T., Strom, P. F., & Cowan, R. A. (2003). Simultaneous Biological Nutrient Removal: Evaluation of Autotrophic Denitrification, Heterotrophic Nitrification, and Biological Phosphorus Removal in Full-Scale Systems. *Water Environment Research*, *75*(2), 138–150. <https://doi.org/10.2175/106143003X140926>
- Liu, Y., Shi, H., Xia, L., Shi, H., Shen, T., Wang, Z., ... Wang, Y. (2010). Study of operational conditions of simultaneous nitrification and denitrification in a Carrousel oxidation ditch for domestic wastewater treatment. *Bioresource Technology*, *101*(3), 901–906.
- Matsumoto, S., Terada, A., & Tsuneda, S. (2007). Modeling of membrane-aerated biofilm: Effects of C/N ratio, biofilm thickness and surface loading of oxygen on feasibility of simultaneous nitrification and denitrification. *Biochemical Engineering Journal*, *37*(1), 98–107. <https://doi.org/10.1016/j.bej.2007.03.013>
- Miller, M. W., Bunce, R., Regmi, P., Hingley, D. M., Kinnear, D., Murthy, S., ... Bott, C. B. (2012). A/B process pilot optimized for nitrite shunt: High rate carbon removal followed by BNR with ammonia-Based cyclic aeration control. *Proceedings of the Water Environment Federation*, *2012*(10), 5808–5825.

- Miller, M. W., Elliott, M., DeArmond, J., Kinyua, M., Wett, B., Murthy, S., & Bott, C. B. (2017). Controlling the COD removal of an A-stage pilot study with instrumentation and automatic process control. *Water Science and Technology*, *75*(11), 2669–2679.
- Mino, T., San Pedro, D. C., & Matsuo, T. (1995). Estimation of the rate of slowly biodegradable COD (SBCOD) hydrolysis under anaerobic, anoxic and aerobic conditions by experiments using starch as model substrate. *Water Science and Technology*, *31*(2), 95–103.
- Münch, E. V., Lant, P., & Keller, J. (1996). Simultaneous nitrification and denitrification in bench-scale sequencing batch reactors. *Water Research*, *30*(2), 277–284.
- Oh, J., & Silverstein, J. (1999). Oxygen inhibition of activated sludge denitrification. *Water Research*, *33*(8), 1925–1937.
- Park, H.-D., Regan, J. M., & Noguera, D. R. (2002). Molecular analysis of ammonia-oxidizing bacterial populations in aerated-anoxic Orbal processes. *Water Science and Technology*, *46*(1–2), 273–280. <https://doi.org/10.2166/wst.2002.0489>
- Park, Hee-Deung, & Noguera, D. R. (2008). Nitrospira community composition in nitrifying reactors operated with two different dissolved oxygen levels. *J Microbiol Biotechnol*, *18*(8), 1470–1474.
- Pochana, K., & Keller, J. (1999). Study of factors affecting simultaneous nitrification and denitrification (SND). *Water Science and Technology*, *39*(6), 61–68. [https://doi.org/10.1016/S0273-1223\(99\)00123-7](https://doi.org/10.1016/S0273-1223(99)00123-7)
- Quast, C., Pruesse, E., Yilmaz, P., Gerken, J., Schweer, T., Yarza, P., ... Glöckner, F. O. (2013). The SILVA ribosomal RNA gene database project: Improved data processing and web-based tools. *Nucleic Acids Research*, *41*(D1), D590–D596. <https://doi.org/10.1093/nar/gks1219>
- Randall, C. W., & Sen, D. (1996). Full-scale evaluation of an integrated fixed-film activated sludge (IFAS) process for enhanced nitrogen removal. *Water Science and Technology*, *33*(12), 155–162. [https://doi.org/10.1016/0273-1223\(96\)00469-6](https://doi.org/10.1016/0273-1223(96)00469-6)
- Regmi, P., Bunce, R., Miller, M. W., Park, H., Chandran, K., Wett, B., ... Bott, C. B. (2015). Ammonia-based intermittent aeration control optimized for efficient nitrogen removal. *Biotechnology and Bioengineering*, *112*(10), 2060–2067. <https://doi.org/10.1002/bit.25611>
- Regmi, P., Miller, M. W., Holgate, B., Bunce, R., Park, H., Chandran, K., ... Bott, C. B. (2014). Control of aeration, aerobic SRT and COD input for mainstream nitrification/denitrification. *Water Research*, *57*, 162–171.

- Rieger, L., Takács, I., & Siegrist, H. (2012a). Improving Nutrient Removal While Reducing Energy Use at Three Swiss WWTPs Using Advanced Control. *Water Environment Research; Alexandria*, 84(2), 170–188.
- Rieger, L., Jones, R. M., Dold, P. L., & Bott, C. B. (2012b). Myths about Ammonia Feedforward Aeration Control. *Proceedings of the Water Environment Federation*, 2012(14), 2483–2502. <https://doi.org/10.2175/193864712811726392>
- Rieger, L., Jones, R. M., Dold, P. L., & Bott, C. B. (2014). Ammonia-based feedforward and feedback aeration control in activated sludge processes. *Water Environment Research*, 86(1), 63–73.
- Roots, P., Wang, Y., Rosenthal, A. F., Griffin, J. S., Sabba, F., Petrovich, M., ... Wells, G. F. (2019). Comammox Nitrospira are the dominant ammonia oxidizers in a mainstream low dissolved oxygen nitrification reactor. *Water Research*.
- Rubio-Rincón, F. J., Lopez-Vazquez, C. M., Welles, L., van Loosdrecht, M. C. M., & Brdjanovic, D. (2017). Cooperation between Candidatus Competibacter and Candidatus Accumulibacter clade I, in denitrification and phosphate removal processes. *Water Research*, 120, 156–164. <https://doi.org/10.1016/j.watres.2017.05.001>
- Schloss, P. D., Westcott, S. L., Ryabin, T., Hall, J. R., Hartmann, M., Hollister, E. B., ... Weber, C. F. (2009). Introducing mothur: Open-Source, Platform-Independent, Community-Supported Software for Describing and Comparing Microbial Communities. *Applied and Environmental Microbiology*, 75(23), 7537–7541. <https://doi.org/10.1128/AEM.01541-09>
- Schraa, O., Rieger, L., Alex, J., & Miletić, I. (2019). Ammonia-based aeration control with optimal SRT control: Improved performance and lower energy consumption. *Water Science and Technology*, 79(1), 63–72.
- Stinson, B., Murthy, S., Bott, C., Wett, B., Al-Omari, A., Bowden, G., ... Clippeleir, H. D. (2013). *Roadmap Toward Energy Neutrality & Chemical Optimization at Enhanced Nutrient Removal Facilities*. Retrieved from <https://www.accesswater.org/publications/-281854/roadmap-toward-energy-neutrality--amp--chemical-optimization-at-enhanced-nutrient-removal-facilities>
- Third, K. A., Burnett, N., & Cord-Ruwisch, R. (2003). Simultaneous nitrification and denitrification using stored substrate (PHB) as the electron donor in an SBR. *Biotechnology and Bioengineering*, 83(6), 706–720.
- Tsuneda, S., Ohno, T., Soejima, K., & Hirata, A. (2006). Simultaneous nitrogen and phosphorus removal using denitrifying phosphate-accumulating organisms in a sequencing batch reactor. *Biochemical Engineering Journal*, 27(3), 191–196. <https://doi.org/10.1016/j.bej.2005.07.004>

- van Kessel, M. A. H. J., Speth, D. R., Albertsen, M., Nielsen, P. H., Op den Camp, H. J. M., Kartal, B., ... Lücker, S. (2015). Complete nitrification by a single microorganism. *Nature*, 528(7583), 555–559. <https://doi.org/10.1038/nature16459>
- Van Loosdrecht, M. C. M., & Henze, M. (1999). Maintenance, endogeneous respiration, lysis, decay and predation. *Water Science and Technology*, 39(1), 107–117. [https://doi.org/10.1016/S0273-1223\(98\)00780-X](https://doi.org/10.1016/S0273-1223(98)00780-X)
- van Loosdrecht, M. C. M., Pot, M. A., & Heijnen, J. J. (1997). Importance of bacterial storage polymers in bioprocesses. *Water Science and Technology*, 35(1), 41–47. <https://doi.org/10.2166/wst.1997.0008>
- Vocks, M., Adam, C., Lesjean, B., Gnirss, R., & Kraume, M. (2005). Enhanced post-denitrification without addition of an external carbon source in membrane bioreactors. *Water Research*, 39(14), 3360–3368.
- Vrečko, D., Hvala, N., Stare, A., Burica, O., Stražar, M., Levstek, M., ... Podbevšek, S. (2006). Improvement of ammonia removal in activated sludge process with feedforward-feedback aeration controllers. *Water Science and Technology*, 53(4–5), 125–132. <https://doi.org/10.2166/wst.2006.098>
- Wankmuller, D., Bilyk, K., Pitt, P., Fredericks, D., Latimer, R., Grandstaff, J., ... Sparks, J. (2017, January 1). *Saving Carbon with SND Using Ammonia Based Aeration Control*. Retrieved from <https://www.accesswater.org/publications/-279792/saving-carbon-with-snd-using-ammonia-based-aeration-control>
- Winkler, M., Coats, E. R., & Brinkman, C. K. (2011). Advancing post-anoxic denitrification for biological nutrient removal. *Water Research*, 45(18), 6119–6130.
- Zeng, R. J., Lemaire, R., Yuan, Z., & Keller, J. (2003). Simultaneous nitrification, denitrification, and phosphorus removal in a lab-scale sequencing batch reactor. *Biotechnology and Bioengineering*, 84(2), 170–178.
- Zhu, G., Peng, Y., Wu, S., Wang, S., & Xu, S. (2007). Simultaneous nitrification and denitrification in step feeding biological nitrogen removal process. *Journal of Environmental Sciences*, 19(9), 1043–1048. [https://doi.org/10.1016/S1001-0742\(07\)60170-3](https://doi.org/10.1016/S1001-0742(07)60170-3)

APPENDIX B: SUPPORTING INFORMATION FOR CHAPTER 7

Example SND Calculation:

Assume:

The anoxic TIN reduction includes what is denitrified in the clarifier, the anaerobic zone (if present), and the anoxic zone. It is assumed that $CSTR4_{out}^{NOx}$ equals the NO_x concentration in the RAS line, which means that any denitrification taking place in the clarifier gets included in the anoxic TIN calculation.

Q_{total} = Total forward flow = influent + RAS + IMLR

Q_{inf} = Influent flow

Q_{RAS} = RAS flow

Q_{IMLR} = IMLR flow

MLE, A2O, and A/O with 4 CSTR:

Aerobic TIN removal (SND) as mg/L in the influent flow:

$$(CSTR1_{out}^{TIN} - CSTR4_{out}^{TIN}) * \frac{Q_{total}}{Q_{inf}}$$

Anoxic TIN removal as mg/L in the influent flow:

$$(CSTR1_{out}^{NOx} * Q_{total} - (CSTR4_{out}^{NOx} * Q_{IMLR} + CSTR4_{out}^{NOx} * Q_{RAS})) * \frac{1}{Q_{inf}}$$

A/O with 5 CSTR:

Aerobic TIN removal (SND) as mg/L in the influent flow:

$$(CSTR0_{out}^{TIN} - CSTR4_{out}^{TIN}) * \frac{Q_{total}}{Q_{inf}}$$

Anoxic TIN removal as mg/L in the influent flow:

$$(CSTR0_{out}^{NOx} * Q_{total} - CSTR4_{out}^{NOx} * Q_{RAS}) * \frac{1}{Q_{inf}}$$

Table B1: Diurnal Flow pattern

Base Flow Rate: 0.3 gpm		
Time (hr)	Multiplier (operator input)	Flow Rate (gpm) = Multiplier*base flow rate
0	0.97	0.291
1	0.85	0.255
2	0.72	0.216
3	0.64	0.192
4	0.58	0.174
5	0.55	0.165
6	0.59	0.177
7	0.77	0.231
8	1.02	0.306
9	1.07	0.321
10	1.15	0.345
11	1.24	0.372
12	1.24	0.372
13	1.23	0.369
14	1.2	0.36
15	1.16	0.348
16	1.13	0.339
17	1.15	0.345
18	1.13	0.339
19	1.17	0.351
20	1.2	0.36
21	1.18	0.354
22	1.13	0.339
23	1.09	0.327

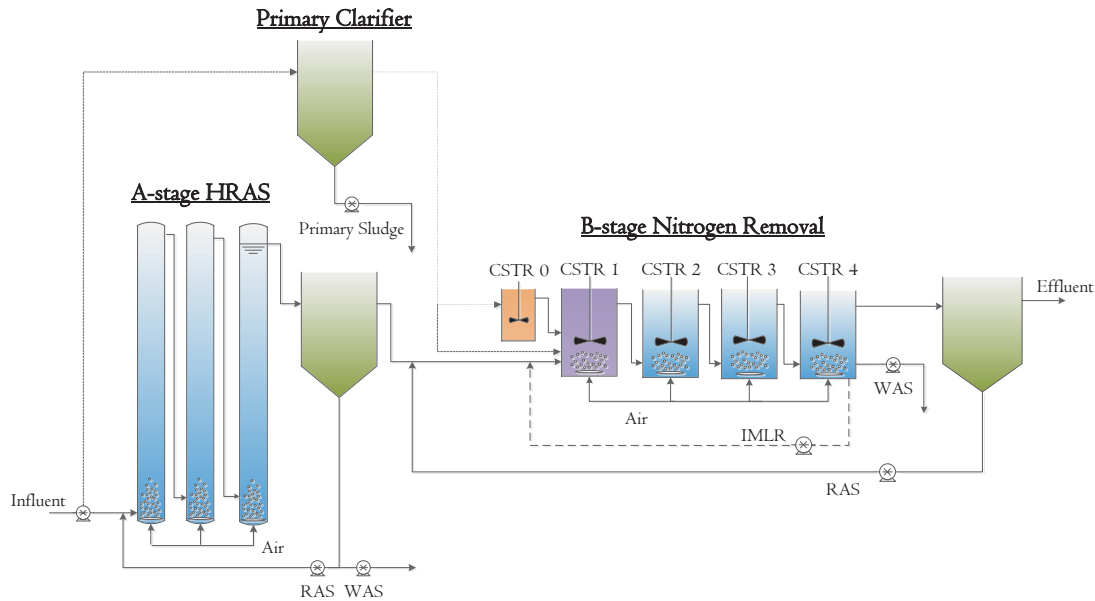


Figure B1: Overall pilot configuration. CSTR 0 was an optional anaerobic zone and could be bypassed. CSTR 1 was either aerobic or anoxic, with or without internal mixed liquor recycle (IMLR). CSTRs 2-4 were aerobic.

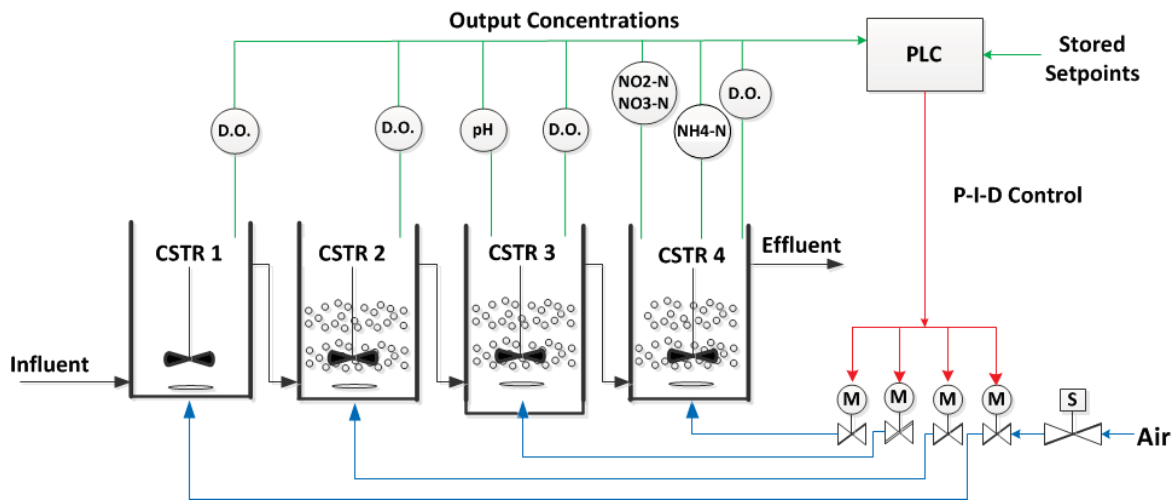


Figure B2: Sensors include dissolved oxygen (Insite Model 10, LA, USA), pH (Foxboro/Invensys, UK) ammonium (WTW VARiON, Germany), nitrate and nitrite (s::can Spectro::lyser, Austria). The anaerobic selector (CSTR 0) had no automated control and is not shown.

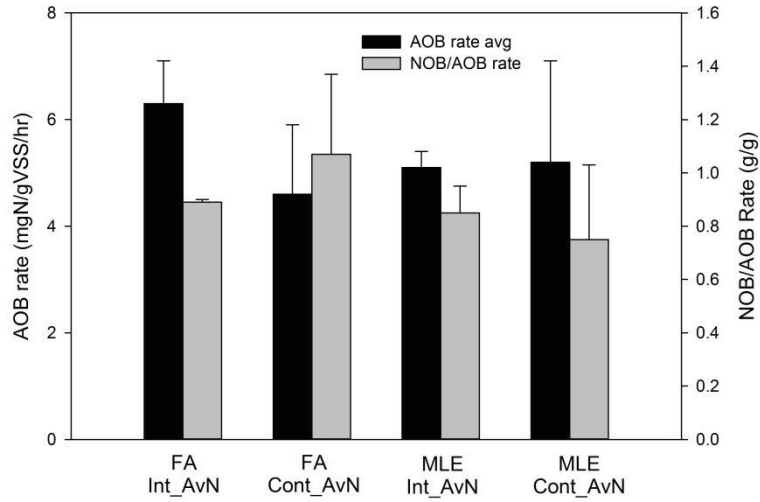


Figure B3: Phase 1 AOB and NOB rates

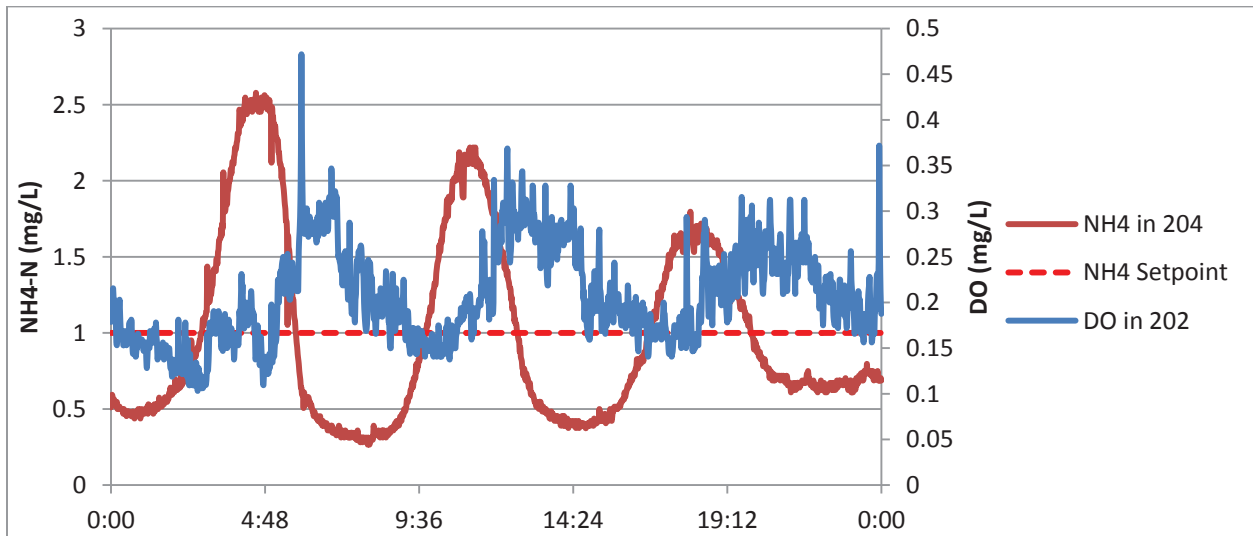


Figure B4: example of ABAC diurnal PID control.

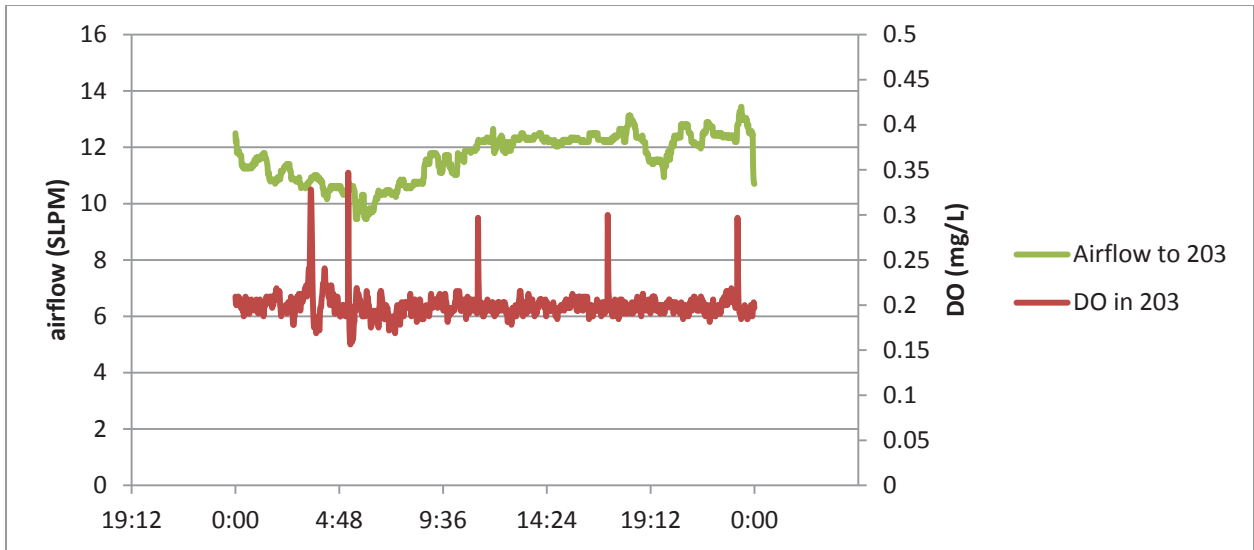


Figure B5: Constant DO setpoint

CHAPTER 8: INTEGRATION OF SIDESTREAM BIOLOGICAL PHOSPHORUS REMOVAL AND PARTIAL DENITRIFICATION/ANAMMOX

Stephanie Klaus, Varun Srinivasan, Dongqi Wang, Chenghua Long, Haydee DeClippeleir, Kartik Chandran, April Gu, Charles B. Bott

ABSTRACT

The integration of biological phosphorus removal (bio-P) and shortcut nitrogen removal processes is challenging because of the conflicting use of influent carbon. The objective of this study was to achieve shortcut nitrogen removal, either via partial nitrification/anammox (PNA) or partial denitrification/anammox (PDNA), simultaneously with biological phosphorus removal. This study took place in a pilot scale A/B process, with a sidestream bio-P reactor, and tertiary anammox polishing. Bio-P occurred in B-stage, with the addition of A-stage WAS fermentate, despite low influent rbCOD concentrations from the A-stage effluent. Nitrite accumulation (maximum of 5.9 mg/L) occurred in B-stage via partial denitrification, and was removed along with ammonia by the tertiary anammox MBBR, with the ability to achieve effluent TIN less than 2 mg/L. Nitrite accumulation and bio-P occurred simultaneously, but this was not sustained and bio-P performance suffered, potentially due to competition for the influent VFA between PAO and other carbon storing organisms.

INTRODUCTION

Partial nitrification/anammox (PNA) in sidestream processes, treating dewatered anaerobically digested sludge liquor, is well established with over 100 full-scale installations (Lackner et al., 2014). The main challenges of achieving mainstream deammonification are NOB out-selection and anammox retention (Cao et al., 2017). NOB repression is easier in sidestream processes due to high free ammonia (FA) concentrations (Anthonisen et al., 1976) and high temperature (Hellings et al., 1998). The challenge of anammox retention can be overcome by a two-phase, separate SRT, system in which nitrifiers and ordinary heterotrophs are in a suspended growth reactor, followed by a completely anoxic anammox moving bed biofilm reactor (MBBR) (Regmi et al., 2015; Ma et al., 2011). However, sustaining NOB out-selection has proven very difficult, and may be an insurmountable obstacle to full-scale adoption of PNA (Wells et al., 2017; Ma et al., 2016; Cao et al., 2017; Lotti et al., 2015)

Due to the difficulty of generating nitrite from partial nitrification, recent research efforts have explored the generation of nitrite from partial denitrification (Du et al., 2017; Le et al., 2019; Wang et al., 2019). While PDNA offers less aeration and external carbon savings than PNA, it still provides a significant savings over full nitrification/denitrification. PNA theoretically provides 60% aeration savings and 100% external carbon saving, while PDNA provides 50% aeration savings and 80% external carbon savings (Ma et al., 2016). The aeration savings is dependent on diverting carbon away from the BNR process (Daigger, 2014), for example by using a high rate activated sludge (HRAS) A-stage process (Böhnke and Diering, 1997; Miller et al., 2017).

While the PDNA concept was originally conceived for sidestream treatment (Kalyuzhnyi et al., 2008; Sharp et al., 2017), it has greater potential for mainstream treatment because of the possibility to take advantage of influent carbon for partial denitrification, and PDNA obviates the need for NOB out-selection in mainstream. In sidestream treatment, external carbon must be utilized for partial denitrification, and NOB out-selection is not a challenge so PNA is the more obvious choice.

Partial denitrification can also be achieved using internally stored carbon, such as polyhydroxyalkanoates (PHAs) and glycogen, in which case no external carbon would be required (if influent VFA is the source of the stored compounds). There are many examples of volatile fatty acids in the influent being stored in an anaerobic zone, and then used for denitrification in a post-aeration anoxic zone (Winkler et al., 2011; Vocks et al., 2005; Alleman and Irvine, 1980), or during intermittent aeration (Zhao et al., 1999). This can be carried out by denitrifying PAO, denitrifying GAO, or other heterotrophs (Tsuneda et al., 2006; Rubio-Rincón et al., 2017; Van Loosdrecht et al., 1997). It is not clear from the literature what factors would cause partial denitrification to nitrite over full denitrification. Recent studies have shown that dGAO may preferentially reduce nitrate to nitrite, and then dPAO reduce nitrite to dinitrogen gas (Wang et al., 2019; Rubio-Rincón et al., 2017). While accumulation of nitrite via partial denitrification by dGAO is desired for treatment by anammox bacteria, GAO compete with PAO for VFA, and can lead to deterioration of bioP performance (Erdal et al., 2003; Lopez-Vazquez et al., 2009).

Sidestream bioP processes are configurations in which the influent is bypassed around the anaerobic zone (Barnard et al., 2017). Sidestream bioP configurations can include RAS fermentation, in which a portion of the RAS (5-10%) is held in an anaerobic reactor with a retention time of one to two days (Vollertsen et al., 2006; Tooker et al., 2016). Alternatively, the retention time of the sidestream reactor can be considerably shorter (1-4 hours) with the addition of supplemental carbon (since fermentation is not occurring in the reactor), such as primary sludge fermentate (Cavanaugh et al., 2012; Tooker et al., 2016).

RAS fermentation was initially investigated as a means to decrease sludge production and nutrient loading to the nutrient removal step, compared to primary sludge fermentation (Andreasen et al., 1997; Novak et al., 2007). It has also been shown that sidestream processes result in more stable bioP performance (Lanham et al., 2013; Onnis-Hayden et al., 2019). Sidestream processes provide protection from wet weather flows, provides VFA from hydrolysis and fermentation, and possible suppression of GAO (Vollertsen et al., 2006; Barnard et al., 2017). The enrichment of PAO over GAO may occur because PAO decay more slowly than GAO under long-term anaerobic conditions (Varga et al., 2018). It has also been suggested that a sidestream reactor may lead to the enrichment of *Tetrasphaera* over *Accumulibacter* (Nguyen et al., 2011) which may lead to greater bioP stability by providing increased microbial diversity (Barnard et al., 2017).

The goal of this study is to integrate PDNA and sidestream bioP, utilizing A-stage WAS fermentation as a supplemental carbon source. The challenge behind integrating biological phosphorus removal and shortcut nitrogen removal in general, is the conflicting use of influent carbon. The goal of shortcut nitrogen removal is to reduce carbon demand for denitrification so that carbon can be diverted. However, if a HRAS A-stage process is utilized for carbon diversion, then there is little to no rbCOD available in the B-stage process for biological phosphorus removal to occur. BioP cannot occur in A-stage because the SRT is too short (less than 1 day) for PAOs to grow. While there has been a study on mesophilic fermentation (35°C) of HRAS A-stage sludge in bench scale batch tests (Cagnetta et al., 2016), this is the first study to examine the fermentation of A-stage sludge as a supplemental carbon source in a continuous flow process.

METHODS

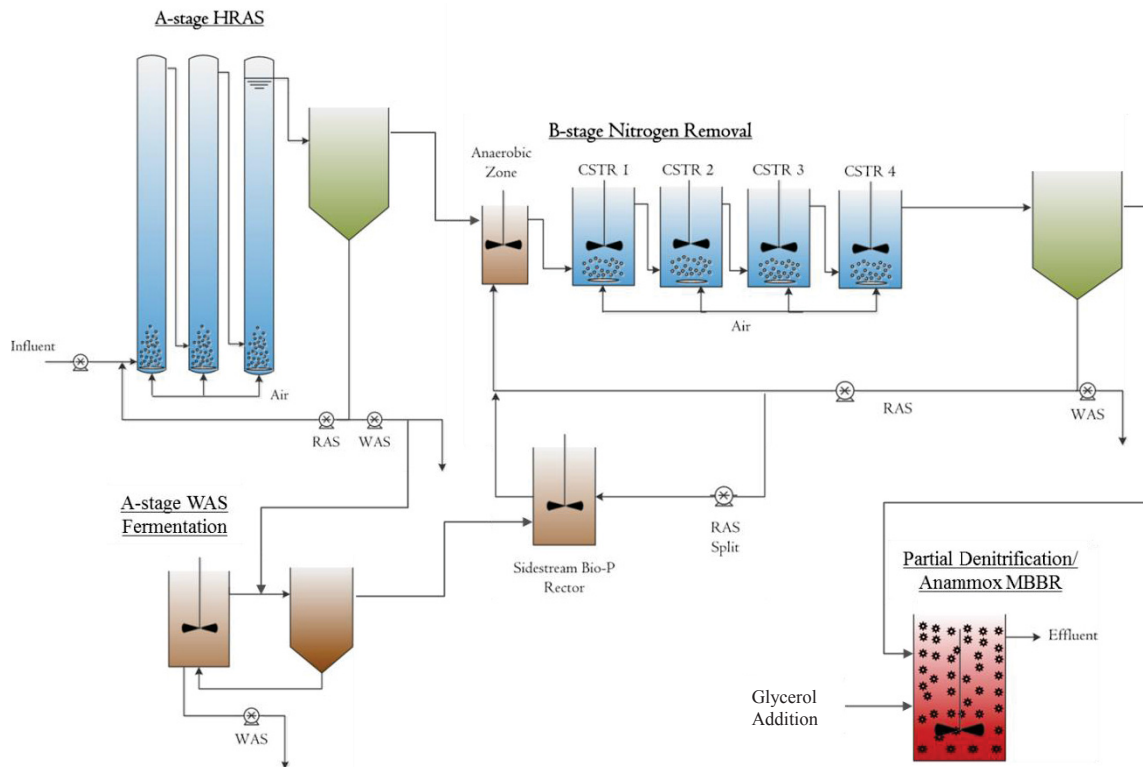


Figure 8.1: Pilot Configuration

Pilot Configuration

This study took place at the A/B pilot located at the Hampton Roads Sanitation District (HRSD) Chesapeake- Elizabeth Plant located in Virginia Beach, VA (Figure 8.1). The influent was temperature controlled to 20°C and fed to the A-stage high rate activated sludge (HRAS) process (45 minute HRT). The A-stage process configuration and process control is detailed in Kinyua et al., 2017. The effluent from the A-stage clarifier fed the B-stage nitrogen removal step (5 hour

HRT). B-stage consisted of 5 reactors in series. The anaerobic selector was 50 liters, was continuously mixed, and covered with ping pong balls to minimize oxygen transfer. The other 4 intermittently aerated CSTRs were 150 liters each for a total volume of 650 liters. Following the secondary clarifier, the B-stage effluent fed an anoxic anammox MBBR with an HRT of 2 hours, total volume of 340 liters, and a 60% fill of K3 media (Anoxkaldnes, Lund, Sweden). The MBBR at times was fed glycerol to induce partial denitrification combined with anammox.

The sidestream bio-P reactor (SBPR) HRT varied depending on the percentage of RAS sent to the sidestream. A portion of the A-stage WAS was fed to a combined fermenter and thickener, and the fermentate was added to the SBPR. The volume of the fermenter was 190 Liters and the thickener was 340 Liters. The A-stage WAS was fed into the thickener along with the fermenter effluent, and then the underflow of the thickener was fed to the fermenter. In this way, the influent provided elutriation of the fermenter effluent. The effluent from the thickener (fermentate) flowed into a 15 liter bucket, where it was pumped into the bottom of the SBPR reactor ($V_{total} = 150$ Liters). The influent to the SBPR consisted of a one-foot piece of PVC pipe, where the RAS and the fermentate were mixed prior to entering the reactor. The influent to the anaerobic selector also consisted of a one-foot section of PVC pipe in which the influent, the RAS, and the SBPR effluent could combine, before entering the reactor. The SBPR was programmed to be mixed for 10 minutes every 3 hours. The anaerobic selector was continuously mixed and covered with ping pong balls to minimize oxygen transfer. CSTR 1 to 4 were each 150 Liters, and the anaerobic selector was 53 Liters. The HRT of the anaerobic selector was 20 minutes.

B-stage sensors included a dissolved oxygen sensor in CSTR 1, CSTR2, CSTR 3, and CSTR 4 (Insite Model 10, LA, USA), ammonium in CSTR 4 (WTW VARiON, Germany), nitrate and nitrite in CSTR 4 (Scan Spectrolyser, Austria), and nitrous oxide (Unisense, Denmark). There was also a NO_x sensor in the MBBR (Hach Nitratax plus sc, Loveland, CO). The sensors were connected to a programmable logic controller (PLC) and then used for proportion-integral-derivative (PID) or PI control. The B-stage was intermittently aerated using ammonia versus NO_x (AvN) control via feedback from the ammonia, nitrate, and nitrite sensors in CSTR 4. AvN intermittent control utilized two independent control loops. The aerobic fraction (air on time divided by total cycle time) was controlled via PID control to meet a NO_x/NH₃ setpoint in CSTR 4. When the air was on, a PI controller manipulated the air valve position via a motor operated valve (MOV) to meet a DO setpoint of 2 mg/L for each reactor. The total cycle time for the duration of the study varied from 16 to 20 minutes. The NO_x sensor in the MBBR fed into a PI feedback controller which controlled the glycerol dosing pump feed rate to meet a NO_x setpoint in the reactor.

Analysis

Performance was monitored through the collection of 24-hour composite samples using automated samplers. The samplers extracted 250 mL at one-hour intervals allowing average

daily influent and effluent characteristics to be measured. Total and volatile suspended solids (TSS and VSS) were analyzed using standard methods 2540D and 2540E respectively (APHA, 2012). Total and soluble COD, OP, total ammonia nitrogen ($\text{NH}_4^+\text{-N} + \text{NH}_3\text{-N}$), $\text{NO}_2^-\text{-N}$, and $\text{NO}_3^-\text{-N}$ were measured with HACH TNTplus kits (Loveland, Colorado) and a HACH DR2800 spectrophotometer (Loveland, CO). Nutrient and soluble COD samples were filtered through 0.45 μm and 1.5 μm filters respectively. Particulate COD (pCOD) was calculated as the difference between total COD and sCOD (1.5 μm filtered). The sCOD measurement includes readily biodegradable and colloidal COD fractions. Daily pH and temperature readings of the reactors were recorded using a handheld pH and temperature meter (Beckman Coulter, Brea, CA). Readings for DO were recorded using a handheld DO sensor (Insite Model 10, LA, USA).

To preserve the mixed liquor samples for PHA analysis, 14 mL of sample was collected in a 15mL centrifuge tube with 0.2 mL of 37% formaldehyde and refrigerated overnight. Then the samples were centrifuged for 3 minutes at 10,000 rpm, decanted, and 10mL of phosphate buffered saline (PBS) was added. The sample was then re-suspended using a vortex mixer, centrifuged for 3 minutes at 10,000 rpm, decanted, and stored at -80°C . The sample was then freeze-dried and PHA was extracted utilizing 3% sulfuric acid, followed by a 3 hours of incubation, and then analyzed via GC-MS as previously described in Lanham et al., 2013.

Concentrations of acetic, propionic, butyric, isobutyric, valeric, isovaleric, and caproic acids were determined by GC-FID as previously described in Kinyua et al., 2017. In short, the A-stage WAS and fermentate samples were filtered through a 0.22 μm filter prior to injection. VFA concentrations were determined from a 0.5-100 mg/L calibration curve prepared from commercial standards (Absolute Standards).

PAO Uptake and Release Tests

Eight liters of mixed liquor were collected in a batch reactor from the last CSTR. The reactor was covered and anaerobic conditions were established. Sodium acetate stock solution (10,000 mgCOD/L) was added to reach 300 mg COD/L in the reactor. Samples were collected every 15 minutes and measured for NO_3^- , NO_2^- , OP and sCOD. In some trials, the ammonia was completely oxidized, and then the NO_x was completely denitrified, and then reaerated to take up the OP prior to the beginning of the anaerobic release period. In other trials the NO_x was not denitrified prior to the beginning of the anaerobic release period. It was determined that as long as there was excess acetate present, the OP release rate was not affected by the presence of NO_x , so after Day 180, the sample was no longer denitrified prior to the anaerobic OP release period. After the anaerobic release phase, the sample was then split into two four liter reactors, one for aerobic OP uptake, and one for anoxic OP uptake. The aerobic reactor was aerated to maintain a DO concentration between 3 and 4 mg/L. Samples were collected every 15 minutes and analyzed for OP. The anoxic reactor was covered and spiked with potassium nitrate stock solution (10,000 mgN/L) to a concentration of 20 mgN/L in the reactor. Samples were collected every 15 minutes,

immediately filtered through 0.45 μ m cellulose acetate filters, and analyzed for OP, sCOD, NO₃⁻, and NO₂⁻.

AOB and NOB Rate Tests

To measure maximum AOB and NOB activity, a 4 L sample was collected from the 4th CSTR and aerated for 30 minutes to oxidize excess COD. The sample was then spiked with NH₄Cl and NaNO₂ so that initial concentrations were 20-30 mg NH₄⁺-N/L and 2-4 mg NO₂⁻-N/L respectively. Temperature was controlled at 20°C via submersion in a water bath. The DO concentration was manually maintained between 2.5 and 4 mg/L using diffused compressed air. The pH was manually maintained at approximately 7.5 through the addition of sodium bicarbonate. The activity tests were conducted for 1 hour with sample collection every 15 minutes. Samples were analyzed for NH₄⁺-N, NO₂⁻-N, and NO₃⁻-N as described above. The AOB rates were calculated as the slope of the NO_x-N production and NOB rates were calculated as the slope of the NO₃⁻-N production. Rates tests were performed every 1-2 weeks.

Long Term Denitrification Test

An 8 Liter sample was collected from the last CSTR and aerated for 48 hours (DO maintained above 3 mg/L) to deplete all external and internally stored carbon. Then the aeration ceased and the sample was split into two 4 Liter reactors, each covered with a Styrofoam lid. One reactor was to measure the endogenous denitrification rate, and the other to measure the denitrification rate from internally stored carbon, after a period of aeration. For the endogenous rate measurement: once the sample went anoxic, samples were taken every 15 minutes for 3 hours. The rate of NO_x reduction was considered the endogenous denitrification rate. For the internally stored carbon test: sodium acetate stock solution was spike to an initial concentration of 250 mgCOD/L for an anaerobic carbon storage phase. Then the reactor was aerated for one hour. Then the reactor was anoxic again, and samples were collected every 15 minutes for 1.5 hours. The NO_x rate was considered the denitrification rate from internally stored carbon, or the post anoxic denitrification rate, since external rbCOD was depleted in the aerated phase. Samples were filtered through 0.45 cellulose acetate filters and analyzed for NO₃⁻-N, NO₂⁻-N, NH₃-N, COD, and OP.

External Carbon Independent Denitrification Rate Tests

A 4 L sample was collected from the last CSTR and covered with a Styrofoam lid. Potassium nitrate stock solution was added so that the initial NO₃-N concentration was 10-20 mg/L, and sodium nitrite stock solution was added so that the initial NO₂-N concentration was 2-6 mg/L. Samples were taken every 15 minutes for 1 hour, filtered through 0.45 μ m cellulose filters, and analyzed for NO₃⁻-N, NO₂⁻-N, NH₃-N, COD, and OP.

Amplicon Sequencing and Analysis

MLSS samples were collected weekly, centrifuged for 3 minutes at 10,000 rpm, supernatant decanted, and stored at -80° C. Samples were then shipped in a single batch to Northeastern University, Boston MA overnight on dry ice. The DNA was extracted and then sent to University of Connecticut-MARS facility for PCR amplification and sequencing. DNA extraction, amplification, and sequencing were performed as detailed in Srinivasan et al., 2019. Amplicon data was rarefied to the minimum total sequence count (22342 sequences) across all samples.

qPCR

The abundance of AOB and NOB was quantified using quantitative polymerase chain reaction (qPCR). Canonical AOB were targeted using the Canonical AOB ammonia mono-oxygenase subunit A (*amoA*) gene (Rotthauwe et al., 1997), while Comammox bacteria were targeted using the Comammox bacteria *amoA* gene (Wang et al, 2018). NOB were targeted using the *Nitrobacter* 16S rRNA gene (Graham et al., 2007) and *Nitrospira* 16S rRNA gene (Kindaichi et al., 2006). Total bacterial abundance was quantified using eubacterial 16S rRNA gene targeted primers (Ferris et al., 1996). Primer sequences are listed in Table C1. qPCR assays were conducted on a CFX384 Touch Real-Time PCR Detection System (BioRad Laboratories, Hercules, CA). Standard curves for qPCR were generated via serial decimal dilutions of plasmid DNA containing specific target gene inserts. qPCR for standard plasmid DNA and sample DNA were conducted in triplicate. Primer specificity and the absence of primer-dimers were confirmed via melt curve analysis of each qPCR profile (Ma et al, 2015; Park et al., 2015).

RESULTS AND DISCUSSION

Overall Operation

The B-stage temperature was $20.8^{\circ}\text{C} \pm 0.9^{\circ}\text{C}$, HRT was 4.9 ± 0.2 hours, mainstream SRT (excluding SBPR) was 9.6 ± 3.2 days and aerobic SRT (a function of the AvN controller) was 5.7 ± 2.4 days over the entire operating period. B-stage operation was divided into four operational phases based on SBPR operation and fermentate addition (Table 8.1). Phases 1 and 4 were at a shorter sidestream HRT with higher fermentate addition, and Phases 2 and 3 were at a longer HRT with low fermentate addition (Phase 2) and no fermentate addition (Phase 3). The idea being that at the longer HRT and SRT, fermentation of the RAS in the SBPR would decrease the need for external carbon. The goal of Phase 4 was to return to the operating conditions in Phase 1, but with tighter control of the fermentate dosage, using the sCOD/OP ratio as a guideline. The sCOD/OP and VFA/OP ratios were calculated as the sCOD or VFA load from the fermentate, divided by the sum of the OP load from the influent (A-stage effluent) and OP load from the fermentate.

Table 8.1: Sidestream BioP Reactor (SBPR) operation for each phase. sCOD/OP was calculated as sCOD added from the fermentate, divided by the sum of the OP in the influent and OP in the fermentate

	Time Period (day)	RAS Split %	SBPR HRT (hour)	SBPR SRT (day)	Fermentate sCOD Addition (mg/L)	sCOD/OP Ratio (gCOD/gP)	VFA/OP Ratio (gHAc/gP)
Phase 1	0 - 188	25%	3.7	9.2±5.5	61.1±19.8	18.2±6.8	7.2±3.2
Phase 2	189-220	5%	20.7	16.0±9.0	8.0±2.2	3.0±1.1	1.2±0.3
Phase 3	221-269	8%	14.2	9.5±3.1	n/a	n/a	n/a
Phase 4	270 - 412	27%	4.0	6.1±1.4	54.9±15.3	16.1±3.4	5.6±1.4

Fermenter Performance

The HRT of the fermenter was 24 hours and SRT was 4.1±0.8 days (excluding the thickener) over the entire study. Average temperature was 20.6°C ± 1.8°C and average pH was 5.5±0.3. The average VFA yield was 0.099±0.040 gCOD/gVSS (0.061±0.021 gCOD/gCOD) and the average sCOD yield was 0.298±0.133 gCOD/gVSS (0.190±0.072 gCOD/gCOD).

Although there were not any previous studies available on an A-stage WAS continuous fermentation process, it was predicted that yields would be less than primary sludge fermentation, and greater than RAS fermentation. Rabinowitz (1985) reported that optimum yields of around 0.09 g HAc/g COD were obtained at a 3.5-5 day SRT in a pilot scale primary sludge fermentation process at 16°-20°C. Elefsiniotis and Oldham 1994 reported 0.05 mg VFA/mgVSS (as HAc) at SRT of 5 days, and Skalsky and Daigger 1995 reported 0.05 mgVFA/mgVS from the operation of 2 full-scale fermenters.

The majority of the total VFA were acetic and propionic acid, followed by butyric and valeric acid (Figure 8.2). Concentration of each VFA both as the individual VFA, and as COD are shown in in Table C2. It is typical in primary sludge fermentation that acetic and propionic acid make up about 80-90% of the total VFA, perhaps with small percentages of butyric and valeric acids, and that acetic and propionic acid occur in approximately at a 1:1 ratio to each other (Rabinowitz 1985; Elefsiniotis and Oldham 1994; Skalsky and Daigger 1995). The average ammonia concentration in the fermentate was 107±31 mgN/L and OP was 34.4±9.3 mgN/L.

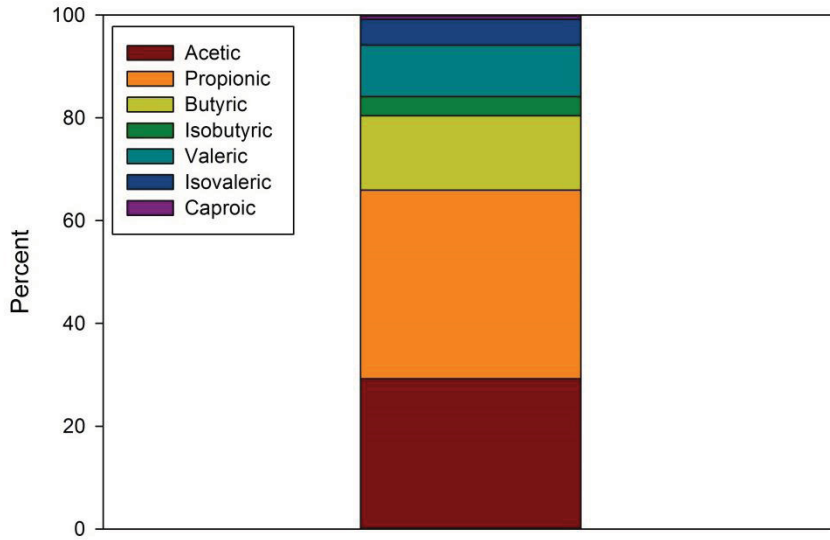


Figure 8.2: Fermentate VFA Fractionation as percent of total VFA on a COD basis.

The total COD (tCOD), soluble COD (sCOD 1.5 um filtered), and VFA load as mg COD/L divided into the influent flow are shown in Figure 8.3. The total COD values were variable and depended on the performance of the thickener. Ideally the total COD addition to the process would be minimized, since it results in a decrease in capacity of B-stage without providing a carbon source for bioP. The average ammonia load from the fermentate divided into the influent flow was 3.0 ± 1.7 mgN/L and OP was 0.9 ± 0.5 mgP/L.

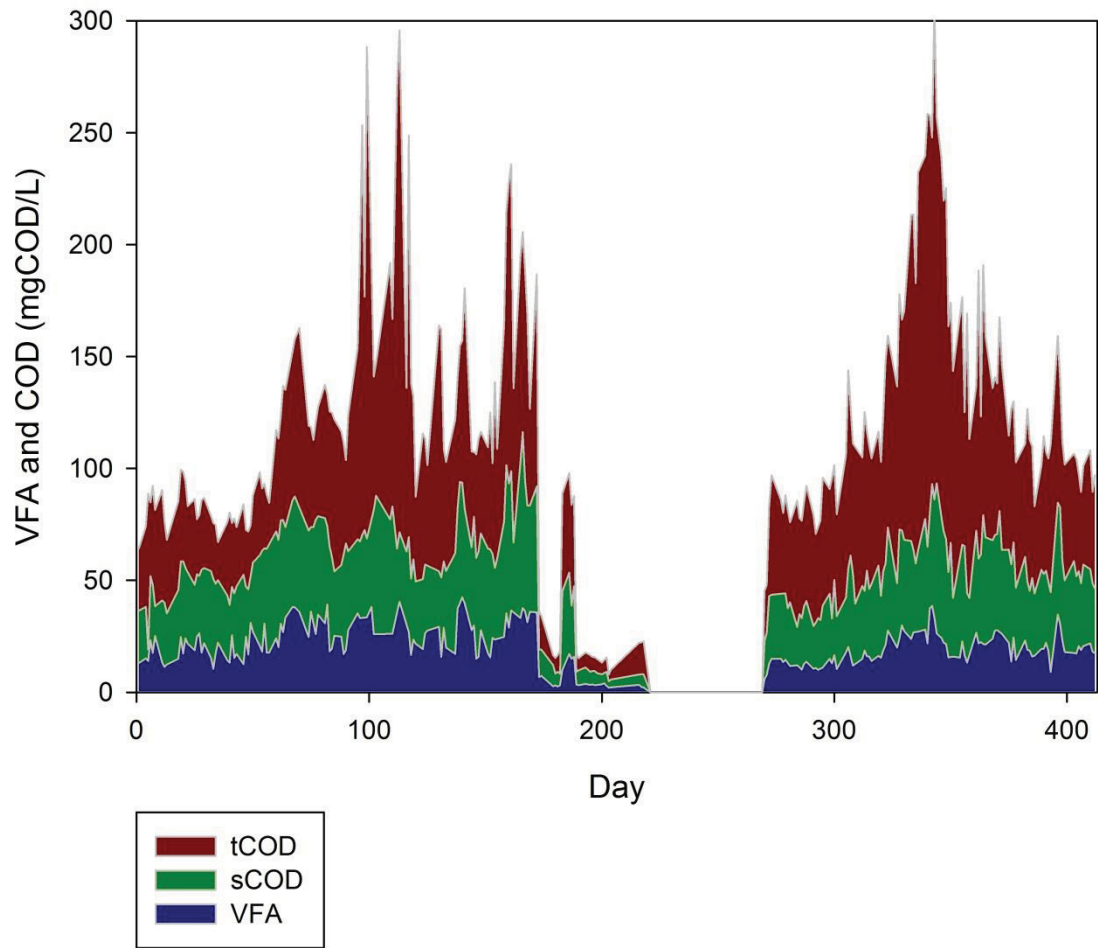


Figure 8.3: tCOD, sCOD, and VFA load to the SBPR in mg COD/L divided into the influent flow.

B-stage effluent phosphorus and nitrite

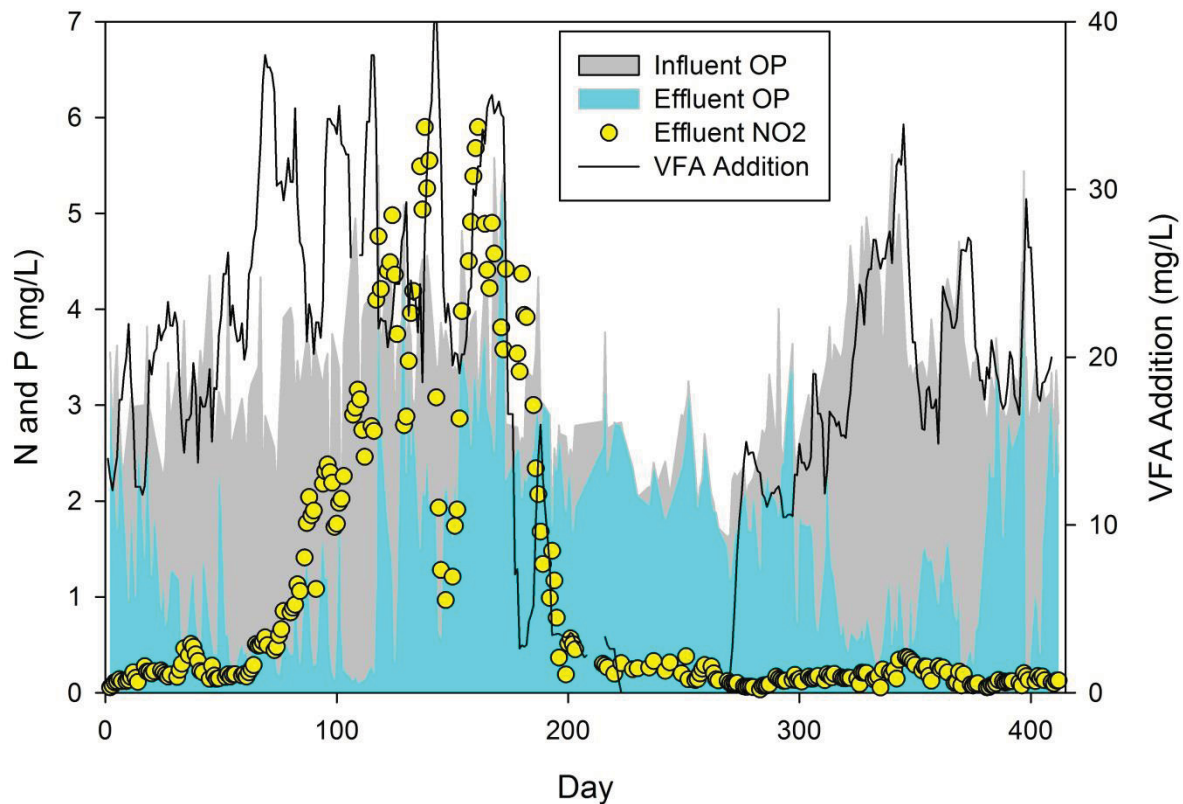


Figure 8.4: Influent OP (combined from influent and fermentate), effluent OP, effluent NO₂, and VFA load to the sidestream divided into the influent flow.

During Days 0 to 100, as the fermentate VFA load was increased, the effluent OP decreased in B-stage (Figure 8.4). Around day 80, nitrite began to accumulate, and effluent nitrite above 2 mgN/L, and effluent OP below 0.5 mgP/L was sustained for a brief period of time (Day 90 to Day 115). Then bioP was lost as nitrite continued to accumulate. It was hypothesized that the nitrite accumulation was due to partial denitrification by organisms utilizing internally stored carbon (perhaps GAO), which were competing with PAO for VFA. A profile in time was taken every 10 minutes at the beginning and end of the air off time on Day 108 (Figure 8.5). This confirmed that nitrite was accumulating during the air off times from partial denitrification. During the air off times, nitrate decreased as nitrite increased, and then during air on times, nitrite decreased as it was being oxidized to nitrate (Figure 8.5). Nitrous oxide also increased during air off times (Figure C1) which also suggests partial denitrification was occurring. Fermentate addition was decreased dramatically from Day 170 to 188, ending Phase 1, and the effluent nitrite decreased in response, confirming that the nitrite accumulation was associated with the VFA addition. The maximum PAO uptake and release rates from batch tests support the hypothesis that bioP was lost due to an excess of external carbon addition (Figure 8.6). From

Day 140 to 160 the PAO uptake and release rates were decreasing, prior to the decrease in fermentate addition (Figure 8.6). Anoxic OP uptake was measured, but not detected in batch tests, and OP profiles during intermittent aeration (Figure C2) did not indicate anoxic OP uptake (although it could not be ruled out entirely).

Phases 2 and 3 (Day 189 to 269) were operated at longer SBPR HRTs with the intention of producing VFA from RAS fermentation, with little to no external fermentate addition. While there was some evidence for some VFA production in the SBPR (as evident by some P release and VFA in the SBPR effluent), it was not enough to lead to appreciable OP removal across B-stage (Figure 8.4). This indicated that either the HRT/SRT of the SBPR needed to be longer, or that a higher mass fraction of the RAS needed to pass through the sidestream. In order to maintain a 20 hour HRT, only 5% of the RAS flow could go to the SBPR with the current reactor volume. In Phase 4 the goal was to add fermentate in a more controlled manner to keep a more consistent COD/OP loading. The goal was to keep the sCOD/OP and VFA/OP ratio high enough to achieve low effluent OP, but below the threshold that may have caused the loss of bioP in Phase 1 (Figures 8.4 and 8.6). In Phase 4, effluent values below 0.5 mgP/L were achieved, but bioP was not stable, and effluent nitrite remained below 0.5 mgN/L.

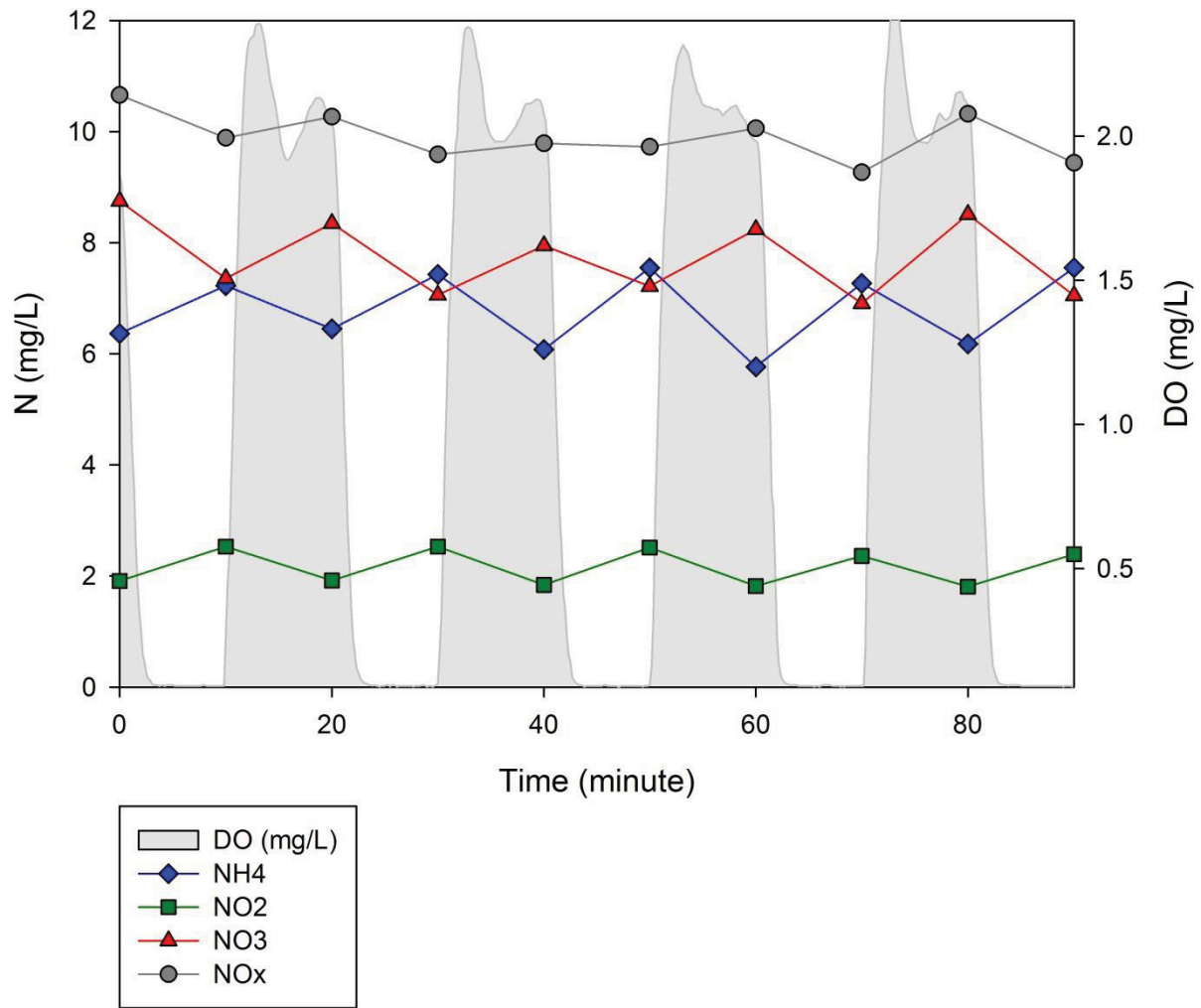


Figure 8.5: Nitrogen profile in time on Day 108 during intermittent aeration in CSTR 4. Grey shaded areas are periods of aeration.

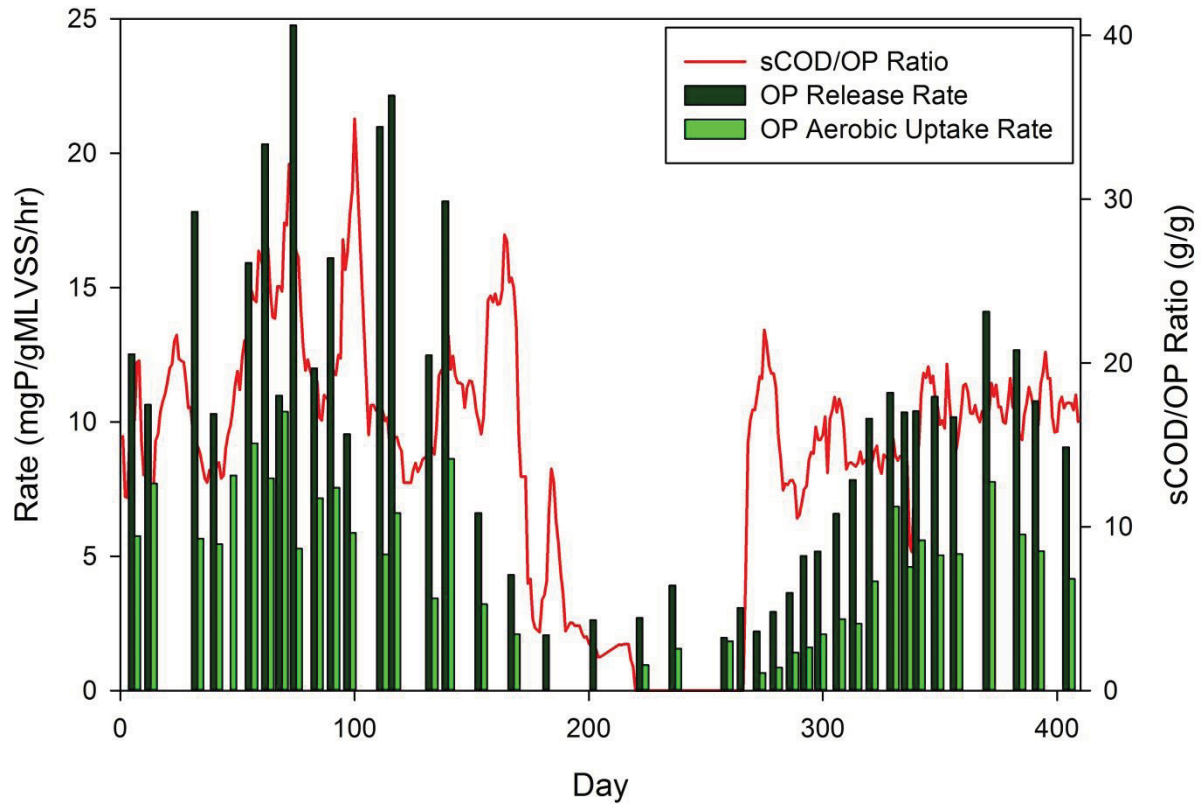


Figure 8.6: Maximum anaerobic OP release rate from batch tests (dark green bar), aerobic OP uptake rate from batch tests (light green bar), and influent sCOD/OP ratio (red line). The sCOD/OP ratio was calculated as the five-day moving average of the sCOD added from the fermentate, divided by the sum of the OP in the influent and OP in the fermentate.

B-stage TIN Removal and Anammox Polishing

TIN removals are shown in Figure 8.7. During Phase 1, glycerol was added to the MBBR to achieve partial denitrification combined with anammox (Figure 8.8). The MBBR carbon dosing controller was set to a nitrate setpoint of 1 mg/L. Effluent TIN was. From Day 154 to 161 there was no external carbon addition to the MBBR, B-stage effluent nitrite was 5.1 ± 0.7 mgN/L, and the effluent TIN from the MBBR was 2.34 ± 0.73 mgN/L. This was only sustained for a week because the fermentate addition was reduced after losing bioP, but this demonstrates the potential of this process, if bioP can be sustained along with nitrite accumulation.

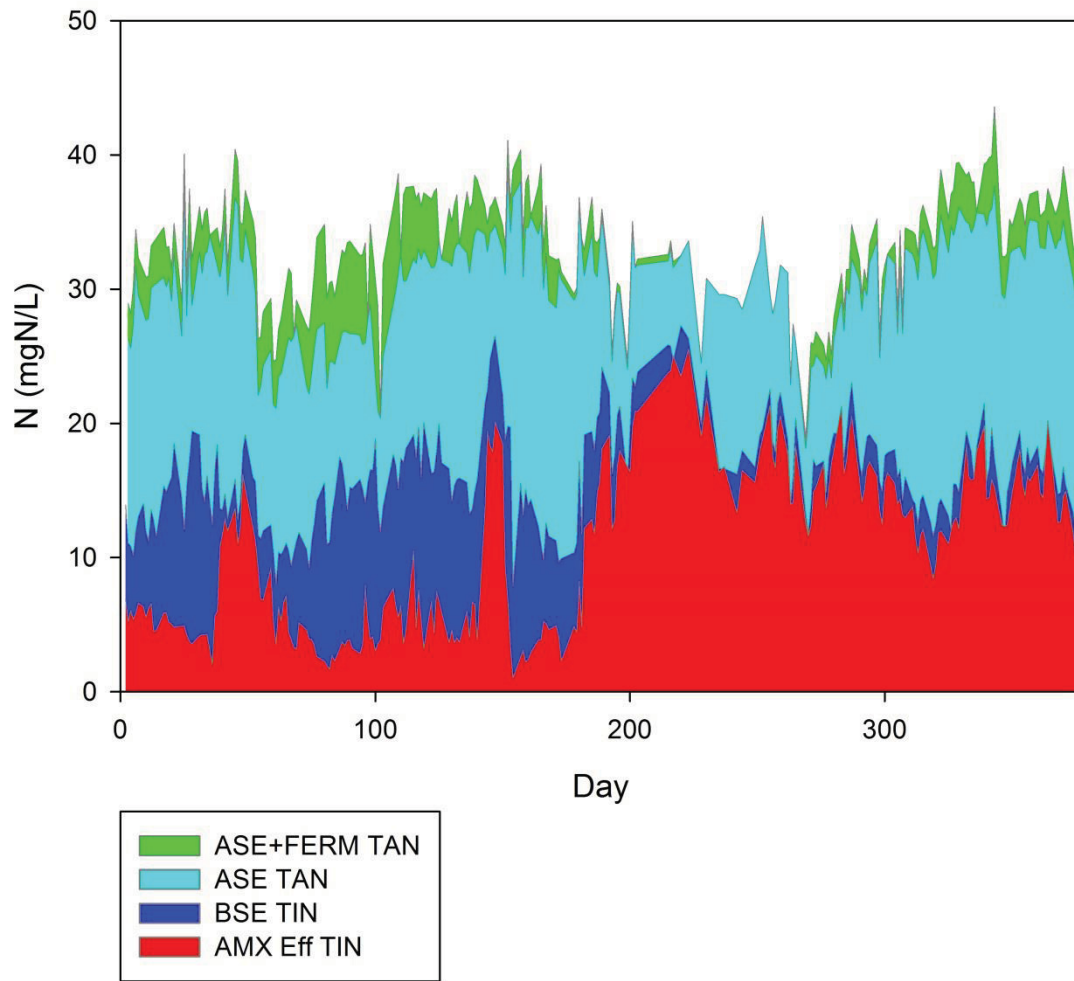


Figure 8.7: Total TIN in the influent (A-stage effluent (ASE) + fermentate), TIN only from A-stage effluent (ASE), TIN in B-stage effluent (BSE), and TIN in the anammox MBBR effluent.

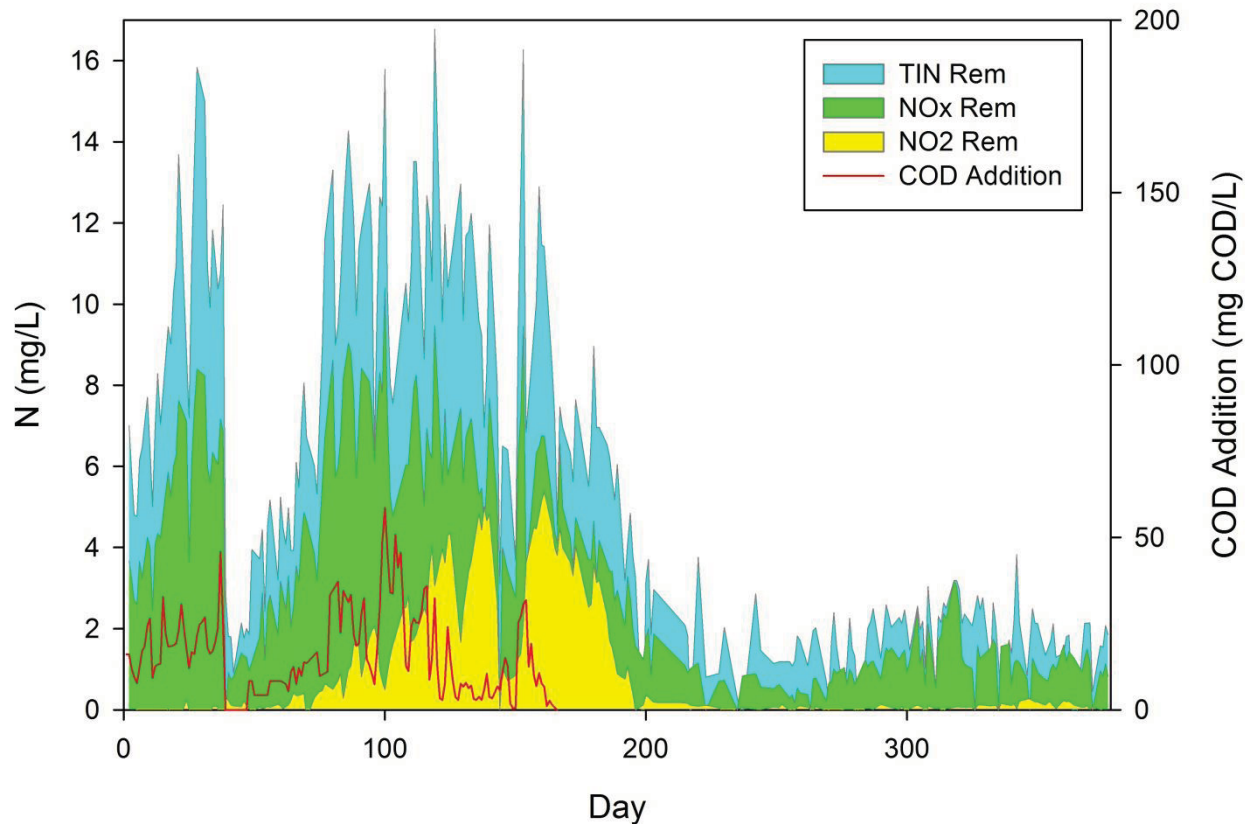


Figure 8.8: TIN removal performance of the MBBR, and glycerol addition (mgCOD/L) to the MBBR.

Microbial Quantification

Throughout the study, NOB rates were higher than AOB rates, with an average NOB/AOB rate ratio of 1.3 ± 0.5 , which supports that nitrite accumulation was not due to NOB out-selection. Figure C3 shows specific AOB and NOB rates from batch tests, and effluent nitrite. If AOB and NOB abundance are equivalent, the ratio of the maximum growth rates (NOB/AOB) should be approximately 0.8 (Dold et al., 2015). In previous studies at the same pilot, without the SBPR and fermentate addition, NOB out-selection was achieved by utilizing intermittent aeration, controlling the aerobic SRT to less than 5 days, and maintaining an ammonia residual above 1 mgN/L (Regmi et al, 2014). The intermittent aeration profile (Figure 8.5) supports the observation that NOB rates were higher than AOB rates. Winkler et al., 2012 coined the term “nitrite loop” for describing partial denitrification from nitrate to nitrite, and then that nitrite being oxidized back to nitrate. This mechanism was hypothesized to result in an imbalance of NOB and AOB, as more nitrite is available to NOB, which was not the product of ammonia oxidation by AOB (Winkler et al., 2012).

The abundance (copies/mL) of canonical AOB, Comammox, *Nitrospira*, *Nitrobacter*, and Eubacteria are shown in Figure C4. *Nitrospira* had the highest abundance by two orders of magnitude, so only *Nitrospira* relative abundance was plotted with effluent nitrite in Figure 8.9. The *Nitrospira* relative abundance appears to trend with effluent nitrite (Figure 8.9), which supports the hypothesis that nitrite accumulation from partial denitrification led to an increase in NOB abundance, i.e nitrite loop (Winkler et al., 2012). What was unusual about these results was the very low relative abundance of amoA. The maximum relative abundance of Canonical AOB amoA was 0.008% and 0.006% for Comammox amoA. Since ammonia oxidation was obviously occurring in the process, there are two possible explanations:

1. The primer utilized for Comammox amoA is fairly new and still under development (Wang et al., 2018), therefore it is possible that more of the *Nitrospira* possess ammonia oxidation capability. Quantitative detection of comammox by qPCR may not be accurate because of primer limitations (Beach and Noguera, 2019).
2. Other organisms apart from Canonical AOB or Comammox bacteria were responsible for ammonia oxidation.

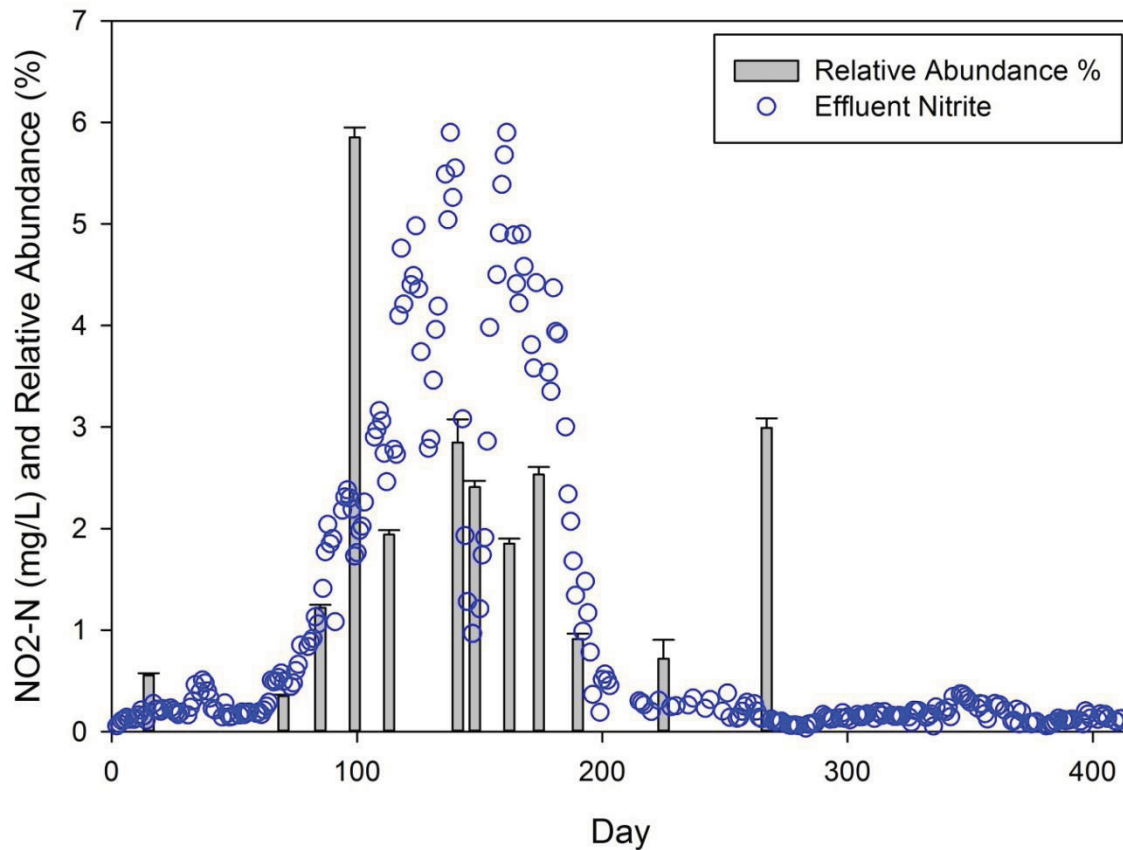


Figure 8.9: qPCR results for Canonical AOB, Comammox, *Nitrospira*, and *Nitrobacter*.

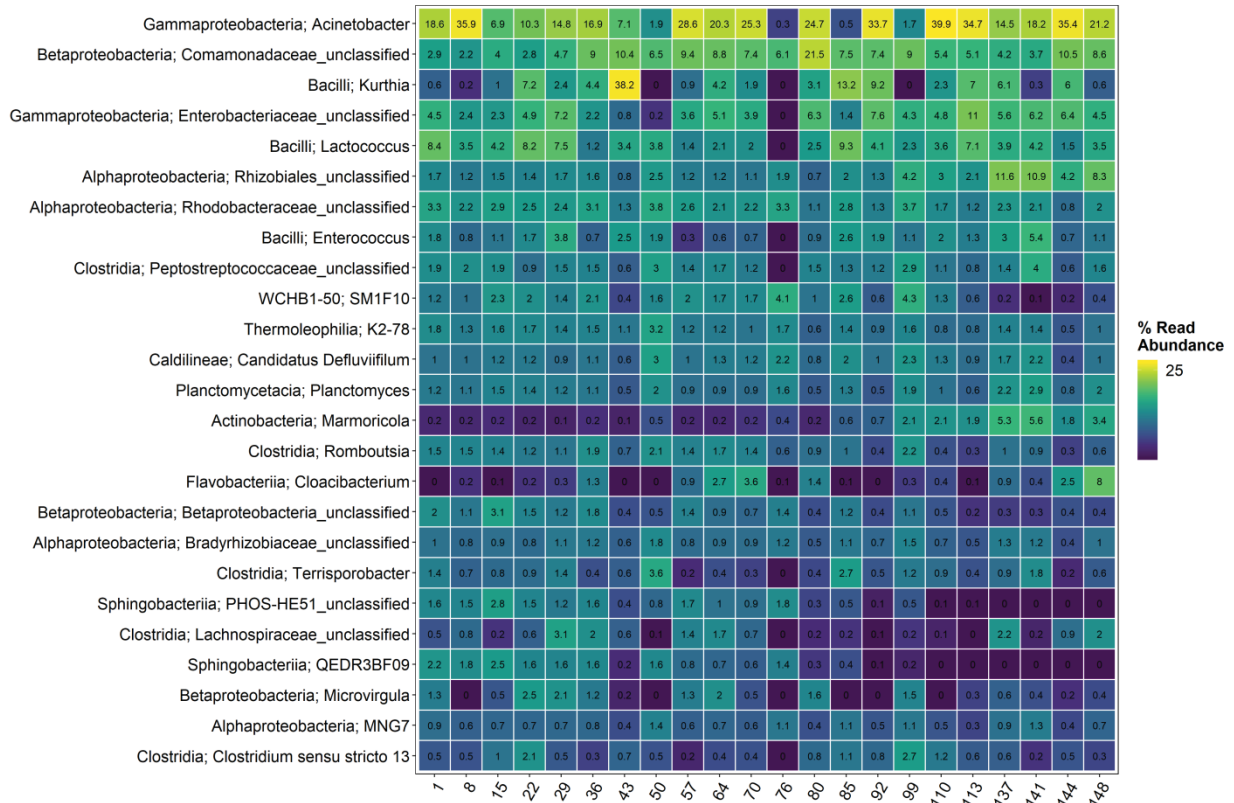


Figure 8.10: Top 25 genera from 16S amplicon sequencing

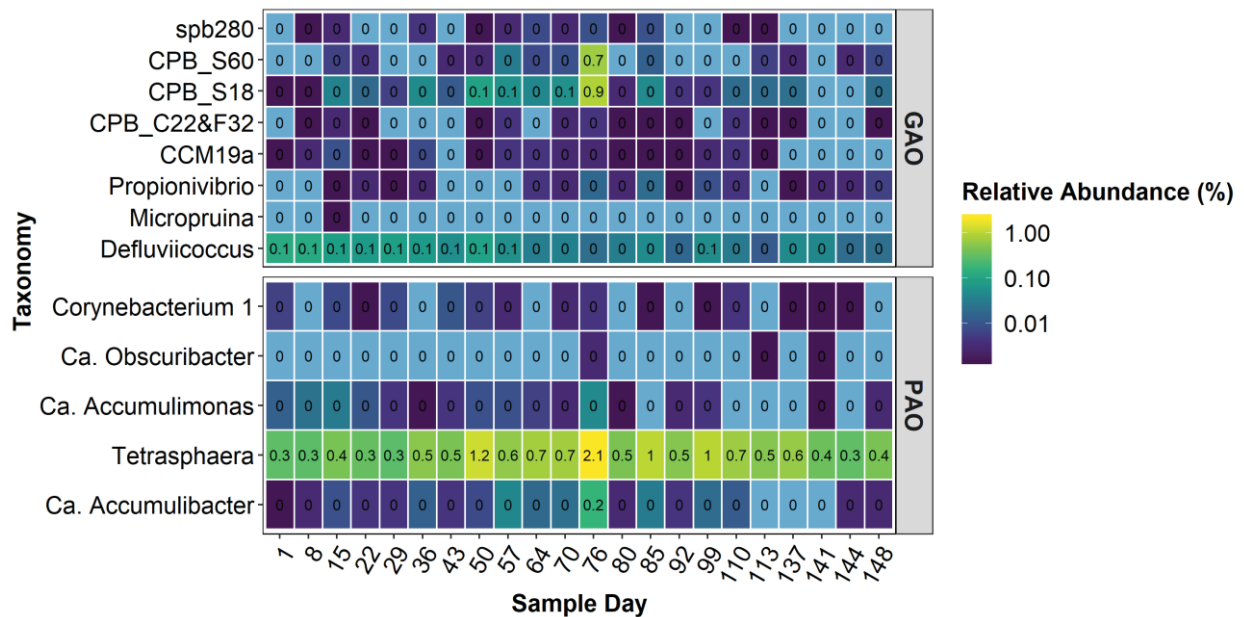


Figure 8.11: Putative PAO and GAO from 16S amplicon sequencing

Unexpectedly, *Acinetobacter* was the most abundant genus detected in the mixed liquor samples (Figure 8.10). *Acinetobacter* were once thought to be the dominant organisms performing polyphosphate accumulation (Fuhs and Chen, 1975; Lötter et al., 1986; Wentzel et al., 1991), but it was later concluded that *Acinetobacter* were not primarily responsible for bioP (Jenkins and Tandoi 1991, Auling et al., 1991; Mino et al., 1998). Because of these findings, *Acinetobacter* is not frequently considered in recent research of bioP processes, but it is difficult to attribute bioP to any of the other putative PAOs in this study, except maybe some to *Tetrasphaera* (Figure 8.11). It has also been demonstrated that *Acinetobacter* is capable of heterotrophic nitrification, but the contribution of *Acinetobacter* in full-scale activated sludge systems is not known (Yao et al., 2013). While it was hypothesized that GAO may be responsible for the denitrification with internally stored carbon, there has not been evidence thus far, and putative GAO were not detected in substantial quantities.

External Carbon Independent Denitrification

During the time of nitrite accumulation in the process, nitrite accumulation was also observed in the external carbon independent denitrification tests. In these tests, a sample was taken from the last aerated reactor and left to go anoxic. Nitrite would continue to accumulate until nitrate was depleted, and only then would nitrite be reduced. This sample was taken from the process in the last aerobic reactor, so no rbCOD was available as an electron donor. Figure 8.12 shows an extended test that lasted for 8 hours. Nitrate was reduced at a rate of 1.8 mgN/gMLVSS/hr and about 50% accumulated as nitrite. This rate of denitrification cannot be explained by endogenous decay, as the NH₄-N increase rate during the test was only 0.03 mgN/gMLVSS/hr, and soluble COD was constant at the beginning and the end of the test. Since OP increased, denitrification cannot be due to dPAO. PHA was measured, and does not appear to be the carbon source for denitrification (Figure 8.12).

Some studies have hypothesized, that post-aerobic denitrification was occurring using internally stored glycogen (Vocks et al., 2005; Winkler et al., 2011). There is also evidence to suggest that dGAOs have a preference for reducing NO₃⁻ to NO₂⁻, causing nitrite accumulation (Rubio-Rincon et al., 2017). However, there are other heterotrophic organisms that can store carbon internally, so it is not necessarily GAO (Van Loosdrecht et al., 1997). Vocks 2008 suggested that an alternative internally stored carbon source may be driving post-anoxic denitrification since denitrification could not be attributed to either PHA or glycogen.

The results from the weekly external carbon independent denitrification tests are shown in Figure 13. The nitrite accumulation in the process corresponds to nitrite accumulation in the batch tests (Figure 8.13). The nitrate reduction rate appears to trend with the VFA addition, which could suggest that increased VFA addition led to higher rates of post-anoxic denitrification. Even with no VFA addition there was still post-anoxic denitrification occurring above expected endogenous rates, most likely because there was still VFA production and storage occurring in the SBPR

during Phase 3. The average specific NO_x reduction rate in the external carbon independent denitrification tests was 1.36 ± 0.34 mgN/gVSS/hr (Figure C5).

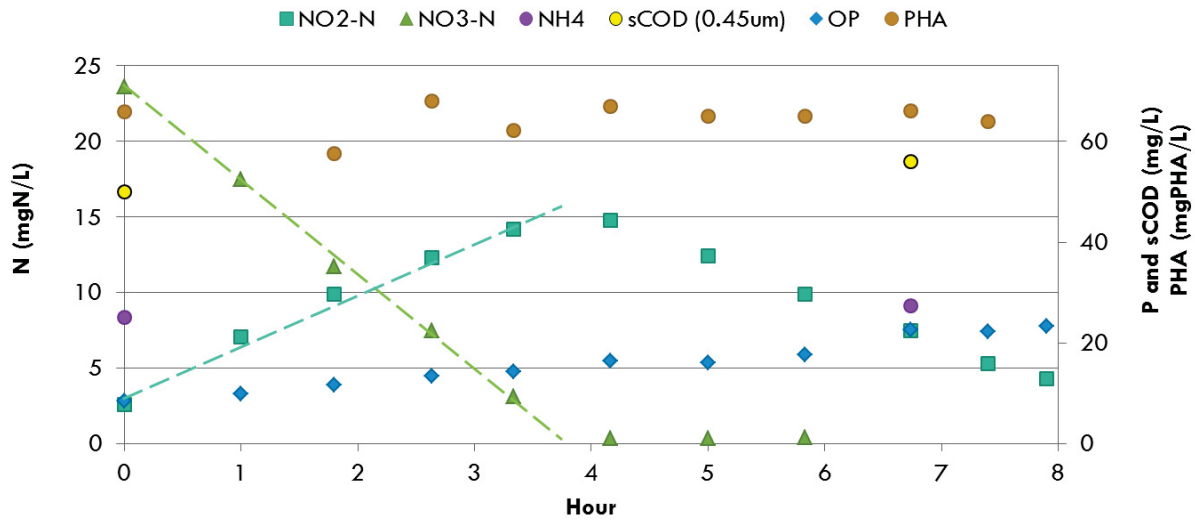


Figure 8.12: External carbon independent denitrification test on Day 116.

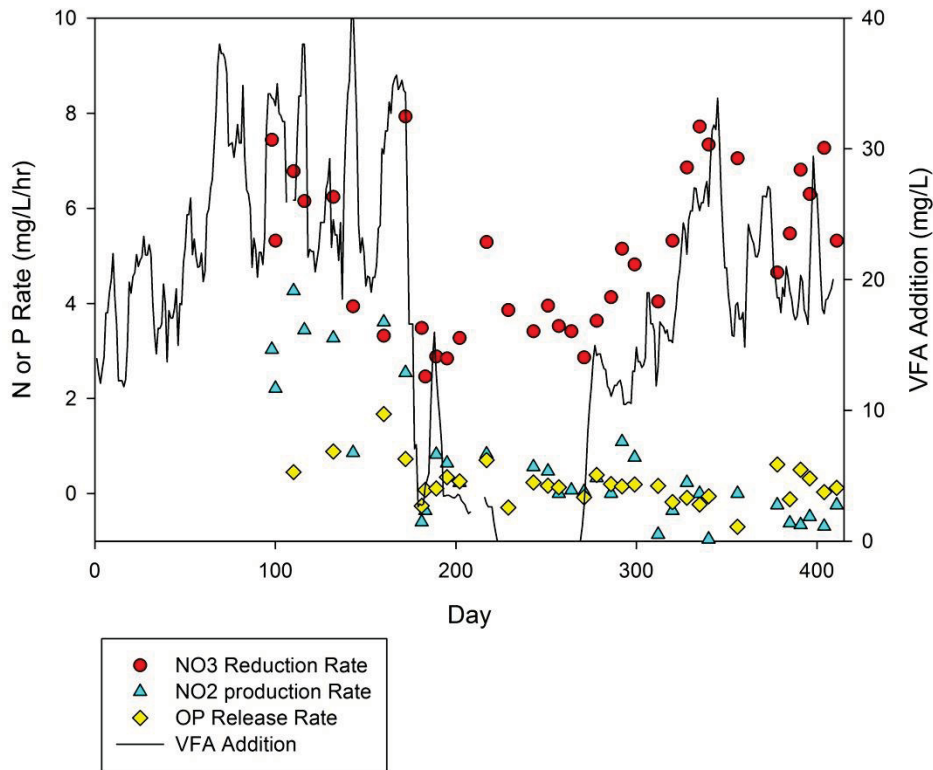


Figure 8.13: Rates from external carbon independent denitrification tests over time and VFA load to the SBPR in mg/L as influent flow. Nitrate reduction is positive, nitrite production and OP release are positive.

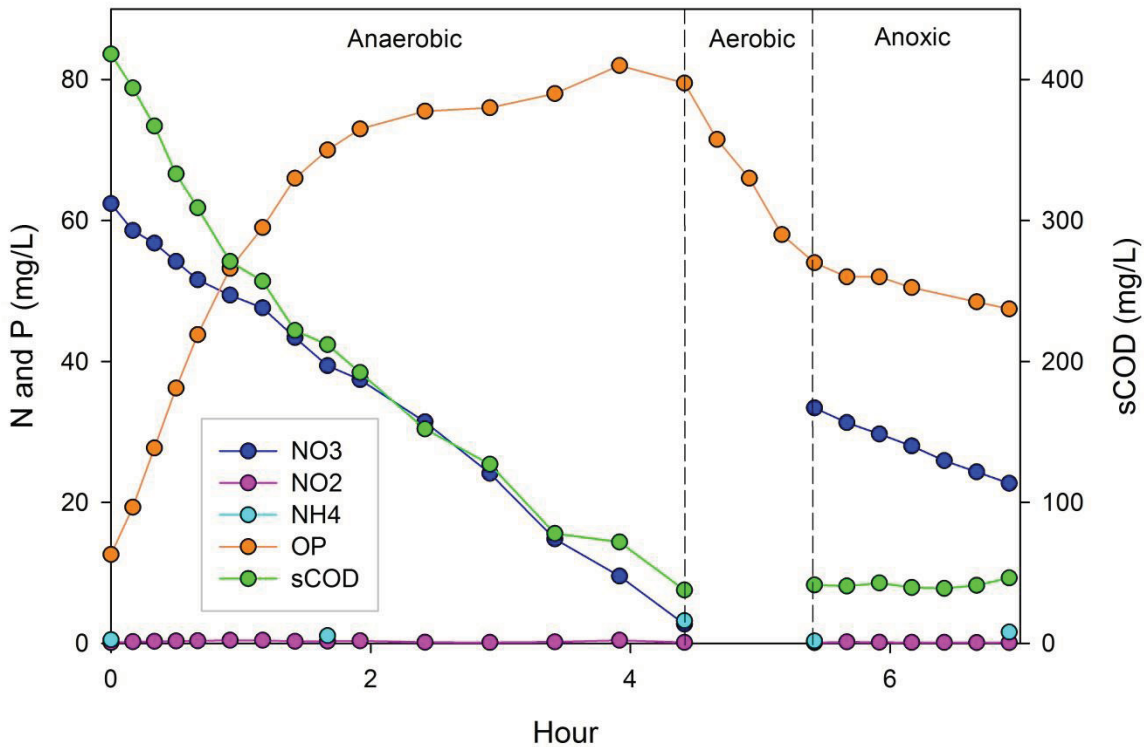


Figure 8.14: Results from the long term denitrification test. The first period is labeled “anaerobic” even though there is nitrate present because this is the OP release and VFA storage period, followed by the aerobic period, then anoxic.

The term post-anoxic denitrification refers to an anoxic zone that follows an aerated zone, without external carbon addition. This is equivalent to the anoxic times of intermittent aeration, once external carbon sources have been depleted. Post-anoxic denitrification typically implies endogenous denitrification, but it is not always specified whether this includes denitrification from internally stored carbon, as internal storage compounds are not typically measured. The long term denitrification test was performed on Day 362 in order to measure the endogenous and post-anoxic denitrification rate (from acetate storage only) (Figure 8.14). There was no nitrite accumulation in this test, so the following denitrification rates are the rate of nitrate reduction. After the sample was aerated for 48 hours, the measured endogenous denitrification rate was 0.48 mgN/gVSS/hr. Typical endogenous denitrification rates are in the range of 0.2-0.8 mgN/gMLSS/hr (Kujawa and Klapwijk, 1999).

The rate of denitrification with acetate as the only carbon source was 2.4 mgN/gVSS/hr. There may have been some endogenous denitrification occurring during the anoxic period with acetate, but it can be assumed that there were no internal carbon stores at the start of the anoxic period after 48 hours of aeration. The acetate was first utilized both for OP release by PAO and for

denitrification by OHO (hour 0 to 2), and then just for denitrification once OP release ended (hour 2 to 4). After a period of 1 hour of aeration to deplete any residual rbCOD, the post-anoxic denitrification rate was 1.3 mgN/gVSS/hr which is less than the rate with acetate as the carbon source, and greater than the endogenous denitrification rate. Since the only available carbon source after 48 hours of aeration was acetate, it can be assumed that internally stored carbon is the electron donor for denitrification. In this case, there was OP uptake in the last anoxic period (0.76 mgP/gVSS/hr), but denitrification in the external carbon independent denitrification tests was not typically associated with OP uptake (Figure 8.13). The average NO_x reduction rate in the external carbon independent batch tests during this time (Day 340 to Day 378) was 1.4±0.2 mgN/gVSS/hr. Interestingly, this is close to the post-anoxic rate that was observed in the batch test after acetate storage (1.3 mgN/gVSS/hr). Vocks 2008 performed similar batch tests using mixed liquor from three full-scale facilities: two UCT processes (with bioP), and one pre-denitrification process without bioP. The average post-anoxic denitrification rates for the UCT processes were 1.6 mgN/gVSS/hr (n=10) and 1.4 mgN/gVSS/hr (n=2), with values ranging from 0.7-2.7 mgN/gVSS/hr and 1.2-1.5 mgN/gVSS/hr. For the facility without bioP the average was 0.6 mgN/gVSS/hr (n=3) ranging from 0.4-0.7 mgN/gVSS/hr. It is possible that post-anoxic denitrification may be occurring more frequently than is recognized in combined bioP and N removal processes, because post-anoxic denitrification without external carbon addition in full scale processes is not common.

Although the concept of denitrification from internal carbon storage is not new (Alleman and Irvine, 1980; van Loosdrecht et al., 1997), there has been a recent interest in exploiting post-anoxic denitrification (and potentially nitrite accumulation) combined with bioP (Winkler et al., 2011; Chen et al., 2013; Liu et al., 2017; Zhao et al., 2019; Wang et al., 2019). These studies propose utilizing variations of an anaerobic/aerobic/anoxic configuration. Winkler et al. (2011) reported greater than 99% inorganic nitrogen and phosphorus removal, and although GAO were thought to be responsible in part for the post-anoxic denitrification, bioP performance was not compromised. Liu et al. (2017) and Zhao et al. (2019) proposed nitrite accumulation via partial nitrification, followed by anoxic denitrification of the nitrite utilizing internally stored carbon. They recognized the challenge of maintaining post-anoxic denitrification by GAO, because of the competition with PAO for the VFA. Wang et al., 2019 operated two SBRs in series, the first was operated in in anaerobic/anoxic/aerobic phases (with added nitrate in the influent), and nitrite was accumulated during the anoxic phase by GAO, followed by an anoxic anammox SBR. It appears that utilizing internally stored carbon for denitrification (by non-PAO) in bioP processes is promising, especially if it results in nitrite accumulation, as long as the PAO are not outcompeted. It would be preferable if the denitrification was being performed by PAO, but it is still unclear how to design a process to guarantee dPAO activity.

CONCLUSIONS

Low effluent TIN (less than 2 mg/L) was achieved via partial denitrification in B-stage followed by anammox in an anoxic MBBR without external carbon addition. Effluent OP less than 0.2 mg/L was achieved via feeding A-stage WAS fermentate to a sidestream RAS reactor (SBPR) in B-stage. The period of the highest TIN removal did not coincide with the period of highest OP removal, as the nitrite accumulation in B-stage could not be sustained along with bioP. It was hypothesized that the organisms performing partial denitrification utilizing internally stored were competing with PAO for VFA, which led to the deterioration of bioP. The long term denitrification test demonstrated that denitrification following an anaerobic and aerobic period was occurring utilizing internally stored carbon. The external carbon independent denitrification tests demonstrated that there was a preference for partial denitrification to nitrite, which corresponded to the VFA load from the A-stage WAS fermentate. PAO were not responsible for the external carbon independent denitrification, as anoxic OP uptake was not observed during the external carbon independent denitrification tests, or the PAO anoxic uptake batch tests. Denitrifying GAO were suspected, but low abundance of GAO were detected using amplicon 16S sequencing. PHA did not appear to be responsible for the denitrification from internally stored carbon, and the carbon source was not able to be identified. An unexpectedly low abundance of *amoA* gene copies (both from canonical AOB and Comammox) were measured via qPCR, so it was not clear which organisms performed ammonia oxidation. Future work includes identifying the internal storage polymer responsible for denitrification, and replicating the high nitrite accumulation by increasing the fermentate loading.

REFERENCES

- Alleman, J. E., & Irvine, R. L. (1980). Storage-induced denitrification using sequencing batch reactor operation. *Water Research*, 14(10), 1483–1488.
- Andreasen, K., Petersen, G., Thomsen, H., & Strube, R. (1997). Reduction of nutrient emission by sludge hydrolysis. *Water Science and Technology; London*, 35(10), 79–85.
- Anthonisen, A. C., Loehr, R. C., Prakasam, T. B. S., & Srinath, E. G. (1976). Inhibition of nitrification by ammonia and nitrous acid. *Journal (Water Pollution Control Federation)*, 835–852.
- Auling, G., Pilz, F., Busse, H. J., Karrasch, S., Streichan, M., & Schön, G. (1991). Analysis of the polyphosphate-accumulating microflora in phosphorus-eliminating, anaerobic-aerobic activated sludge systems by using diaminopropane as a biomarker for rapid estimation of *Acinetobacter* spp. *Applied and Environmental Microbiology*, 57(12), 3585–3592.
- Barnard, J. I., Dunlap, P., & Steichen, M. (2017). Rethinking the mechanisms of biological phosphorus removal. *Water Environment Research*, 89(11), 2043–2054.
<https://doi.org/10.2175/106143017X15051465919010>

- Beach, N. K., & Noguera, D. R. (2019). Design and Assessment of Species-Level qPCR Primers Targeting Comammox. *Frontiers in Microbiology*, 10. <https://doi.org/10.3389/fmicb.2019.00036>
- Boehnke, D. B., & Diering, D. B. (1997). Cost-effective wastewater treatment process for removal of... *Water Engineering & Management*, 144(5), 30–34.
- Cagnetta, C., Coma, M., Vlaeminck, S. E., & Rabaey, K. (2016). Production of carboxylates from high rate activated sludge through fermentation. *Bioresource Technology*, 217, 165–172. <https://doi.org/10.1016/j.biortech.2016.03.053>
- Cao, Y., van Loosdrecht, M. C. M., & Daigger, G. T. (2017). Mainstream partial nitrification–anammox in municipal wastewater treatment: Status, bottlenecks, and further studies. *Applied Microbiology and Biotechnology*, 101(4), 1365–1383. <https://doi.org/10.1007/s00253-016-8058-7>
- Chen, H., Yang, Q., Li, X., Wang, Y., Luo, K., & Zeng, G. (2013). Post-anoxic denitrification via nitrite driven by PHB in feast–famine sequencing batch reactor. *Chemosphere*, 92(10), 1349–1355. <https://doi.org/10.1016/j.chemosphere.2013.05.052>
- Daigger, G. T. (2014). Oxygen and Carbon Requirements for Biological Nitrogen Removal Processes Accomplishing Nitrification, Nitritation, and Anammox. *Water Environment Research*, 86(3), 204–209. <https://doi.org/10.2175/106143013X13807328849459>
- Dold, P., Du, W., Burger, G., & Jimenez, J. (2015). Is Nitrite-Shunt Happening in the System? Are NOB Repressed? *Proceedings of the Water Environment Federation*, 2015(13), 1360–1374.
- Du, R., Cao, S., Li, B., Niu, M., Wang, S., & Peng, Y. (2017). Performance and microbial community analysis of a novel DEAMOX based on partial-denitrification and anammox treating ammonia and nitrate wastewaters. *Water Research*, 108, 46–56. <https://doi.org/10.1016/j.watres.2016.10.051>
- Elefsiniotis, P., & Oldham, W. K. (1994). Anaerobic acidogenesis of primary sludge: The role of solids retention time. *Biotechnology and Bioengineering*, 44(1), 7–13. <https://doi.org/10.1002/bit.260440103>
- Erdal, U. G., Erdal, Z. K., & Randall, C. W. (2003). The competition between PAOs (phosphorus accumulating organisms) and GAOs (glycogen accumulating organisms) in EBPR (enhanced biological phosphorus removal) systems at different temperatures and the effects on system performance. *Water Science and Technology*, 47(11), 1–8. <https://doi.org/10.2166/wst.2003.0579>
- Ferris, M. J., Muyzer, G., & Ward, D. M. (1996). Denaturing gradient gel electrophoresis profiles of 16S rRNA-defined populations inhabiting a hot spring microbial mat community. *Applied and Environmental Microbiology*, 62(2), 340–346.

- Fuhs, G. W., & Chen, M. (1975). Microbiological basis of phosphate removal in the activated sludge process for the treatment of wastewater. *Microbial Ecology*, 2(2), 119–138. <https://doi.org/10.1007/BF02010434>
- Graham, D. W., Knapp, C. W., Van Vleck, E. S., Bloor, K., Lane, T. B., & Graham, C. E. (2007). Experimental demonstration of chaotic instability in biological nitrification. *The ISME Journal*, 1(5), 385–393. <https://doi.org/10.1038/ismej.2007.45>
- Hellinga, C., Schellen, A., Mulder, J. W., van Loosdrecht, M. v., & Heijnen, J. J. (1998). The SHARON process: An innovative method for nitrogen removal from ammonium-rich waste water. *Water Science and Technology*, 37(9), 135–142.
- Jenkins, D., & Tandoi, V. (1991). The applied microbiology of enhanced biological phosphate removal—Accomplishments and needs. *Water Research*, 25(12), 1471–1478. [https://doi.org/10.1016/0043-1354\(91\)90177-R](https://doi.org/10.1016/0043-1354(91)90177-R)
- Kalyuzhnyi, S. V., Gladchenko, M. A., Kang, H., Mulder, A., & Versprille, A. (2008). Development and optimisation of VFA driven DEAMOX process for treatment of strong nitrogenous anaerobic effluents. *Water Science and Technology*, 57(3), 323–328. <https://doi.org/10.2166/wst.2008.044>
- Kindaichi, T., Kawano, Y., Ito, T., Satoh, H., & Okabe, S. (2006). Population dynamics and in situ kinetics of nitrifying bacteria in autotrophic nitrifying biofilms as determined by real-time quantitative PCR. *Biotechnology and Bioengineering*, 94(6), 1111–1121. <https://doi.org/10.1002/bit.20926>
- Kinyua, M. N., Miller, M. W., Wett, B., Murthy, S., Chandran, K., & Bott, C. B. (2017). Polyhydroxyalkanoates, triacylglycerides and glycogen in a high rate activated sludge A-stage system. *Chemical Engineering Journal*, 316, 350–360. <https://doi.org/10.1016/j.cej.2017.01.122>
- Kujawa, K., & Klapwijk, B. (1999). A method to estimate denitrification potential for predenitrification systems using NUR batch test. *Water Research*, 33(10), 2291–2300. [https://doi.org/10.1016/S0043-1354\(98\)00459-X](https://doi.org/10.1016/S0043-1354(98)00459-X)
- Lackner, S., Gilbert, E. M., Vlaeminck, S. E., Joss, A., Horn, H., & van Loosdrecht, M. C. M. (2014). Full-scale partial nitrification/anammox experiences – An application survey. *Water Research*, 55, 292–303. <https://doi.org/10.1016/j.watres.2014.02.032>
- Lanham, A. B., Oehmen, A., Saunders, A. M., Carvalho, G., Nielsen, P. H., & Reis, M. A. M. (2013). Metabolic versatility in full-scale wastewater treatment plants performing enhanced biological phosphorus removal. *Water Research*, 47(19), 7032–7041. <https://doi.org/10.1016/j.watres.2013.08.042>
- Le, T., Peng, B., Su, C., Massoudieh, A., Torrents, A., Al-Omari, A., ... Clippeleir, H. D. (2019). Impact of carbon source and COD/N on the concurrent operation of partial denitrification

- and anammox. *Water Environment Research*, 91(3), 185–197.
<https://doi.org/10.1002/wer.1016>
- Liu, J., Yuan, Y., Li, B., Zhang, Q., Wu, L., Li, X., & Peng, Y. (2017). Enhanced nitrogen and phosphorus removal from municipal wastewater in an anaerobic-aerobic-anoxic sequencing batch reactor with sludge fermentation products as carbon source. *Bioresource Technology*, 244, 1158–1165. <https://doi.org/10.1016/j.biortech.2017.08.055>
- Lopez-Vazquez, C. M., Oehmen, A., Hooijmans, C. M., Brdjanovic, D., Gijzen, H. J., Yuan, Z., & van Loosdrecht, M. C. M. (2009). Modeling the PAO–GAO competition: Effects of carbon source, pH and temperature. *Water Research*, 43(2), 450–462.
<https://doi.org/10.1016/j.watres.2008.10.032>
- Lotter, L. H., Wentzel, M. C., & Loewenthal, R. E. (1986). A study of selected characteristics of *Acinetobacter* spp. Isolated from activated sludge in anaerobic/anoxic/aerobic and aerobic systems. *Water SA*, 12(4), 203–208.
- Lotti, T., Kleerebezem, R., Hu, Z., Kartal, B., de Kreuk, M. k., van Erp Taalman Kip, C., ... van Loosdrecht, M. c. m. (2015). Pilot-scale evaluation of anammox-based mainstream nitrogen removal from municipal wastewater. *Environmental Technology*, 36(9), 1167–1177. <https://doi.org/10.1080/09593330.2014.982722>
- Ma, B., Wang, S., Cao, S., Miao, Y., Jia, F., Du, R., & Peng, Y. (2016). Biological nitrogen removal from sewage via anammox: Recent advances. *Bioresource Technology*, 200, 981–990. <https://doi.org/10.1016/j.biortech.2015.10.074>
- Ma, B., Zhang, S., Zhang, L., Yi, P., Wang, J., Wang, S., & Peng, Y. (2011). The feasibility of using a two-stage autotrophic nitrogen removal process to treat sewage. *Bioresource Technology*, 102(17), 8331–8334. <https://doi.org/10.1016/j.biortech.2011.06.017>
- Ma, Y., Sundar, S., Park, H., & Chandran, K. (2015). The effect of inorganic carbon on microbial interactions in a biofilm nitrification–anammox process. *Water Research*, 70, 246–254. <https://doi.org/10.1016/j.watres.2014.12.006>
- Miller, M. W., Elliott, M., DeArmond, J., Kinyua, M., Wett, B., Murthy, S., & Bott, C. B. (2017). Controlling the COD removal of an A-stage pilot study with instrumentation and automatic process control. *Water Science and Technology*, 75(11), 2669–2679.
<https://doi.org/10.2166/wst.2017.153>
- Mino, T., van Loosdrecht, M. C. M., & Heijnen, J. J. (1998). Microbiology and biochemistry of the enhanced biological phosphate removal process. *Water Research*, 32(11), 3193–3207.
[https://doi.org/10.1016/S0043-1354\(98\)00129-8](https://doi.org/10.1016/S0043-1354(98)00129-8)
- Nguyen, H. T. T., Le, V. Q., Hansen, A. A., Nielsen, J. L., & Nielsen, P. H. (2011). High diversity and abundance of putative polyphosphate-accumulating Tetrasphaera-related

- bacteria in activated sludge systems. *FEMS Microbiology Ecology*, 76(2), 256–267. <https://doi.org/10.1111/j.1574-6941.2011.01049.x>
- Novak, J. T., Chon, D. H., Curtis, B.-A., & Doyle, M. (2007). Biological Solids Reduction Using the Cannibal Process. *Water Environment Research*, 79(12), 2380–2386. <https://doi.org/10.2175/106143007X183862>
- Onnis-Hayden, A., Srinivasan, V., Tooker, N. B., Li, G., Wang, D., Barnard, J. L., ... Gu, A. Z. (n.d.). Survey of Full Scale Side-Stream Enhanced Biological Phosphorus Removal (S2EBPR) Systems and Comparison with Conventional EBPRs in North America: Process Stability, Kinetics and Microbial Populations. *Water Environment Research*, 0(ja). <https://doi.org/10.1002/wer.1198>
- Park, H., Sundar, S., Ma, Y., & Chandran, K. (2015). Differentiation in the microbial ecology and activity of suspended and attached bacteria in a nitrification-anammox process. *Biotechnology and Bioengineering*, 112(2), 272–279. <https://doi.org/10.1002/bit.25354>
- Rabinowitz, B. (1985). *The role of specific substrates in excess biological phosphorus removal* (PhD Thesis). University of British Columbia.
- Regmi, P., Miller, M. W., Holgate, B., Bunce, R., Park, H., Chandran, K., ... Bott, C. B. (2014). Control of aeration, aerobic SRT and COD input for mainstream nitrification/denitrification. *Water Research*, 57, 162–171.
- Rothauwe, J. H., Witzel, K. P., & Liesack, W. (1997). The ammonia monooxygenase structural gene amoA as a functional marker: Molecular fine-scale analysis of natural ammonia-oxidizing populations. *Applied and Environmental Microbiology*, 63(12), 4704–4712.
- Rubio-Rincón, F. J., Lopez-Vazquez, C. M., Welles, L., van Loosdrecht, M. C. M., & Brdjanovic, D. (2017). Cooperation between Candidatus Competibacter and Candidatus Accumulibacter clade I, in denitrification and phosphate removal processes. *Water Research*, 120, 156–164. <https://doi.org/10.1016/j.watres.2017.05.001>
- Sharp, R., Niemiec, A., Khunjar, W., Galst, S., & Deur, A. (2017). Development of a novel deammonification process for cost effective separate centrate and main plant nitrogen removal. *International Journal of Sustainable Development and Planning*, 12(1), 11–21. <https://doi.org/10.2495/SDP-V12-N1-11-21>
- Skalsky, D. S., & Daigger, G. T. (1995). Wastewater solids fermentation for volatile acid production and enhanced biological phosphorus removal. *Water Environment Research*, 67(2), 230–237. <https://doi.org/10.2175/106143095X131402>
- Srinivasan, V. N., Li, G., Wang, D., Tooker, N. B., Dai, Z., Onnis-Hayden, A., ... Gu, A. Z. (2019). Oligotyping and Genome-Resolved Metagenomics Reveal Distinct Candidatus Accumulibacter Communities in Full-Scale Side-Stream versus Conventional Enhanced Biological Phosphorus Removal (EBPR) Configurations. *BioRxiv*, 596692.

- Tooker, N. B., Barnard, J. L., Bott, C., Carson, K., Dombrowski, P., Dunlap, P., ... Phillips, H. (2016). Side-Stream Enhanced Biological Phosphorus Removal as a Sustainable and Stable Approach for Removing Phosphorus from Wastewater. *WEF/IWA Nutrient Removal and Recovery*.
- Tsuneda, S., Ohno, T., Soejima, K., & Hirata, A. (2006). Simultaneous nitrogen and phosphorus removal using denitrifying phosphate-accumulating organisms in a sequencing batch reactor. *Biochemical Engineering Journal*, 27(3), 191–196. <https://doi.org/10.1016/j.bej.2005.07.004>
- van Loosdrecht, M. C. M., Pot, M. A., & Heijnen, J. J. (1997). Importance of bacterial storage polymers in bioprocesses. *Water Science and Technology*, 35(1), 41–47. <https://doi.org/10.2166/wst.1997.0008>
- Varga, E., Hauduc, H., Barnard, J., Dunlap, P., Jimenez, J., Menniti, A., ... Takács, I. (2018). Recent advances in bio-P modelling – a new approach verified by full-scale observations. *Water Science and Technology*, 78(10), 2119–2130. <https://doi.org/10.2166/wst.2018.490>
- Vocks, M., Adam, C., Lesjean, B., Gnirss, R., & Kraume, M. (2005). Enhanced post-denitrification without addition of an external carbon source in membrane bioreactors. *Water Research*, 39(14), 3360–3368.
- Vocks, Martin. (2008). *Extensive biological nutrients removal in membrane bioreactors: Mechanisms, influences and optimisations* (VerlDrHut). Retrieved from http://bvbr.bib-bvb.de:8991/F?func=service&doc_library=BVB01&local_base=BVB01&doc_number=017079994&sequence=000001&line_number=0001&func_code=DB_RECORDS&service_type=MEDIA
- Vollertsen, J., Petersen, G., & Borregaard, V. R. (2006). Hydrolysis and fermentation of activated sludge to enhance biological phosphorus removal. *Water Science and Technology*, 53(12), 55–64. <https://doi.org/10.2166/wst.2006.406>
- Wang, M., Huang, G., Zhao, Z., Dang, C., Liu, W., & Zheng, M. (2018). Newly designed primer pair revealed dominant and diverse comammox amoA gene in full-scale wastewater treatment plants. *Bioresour Technol*, 270, 580–587. <https://doi.org/10.1016/j.biortech.2018.09.089>
- Wang, X., Wang, S., Zhao, J., Dai, X., Li, B., & Peng, Y. (2016). A novel stoichiometries methodology to quantify functional microorganisms in simultaneous (partial) nitrification-endogenous denitrification and phosphorus removal (SNEDPR). *Water Research*, 95, 319–329. <https://doi.org/10.1016/j.watres.2015.12.046>
- Wang, X., Zhao, J., Yu, D., Du, S., Yuan, M., & Zhen, J. (2019). Evaluating the potential for sustaining mainstream anammox by endogenous partial denitrification and phosphorus removal for energy-efficient wastewater treatment. *Bioresour Technol*, 284, 302–314. <https://doi.org/10.1016/j.biortech.2019.03.127>

- Wells, G. F., Shi, Y., Laurenzi, M., Rosenthal, A., Szivák, I., Weissbrodt, D. G., ... Morgenroth, E. (2017). Comparing the Resistance, Resilience, and Stability of Replicate Moving Bed Biofilm and Suspended Growth Combined Nitrification–Anammox Reactors. *Environmental Science & Technology*, *51*(9), 5108–5117. <https://doi.org/10.1021/acs.est.6b05878>
- Wentzel, M. C., Lötter, L. H., Ekama, G. A., Loewenthal, R. E., & Marais, G. v R. (1991). Evaluation of Biochemical Models for Biological Excess Phosphorus Removal. *Water Science and Technology*, *23*(4–6), 567–576. <https://doi.org/10.2166/wst.1991.0506>
- Winkler, M., Coats, E. R., & Brinkman, C. K. (2011). Advancing post-anoxic denitrification for biological nutrient removal. *Water Research*, *45*(18), 6119–6130.
- Winkler, M. K. H., Bassin, J. P., Kleerebezem, R., Sorokin, D. Y., & van Loosdrecht, M. C. M. (2012). Unravelling the reasons for disproportion in the ratio of AOB and NOB in aerobic granular sludge. *Applied Microbiology and Biotechnology*, *94*(6), 1657–1666. <https://doi.org/10.1007/s00253-012-4126-9>
- Yao, S., Ni, J., Ma, T., & Li, C. (2013). Heterotrophic nitrification and aerobic denitrification at low temperature by a newly isolated bacterium, *Acinetobacter* sp. HA2. *Bioresource Technology*, *139*, 80–86. <https://doi.org/10.1016/j.biortech.2013.03.189>
- Zhao, H. W., Mavinic, D. S., Oldham, W. K., & Koch, F. A. (1999). Controlling factors for simultaneous nitrification and denitrification in a two-stage intermittent aeration process treating domestic sewage. *Water Research*, *33*(4), 961–970. [https://doi.org/10.1016/S0043-1354\(98\)00292-9](https://doi.org/10.1016/S0043-1354(98)00292-9)
- Zhao, J., Wang, X., Li, X., Jia, S., Wang, Q., & Peng, Y. (2019). Improvement of partial nitrification endogenous denitrification and phosphorus removal system: Balancing competition between phosphorus and glycogen accumulating organisms to enhance nitrogen removal without initiating phosphorus removal deterioration. *Bioresource Technology*, *281*, 382–391. <https://doi.org/10.1016/j.biortech.2019.02.109>

APPENDIX C: SUPPORTING INFORMATION FOR CHAPTER 8

Table C1: qPCR Primers

Target Gene	qPCR Primer	Sequence (5'-3')
Nitrospira 16S	NSPRA-675f	GCGGTGAAATGCGTAGAKATCG
	NSPRA-746r	TCAGCGTCAGRWAYGTTCCAGAG
	Nspra-723Taq	CGCCGCCTTCGCCACCG
Nitrobacter 16S	Nitro-1198f	ACCCCTAGCAAATCTCAAAAAACCG
	Nitro-1423r	CTTCACCCCAGTCGCTGACC
	Nitro-1374Taq	AACCCGCAAGGGAGGCAGCCGACC
Canonical AOB amoA	amoA-1F	GGGGTTTCTACTGGTGGT
	amoA-2R	CCCCTCKGSAAAGCCTTCTTC
Universal 16S	1055F	ATGGCTGTCGTCAGCT
	1392R	ACGGGCGGTGTGTAC
Comammox amoA	comamoA AF	AGGNGAYTGGGAYTTCTGG
	comamoA SR	CCGVACATACATRAAGCCCAT

Table C2: Fermentate VFA fractionation concentrations

	Average Concentration (mg/L as each VFA)	Average Concentration (mg/L as COD)
Acetic	350±120	375±128
Propionic	290±73	438±111
Butyric	107±44	195±79
Isobutyric	26.0±12.2	47.2±22.1
Valeric	65.5±35.9	133.7±73.2
Isovaleric	32.6±15.8	66.5±32.2
Caproic	9.2±2.6	20.4±5.8

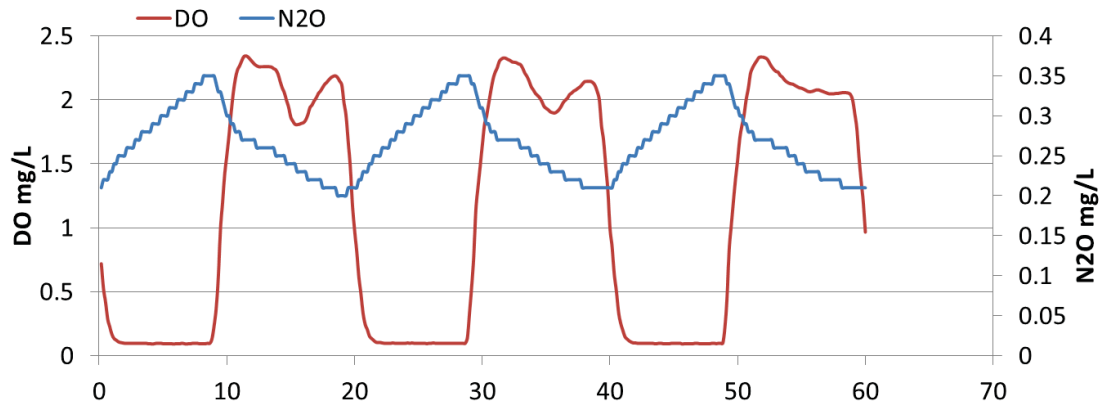


Figure C1: Nitrous oxide production from sensor readings for a 60 minute period

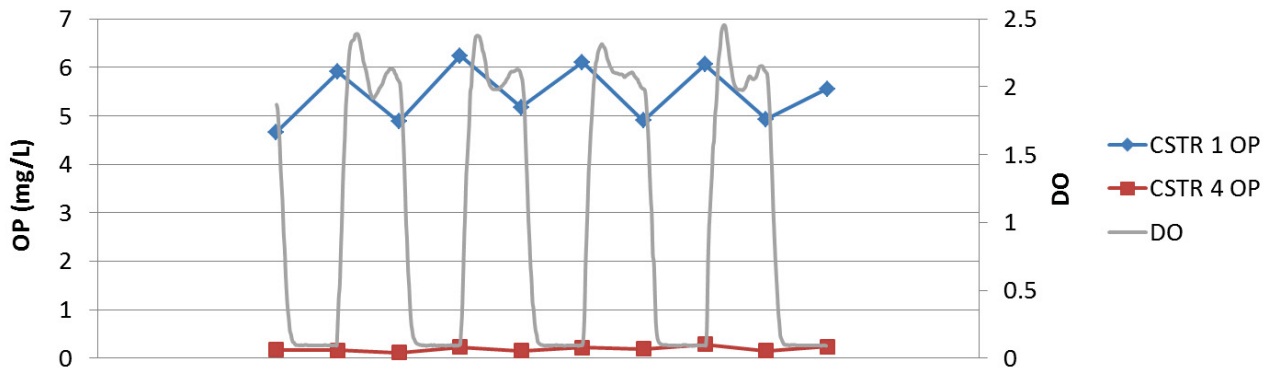


Figure C2: OP profile in time, in reactor during intermittent aeration (10 minute air on/10 minute air off cycle).

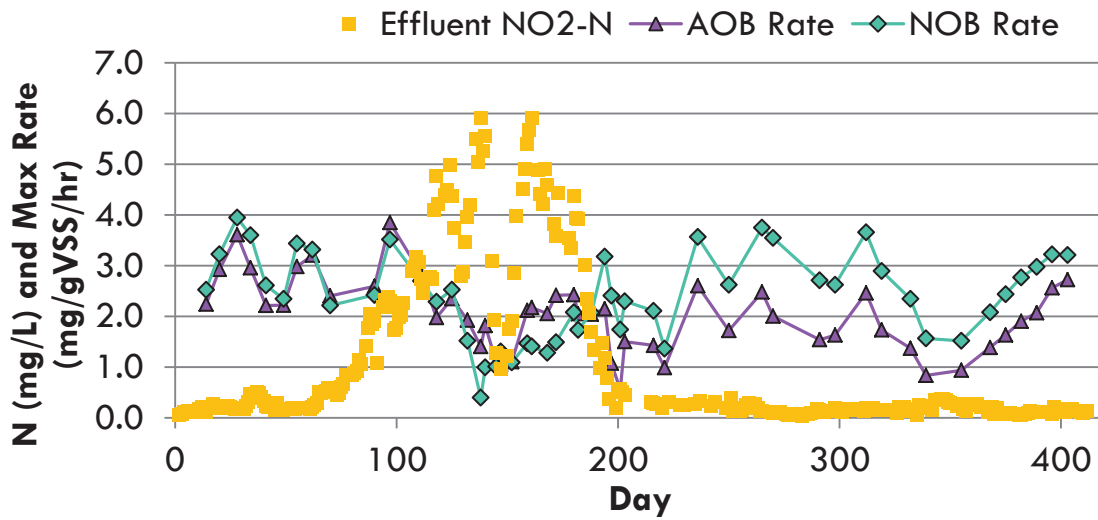


Figure C3: AOB and NOB rates from maximum activity tests and B-stage effluent nitrite

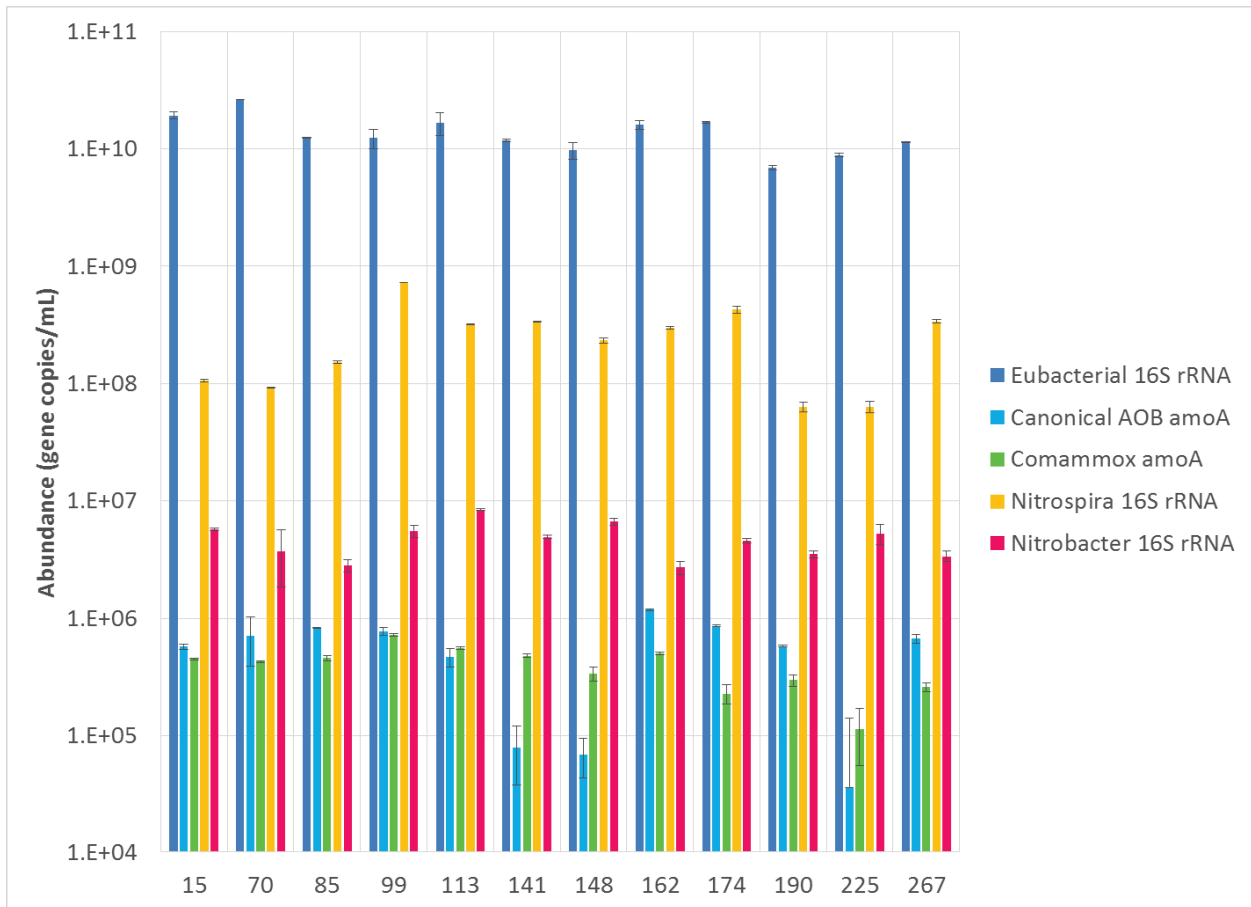


Figure C4: The abundance (copies/mL) of canonical AOB, Comammox, Nitrospira, Nitrobacter, and Eubacteria

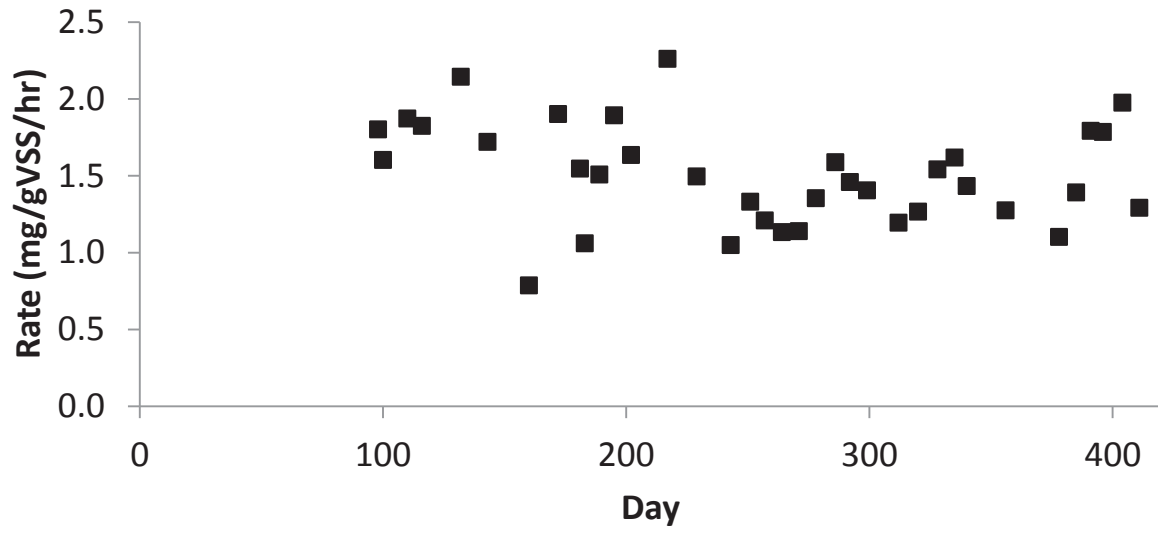


Figure C5: Specific NO_x reduction rates for the external carbon independent batch tests